



<https://theses.gla.ac.uk/>

Theses Digitisation:

<https://www.gla.ac.uk/myglasgow/research/enlighten/theses/digitisation/>

This is a digitised version of the original print thesis.

Copyright and moral rights for this work are retained by the author

A copy can be downloaded for personal non-commercial research or study, without prior permission or charge

This work cannot be reproduced or quoted extensively from without first obtaining permission in writing from the author

The content must not be changed in any way or sold commercially in any format or medium without the formal permission of the author

When referring to this work, full bibliographic details including the author, title, awarding institution and date of the thesis must be given

Enlighten: Theses

<https://theses.gla.ac.uk/>
research-enlighten@glasgow.ac.uk

The Investigation of Two Novel PDE4A Enzymes

A thesis submitted to the

FACULTY OF BIOMEDICAL AND LIFE SCIENCES

For the degree of

DOCTOR OF PHILOSOPHY

By

Lee Ann Johnston

Division of Biochemistry & Molecular Biology

Institute of Biomedical and Life Sciences

University of Glasgow

October 2002

ProQuest Number: 10390627

All rights reserved

INFORMATION TO ALL USERS

The quality of this reproduction is dependent upon the quality of the copy submitted.

In the unlikely event that the author did not send a complete manuscript and there are missing pages, these will be noted. Also, if material had to be removed, a note will indicate the deletion.



ProQuest 10390627

Published by ProQuest LLC (2017). Copyright of the Dissertation is held by the Author.

All rights reserved.

This work is protected against unauthorized copying under Title 17, United States Code
Microform Edition © ProQuest LLC.

ProQuest LLC.
789 East Eisenhower Parkway
P.O. Box 1346
Ann Arbor, MI 48106 – 1346

GLASGOW
UNIVERSITY
LIBRARY:

12 960

copy 2

Declaration

I declare that the work described in this thesis has been carried out by myself unless otherwise cited or acknowledged. It is entirely of my own composition and has not, in whole or in part, been submitted for any other degree.

Lee Ann Johnston

October 2002

Abstract

As the central function of PDEs within cells is to control the levels of the cyclic nucleotides, it was surprising to find that the *PDE4A* gene encoded a splice variant, called PDE4A7 (2EL) that is catalytically inactive. This protein was investigated further by firstly determining its intracellular localisation using the methods of subcellular fractionation and Laser Scanning Confocal Microscopy (LSCM). Interestingly, PDE4A7 when over-expressed in COS-1 cells was found exclusively within the nuclear compartment. This was in contrast to that of the catalytically active long isoform, PDE4A4B, which was found to be extranuclear. Subcellular fractionation studies revealed that the major fraction of PDE4A4B was localised within the cytosolic (S2) fraction, whereas PDE4A7 was localised exclusively within the low speed particulate (P1) fraction. Therefore, despite sharing identical core regions, both PDE4A4B and PDE4A7 were found in completely different compartments. Using chimeric constructs, I firstly demonstrated that the central core was exclusively located to the particulate (P1) fraction even in the absence of the PDE4A7 N-terminal region. Secondly, I demonstrated that replacing the C-terminal of PDE4A7 with 19 amino acids from the C-terminal region that is common to all the active PDE4As was enough to cause re-distribution of a fraction of the PDE4A7 central core to the cytosolic (S2) fraction. These analyses established that the cytosolic targeting observed with the active PDE4A enzymes can be attributed to a small portion of sequence located within their C-terminal regions.

In Chapter 4, the yeast two hybrid screening procedure was used to try and identify binding partners for PDE4A7. Proteins identified as potential binding partners for PDE4A7 included; CREB binding protein (CBP), RanBPM9 and mRNA from the KIAA0160 gene. However, upon further analysis I demonstrated that both CBP and RanBPM9 were false positives generated from the yeast two-hybrid screen. The interaction between PDE4A7 and the mRNA from the KIAA0160 gene has yet to be re-evaluated.

In Chapter 5, I used the methods of gene microarray and RT-PCR to address whether the functional role of PDE4A7 within the nucleus was to control the expression levels of other genes. Gene microarray results demonstrated that the expression levels of a large number of genes changed in response to the over-expression of PDE4A7. Next, RT-PCR was used in an attempt to verify a small number of these changes. However, RT-PCR analysis did not support the changes observed with gene microarray. It was concluded that microarray had generated false positive data for these particular genes.

As yet the basis for the nuclear targeting of PDE4A7 and the function of this protein within this compartment remains to be elucidated.

Finally, in Chapter 6, I performed partial characterisation studies on a novel PDE4A isoform, called HSPDE4A11. Transient expression of HSPDE4A11 in COS-7 cells allowed the detection of a 118kDa protein in both the soluble and particulate fractions. The soluble and particulate forms of HSPDE4A11 exhibited similar K_m values for cAMP hydrolysis ($\sim 2.5\mu\text{M}$) and V_{max} values.

Acknowledgements

I would firstly like to thank Prof. M. Houslay for his guidance, help, patience and supervision during the course of my Ph.D.

Thanks to everyone in the Gardiner Lab for their technical help and friendship, especially to Elaine Huston for her guidance and to Catherine, who has been a great wee pal over the last few years.

I would also like to thank Gordon, who has been very supportive, helpful and patient with moody ole me!!

My biggest thanks goes to my mum and dad for all their encouragement and support over the past few years.

Table of Contents

Declaration.....	ii
Abstract.....	iii
Acknowledgements.....	v
Table of contents.....	vi
List of Figures.....	x
List of Tables.....	xii
Abbreviations.....	xiii

Chapter 1

General Introduction.....	1
1.1. Cyclic nucleotide signalling pathways.....	1
1.1.1. Generation and detection of cAMP.....	1
1.1.2. G protein coupled receptors.....	1
1.1.3. Adenylyl cyclase.....	2
1.1.4. Protein Kinase A.....	4
1.1.5. cAMP signalling independent from PKA.....	5
1.2. Phosphodiesterase enzymes.....	7
1.2.1. PDE1 enzyme family.....	8
1.2.2. PDE2 enzyme family.....	8
1.2.3. PDE3 enzyme family.....	9
1.2.4. PDE4 enzyme family.....	9
1.2.5. PDE5 enzyme family.....	10
1.2.6. PDE6 enzyme family.....	10
1.2.7. PDE7 enzyme family.....	11
1.2.8. PDE8 enzyme family.....	11
1.2.9. PDE9 enzyme family.....	12
1.2.10. PDE10 enzyme family.....	12
1.2.11. PDE11 enzyme family.....	12
1.3. Compartmentalisation of cAMP signalling.....	15
1.4. PDE4 Phosphodiesterases.....	16
1.4.1. PDE4A subfamily.....	20
1.4.1.1. PDE4A localisation and targeting.....	20
1.4.1.2. Regulation of PDE4As.....	21
1.4.2. PDE4B subfamily.....	22
1.4.3. PDE4C subfamily.....	23
1.4.4. PDE4D subfamily.....	23
1.4.4.1. PDE4D localisation and targeting.....	23
1.4.4.2. Regulation of PDE4Ds.....	24
1.5. Transcriptional regulation of PDE4s.....	25
1.6. Importance of PDE4s.....	26

Chapter 2

Materials and methods	28
2.1. Mammalian cell culture	28
2.1.1. Cell culture techniques.....	28
2.1.1.1. COS-1 and COS-7 cell lines.....	28
2.1.1.2. HEK-293 cell line.....	28
2.1.1.3. Maintenance of cell lines.....	28
2.1.2. Transfection of COS-1 cells with plasmid DNA.....	29
2.1.3. Transfection of HEK-293 cells with plasmid DNA.....	29
2.2. Biochemical techniques	29
2.2.1. General subcellular fractionation of cells.....	30
2.2.2. Immunoprecipitation.....	30
2.2.3. Quantification of protein.....	31
2.2.4. SDS-polyacrylamide gel electrophoresis.....	31
2.2.4.1. Preparation of samples.....	31
2.2.4.2. Molecular weight protein standards.....	32
2.2.4.3. Casting and running tris-glycine gels.....	32
2.2.4.4. Transfer of proteins onto nitrocellulose.....	32
2.2.4.5. Immunoblotting.....	33
2.2.5. Laser Scanning Confocal microscopy (LSCM).....	33
2.3. Molecular techniques	34
2.3.1. Small scale production of DNA.....	34
2.3.2. Large scale production of DNA.....	35
2.3.3. DNA and RNA quantification.....	35
2.3.4. Glycerol stock production.....	36
2.3.5. Agarose gel electrophoresis.....	36
2.3.6. Gel extraction of DNA.....	37
2.3.7. Restriction digestion of DNA.....	37
2.3.8. DNA ligation.....	37
2.3.9. Reverse transcription polymerase chain reaction (RT-PCR).....	37
2.3.9.1. RNA isolation.....	37
2.3.9.2. First strand cDNA synthesis.....	38
2.3.9.3. PCR reaction.....	38
2.3.10. Cloning and PCR.....	39
2.3.10.1. PCR conditions used for generating PDE4A7 cDNA containing the nuclear export signal (NES) of PKI α and for incorporating EcoRI and BamHI sites onto PDE4A7.....	39
2.3.10.2. Transformation of Ecoli with plasmid DNA.....	39
2.3.10.3. TOPO cloning.....	40
2.3.10.4. PCR screening of colonies.....	40
2.3.11. DNA sequencing.....	41
2.3.11.1. Sequence analysis.....	41
2.4. Yeast two hybrid analysis	41
2.4.1. Testing the bait plasmid for toxicity effects, transcriptional activation and effects on yeast mating efficiency.....	41
2.4.2. Preparation of SD/-Ade/-His/-Leu/-Trp plates.....	41
2.4.3. Preparation of competent yeast cells.....	42
2.4.4. Transformation of DNA into yeast.....	42
2.4.5. Protein extraction from yeast.....	43
2.4.6. Small scale yeast mating.....	43
2.4.7. Large scale yeast mating.....	43
2.4.8. Assay for β -galactosidase activity.....	44
2.4.9. Plasmid isolation from yeast cells.....	44
2.5. Gene microarray analysis	45

Chapter 3

Intracellular targeting of PDE4As.....	47
3.1. Introduction.....	47
3.2. Results	47
3.2.1. Subcellular distribution of PDE4A4B and PDE4A4C (h6.1) in COS-1 cells.....	48
3.2.2. Analysis of transfected COS-1 cells using Laser Scanning Confocal Microscopy (LSCM).....	48
3.2.3. Subcellular localisation of PDE4A7 (2EL).....	54
3.2.4. Subcellular distribution of the PDE4A7 chimeras, hyb1 and hyb2 in COS-1 cells.....	56
3.2.5. Expression of hyb1 truncates in COS-1 cells.....	61
3.2.6. Conclusions from targeting analysis of PDE4As.....	70
3.2.7. Attempt to identify nuclear import and export signals on PDE4A7 and PDE4A4B, respectively.....	70
3.2.8. Mutational analysis of the putative nuclear import signal of PDE4A7.....	72
3.2.9. Mutational analysis of the putative export signal in hyb1.....	72
3.2.10. Engineering an NES to the C-terminal of PDE4A7.....	75
3.3. Discussion.....	79

Chapter 4

An attempt to identify PDE4A7 (2EL) interacting proteins.....	82
4.1. Introduction.....	82
4.1.1. The yeast two hybrid principle.....	82
4.2. Results.....	85
4.2.1. Constructing the bait plasmid.....	86
4.2.2. Digestion of pGBKT7 vector and PDE4A7 insert.....	84
4.2.3. Restriction analysis of pGBK17-PDE4A7.....	90
4.2.4. Verification of PDE4A7 protein expression in the AH109 yeast reporter strain.....	90
4.2.5. Testing for PDE4A7 bait protein toxicity effects.....	91
4.2.6. Yeast mating.....	94
4.2.7. Testing for β -galactosidase activity.....	94
4.2.8. Rescue of the library plasmid.....	96
4.2.9. Proteins found to interact with PDE4A7 in the yeast two hybrid screen.....	96
4.2.10. Attempt to confirm protein-protein interaction by immunoprecipitation.....	103
4.2.11. Re-evaluating the possible interaction of PDE4A7 with RanBPM and CBP using the small scale Y2H.....	106
4.3. Discussion.....	108

Chapter 5

Assessing the potential effects of PDE4A7 (2EL) on gene regulation.....	109
5.1. Introduction.....	109
5.2. Results.....	110
5.2.1. Expression of PDE4A7 in HEK-293 cells.....	110
5.2.2. Using microarray to detect changes in gene expression in response to expression of recombinant PDE4A7.....	112
5.2.3. Using RT-PCR to detect changes in gene expression in response to PDE4A7 Over-expression.....	116
5.2.4. Primer design.....	116
5.2.5. Checking for PDE4A7 expression in HEK-293 cells.....	127
5.3. Discussion.....	138

Chapter 6

Partial characterisation of the novel cyclic AMP-specific phosphodiesterase PDE4A11(TM3).....	140
6.1. Introduction.....	140
6.2. Results.....	144
6.2.1. Distinguishing between the different PDE4A long forms.....	144
6.2.2. Localisation of HSPDE4A11 in transiently transfected COS-7 cells.....	149
6.3. Kinetic evaluation of HSPDE4A11.....	152
6.3.1. Km and relative Vmax values of PDE4A11 expressed in transfected COS-7 cells.....	152
6.4. Discussion.....	156

Chapter 7

General discussion.....	157
References.....	164

List of Figures

Chapter 1

Figure 1.1	cAMP signalling.....	6
Figure 1.2	Schematic representation of PDE4 enzymes.....	18
Figure 1.3	PDE4 mRNA transcripts generated from the human PDE4A, PDE4B, PDE4C and PDE4D genes.....	19

Chapter 3

Figure 3.1	Sequence alignment of PDE4A4B, h6.1, PDE4A7, hyb1 and hyb2.....	50
Figure 3.2	Distribution of the PDE4A4B (PDE46) in COS-1 cells.....	52
Figure 3.3	Distribution of PDE4A4C (h6.1) in COS-1 cells.....	53
Figure 3.4	Distribution of PDE4A7 (2EL) in COS-1 cells.....	55
Figure 3.5	Subcellular localisation of hyb1.....	59
Figure 3.6	Subcellular localisation of hyb2.....	60
Figure 3.7	Alignment of hyb1 and PDE4A7 (2EL) with engineered hyb1 chimeras.....	64
Figure 3.8	Subcellular localisation of delta N-C terminal.....	66
Figure 3.9	Subcellular localisation of delta 309.....	67
Figure 3.10	Subcellular localisation of delta 328.....	68
Figure 3.11	Subcellular localisation of delta 410.....	69
Figure 3.12	Subcellular localisation of PDE4A7 containing import mutation 1.....	73
Figure 3.13	Subcellular localisation of PDE4A7 containing import mutation 2.....	74
Figure 3.14	Engineering the NES of PKI α to the C-terminal of PDE4A7.....	77
Figure 3.15	Subcellular localisation of PDE4A7 containing a NES.....	78

Chapter 4

Figure 4.1	The yeast two-hybrid principle.....	84
Figure 4.2	Incorporation of EcoRI and BamHI restriction sites into PDE4A7 cDNA.....	87
Figure 4.3	Digestion of the pGBKT7 vector and PDE4A7 cDNA.....	88
Figure 4.4	Identification of pGBKT7 vectors containing the PDE4A7 insert.....	89
Figure 4.5	Restriction analysis of putative pGBKT7/PDE4A7 DNA.....	92
Figure 4.6	Verification of expression of PDE4A7 in AH109 yeast cells.....	93
Figure 4.7	Testing positive colonies for β -galactosidase activity.....	95
Figure 4.8	Sequence alignment of the insert demonstrating homology to CREB binding protein (CBP).....	98
Figure 4.9	Sequence alignment of inserts demonstrating homology to the RanBPM9 protein.....	99
Figure 4.10	Sequence alignment of the insert that demonstrated homology to human mRNA for the KIAA0160 gene.....	101
Figure 4.11	Testing for the <i>in vivo</i> interaction of CBP with PDE4A7.....	105
Figure 4.12	Re-testing the interaction of PDE4A7 with RanBPM and CBP.....	107

Chapter 5

Figure 5.1	Expression of PDE4A7 in HEK-293 cells.....	111
Figure 5.2	Display of genes upregulated in response to over-expression of PDE4A7 in HEK-293 cells.....	114
Figure 5.3	Display of genes downregulated in response to over-expression of PDE4A7 in HEK-293 cells.....	115
Figure 5.4	Nucleotide sequence of the A2AR (NCBI: S46950).....	118
Figure 5.5	Nucleotide sequence of CREB protein (NCBI: M31630).....	119
Figure 5.6	Nucleotide sequence of the MAP1B protein (NCBI: XM003704).....	120
Figure 5.7	Nucleotide sequence of the C3 protein (NCBI: M29871).....	121
Figure 5.8	Nucleotide sequence of the FLCK protein (NCBI: M10119).....	121
Figure 5.9	Nucleotide sequence of the CLK2 protein (NCBI: XM002188).....	122
Figure 5.10	Nucleotide sequence of the A2BR (NCBI: X68487).....	123
Figure 5.11	Nucleotide sequence of cyclophilin (NCBI: X52851).....	124
Figure 5.12	Detecting expression of PDE4A7 in cell lysates used for RT-PCR analysis.....	130
Figure 5.13	Changes in the adenosine A2A receptor (A2AR) transcript level in response to over-expression of PDE4A7.....	131
Figure 5.14	Changes in cAMP response element binding protein (CREB) transcript level in response to over-expression of PDE4A7.....	132
Figure 5.15	Changes in microtubule-associated protein 1B (MAP1B) transcript level in response to over-expression of PDE4A7.....	133
Figure 5.16	Changes in C3 botulinum toxin substrate (C3) transcript level in response to over-expression of PDE4A7.....	134
Figure 5.17	Changes in ferritin light chain kinase (FLCK) transcript level in response to over-expression of PDE4A7.....	135
Figure 5.18	Changes in protein kinase CLK2 (CLK2) transcript level in response to over-expression of PDE4A7.....	136

Chapter 6

Figure 6.1	PDE4A gene structure.....	142
Figure 6.2	Amino acid sequence of HSPDE4A11 (TM3).....	143
Figure 6.3	Immunoprobng HSPDE4A11 and HSPDE4A4B lysates with the HSPDE4A4B N-terminal specific antisera.....	146
Figure 6.4	Immunoprobng HSPDE4A11 and HSPDE4A4B lysates with the HSPDE4A10 N-terminal specific antisera.....	147
Figure 6.5	Immunoprobng HSPDE4A11 and HSPDE4A4B lysates with general PDE4A antisera.....	148
Figure 6.6	Subcellular distribution of HSPDE4A11.....	151
Figure 6.7	Analysis of the Km for particulate PDE4A11 expressed in COS-7 cells.....	154
Figure 6.8	Analysis of the Km for soluble PDE4A11 expressed in COS-7 cells.....	155

List of Tables

Chapter 1

Table 1.1	The regulation of the multiple adenylyl cyclase isoforms.....	3
Table 1.2	Phosphodiesterase superfamily.....	14

Chapter 3

Table 3.1	Distribution of PDE4A4B, h6.1, hyb1 and hyb2 in COS-1 cells.....	58
Table 3.2	Distribution of delta 309 and delta 410 in COS-1 cells.....	63
Table 3.3	Table showing the sense and antisense primers used to incorporate the NES of PKI α onto the C-terminal of PDE4A7.....	75

Chapter 4

Table 4.1	Nucleotide sequences of inserts identified from the Y2H study.....	97
------------------	--	----

Chapter 5

Table 5.1	Table showing primers and conditions used for RT-PCR reactions.....	126
Table 5.2	Comparison of the predicted and observed molecular sizes (in bp) for target genes.....	129
Table 5.3	Comparison of the gene expression changes detected using gene microarray and RT-PCR arrays.....	137

Chapter 6

Table 6.1	Distribution of HSPDE4A11 and HSPDE4A4B in COS-7 cells.....	147
Table 6.2	Properties of HSPDE4A11 expressed in COS-7 cells.....	153
Table 6.3	Comparison of the relative V_{max} obtained for soluble (S2) HSPDE4A4B and HSPDE4A11.....	153

Abbreviations

aa	amino acid
A2AR	adenosine A2A receptor
A2BR	adenosine A2B receptor
AD	activation domain
Ade	adenine
AC	adenylyl cyclase
AKAP	A kinase anchoring prote
bp	base pair
BD	binding domain
Ca /Ca.M	calcium/calmodulin
cAMP	cyclic 3'5' adenosine mono phosphate
CAT	chloramphenicol acetyltransferase
C3	C3 botulinum toxin substrate
CLK2	protein kinase CLK2
CREB	cAMP response element binding protein
cDNA	complementary DNA
cGMP	cyclic guanosine mono phosphate
DEAE	diethyl aminoethyl
DMEM	Dulbecco's modification of Eagle's Medium
DMSO	dimethylsulphoxide
DNA	deoxyribonucleic acid
dNTP	deoxynucleotide triphosphate
DTT	dithiothreitol
FLCK	ferritin light chain kinase
ECL	Enhanced chemiluminescence
EDTA	Diaminoethanetetra-acetic acid
EGF	epidermal growth factor
EGTA	Ethylene glycol-bis(β -aminoethyl ether)-N,N,N',N'-tetraacetic acid
ERK	Extracellular regulated kinase
FCS	foetal calf serum
GPCR	G-protein coupled receptor
G-protein	guanine nucleotide binding regulatory protein
GTP	guanosine triphosphate
HEK	Human embryonic kidney
HEPES	N-2-Hydroxyethylpiperazine-N'-2-ethanesulfonic acid
His	histidine
IBMX	isobutylmethylxanthine
IGF	Insulin-like growth factor
IL	interleukin

IFN γ	interferon gamma
IRS1/IRS2	insulin receptor substrate 1 (or 2)
KHEM	potassium (K), HEPES, EGTA, Magnesium
K _m	Michealis-Menton
kDa	kiloDaulton
LB	Luria-Bertoni
Lcu	leucine
LR	linker region
LSCM	Laser scanning Confocal Microscopy
MAP kinase	mitogen activated protein kinase
MAP1B	microtubule-associated protein 1B
MEK	MAPK kinase
mRNA	messenger RNA
NBCS	new born calf serum
NES	nuclear export signal
NLS	nuclear localisation signal
NPC	nuclear pore complex
OD ₆₀₀	optical density (e.g at 600nm)
ORF	open reading frame
PA	phosphatidic acid
PTF-1	pancreatic transcription factor-1
PAGE	Polyacrylamide gel electrophoresis
PBS	phosphate buffered saline
PCR	polymerase chain reaction
PDE	phosphodiesterase
PI 3-kinase	Phosphatidyl inositol 3-kinase
PKA	protein kinase A
PKC	protein kinase C
PKI	PKA inhibitor protein
PMA	Phorbol 12- myristate 13-acetate
QDO	quadruple dropout
RanBPM	Ran binding protein
pRb	Retinoblastoma protein
RNA	ribonucleic acid
RT	reverse transcription
RT-PCR	reverse transcription-polymerase chain reaction
SD	synthetic dropout
SDS	sodium dodecyl sulphate
SH2 domain	Src homology 2 domain
SH3 domain	Src homology 3 domain
SHP-1	Src homology 2 domain-containing protein tyrosine phosphatase-1
SV40	simian virus large T-antigen
TAE	tris/acetate/EDTA

TBS	tris buffered saline
TCR	T cell receptor
TE	tris/EDTA
TEMED	N,N,N',N'-Tetramethyl-ethylenediamine
TGF	Transforming growth factor
Trp	tryptophan
UCR	upstream conserved region
VSMC	Vascular smooth muscle cell
X-gal	5-bromo-4-chloro-3-indolyl- β -D-galactopyranoside
Y2H	yeast two-hybrid
YPD	Yeast extract Peptone and Dextrose
YPDA	YPD medium supplemented with adenine

Chapter 1

General Introduction

1.1 Cyclic nucleotide signalling pathways

1.1.1 Generation and detection of cAMP

Cyclic adenosine monophosphate (cAMP) was first discovered in 1957 [Sutherland et al., 1958] and cyclic guanosine monophosphate (cGMP) was first identified as an important signalling molecule in 1963 by Ashman [Ashman et al., 1963]. Since their discovery both cAMP and cGMP have been found to regulate a wide range of different cellular processes including neurotransmission, glycogenolysis, transcription, and inflammatory processes [Verne et al., 1973; Montminy, 1997; Torphy, 1998] and cAMP has also been shown to regulate cell growth and differentiation [Lui, 1982]. The production and detection of cAMP will be discussed in brief, followed by an 'in depth' discussion of the targeting and regulation of phosphodiesterases (PDEs), which are the enzymes that catalyse the hydrolysis of these cyclic nucleotides.

1.1.2 G protein coupled receptors

The events preceding the production of cAMP include a ligand such as a hormone or neurotransmitter binding to its cognate G protein coupled receptor (GPCR), which then stimulates G_{α} to activate adenylyl cyclase and produce cAMP (cAMP signalling pathway is illustrated in *figure 1.1*). This process is discussed in more depth below.

Although over 1000 GPCRs exist, each share a common general structure composed of an extracellular N-terminal followed by seven transmembrane domains that are connected by three extracellular and three intracellular loops and end with a cytoplasmic C-terminal tail [Gether et al., 1998; Hamm, 1998]. Prior to activation, G proteins exist as heterodimers composed of an α subunit (which bears the guanine nucleotide site) associated with a $\beta\gamma$ subunit dimer. After ligand binding, GPCRs undergo a conformational change that exposes residues capable of interacting with particular G proteins. The N-terminal region of G_{α} can then interact with residues in the third cytoplasmic loop of the activated GPCR [Martin et al., 1996]. This interaction results in a conformational change in the G proteins that results in the exchange of GDP for GTP in

the α subunit. The $G\alpha$ subunit dissociates from the $G\beta\gamma$ subunit dimer and goes on to activate adenylyl cyclase and $G\beta\gamma$ can also go on and activate downstream effectors [Gether and Ulrik, 2000; Hamm, 1998]. It should also be noted that there are different $G\alpha$ subunits that can serve to activate or inhibit adenylyl cyclase. De-activation of this process ensues when GTP is hydrolysed back to GDP by the intrinsic GTPase activity of the $G\alpha$ subunit. There are of course additional mechanisms that de-activate GPCR signals which are reviewed elsewhere [Bunemann and Hooley, 1999].

1.1.3 Adenylyl cyclase

The adenylyl cyclase enzyme family consists of nine isoforms that all catalyse cAMP from ATP when activated by $G\alpha$ -GTP. However, regulation of these enzymes is by no means a simple process as they can also be regulated by PKA, PKC, calcium (Ca^{2+}), calcium/calmodulin (Ca^{2+}/CaM), $G\alpha$ and $G\beta\gamma$ in an isoform-specific fashion [Hanoune et al., 2001; Patel et al., 2001].

Each adenylyl cyclase isoform demonstrates a common overall structure consisting of two transmembrane domains (M1 and M2) that are each composed of six transmembrane domains and two large cytoplasmic loops (C1 and C2), which can be further sub-divided into the regions of C1 α , C1 β , C2 α and C2 β (*figure 1.1*) [Hurley, 1999; Tesmer et al., 1998]. The C1 α and C2 α regions form the catalytic site of adenylyl cyclase. The C2 α region provides the site of interaction for $G\alpha$ and $G\beta\gamma$ [Tang and Gilman, 1995; Yan, Huang et al., 1997]. The C1 β region provides the domain that mediates the regulation of certain adenylyl cyclase isoforms by PKA, calcium, Ca^{2+}/CaM etc (as described above) [Tesmer and Sprang, 1998]. The effect this regulation has on enzyme activity depends on the isoform. Forskolin can activate all the adenylyl cyclases, except AC-IX, by stabilizing the interactions between the two cytoplasmic domains [Sunahara et al., 1997]. The differences found in cAMP responsiveness in different tissues can be accounted for by different expression patterns of the differentially regulated adenylyl cyclases (Table 1.1). The main intracellular detector of cAMP is the cAMP-dependent protein kinase (PKA) [Taylor, Knighton et al., 1992] other targets regulated by cAMP include cyclic nucleotide gated ion channels [Pedarzani and Storm, 1995] and the GTP exchange proteins of Epac [de Rooij, Zwartkruis et al., 1998; Kawasaki, Springett et al., 1998].

Response to cAMP signalling pathway component ^a						
AC Isoform	Gs α	G α	G $\beta\gamma$	Ca ²⁺	Protein kinases	Human chromosome
AC-I	↑	↓ (CaM- or FSK-stimulated activities)	↓	↑ (CaM) ↓ (CaM kinase IV)	↑ PKC (weak) ↓ (CaM kinase IV)	7p12
AC-II	↑	→	↑ (when stimulated by G α s)		↑ (PKC)	5p15
AC-III	↑	↓		↑ (CaM) (in vitro) ↓ (CaM kinase II)	↑ PKC (weak) (in vitro) ↓ (CaM kinase II)	2p22-24
AC-IV	↑		↑		↑ (PKC)	14q11.2
AC-V	↑	↓	↓ (β 1 γ 2)	↓ (<1 μ M)	↓ (PKA) ↑ (PKC α/ζ)	3q13.2-q21
AC-VI	↑	↓	↓ (β 1 γ 2)	↓ (<1 μ M)	↓ (PKA, PKC)	12q12-13
AC-VII	↑		↑		↑ (PKC)	16q12-13
AC-VIII	↑	↓ (Ca ²⁺ Rises)		↑ (CaM)	→ (PKC)	8q24
AC-IX	↑	↓		↓ (calcineurin)		16p13.3

Table 1.1 The regulation of the multiple adenylyl cyclase isoforms [Hanoune and Defer., 2001].

Key: ↑, positive regulatory response; ↓, negative regulatory response; →, neutral response

1.1.4 Protein Kinase A

The most extensively studied intracellular receptor of cAMP is PKA. In its inactive state, PKA exists as a heterotetramer composed of two catalytic subunits (C) bound to a regulatory subunit dimer (R). When four molecules of cAMP bind to the regulatory subunit dimer, a conformational change ensues, which causes dissociation of the enzyme into an R subunit and two C subunits that can phosphorylate substrate proteins on serine or threonine residues in an RRXS/T motif (*figure 1.1*) [reviewed in Skalhogg and Tasken, 2000 and the substrates of PKA are reviewed in Shabb, 2001]. Multiple isoforms of both the R and C subunits exist, leading to different isoforms that possess different biochemical characteristics. The R subunits are encoded by four different genes (RI α , RI β , RII α and RII β) [Lee et al., 1983; Scott et al., 1987] with alternative splice variants reported for RI α [Solberg et al., 1997]. Three different genes (C α , C β and C γ) encode the C subunit with alternative splice variants reported for both C α and C β [Chrivia et al., 1988]. The PKAI holoenzymes (RI α and RI β) exist as soluble species and are activated by weak cAMP signals, whereas PKAII (RII α and RII β) associate with the particulate fraction of the cell and are activated only by high and persistent cAMP signals [Taylor et al., 1992]. RI α and RII α are ubiquitously expressed whereas RII β has been found expressed predominantly in endocrine, brain, fat and reproductive tissues [Taylor et al., 1992].

PKAII is localised to specific intracellular locations by associating with targeting proteins called A-kinase anchoring proteins (AKAPs). AKAPs are a family of proteins that demonstrate little sequence similarity to each other but all possess a RII binding domain [Felicciello et al., 2001; Michel and Scott, 2002]. This domain is an amphipathic helix that binds to the first 30 amino acids in the N-terminal of the RII subunit dimer, a region that is also responsible for promoting the dimerization of the RII subunits [Li and Rubin, 1995; Newlon et al., 1997]. Each AKAP contains a unique targeting domain, responsible for directing the PKA holoenzymes to the appropriate cellular location [Colledge and Scott, 1999]. Most AKAPs preferentially bind to the RII subunits of PKA. However, recently a family of dual function AKAPs, capable of binding to both RI and RII subunit dimers, have been identified [Banky et al., 2000; Felicciello et al., 2001].

1.1.5 cAMP signalling independent from PKA

cAMP can activate the small GTPases of Rap1 and Rap2 in a PKA-independent manner by directly activating the guanine nucleotide exchange factor (GEF) Epac (exchange protein directly activated by cAMP) [de Rooij et al., 1998; Kawasaki et al., 1998]. The Epac family consists of three members: Epac1, Epac2 and Repac (for related to Epac) [de Rooij et al., 2000]. The N-terminals of Epac1 and Epac2 contain one and two cAMP binding sites respectively, which, in the absence of cAMP act as an inhibitory domain to these proteins. Upon the binding of cAMP to these domains, a conformational change ensues that allows the GEF domain, located in the C-terminal catalytic site, to specifically activate both the Rap1 and Rap2 GTPases [de Rooij et al., 2000]. Also located within the N-terminal of Epac1 is a DEP domain (for Disheveled, Eg1-10 and pleckstrin [Ponting and Bork, 1996]), found responsible for the membrane localisation of this protein [de Rooij et al., 2000]. Repac lacks the cAMP binding domains and, as a result, remains constitutively active.

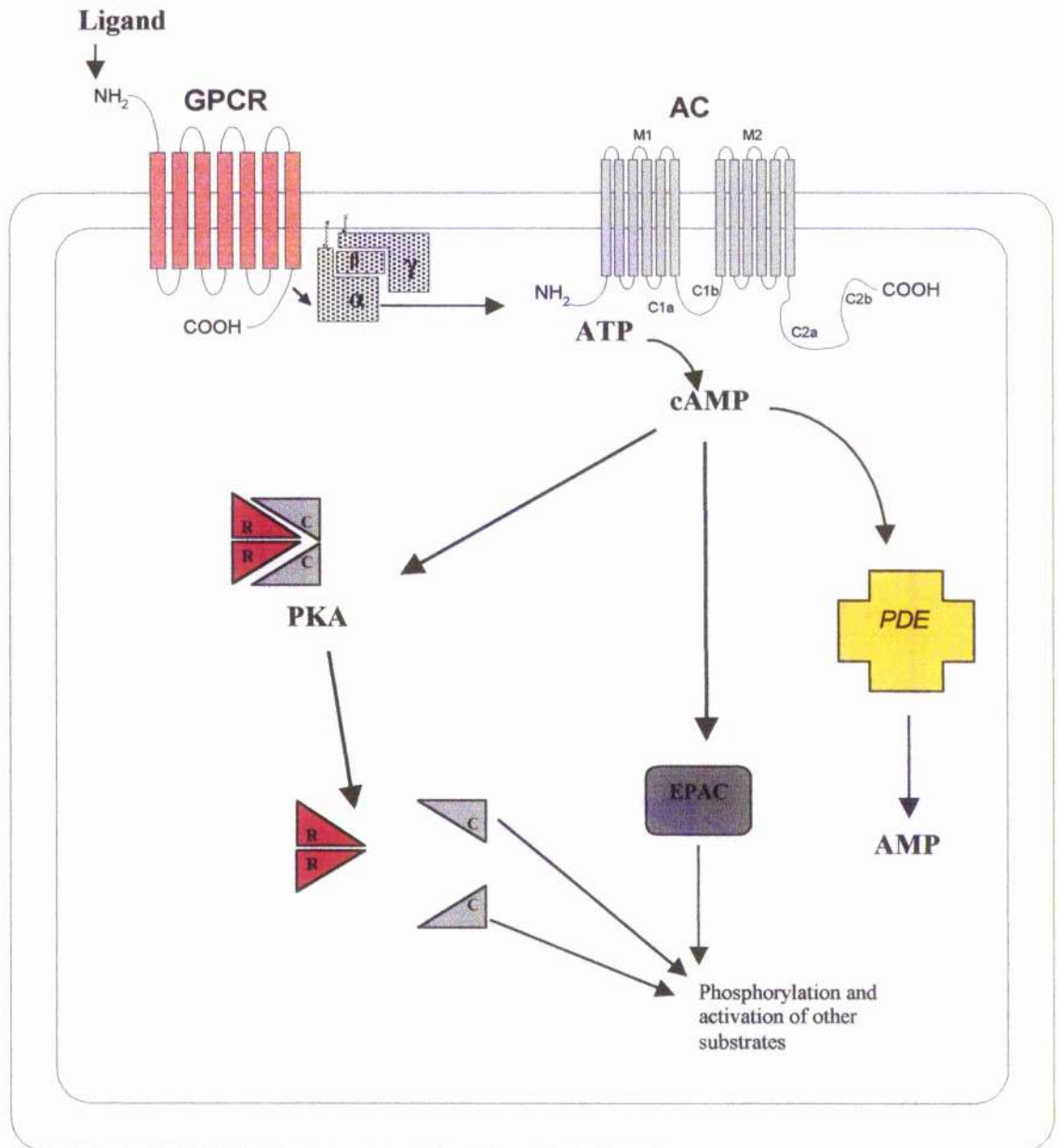


Figure 1.1 cAMP signalling. cAMP generation begins with ligand binding to its cognate seven transmembrane domain receptor. The activated receptor stimulates the release of the G α subunit from the $\beta\gamma$ subunit dimer. G α then diffuses along the membrane and interacts with adenylyl cyclase, which results in either activation or inhibition in the production of cAMP. If it is G α_s , then cAMP will be produced, which then binds to the regulatory subunits of PKA causing the release of the catalytic subunits that can phosphorylate a number of other target proteins. cAMP degradation is catalysed by the phosphodiesterase enzymes.

1.2 Phosphodiesterase enzymes

PDE activity was first discovered in heart tissues, soon after the discovery of cAMP [Sutherland and Rall, 1958]. Following this, many other PDEs have since been discovered and characterised. These enzymes hydrolyse the 3'-5' phosphodiester bond of either cAMP and/or cGMP to generate inactive 5'-nucleoside monophosphates. PDEs are encoded by 21 different genes, the products of which are classified into 11 families based on primary amino acid sequence, substrate specificity, regulatory properties and their sensitivity to different inhibitors [reviewed in Houslay, 2001]. Further complexity arises within each family as a result of alternative mRNA 5' splicing, which yields isoforms with unique N-terminal sequences. There are also members that undergo 5' and 3' mRNA splicing, which generate isoforms containing unique N- and C-terminal regions. This has been demonstrated for members of the PDE1 and PDE4 enzyme families.

The unique N-terminal sequence has been found to confer targeting and regulatory properties on these enzymes, for example the calmodulin-binding domains on PDE1 enzymes, the GAF domains of PDE2, PDE5 and PDE6 and membrane association of PDE3s is mediated by their hydrophobic N-terminal portion. These various features are discussed in depth later. As PDEs can be regulated by other signals, they serve as a point of cross-talk between different signalling cascades [Conti et al. 1995; reviewed in Houslay, 2001]. Despite the diversity of PDEs, they each share a degree of structural homology. This relates to the catalytic domain, which is located towards the C-terminus of all PDEs and is typically around 275 amino acids in size. This domain demonstrates a sequence homology of 80% between isoforms of the same gene family and 25-40% sequence identity between isoenzymes from different gene families [Charbonneau et al., 1986]. The catalytic core also contains a PDE-specific sequence motif of HD(X)₂H(X)₄N and two consensus Zn²⁺-binding domains [Beavo, 1995].

Due to the large number of PDE enzymes, a system of nomenclature was developed for describing them [Beavo et al., 1994]. This can be demonstrated by using HSPDE4A4 as an example where 'HS' indicates the species of origin in this case *Homo sapiens*, PDE4 refers to the gene family, 'A' refers to the gene and '4' refers to the splice variant. A letter after the splice variant number refers to the GenBank report for a specific splice variant that has been cloned separately by two or more groups.

PDEs tightly control the levels of cAMP and cGMP during hormonal stimulation. The targeting of these enzymes to different cellular locations serves to channel cAMP or cGMP to the appropriate intracellular detector and can also keep the cAMP or cGMP

signal confined to a particular sub-compartment of the cell [Houslay and Milligan, 1997]. Therefore, PDEs have an important role in dictating the cellular response to hormone or neurotransmitter stimulation. Each of the 11 PDE families are discussed in more depth below with Table 1.2 summarising the general characteristics of each family.

1.2.1 PDE1 enzyme family

The existence of a calcium stimulated PDE was first identified in rat brain [Kakiuchi, 1970]. The PDE1 family of enzymes are encoded by three different genes: PDE1A, which encodes two splice variants (PDE1A1 and PDE1A2); PDE1B encodes one splice variant (PDE1B1) and PDE1C encodes five splice variants (PDE1C1, PDE1C2, PDE1C3, PDE1C4 and PDE1C5) [Kakkar et al., 1999; Sonnenburg et al., 1998]. The multiple splice variants of this family result from alternative 5' and 3' mRNA splicing, generating enzymes with unique N- and C-termini. PDE1 enzymes are able to hydrolyse both cAMP and cGMP, although the PDE1A and PDE1B1 enzymes demonstrate a higher affinity for cGMP than cAMP, whereas the PDE1C enzymes hydrolyse both these cyclic nucleotides equally well. PDE1 enzymes are activated by the binding of Ca^{2+} /Calmodulin (Ca^{2+} /CaM) to paired domains located within their N-terminal regions. Their affinity for CaM differs for each of the PDE1 isoforms [reviewed in Kakkar et al, 1999].

Phosphorylation of certain PDE1 splice variants by either PKA or Cam kinase II reduces their affinity for CaM and results in a reduction of PDE1 enzyme activity [Hashimoto et al., 1989; Sharma and Wang, 1985]. The PDE1 enzyme family demonstrates a broad tissue distribution with the highest expression found in the testis, heart and neural tissues. These enzymes are postulated to have specific functional roles in neuronal functions as their expression is selective to particular brain areas including the cortex, regions of the hippocampus and the dentate gyrus [Juilfs et al., 1997; Yan et al., 1996].

1.2.2 PDE2 enzyme family

The PDE2 splice variants are encoded by a single gene called PDE2A. This gene encodes the three splice variants of PDE2A1, PDE2A2 and PDE2A3, which are found distributed between the soluble and particulate fraction of cells [reviewed in Beavo, 1995]. PDE2 enzymes localised to the particulate fraction of cells contain hydrophobic N-terminals, which may mediate membrane association. These enzymes can hydrolyse both cAMP (K_m 15-30 μ M) and cGMP (K_m 30-50 μ M), with affinity for nucleotide hydrolysis

increased by the binding of cGMP to allosteric non-catalytic cGMP sites located within the N-terminal portion of PDE2s [Manganiello et al., 1990].

PDE2 expression is high within the adrenal cortex, olfactory neurons and a subset of goblet cells. These enzymes have been implicated as having important functional roles in catecholamine secretion [MacFarland et al., 1997], regulation of calcium channels [Hartzell and Fischmeister, 1986] and olfactory signalling [Juilfs et al., 1997]. However, little is known about the functional role of this enzyme family.

1.2.3 PDE3 enzyme family

Both cAMP and cGMP can act as substrates for the PDE3 enzymes, therefore, both these nucleotides compete for hydrolysis by these enzymes. Nevertheless, cGMP hydrolysis is so low that this group of enzymes are effectively cAMP-specific. PDE3 isoforms are encoded by the two genes of PDE3A and PDE3B [Meacci et al., 1992]. PDE3A is abundant in the cardiovascular system and airways [Harrison et al., 1986, MacPhee et al., 1986] and PDE3B is abundant in adipose tissue [Degerman et al., 1997]. These enzymes are found distributed between the soluble and particulate fractions of cells. Located within the N-terminal of PDE3s is a hydrophobic region of sequence that has been suggested to mediate membrane association [Shakur et al., 2000]. Both PDE3A and PDE3B can be phosphorylated and activated by PKA on sequence present within their N-termini [Manganiello et al., 1992]. In adipocytes, insulin promotes the phosphorylation and activation of PDE3B in a process involving insulin-receptor substrate-1 (IRS-1), phosphatidylinositol 3-kinase (PI3-K) and insulin-stimulated protein kinase (PDE3IK) [Rahn et al., 1996]. Activation of PDE3B lowers cAMP levels, which results in dephosphorylation and inactivation of hormone-sensitive lipase (HSL) coupled with a decrease in lipolysis in white fat (adipocytes) [Rahn et al., 1996]. PDE3 enzymes have also been implicated to have a role in processes such as cardiac function, platelet aggregation and regulation of blood pressure [reviewed in Beavo, 1995].

1.2.4 PDE4 enzyme family

The PDE4 enzyme family are encoded by the four genes of PDE4A, PDE4B, PDE4C and PDE4D and because the products of these genes, their localisation and regulation are reviewed in a later section (Section 1.4), they will be omitted from discussion in this overview section.

1.2.5 PDE5 enzyme family

PDE5 cDNA was first isolated from bovine lung [McAllister-Lucas et al., 1993]. The PDE5 family of enzymes are encoded by a single gene called PDE5A, which encodes for the two splice variants of PDE5A1 and PDE5A2 that are specific for the hydrolysis of cGMP [Loughney et al., 1998; Kotera, Fujishige et al., 1999; Stacey, Rulten et al., 1998]. Located within the N-terminal portion of PDE5 are two high affinity, non-catalytic cGMP-binding sites (GAF domains) [Turko et al., 1996]. Once cGMP occupies both of these sites, PDE5 can be phosphorylated by either PKA or PKG. Although no clear functional consequence for this has been identified [Thomas et al., 1992], it has been suggested that phosphorylation by these kinases may serve to up-regulate PDE5 activity.

PDE5 is expressed as a cytosolic species in platelets, spleen, lung and vascular smooth muscle cells (VSCM) [Loughney et al., 1998; Stacey et al., 1998]. Zaprinst and sildenafil are potent inhibitors of PDE5 enzymes, with sildenafil (Viagra) marketed for the treatment of male erectile dysfunction [Corbin and Francis, 1999; Gopal et al., 2001].

1.2.6 PDE6 enzyme family

PDE6 has been found localised to the rod and cone cells of the retina and has a major role in the process of visual signal transduction. PDE6 enzymes specifically hydrolyse cGMP and contain two allosteric cGMP binding sites (GAF domains) that are located within their N-terminal regions. These enzymes exist either as heterotetramers composed of variations in catalytic units, either of α and β if in rod cells or as homotetramers consisting of two α ' if in cone cells. Each catalytic dimer is complexed with two inhibitory γ -subunits when cGMP is bound [Artemyev et al., 1998; Mou and Cote, 2001]. Soluble PDE6 contains an additional δ -subunit responsible for conferring solubility on the enzymes by masking their membrane binding motifs [Florio et al., 1996]. Following illumination, a photon activates rhodopsin, which promotes the GDP/GTP exchange of transducin. The GTP-bound α -subunit of transducin interacts with and releases the inhibitory γ -subunits of PDE6, resulting in an increase in PDE6 activity. cGMP is hydrolysed, which causes the dissociation of cGMP from the cGMP-gated channels followed by their closure.

1.2.7 PDE7 enzyme family

PDE7 was first discovered by a genetic screening procedure, which was developed in yeast to identify high affinity cAMP PDE cDNA clones. The PDE7 enzyme family demonstrates a high specificity for cAMP (K_m 0.2-1 μ M) and are resistant to inhibition by a number of common PDE inhibitors. PDE7s are encoded by two genes: PDE7A [Bloom and Beavo, 1996; Han et al., 1997] and PDE7B [Gardner et al., 2000]. PDE7A encodes for three splice variants (PDE7A1, PDE7A2 and PDE7A3), which each possess unique N-terminal regions. The N-terminal region of PDE7A1 and PDE7A2 impose differential intracellular targeting on these enzymes as PDE7A1 is found associated with both the soluble and particulate fractions of cardiac and skeletal muscle whereas PDE7A2, which possesses a hydrophobic N-terminal region, promotes particulate association in these cells [Han et al., 1997].

Interest developed in PDE7A1 when it was found induced with the onset of T-cell activation. It has been suggested to play a crucial role in promoting T cell activation and proliferation [Li et al., 1997]. Recently PDE7A3 was also suggested to be actively involved in this process [Glavas et al., 2001].

PDE7B transcripts have been identified in the putamen, caudate nucleus, heart and skeletal muscle, but its functional role is yet unclear [Gardner et al., 2000].

1.2.8 PDE8 enzyme family

The PDE8 family of enzymes are encoded by the two genes, PDE8A [Fisher et al., 1998; Soderling et al., 1998] and PDE8B [Hayashi et al., 1998]. The PDE8 enzymes are specific for the hydrolysis of cAMP (K_m 70nM) and are resistant to inhibition by the non-selective (general) PDE inhibitor, IBMX. Located within the N-terminal regions of PDE8 is a PAS domain (for Per, ARNT and Sim proteins, where this domain was originally identified), which in other proteins mediates homomeric and heteromeric protein-protein interactions [reviewed in Soderling and Beavo, 2000]. The function of the PAS domain in PDE8 is not yet known. PDE8A expression is most abundant in the testis, ovary, small intestine and colon [Fisher et al., 1998], whereas PDE8B is most highly expressed in the thyroid gland [Hayashi et al., 1998]. Again a functional role for PDE8 enzymes has yet to be established although, recently, the PDE8A1 splice variant was shown to be induced in response to T cell activation [Glavas et al., 2001].

1.2.9 PDE9 enzyme family

PDE9 was first identified by bioinformatic screening of an expressed sequence tag (EST) database for entities having a PDE motif. The PDE9 family is composed of four splice variants encoded by the PDE9A gene generated as a result of alternative 5' mRNA splicing [Fisher et al., 1997; Soderling et al., 1998]. cGMP is hydrolysed with high affinity by PDE9s (K_m 70 μ M). They, like PDE8 are also insensitive to selective inhibitors such as sildenafil (PDE5), rolipram (PDE4) as well as the non-selective PDE inhibitor IBMX. PDE9 mRNA demonstrates a wide tissue distribution. As yet no functional role for PDE9 is known [Guipponi et al., 1998] although it has been postulated that PDE9, with its high affinity for cGMP and broad tissue distribution, may serve to maintain the basal levels of cAMP.

1.2.10 PDE 10 enzyme family

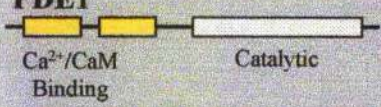
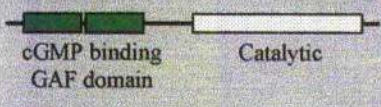
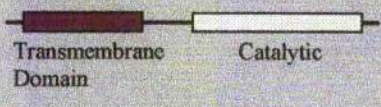
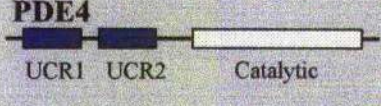
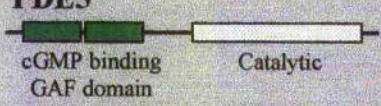
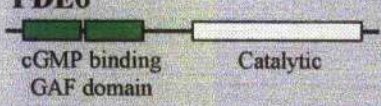
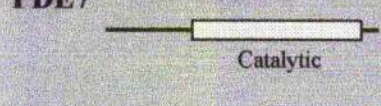
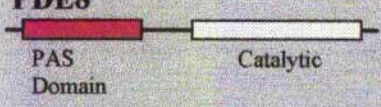
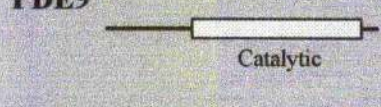
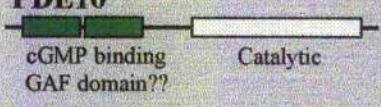
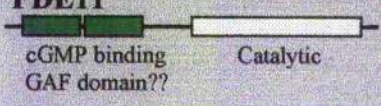
PDE10 was identified using bioinformatics to search an EST database for entities having a PDE motif. To date, the PDE10 family contains two splice variants that are encoded by the PDE10A gene (PDE10A1 and PDE10A2) and are capable of hydrolysing both cAMP (K_m 0.26 μ M) and cGMP (K_m 7.2 μ M) [Fujishige et al., 1999; Loughney et al. 1999; Soderling et al., 1999]. These enzymes are inhibited by the non-selective PDE inhibitor of IBMX. Located within the N-terminal of PDE10 are two domains that resemble the cGMP binding domains of PDE2, PDE5 and PDE6. However, as yet, any regulatory role they impose on PDE10 remains to be resolved [reviewed in Soderling and Beavo, 2000]. That cAMP can inhibit cGMP hydrolysis PDE10 led to their classification as the cAMP-inhibited cGMP PDEs. PDE10 mRNA has been identified in a number of tissues with abundance detected in the brain and testis [Fujishige et al., 1999].

1.2.11 PDE11 enzyme family

The PDE11 family was also discovered by bioinformatic screening of an Incyte database for entities containing a PDE motif. Three PDE11 splice variants are postulated to arise from the PDE11A gene, however, PDE11A1 is the only splice variant to have been characterised to date. PDE11A1 can hydrolyse both cAMP (K_m 1.04 μ M) and cGMP (K_m 0.52 μ M) and can be potently inhibited by dipyridamole and IBMX [Fawcett et al., 2000]. Contained within the N-terminal region of PDE11 is a domain that is homologous to the cGMP-binding domain of PDE2, PDE5, PDE6 and PDE10, as yet no regulatory role is

known for this domain [Fawcett et al., 2000]. PDE11A transcripts have been detected in skeletal muscle, prostate, kidney, liver, testis, pituitary and salivary glands, but the functional role of this enzyme remains to be elucidated [Yuasa et al., 2000].

Table 1.2 Phosphodiesterase superfamily

PDE Family	Genes	Substrate Specificity	Inhibitors	Examples of Regulation
PDE1 	PDE1A PDE1B PDE1C	cAMP and cGMP	Nicardipine, Methoxymethyl-IBMX Vinpocetine, KS-505a	Stimulated by Ca ²⁺ / calmodulin. Phosphorylated by PKA/PKG
PDE2 	PDE2A	cAMP and cGMP	EHNA	Stimulated by cGMP
PDE3 	PDE3A PDE3B	cAMP and cGMP	Cilostimide, Milrinone, Enoximone,	cGMP can inhibit cAMP hydrolysis. Phosphorylated and activated by PKA and by insulin-dependent kinases.
PDE4 	PDE4A PDE4B PDE4C PDE4D	cAMP Specific	Rolipram, Denbufylline	Phosphorylated by PKA and by ERK2. Long isoforms activated by phosphatidic acid.
PDE5 	PDE5A PDE5B	cGMP Specific	Zaprinast Sildenafil Dipyridamole	cGMP binding results in phosphorylation by PKA/PKG
PDE6 	PDE6A PDE6B PDE6C	cGMP Specific	Zaprinast, Dipyridamole	Stimulated by transducin, when activated by photons. Inhibited by γ subunit.
PDE7 	PDE7A PDE7B	cAMP Specific	None reported	None reported
PDE8 	PDE8A PDE8B	cAMP Specific	Dipyridamole (K _i = 4.5 μ M)	None reported
PDE9 	PDE9A	cGMP Specific	SCH 518666 Zaprinast	None reported
PDE10 	PDE10A	cAMP and cGMP	None reported	None reported
PDE11 	PDE11A	cAMP and cGMP	Zaprinast, Dipyridamole	None reported

1.3 Compartmentalisation of cAMP signalling

It was first realised that cAMP signalling could be confined to a particular subcellular compartment from studies reporting that the activation of two receptors which both stimulated adenylyl cyclase could generate quite different cellular responses. The earlier examples of compartmentalised cAMP signalling was demonstrated by Keely [Keely, 1977] where the stimulation of rat heart with either epinephrine (β_2 adrenoreceptor agonist) or prostaglandin E1 (PGE1) led to an increase in cAMP levels and activation of PKA. However, only epinephrine was found to phosphorylate and activate glycogen phosphorylase. The most conclusive evidence was generated by studies performed by Hayes et al [Hayes et al., 1980], whereby stimulation of cultured rat myocytes with isoproterenol or PGE1 led both to increases in cAMP and subsequent activation of PKA. However, only isoproterenol stimulation led to contractile activity and the phosphorylation of a number of proteins whereas PGE1 stimulation resulted in no cellular response. These studies demonstrated that isoproterenol and epinephrine-mediated cAMP signalling occur in different compartments to the cAMP response generated by PGE1.

Several studies have illustrated the importance of PDEs in generating a compartmentalised response. For example, exposure of one half of a frog ventricular myocyte to isoproterenol, led to increases in cAMP and activation of PKA. This resulted in the phosphorylation and stimulation of 'local' L-type Ca^{2+} channels (within the vicinity of agonist stimulation), but had little effect on Ca^{2+} channels located in the other half of the cell [Jurevicius and Fischmeister, 1996]. In contrast, treatment of one half of the cell with the non-selective PDE inhibitor IBMX, followed by isoproterenol stimulation resulted not only in the stimulation of Ca^{2+} channels locally, but also of those channels distant from the site of agonist/inhibitor administration [Jurevicius and Fischmeister, 1996]. This study demonstrated that PDEs are important in constraining the diffusion of cAMP and keep it contained within a particular subcellular location.

Studies performed by Dousa [Dousa, 1999] have demonstrated that PDE3 and PDE4 enzymes can control distinct pools of cAMP in the mesangial cells of kidney glomeruli. Inhibition of PDE3 enzymes in these cells by treatment with the PDE3-selective inhibitor cilostamide caused increases in cAMP, which inhibited mitotic DNA synthesis [Matousovic et al., 1995]. In contrast, the inhibition of PDE4 enzyme activity with the PDE4-selective inhibitor rolipram caused no effect on mitotic DNA synthesis. However, the rolipram-mediated increases in cAMP were found to inhibit the production

of reactive oxygen metabolite (ROM), which has a pathogenic role in glomerulonephritis [Chini et al., 1997]. In contrast to this, PDE3 inhibition had no effect on ROM production.

Therefore, the cellular response resulting from ligands that increase cAMP levels depends on a number of factors, including the isoforms of adenylyl cyclase, PKA and PDE that are expressed by the cell and also on their localisation. For example, adenylyl cyclase can be localised to discrete regions of the plasma membrane, certain isoforms of PKA are anchored to specific cellular domains by interacting with AKAPs and PDE isoforms can associate with particular cellular compartments by interacting with different binding partners [Houslay and Milligan, 1997]. PDEs are important in maintaining steep cAMP gradients and preventing levels of this nucleotide from becoming uniform. They also channel cAMP so that only particular PKA isoforms become activated [Houslay and Milligan, 1997].

1.4 PDE4 Phosphodiesterases

The PDE4 family of enzymes are encoded by four genes: PDE4A (chromosome 19p13.1) [Davis et al., 1989; Sullivan et al., 1998], PDE4B (chromosome 1) [Szpirer et al., 1995], PDE4C (chromosome 19p13.2) [Sullivan et al., 1999] and PDE4D (chromosome 5) [Szpirer et al., 1995]. Each of these genes encodes for multiple splice variants produced as a result of alternative 5' mRNA splicing [reviewed in Houslay, 2001 and Muller et al., 1996]]. PDE4A1 (RD1) was the first PDE to be cloned and was identified by screening a rat brain cDNA library using the product of the *Drosophila melanogaster dunce* gene as a probe [Davis et al., 1989]. All PDE4 isoenzymes specifically hydrolyse cAMP and are resistant to regulation by either Ca^{2+}/CaM or cGMP. The compound rolipram acts as a competitive inhibitor of PDE4s and interacts with their catalytic site.

The catalytic site of PDE4 is ~320-350 amino acids in size and shows common similarity to the other PDE enzyme classes [Charbonneau et al., 1986]. Located N-terminal to the catalytic domain are two regions of conserved sequence referred to as upstream conserved region 1 (UCR1) and 2 (UCR2), which are 60 amino acids and 80 amino acids in size, respectively (*figure 1.2*) [reviewed in Houslay, 2001]. There are two splice junctions that generate active PDE4s and these determine whether the product enzyme will contain one or both of these UCRs (*figure 1.2 and figure 1.3*). Those enzymes containing both UCR1 and UCR2 are referred to as long isoforms, whereas those that lack a UCR1, but contain a UCR2, are referred to as short isoforms (*figure 1.2 and figure 1.3*). Additionally, there are enzymes such as PDE4A1 (RD1) and PDE4D2 that lack a UCR1 and are missing the N-terminal portion of UCR2; these enzymes are referred

to as super-short isoforms (*figure 1.2 and figure 1.3*). The two regions of hypervariable sequence that connect UCR1 to UCR2 and UCR2 to the catalytic domain are referred to as linker region 1 and 2 (LR1 and LR2), respectively [reviewed in Houslay, 2001]. LR1 and LR2 demonstrate no sequence similarity between different sub-families.

That the UCR1 and UCR2 domains have been evolutionary conserved suggests they are important to the functioning of these enzymes. ‘Yeast two hybrid’ studies and ‘pull down assays’ using various portions of PDE4D3 cDNA have revealed that the C-terminal portion of UCR1 can interact with the N-terminal portion of UCR2 [Beard et al., 2000]. This interaction can be blocked by mutating the positively charged residues of Arg-98 and Arg-101 in the UCR1 region to alanine, or by mutating the negatively charged residues of Glu-146, Glu-147 and Asp-149 in UCR2 to alanine, indicating these domains associate by electrostatic interactions [Beard et al., 2000]. Phosphorylation of Ser⁵⁴ in the UCR1 domain was found to ablate the interaction between UCR1 and UCR2 and alters the conformation of the catalytic unit. However this has no effect on enzyme activity [Beard et al., 2000]. The UCR1 and UCR2 domains are postulated to form a module that regulates the PDE4 catalytic domain.

As well as possessing these highly conserved domains certain PDE4 isoforms also have a unique N-terminal sequence, which confers distinct targeting and regulatory properties on the enzyme [Houslay, 1996; Michie et al., 1995]. The first evidence that a PDE could be targeted by virtue of its unique N-terminal sequence came from studies performed on the super-short PDE4A1 enzyme (RD1) [Shakur et al., 1993]. PDE4A1 associates with the plasma membrane and golgi apparatus. However, the removal of the 25 amino acid unique N-terminal, to generate Met²⁶-RD1, produced an enzyme that was entirely cytosolic [Scotland and Houslay, 1995; Shakur et al., 1993]. Additionally, Met²⁶-RD1 was also found to have a Vmax twice that of PDE4A1. This suggested that the targeting and regulation of the activity of PDEs could be imposed, in part, by their unique N-terminal regions. To further test this theory, the 25 amino acid N-terminal of PDE4A1 was fused to the cytosolic enzyme of chloramphenicol acetyltransferase (CAT), which caused this normally soluble enzyme to become completely membrane-associated [Scotland and Houslay, 1995]. This provided the definitive evidence that the N-terminal region of PDEs direct their intracellular targeting. This has since been demonstrated for many other PDEs [Houslay et al., 1995].

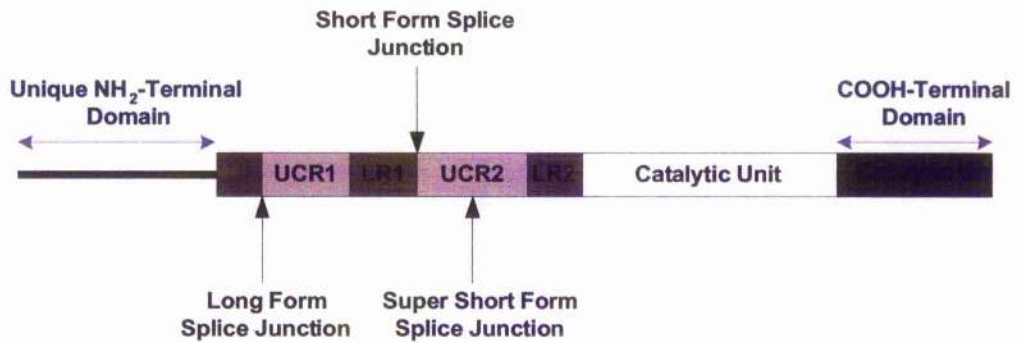


Figure 1.2 Schematic representation of PDE4 enzymes. This figure shows a schematic representation of a typical long PDE4 enzyme. The unique N-terminal is shown as a thick black line. The upstream conserved regions (UCR1 and UCR2) are coloured in light grey, the linker regions (LR1 and LR2) are shown in dark grey, the catalytic domain is shown in white and the C-terminal domain is shown in black. The positions of the splice junctions that are responsible for producing long, short and supershort isoforms are marked by arrows.

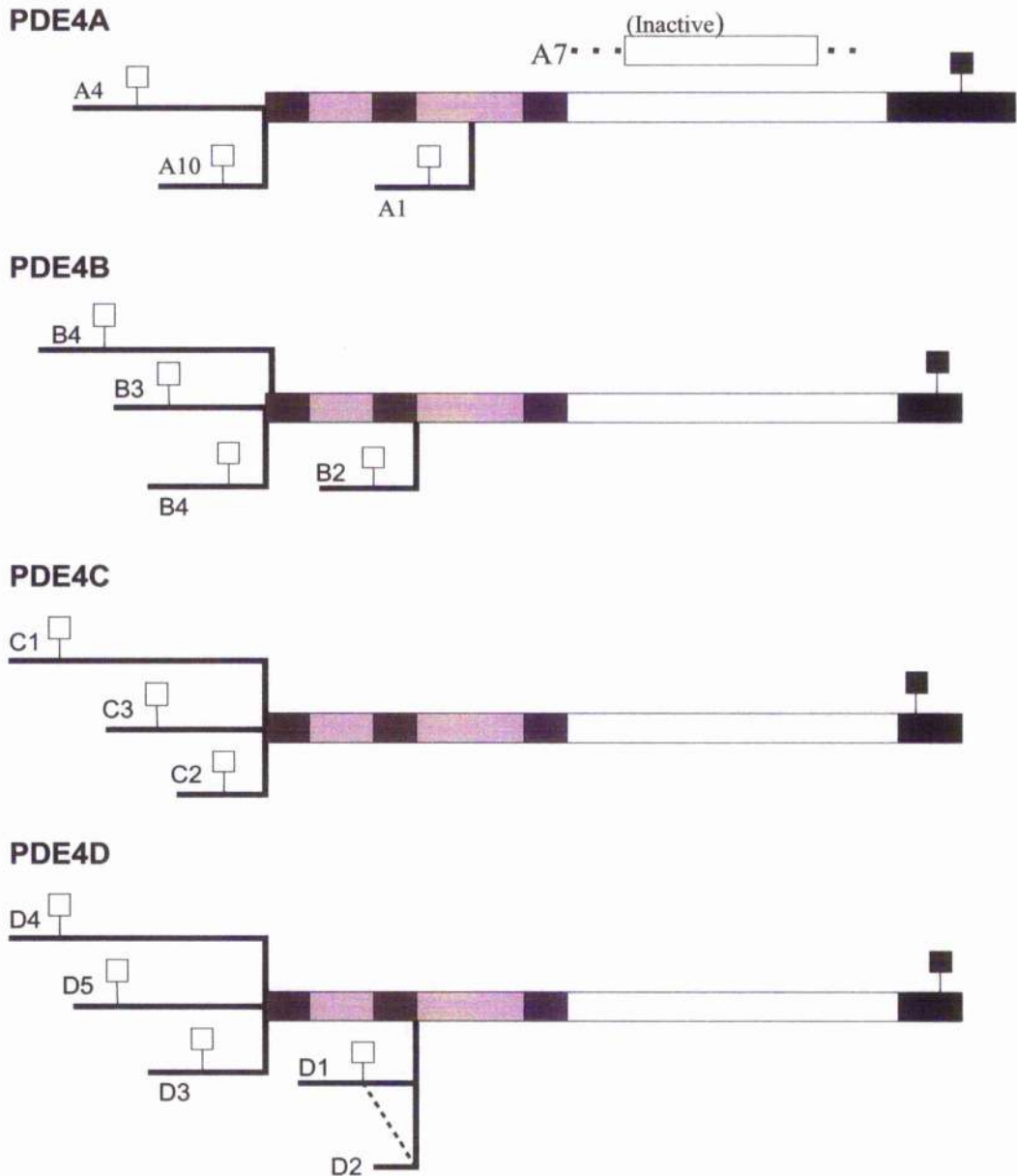


Figure 1.3 PDE4 mRNA transcripts generated from the human PDE4A, PDE4B, PDE4C and PDE4D genes. This figure shows a diagrammatic illustration of the mRNA transcripts that are generated from the four PDE4 gene groups. The initiator and termination codons are marked with white-filled and black-filled squares, respectively. The upstream conserved regions (UCR1 and UCR2) are shown in light grey, the linker regions are shown in dark grey, the catalytic core is in white and the C-terminal domain is shown in black. The dashed line connecting transcripts D1 and D2 indicates the region of sequence in PDE4D1 that is spliced out in PDE4D2.

1.4.1 PDE4A subfamily

There are five different splice variants encoded by both the human and rat PDE4A gene including PDE4A4B (PDE46) [Sullivan et al., 1998] (rodent homologue PDE4A5 [McPhee et al., 1995]), PDE4A10 (so called in human and rat) [Rena et al., 2001] and PDE4A11 (TM3; unpublished), which are all long isoforms that each contain a unique N-terminal sequence that is generated as a result of alternative 5'mRNA splicing. There is also the supershort isoform called PDE4A1, which lacks a UCR1 and contains a truncated UCR2 [Davis et al., 1989; Sullivan et al., 1998] and the highly unusual N- and C-terminally truncated PDE4A7 (2EL) [Horton et al., 1995]. All the transcripts generated from the human PDE4A gene are shown schematically in *figure 1.3*. The rat RNPDE4A8 (RPDE39) has no human or mouse homologue [Bolger et al., 1996].

PDE4A7 was isolated from a human T cell library and is devoid of catalytic activity [Horton et al., 1995]. It is the only PDE4 found to possess a unique N- and C-terminal domain due to alternative 5' and 3' mRNA splicing. The 34 base pair insert within the highly conserved catalytic domain is responsible for making this enzyme inactive and causes the frameshift that results in the premature termination of the transcript [Horton et al., 1995]. The cellular function of PDE4A7 remains to be elucidated.

1.4.1.1 PDE4A localisation and targeting

The first evidence that PDEs could be targeted to specific subcellular compartments by virtue of sequence located within their unique N-terminals came from studies performed on PDE4A1 [Scotland and Houslay, 1995; Shakur et al., 1993]. PDE4A1 localises specifically to the membrane and golgi apparatus and is therefore associated exclusively with the particulate fraction of cells [Pooley et al., 1997]. This is in contrast to the homologues PDE4A4B and PDE4A5, which are distributed between both the soluble and particulate fraction of cells [Huston et al. 1996; O'Connell et al., 1996]. The particulate localisation of these enzymes is governed in part by their proline- and arginine-rich N-terminal domains, which mediate their interaction with the SH3 domains of other proteins such as the SRC-related tyrosyl kinases LYN and FYN and the cytoskeletal protein fodrin [Huston et al., 1996; O'Connell et al., 1996]. Deletion of the N-terminal of PDE4A4B caused a notable loss of this species from the membrane ruffles. However, did not completely ablate particulate association [Huston et al., 1996]. An additional proline- and arginine-rich domain has been identified in the LR2 region of PDE4A4B, which can also bind the SH3 domains of LYN and FYN, demonstrating that regions other than the unique

N-terminal are responsible for directing PDEs to their cellular location [McPhee et al., 1999]. This point was further reinforced with studies performed on the rat homologue PDE4A5, whereby the N-terminal of UCR2 was found to be partly responsible for mediating the membrane association of this enzyme [Beard et al., 2002]. Interestingly, the particulate PDE4A4B isoform demonstrates a higher affinity for rolipram than its soluble counterpart suggesting that the interaction of the PDE4A4B N-terminal with SH3 domain containing proteins induces a conformational change in the enzyme. Therefore, the N-terminal not only mediates targeting of PDEs, but can also control the conformation of the catalytic unit, as indicated by changes in activity and in sensitivity to the selective inhibitor rolipram.

In cells undergoing apoptosis, the unique N-terminal region of PDE4A5 is cleaved by caspase 3, thus preventing its interaction with the SH3 domain of LYN. This results in a re-distribution of the PDE4A5 enzyme [Huston et al., 2000]. PDE4A5 has been reported to have a role in promoting cell survival, as over-expression of PDE4A5 in Rat-1 cells protected them against staurosporine-induced apoptosis [Huston et al., 2000].

The PDE4A10 and PDE4A4B long isoforms differ in sequence only at their unique N-termini yet are targeted differently and possess distinct kinetic properties. PDE4A10 is predominantly localised to the perinuclear region of COS-1 cells, whereas PDE4A4B predominates at the cell margins and cortical cytoskeleton [Huston et al., 1996; O'Connell et al., 1996; Rena et al., 2001]. Both these enzymes can associate with the SH3 domains of LYN as they both share the proline- and arginine-rich LR2 region. However, PDE4A4B has a much higher affinity for LYN because it contains the additional proline- and arginine-rich sequence within its unique N-terminal (as already discussed). The differences in the unique N-terminals of PDE4A4B and PDE4A10 also causes their catalytic sites to adopt distinct conformations as detected by the greater sensitivity of PDE4A10 to rolipram [Rena et al., 2001].

1.4.1.2 Regulation of PDE4As

Challenge of U937 cells with lipopolysaccharide (LPS) or interferon- γ (IFN- γ) leads to activation of PDE4A4B [MacKenzie and Houslay, 2000] and the stimulation of 3T3-F442A pre-adipocytes with growth hormone causes the phosphorylation and activation of PDE4A5 (rat homologue of PDE4A4) [MacKenzie et al., 1998]. The activation of both these enzymes can be prevented by treatment of these cells with the phosphatidylinositol-3 kinase (PI3-kinase) inhibitor wortmannin or the immunosuppressant rapamycin. Stimulation of PDE4A4B and PDE4A5 activity is mediated through a pathway involving

the PI3-kinase mediated activation of p70S6 kinase [MacKenzie et al., 1998; MacKenzie and Houslay, 2000]. The activation of PDE4A5 in 3T3-F442A cells serves to block their differentiation into adipocytes.

Phosphatidic acid (PA) and phosphatidylserine (PS) can also activate PDE4A long isoforms by interacting with a region in the UCR1 domain [Nemoz et al., 1997]. These phospholipids have no effect on the activity of the PDE4A short isoforms because they lack the UCR1 domain. The lack of selectivity between different acidic phospholipids probably indicates a charge-charge interaction. This is in marked contrast to the selective interaction of PDE4A1 with PA, which occurs through binding to the TAPAS1 domain.

PDE4As are not susceptible to the inhibitory phosphorylation by ERK2 because they cannot be recognised as substrates. This is because the first proline of the P-x-S/T-P ERK2 consensus motif is replaced by an arginine [Alvarez et al., 1991].

1.4.2 PDE4B subfamily

There are currently four isoforms encoded by the PDE4B gene, including the three long isoforms of PDE4B1, PDE4B3, PDE4B4 and the short PDE4B2 isoform [Huston et al., 1997]. All of the transcripts generated from the human PDE4B gene are shown schematically in *figure 1.3*. All these enzymes have been found distributed between the particulate and soluble fractions of the cell. The particulate isoforms must interact with different binding partners as they are released differently with the use of different detergents. cAMP and phospholipids can impose different regulatory effects on the multiple PDE4B splice variants. For example, phosphorylation of PDE4B1 on Ser⁶⁵⁹ by ERK2 imposes an inhibitory effect, whereas phosphorylation of PDE4B2 on its cognate serine residue (Ser⁴⁸⁷) serves to activate this isoform [Baillie et al., 2000]. Also, phosphatidic acid (PA) activates the long PDE4B1 isoform yet has no effect on the activity of the PDE4B2 short isoform [Nemoz et al., 1997], indicating again a need for UCR1 in mediating activation by PA.

Interestingly, PDE4B2 accounts for 95-100% of total cellular PDE4 mRNA in neutrophils and monocytes stimulated with LPS [Wang et al., 1999; Jin and Conti, 2002]. This suggests that PDE4Bs may have an important role in mediating the immune response and in the future may serve as targets for anti-inflammatory drugs [Jin and Conti, 2002].

1.4.3 PDE4C subfamily

The human PDE4C gene is located on chromosome 19p13.1 and encodes for the three long forms: PDE4C1, PDE4C2 and PDE4C3 [Owens et al., 1997; Sullivan et al., 1999]. The transcripts generated from the human PDE4C gene are shown schematically in *figure 1.3*. As yet no short PDE4C isoforms have been identified and their occurrence has been postulated to be very unlikely due to the extremely short introns at the position of predicted splice junctions [Sullivan et al., 1999]. That PDE4C demonstrates a very specific tissue distribution, suggests that they have a particular functional role. Long PDE4C isoforms like all the other long form PDE4s are susceptible to the inhibitory phosphorylation of ERK2 on Ser⁵³⁵ within the catalytic unit [Baillie et al., 2000]

1.4.4 PDE4D subfamily

The PDE4D gene encodes for the short and super-short isoforms of PDE4D1 and PDE4D2, respectively and the three long isoforms of PDE4D3, PDE4D4 and PDE4D5. These differ by virtue of their extreme N-terminals, generated as a result of alternative 5'mRNA splicing [Bolger et al., 1997]. All the transcripts generated from the human PDE4D gene are shown in *figure 1.3*. These isoforms differ in their tissue distributions, intracellular distribution and regulation by phosphorylation.

1.4.4.1 PDE4D localisation and targeting

Generally, PDE4D1 and PDE4D2 exist as soluble species [Erdogan and Houslay, 1997], whereas the long PDE4D isoforms are distributed between the particulate and soluble fractions of cells [Jin et al., 1998]. The particulate association of these enzymes is mediated by their ability to interact with other proteins via their N-terminal domains, as discussed below.

PDE4D3 has been found localised to the centrosomal region in Sertoli cells (testis), where it has been found in a complex with PKA and the centrosomal PKA anchor protein AKAP450 [Tasken et al., 2001]. In heart tissues, PDE4D3 is localised to the perinuclear region by virtue of 15 residues of sequence located within its unique N-terminal, which mediates the interaction with the muscle selective A-Kinase Anchoring Protein (mA_KAP) [Dodge et al., 2001]. Recently, it has been reported that PDE4D3 can be targeted to the golgi and centrosomes in certain cells by associating with the protein myomegalin [Verde et al., 2001]. This targeting of PDE4D3 to specific sub-compartments in the cell may serve

to bring PDE4D3 to the sites of PKA action and allow the control of local cAMP levels and levels of PKA activity.

PDE4D4 interacts with the SRC homology 3 (SH3) domains of the proteins LYN, FYN, SRC and the cytoskeletal protein fodrin, an interaction that is mediated by the unique proline- and arginine-rich 136 amino acid N-terminal region [Beard et al., 1999]. Unlike PDE4A4B, PDE4D4 demonstrates no preference for any particular SH3 domain-containing proteins [Beard et al., 1999].

The 88 amino acid N-terminal of PDE4D5 allows it to interact with the WD-repeat protein RACK1 (receptor for activated C-kinase) [Yarwood et al., 1999]. Amino acids 12-29 of the PDE4D5 N-terminal are found to be absolutely necessary for the binding of RACK1 [Yarwood et al., 1999]. Additionally native RACK1 and PDE4D5 have been found to interact constitutively in numerous other cell types including HEK-293, SK-N-SH cells and 3T3-F442A fibroblasts. As yet the functional significance of this interaction remains to be elucidated.

1.4.4.2 Regulation of PDE4Ds

PDE enzymes can also be regulated by the post-translational modification of phosphorylation. Contained within the N-terminal of PDE4D3 are two PKA phosphorylation sites positioned at Ser¹³ and Ser⁵⁴ [Hoffman et al., 1998; Sette and Conti, 1996]. Phosphorylation of Ser⁵⁴ is responsible for activating PDE4D3 activity, suggesting that other long forms could be substrates for PKA as this Ser⁵⁴ site is located within the highly conserved UCR1 domain. Once phosphorylated, PDE4D3 demonstrates a heightened sensitivity to inhibition by rolipram, indicating that it has undergone a conformational change.

PDE4D3 also harbours an ERK2 phosphorylation site within its C-terminal catalytic region, positioned at Ser⁵⁷⁹. ERK2 phosphorylation inhibits PDE4D3 activity [Hoffman et al., 1999], an effect that has also been reported for all other long PDE4 isoforms with the exception of the PDE4As [Baillie et al., 2000]. PDE4As are not recognised by ERK2 because the first proline of the P-x-S/T-P ERK2 consensus motif is replaced by an arginine [Alvarez et al., 1991]. Encompassing this ERK2 phosphorylation site in PDE4s are a KIM domain and FQF domain that seem to mediate the docking of ERK2. This was shown when mutation of these domains ablated the ability of ERK2 to bind to and phosphorylate PDE4D3 [MacKenzie et al., 2000]. The short isoform of PDE4D1 also possesses the ERK2 consensus motif but, in contrast to PDE4D3, PDE4D1 is activated by ERK2 phosphorylation [Baillie et al., 2000].

EGF stimulation of COS-1 cells over-expressing PDE4D3, induces inhibitory phosphorylation of this enzyme by ERK2, an effect that has also been demonstrated in cells where PDE4D3 is expressed natively [MacKenzie et al., 2000]. The resultant increase in cAMP causes activation of PKA, which then phosphorylates and re-activates PDE4D3. Therefore, PKA is able to reverse the ERK2 inhibitory effect [MacKenzie et al., 2000]. This provided evidence of cross-talk between ERK2 and cAMP signalling.

Both PDE4D3 and PDE4D5 are phosphorylated and activated by PKA in vascular smooth muscle cells (VSCM) in response to forskolin treatment [Liu and Maurice., 1999]. In addition, PDE4D3 was also found to be phosphorylated and activated by the PKC-mediated activation of the Raf-MEK-ERK cascade in these cells rather than inhibited, in response to Angiotensin II (AngII) [Liu and Maurice, 1999]. Interestingly, stimulation of these VSCMs with both forskolin and AngII appeared to result in the activation and translocation of a small fraction of particulate PDE4D3 into the cytosolic fraction [Liu and Maurice, 1999].

PA has been shown to interact directly with sequence present within the N-terminal region of PDE4D3, which overlaps into the UCR1 domain [Grange et al., 2000]. This interaction causes the same increase in activity in this enzyme that would result from phosphorylation by PKA. The PDE4D short forms are unaffected by PA, possibly because they lack the required UCR1 region [Grange et al., 2000].

PDE4D5 is activated in human aortic smooth muscle (HASM) cells in response to phorbol 12-myristate 13-acetate (PMA), which is surprising as ERK2 phosphorylation normally results in the inhibition of this enzyme. In this case however, ERK2 does inhibit PDE4D5 but it also promotes the generation of prostaglandin E2 (PGF2), which stimulates adenylyl cyclase to produce cAMP. This leads to the activation of PKA, which phosphorylates PDE4D5, ablates the inhibitory effect imposed by ERK2 phosphorylation and results in the activation of PDE4D5 [Baillie et al., 2001].

1.5 *Transcriptional regulation of PDE4s*

The expression patterns of PDE4s in cells can be regulated in response to chronic hormonal stimulation [reviewed in Conti and Jin, 1999]. For example, the induction of PDE4D1 and PDE4D2 has been noted in a number of cell types. This was first demonstrated in Sertoli cells where treatment with follicle stimulating hormone (FSH), caused an increase in the levels of PDE4D1 and PDE4D2 mRNA after 1 hour and reached maximum levels between 3 and 12 hours. This effect could be mirrored by treatment of these cells with cAMP analogs [Swinnen et al., 1991]. An increase in PDE4D1 and

PDE4D2 mRNA levels in response to cAMP analogs, have been reported in a number of other cell types including Mono-Mac-6 cells [Verghese et al., 1995], L6 myoblasts [Naro et al., 1999], FRTL-thyroid cells [Jin et al., 1998] and Jurkat cells [Erdogan and Houslay, 1997]. FSH and thyroid stimulating hormone (TSH) stimulation of Sertoli cells and FRTL-5 thyroid cells respectively, induce the expression of only PDE4D1 and PDE4D2 with no effect on the regulation of the other PDE4Ds. This led to the discovery that the expression of PDE4D1 and PDE4D2 were controlled by a distinct promoter from that of the other long form PDE4Ds [Vicini and Conti, 1997].

The levels of PDE4A and PDE4B mRNA transcripts are also found regulated in response to chronic activation of adenylyl cyclase. For example, PDE4A and PDE4B transcripts increase with the elevation of cAMP levels in Mono-Mac-6 cells [Verghese et al., 1995] and U937 cells [Torphy et al., 1992]. In one report elevated cAMP levels in Jurkat cells led to reduced levels of PDE4A mRNA [Erdogan and Houslay, 1997].

1.6 Importance of PDE4s

The importance of PDEs in mediating cAMP signalling was first demonstrated in very early studies whereby fruit flies containing mutations in the *Drosophila dunce* PDE gene demonstrated impairments in their learning behaviour and caused female sterility [Davis and Dauwalder, 1991]. PDE4D (mammalian homologue *Drosophila dunce*) is important for growth and fertility in mice. This was demonstrated by recent studies whereby mice containing targeted disruption of the PDE4D gene were of reduced body weight, viability and the female mice were notably less fertile [Jin et al., 1999].

cAMP has been found to inhibit the function of cells involved in generating an inflammatory response. That PDE4 activity plays a major role in mediating the cAMP levels in inflammatory cells such as neutrophils, eosinophils, mast cells and basophils, it was not surprising to find that PDE4 inhibitors can suppress the inflammatory response by elevating cAMP levels. Clinical trials are being performed on PDE4 inhibitors for the treatment of diseases such as asthma [Torphy, 1998] chronic obstructive pulmonary disease (COPD) [Torphy et al., 1999], atopic dermatitis [Hanifin et al., 1996] and multiple sclerosis [Dinter, 2000]. Unfortunately, nausea and emesis are side-effects still associated with general PDE4 inhibitors because these enzymes are also expressed highly in many other tissues including the brain. Development of PDE4 isoform specific inhibitors may help to overcome these pitfalls. For example, a PDE4 isoform receiving much interest is that of PDE4B2. This enzyme is the most predominant isoform expressed in neutrophils, monocytes and leukocytes, therefore, provides an ideal anti-inflammatory target [Wang et

al., 1999]. Because the expression of PDE4B2 is low in the brain, development of PDE4B2 specific inhibitors would provide a means of treating inflammatory diseases in which monocytes and neutrophils were the mediators, without the side-effect of emesis.

My interest in PDE4A7 developed following the discovery that this PDE4A isoform was devoid of any cAMP-specific catalytic activity. I decided to investigate its intracellular localisation using the methods of subcellular fractionation and Laser Scanning Confocal Microscopy (LSCM). This work uncovered the interesting finding that PDE4A7 was localised exclusively within the nucleus. Using a series of chimeras I then made attempts to gain insight into the basis of the intracellular targeting of this protein. In Chapter 4 I used the yeast two-hybrid screening method in an attempt to identify possible binding partners of PDE4A7, with the hope that this would give insight into its functional role. The methods of gene microarray and RT-PCR analysis were used in Chapter 5 to address whether the functional role of PDE4A7 within the nucleus was to control the expression levels of other genes involved in cAMP signalling. In addition, I also performed some characterisation studies on the novel PDE4A long isoform called PDE4A11 (TM3).

Chapter 2

Materials and Methods

In the following section, the names of companies from where reagents were purchased are given in the parentheses. Where no company name is mentioned, the reagent was purchased from either Sigma or Fisons and were of analytical grade.

2.1 Mammalian cell culture

2.1.1 Cell culture techniques

2.1.1.1 COS-1 and COS-7 cell lines

COS-1 and COS-7 cells (ATCC CRL-1650 and CRL-1651 respectively) are both African green monkey kidney fibroblast-like cell lines, which were derived from the CV-1 cell line by transformation by an origin-defective mutant of SV40 (Gluzman, 1981).

2.1.1.2 HEK-293 cell line

HEK-293 cells are a human embryonic kidney cell line (ATCC CRL-1573), which have an epithelial cell morphology (Harrison, Graham et al. 1977).

2.1.1.3 Maintenance of cell lines

COS-1, COS-7 and HEK-293 cells were all maintained in the cell culture medium of Dulbecco's Modified Eagle's Medium (DMEM) that had been supplemented with 2mM L-glutamine, 10% (v/v) foetal bovine calf serum (FBCS) and 100units/ml of penicillin/streptomycin at 37°C in a 5% CO₂ atmosphere. Cells were passaged upon reaching ~90% confluency, which involved rinsing the cells with pre-warmed phosphate buffered saline (PBS) followed by incubation with 2-4mls of 0.25% trypsin/0.03% EDTA solution until the cells detached. The detached cells were resuspended in 8mls of fresh culture medium, transferred to a sterile 50ml centrifuge tube and pelleted by centrifuging at 3000 rpm for 3mins in the MSE Mistral 1000 swinging bucket centrifuge. Medium was removed from the pelleted cells, which were then resuspended in 10mls of fresh culture medium. The

cells were then diluted 1:5 into new culture flasks containing pre-warmed fresh culture medium.

2.1.2 Transfection of COS-1 cells with plasmid DNA

Cells at ~70% confluency were passaged 24hrs before transfection and seeded onto new 100mm plates at ~ 50% confluency. 10 μ g of DNA was diluted in 250 μ l of Tris-EDTA (TE) buffer (1mM Ethylenediaminetetra-acetic acid (EDTA), 10mM Tris/HCl, pH 7.5) in a sterile tube, to which 200 μ l of DEAE dextran solution (10mg/ml in PBS) was added. This mixture was incubated for 15mins at room temperature to allow DNA-DEAE dextran complexes to which 5mls of transfection medium and 5 μ l of 100mM chloroquine were added. This mixture was added to a 100mm dish of monolayer cells and incubated at 37°C in an atmosphere of 5% CO₂ for 3-4 hrs. After incubation the cells were shocked with 10% DMSO (dissolved in sterile PBS) for 2mins and then rinsed twice with 10mls of PBS. After washing, 10mls of growth medium was added to each plate of cells, which were then incubated at 37°C for ~48-72hrs in an atmosphere of 5% CO₂.

2.1.3 Transfection of HEK-293 cells with plasmid DNA

Cells at ~70% confluency were passaged 24hrs prior to transfection and seeded onto 100mm dishes at ~40-50% confluency. 5 μ g of DNA was diluted in 50 μ l sterile HEPES-buffered saline (HBS) buffer (20mM HEPES, 150mM NaCl (pH 7.4)) in a sterile tube. In a separate sterile tube 30 μ l of DOTAP (Roche) was mixed with 70 μ l of HBS. This DOTAP solution was added the nucleic acid solution, mixed by pipetting and incubated at room temperature for 15mins. 14mls of growth medium (DMEM containing 10% (v/v) new born foetal calf serum (NCBS)) was added to the DOTAP/nucleic acid solution, mixed and added to cells, which were then incubated overnight at 37°C in an atmosphere of 5% CO₂. The next day this culture medium was removed from the cells and replaced with fresh growth medium (DMEM containing 10% (v/v) foetal calf serum). Cells were incubated for a further 48hrs at 37°C in an atmosphere of 5% CO₂.

2.2 Biochemical Techniques

During cell lysis procedures, cells were maintained on ice and buffers were also pre-chilled to minimise the effect of protein degradation.

2.2.1 General subcellular fractionation of cells

Approximately 48hrs after transfection cell plates were transferred from the 37°C incubator onto ice. After removing the growth medium, cells were rinsed once with ice-cold PBS (5mls/100mm dish) and drained before the addition of ice-cold complete KHEM buffer (50mM HEPES-KOH (pH 7.4), 50mM KCl, 10mM EGTA, 1.92mM MgCl₂ supplemented with 1mM dithiothreitol (DTT) and protease inhibitors) (2mls/100mm dish), which was incubated with the cells for 5mins at 4°C and then drained. The cells from 100mm dishes were scraped into a 1.5ml eppendorf and were disrupted by passing the cell lysate 30 times through a 26_{1/2} gauge needle attached to a disposable 1ml syringe.

Cell lysates were centrifuged at 2000rpm for 10mins at 4°C to produce the low speed pellet fraction (P1) that is enriched in nuclear and cytoskeletal components. The resultant supernatant was then centrifuged at 75000g for 30mins at 4°C (Beckman TL-100 ultracentrifuge), which produced a high speed supernatant fraction enriched in cytosolic proteins and a high speed pellet fraction (P2) enriched in plasma membranes, endoplasmic reticulum, lysosomes, endosomes and golgi vesicles. Both the P1 and P2 pellets were washed twice in 500µl of ice-cold complete KHEM and then resuspended in the same volume of complete KHEM as the S fraction. Each of the cell fractions were aliquoted, snap frozen and stored at -80°C until required.

2.2.2 Immunoprecipitation

Growth medium was removed and the cells were washed with 5mls ice-cold PBS, drained and then scraped into 500µl of ice-cold 3T3-lysis buffer (20mM N-2-Hydroxyethylpiperazine-N'-2-ethanesulfonic acid (HEPES), pH 7.4, 50mM NaCl, 50mM NaF, 10% glycerol, 1% triton X-100, 10mM Ethyleneglycol-bis(P-aminoethylether)-N,N,N',N'-Tetra-acetic acid (EGTA), 30mM sodium pyrophosphate and protease inhibitor cocktail was added). Cells were homogenised with 20 strokes of a 26_{1/2} gauge needle attached to a disposable 1ml syringe. Cell lysates were clarified by low speed centrifugation (3000rpm at 4°C for 10mins). 50µl of protein A beads were washed in 500µl of complete 3T3-lysis buffer and pelleted by centrifuging at 3000rpm for 2mins at 4°C in a refrigerated bench top centrifuge. These beads were used to pre-clear the supernatant (cell lysate) for 30mins at 4°C with end-over-end rotation. The protein A beads were recovered by centrifugation (3000rpm at 4°C for 3mins) the supernatant was transferred to a clean 1.5ml eppendorf. The antibody for detection of the target protein was added to the supernatant (cell lysate) at the optimal concentration (0.2-2µg) and

incubated for 2hrs at 4°C with end-over-end mixing. This mixture was then added to a fresh eppendorf containing 50µl of protein A beads (that had been washed with 3T3 lysis buffer) and incubated at 4°C for a further hour. The immune complexes were recovered by low speed centrifugation at 3000rpm at 4°C for 3mins. To remove any non-specific protein, beads were washed three times with 500µl of chilled 3T3-lysis buffer followed by another wash with 500µl of ice-cold PBS. All the supernatant was removed and the beads were resuspended in 60µl of 2X SDS sample buffer and boiled for analysis by SDS-PAGE electrophoresis. With every immunoprecipitation an additional lysate was prepared and used as a control to run in parallel with the experimental immunoprecipitation. Instead, this control lysate was incubated with control IgG rather than the primary antibody of interest.

2.2.3 Quantification of protein

To quantify the protein concentration of sample cell lysates, protein assays were performed in 96 well microtitre plates. A spectrophotometric standard curve of protein concentration was produced using 0-5µg bovine serum albumin (BSA) dissolved in distilled water. Quantifying the amount of protein in cell lysates involved adding 2µl of sample to a well in the 96 microtitre plate followed by 200µl of Bio-Rad reagent diluted 1:5 with distilled water. Each sample was analysed in triplicate. The plate was analysed using a MRX microtitre plate reader (Dynex Technologies), which read sample absorbances at 590nm. The Revelation software package was used to construct a standard curve of absorbances from the BSA standards. Least squared regression analysis was used to determine the line of best fit and the equation of this line was used to calculate the protein concentration of each sample.

2.2.4 SDS-polyacrylamide gel electrophoresis

2.2.4.1 Preparation of samples

Cell lysates were assayed for protein concentration and diluted 1:5 with 5X Laemmli sample buffer (260mM Tris/HCl (pH 6.7), 55.5% glycerol, 8.8% SDS, 0.007% bromophenol blue, 11.1% β-mercaptoethanol (Laemmli, Beguin et al. 1970)) to give a final protein concentration of 20µg. Samples were then boiled for 5mins to denature the protein.

2.2.4.2 *Molecular weight protein standards*

The prestained molecular markers contained the following proteins as standards: myosin (250kDa); β -galactosidase (150kDa); phosphorylase b (100kDa) bovine serum albumin (BSA) (75kDa); ovalbumin (50kDa); carbonic anhydrase (37kDa); soybean trypsin inhibitor (25kDa); lysozyme (15kDa) and aprotinen (10kDa).

2.2.4.3 *Casting and running tris-glycine gels*

The Protcan II xi Cell (BIO-RAD) gel apparatus was assembled in accordance with the manufacturer's instructions. A resolving gel containing the appropriate percentage of acrylamide for the size of the proteins to be separated, which was usually 10% (10% acrylamide:N,N'-methylenebisacrylamide mix, 375mM Tris/HCl (pH 8.8), 0.1% SDS, 0.1% Ammonium persulphate, 0.06% N,N,N',N'-tetramethylethylenediamine (TEMED)) was poured between the gel plates and overlaid with water to produce an even surface. After allowing the gel to set for 1hr the water was removed and a comb was inserted between the plates before pouring a 5% stacking gel (5% 29:1 acrylamide:N,N'-methylenebisacrylamide mix, 125mM Tris/HCl (pH 6.8), 0.1% SDS, 0.1% Ammonium persulphate, 0.1% TEMED). When the stacking gel had set, the comb was removed and the wells were washed with tank buffer (192mM Glycine, 25mM Tris, 0.15% SDS), to remove any excess acrylamide solution. The gels were then placed in a running tank where both the upper and lower reservoir were filled with tank buffer. Protein samples already mixed and boiled with the appropriate amount of 5X laemmli's were loaded into the wells. The gels were then run at the appropriate current (8 milliamps overnight) until the dye front reached the bottom of the gel.

2.2.4.4 *Transfer of proteins onto nitrocellulose*

Following electrophoresis the gels were placed into a transfer cassette. In summary, a piece of sponge (from cassette apparatus) was soaked in transfer buffer (192mM Glycine, 25mM Tris, 20% Methanol) and placed into the cassette. Two pieces of Whatman filter paper and a piece of Protran nitrocellulose (Schleicher & Schuell) were cut to fit the gel slice and were also soaked in transfer buffer. The Whatmann filter paper was placed on top of the sponge followed by the gel slice, Protran nitrocellulose, another piece of Whatmann filter paper and finally another piece of sponge. During assembly of this sandwich care was taken to ensure all air bubbles were excluded from each of the layers.

The cassette was closed and placed into the tank with the nitrocellulose side of cassette towards the positive electrode. The tank was filled with transfer buffer and the proteins transferred for 0.05 amps overnight or 0.8 amps for 1hr.

2.2.4.5 Immunoblotting

After transfer, the nitrocellulose was rinsed with distilled water and then incubated at room temperature with Ponceau S stain (0.1% Ponceau, 3% Trichloroacetic acid) until protein bands appeared. The nitrocellulose was then rinsed several times with TBS-Tween 20 (137mM NaCl, 20mM Tris/HCl (pH 7.6), 0.1% Tween 20) before proceeding with immunological detection. To block any unoccupied protein binding sites, the nitrocellulose membrane was incubated with 5% skimmed milk in TBS-Tween 20 for 1hr with gentle shaking at room temperature, followed by three 5min washes with TBS-Tween 20. The antibody specific to the protein of interest was diluted to the appropriate concentration in 10mls of TBS-Tween 20 (containing 1% skimmed milk powder) and incubated with the nitrocellulose for 2hrs at room temperature with vigorous shaking. The nitrocellulose was then washed several times with TBS-Tween 20. The secondary antibody, which was a horse-radish peroxidase conjugated antibody directed against the primary antibody, was diluted to the appropriate concentration in 10mls TBS-Tween 20 (containing 1% skimmed milk powder) and incubated with the nitrocellulose membrane at room temperature for 1hr with vigorous shaking. After three 5min washes with TBS-Tween 20, the membrane was incubated with reagents from the enhanced chemiluminescence (ECL) kit (Amersham) according to the manufacturers instructions and exposed to Kodak X-ray film for different lengths of time, Film was developed in the Kodak X-omat.

2.2.5 Laser Scanning Confocal Microscopy (LSCM)

COS-1 cells were plated out onto coverslips (18mm X 18mm) at ~40% confluency 24hrs prior to transfection. Cells were then transfected with the required plasmid DNA. 48hrs after transfection, cells were fixed for 10mins in 4% paraformaldehyde (dissolved in Tris buffered saline (TBS) (150mM NaCl, 20mM Tris, pH 7.4) followed by three 5min washes with 5mls of TBS. COS-1 cells were then permeabilised by performing three 5min incubations with 200µl of 0.2% triton in TBS, followed by a blocking step consisting of three 5min incubations with blocking buffer (either 20% goat serum and 4% BSA or 20% donkey serum and 4% BSA dissolved in TBS). The primary antibody was diluted to the

required concentration in dilutant buffer (10% blocking buffer diluted with TBS) and 200 μ l of this mix was added to the slide and left to incubate at room temperature for 2hrs. Slides were then washed with three changes of blocking buffer and incubated with 200 μ l of 1:200 diluted Alexa 594-conjugated anti-rabbit IgG (Molecular Probes) or Alexa 594-conjugated anti-donkey IgG (Molecular Probes) for 1hr. Cells were then washed five times with TBS before mounting the coverslips on microscope slides with Immunomount (Sandon).

Cells were visualised using the Zeiss Axiovert 100 laser scanning confocal microscope (Zeiss, Oberkochen, Germany) using a Zeiss Plan-Apo 63 X 1.4 NA oil immersion objective. The Alexa 594-conjugated secondary antibodies were both excited at 543nm and detected at 590nm.

2.2.6 Phosphodiesterase assay

Phosphodiesterase activity was measured using a modification of the two step procedure of Thompson and Appleman [Thompson and Appleman., 1971], as described previously by Marchmont and Houslay [Marchmont and Houslay., 1980]. The first step is the hydrolysis of the ³H-cyclic nucleotide (8 position of the adenine or guanine ring) by the phosphodiesterases, which generates labelled nucleotide monophosphate. In the second step, incubation with snake venom, (which has 5'-nucleotidase activity) converts the mono-phosphate ring to the corresponding labelled nucleoside. The unhydrolysed cyclic nucleotide was separated from the nucleoside by batch binding of the mixture to Dowex 1X8-400 anion exchange resin. This binds only the charged nucleotides and leaves behind the uncharged nucleosides

2.2.6.1 Activation of Dowex 1X8-400 anion exchange resin

To activate the Dowex 1X8-400 resin, 4L of 1M NaOH was added to 400g of the resin and gently mixed for 15mins at room temperature. After allowing the resin to settle by gravity the supernatant was removed and the resin was washed 30 times with 4L of distilled water. After the final wash the resin was resuspended in 4L of 1M HCl and gently mixed for 15mins at room temperature before being allowed to settle. The resin was then washed 3 times with 4L of distilled water until the supernatant had a pH of 3. The activated resin was stored as a 1:1 slurry with distilled water at 4°C until required.

2.2.6.2 *Preparation of assay tubes*

The appropriate volume of cell lysate was added to each 1.5ml eppendorf tube and made up to a volume of 50 μ l by adding 20mM Tris, pH 7.4. All assay tubes were incubated on ice and each sample was performed in duplicate. 50 μ l of 2 μ M cAMP containing 3 μ Ci [³H]cAMP in 20mM Tris/HCl/10mM MgCl₂ (pH 7.4) was added to all tubes and mixed by vortexing. These tubes were incubated at 30°C for 10mins and boiled for 2mins. After cooling the assay tubes on ice for 1.5mins, 25 μ l of 1mg/ml snake venom (diluted in 20mM Tris, pH 7.4) was added to each tube. These samples were then incubated for 10mins at 30°C. The tubes were transferred back to ice and 400 μ l of a 1:1:1 Dowex/ethanol/water mix was added to all the tubes and mixed by vortexing. The tubes were then incubated on ice for 20min before vortexing the samples again. The dowex resin was pelleted by centrifuging at 13000rpm and 150 μ l of the resultant supernatant was added to 1ml of Opti-scint scintillation fluid and counted on a Wallac 1409 liquid scintillation counter.

2.3 **Molecular techniques**

To prevent any contamination all glassware, tubes, tips, buffers and media used for molecular biology were sterilised.

2.3.1 ***Small scale production of DNA***

A sterile universal containing 5mls of L-broth (170mM NaCl, 0.5% (w/v) BactoYeast Extract, 1% (w/v) Bacto-Tryptone, pH 7.5) supplemented with 50 μ g/ μ l of ampicillin was inoculated from a glycerol stock of bacteria (transformed with the plasmid of interest) using a sterile pipette tip. The culture was incubated at 37°C overnight with agitation. Cells were then pelleted by centrifuging at 3000rpm for 15mins. The DNA was extracted using the QIAprep Spin Miniprep Kit (Qiagen) according to the manufacturer's instructions. In brief, the pelleted cells were resuspended in 250 μ l of buffer P1 (resuspension buffer) and transferred to a microfuge tube. 250 μ l of buffer P2 (lysis buffer) was added and the tubes were mixed and then incubated at room temperature for 4mins. 350 μ l of buffer N3 (neutralisation buffer) was added and the solutions were mixed again before centrifuging at 13000rpm for 10mins. The supernatant was added to a QIAprep column by decanting and centrifuged for 60secs. The flow-through was discarded and the column was washed with 750 μ l of buffer PE. The column was centrifuged for 1min prior

to the elution of the bound DNA. To elute the DNA from the column, 50 μ l of buffer EB was applied to the centre of the column and incubated at room temperature for 1min before centrifuging at 13000rpm for 1min to collect the DNA.

2.3.2 Large scale production of DNA

500mls of sterile L-broth supplemented with 50 μ g/ μ l of ampicillin was inoculated from a glycerol stock of bacteria (transformed with the plasmid of interest) using a sterile pipette tip. The culture was incubated overnight at 37 $^{\circ}$ C with vigorous agitation. The cells were pelleted by centrifugation at 6000g for 15mins at 4 $^{\circ}$ C. The bacterial pellet was resuspended in 10mls of buffer P1 (resuspension buffer), followed by the addition of 10mls of buffer P2 (lysis buffer), which was mixed by inverting 4-6 times. Cells were then incubated at room temperature for 5mins. After incubation, 10mls of chilled buffer P3 (neutralisation buffer) was added and mixed with the lysed cells, followed by a 15min incubation on ice. The sample was centrifuged at 10000g for 30mins at 4 $^{\circ}$ C. Meanwhile a QIAGEN-tip 500 was equilibrated by adding 10mls of buffer QBT and allowed to empty by gravity flow. The supernatant from the previous spin was added, and allowed to flow through the column before washing twice with 10mls of buffer QC. The DNA was eluted from the column using 15mls of buffer QF. To precipitate the DNA 0.7 volumes of room-temperature isopropanol was added to the eluate, mixed and centrifuged at 15000g for 30mins at 4 $^{\circ}$ C. The supernatant from this spin was removed and the remaining DNA pellet was washed with 5mls of room-temperature 70% ethanol and centrifuged at 15000g for 10mins. The remaining DNA pellet was allowed to air-dry for 5-10mins, before it was resuspended in 500 μ l of TE buffer pH 8.0.

2.3.3 DNA and RNA quantification

Both DNA and RNA concentrations were quantified spectrophotometrically using a WPA lightwave UV spectrophotometer blanked with distilled water. 5 μ l of DNA or RNA were diluted to 1ml with distilled water and absorbance measurements were taken at 260nm and 280nm. The concentration of DNA or RNA was calculated using the following spectrophotometric conversions:

An absorbance of 1 at 260nm corresponds to	50 μ g/ml of double stranded DNA
	33 μ g/ml of single stranded DNA
	40 μ g/ml of single stranded RNA

The ratio between the absorbance measurements at 260nm and 280nm indicates the purity of the nucleic acid. DNA or RNA, in solution, typically have $A_{260}:A_{280}$ ratios of 1.8 and 2 respectively. Ratio values lower than these indicate that the nucleic acid may be contaminated.

2.3.4 Glycerol stock production

600 μ l from an overnight culture of transformed cells containing the DNA of interest was transferred aseptically into a sterile screw top cryovial and mixed with 400 μ l of sterile 80% glycerol. This glycerol stock was stored at -80°C .

2.3.5 Agarose gel electrophoresis

DNA was separated and visualised using ethidium bromide agarose gels, the concentration of agarose used was dependent on the size of DNA fragment to be separated (see table below). The 1% agarose mix was dissolved in 1 X TAE buffer (40mM Tris/HCl, pH 8.0, 1mM EDTA, 0.114% glacial acetic acid) and heated until the agarose dissolved. The agarose was allowed to cool slightly before the addition of 1 μ l ethidium bromide. The agarose/ethidium bromide mix was then added to the pre-assembled casting tray minigel apparatus and allowed to set. The combs and stoppers were removed and the tank was filled with 1X TAE buffer. Samples were diluted 6:1 in 6X loading dye (0.25% Bromophenol Blue, 0.25% xylene cyanol blue, 30% glycerol in water) and loaded into the sample wells. In order to size the DNA fragments, the molecular size markers of either Marker X (Promega) or the 1kb ladder marker (Promega) were loaded alongside the samples. The gel was run at 50 volts until the dye front moved through the gel. Due to the presence of intercalating ethidium bromide dye the resultant DNA bands could be visualised with UV transillumination.

Percentage Gel	Size of Fragment (kb)
0.9	0.5-7
1.2	0.4-6
1.5	0.2-3
2	0.1-2

2.3.6 Gel extraction of DNA

DNA of interest was isolated from an agarose gel using the QIAquick Gel Extraction Kit (Qiagen) according to the manufacturer's instructions. Briefly, DNA was excised from the agarose gel and weighed in an eppendorf to which three volumes of Buffer QG to one volume of gel was added. This was incubated at 50°C for 10mins until the gel had dissolved and then one gel volume of isopropanol was added to the sample and mixed. The DNA sample was added to a QIAquick column and centrifuged at 13000rpm for 1min. The column was washed with 750µl of Buffer PE and centrifuged at 13000rpm for 1min twice to remove any residual buffer. The DNA was eluted from the column by adding 30µl of buffer EB to the centre of the membrane, which was allowed to stand for 1min before centrifuging at 13000rpm for 1min.

2.3.7 Restriction digestion of DNA

The restriction enzyme and the appropriate restriction buffer used depended on the site(s) of digestion. The enzymes used for digestion were supplied by Promega. DNA was digested with the appropriate enzyme(s) by incubating the digestion mixture at 37°C for 1-2hrs.

2.3.8 DNA ligation

DNA and vector DNA were ligated using the Rapid DNA Ligation Kit (Roche). Briefly, 100ng of restriction digested DNA, at 1:2 and 1:5 ratios (v/v) of vector:insert DNA were added to a sterile 0.5ml eppendorf and made up to a final volume of 10µl by the addition of 1X DNA dilution buffer. To the DNA mix 10µl of 2X T4 DNA ligation buffer and 1µl of T4 DNA-ligase were added and mixed. The tube contents were mixed and incubated at room temperature for 5mins.

2.3.9 Reverse transcription polymerase chain reaction (RT-PCR)

2.3.9.1 RNA isolation

Briefly, total RNA was extracted from cells by firstly aspirating off the growth medium and then adding 600µl of RLT lysis buffer to each plate. The cells were then scraped into eppendorfs and mixed by pipetting to remove any cell clumps. Samples were

homogenised by passing the lysates five times through a 20-gauge needle fitted to a syringe. 600µl of 70% ethanol was added to the lysates and mixed by pipetting. The lysate was then added to an RNAeasy spin column and centrifuged for 15secs at 8000rpm. 700µl of buffer RW1 was added to the column and allowed to incubate at room temperature for 5mins before centrifuging for 15secs at 8000rpm. The columns were washed twice with 500µl of buffer RPE followed by centrifuging for 15secs at 8000rpm each time. To ensure that ethanol was completely removed, the columns were centrifuged at full speed for 1min. Columns were transferred to a clean collection tube where RNA was eluted from the column by adding 30µl of RNase-free water directly to the column and centrifuging for 1min at 8000rpm.

2.3.9.2 *First strand cDNA synthesis*

First strand cDNA was synthesised using in accordance with the instruction manual from Promega. Briefly, 2µg of RNA was mixed with 2µl of 1µg oligo (dT) primer and made up to a total volume of 10µl by adding water in a sterile microfuge tube. This mixture was mixed, centrifuged briefly to collect sample in the bottom of the tube and then heated to 70°C for 5mins before incubation on ice for 5mins. This mix was again centrifuged briefly to collect the solution at the bottom of the microfuge tube. To this mix 5µl of AMV Reverse Transcriptase 5X Reaction Buffer, 40 units of RNasin Ribonuclease inhibitor, 30 units of AMV Reverse Transcriptase, 2.5µl of dNTP mix, and 40mM sodium pyrophosphate (which had already been prewarmed to 42°C) were added and made up to a total volume of 25µl using RNase-free water. The sample was mixed again and centrifuged briefly to collect contents. Samples were then incubated at 42°C for 60mins, followed by heating to 95°C for 5mins. cDNA was then stored at -20°C until it was required.

2.3.9.3 *PCR reaction*

PCR was performed using Platinum Pfx DNA Polymerase (Life Technologies) in accordance with the manufacturer's instructions. Briefly, 1µg cDNA (generated in 2.2.9.2) was added to 5µl of 10X Pfx amplification buffer, 1.5µl of 10mM dNTPs, 1µl 50mM MgSO₄, 1µl (50pmol/µl) of each of sense and antisense primers for detection of the transcript of interest, 1µl (50pmol/µl) of sense and antisense primers for cyclophylin, 1µl of Platinum Pfx DNA Polymerase and made up to a total volume of 50µl with RNase-free water. The PCR conditions used were as follows:

94°C	2mins	35 cycles
94°C	15secs	
55°C (variable depending on T _m of primer)	30secs	
68°C	60secs	

2.3.10 Cloning and PCR

2.3.10.1 PCR conditions used for generating PDE4A7 cDNA containing the nuclear export signal (NES) of PKI α and for incorporating EcoRI and BamHI sites onto PDE4A7

The amplification of PDE4A7 DNA either containing the nuclear export signal of PKI α or EcoRI and BamHI restriction sites was performed using the Expand High Fidelity PCR System (Roche). Briefly in one sterile vial 400ng of PDE4A7 DNA was added to a tube containing master mix 1 buffer (1 μ l of each of the sense and antisense primers (50pmol/ μ l), 2 μ l of each dNTP (10mM) and made up to a final volume of 50 μ l with sterile water). In a separate vial, master mix 2 buffer was prepared (10 μ l of 10X Expand High Fidelity buffer containing 15mM MgCl₂ was mixed with 0.75 μ l of the Expand High Fidelity PCR System enzyme mix and made up to a total volume of 50 μ l with sterile water). Then 25 μ l of mastermix 1 was mixed with 25 μ l of mastermix 2 in a separate sterile PCR tube. The PCR conditions used were as follows:

94°C	2mins	30 cycles
94°C	15secs	
55°C (variable depending on T _m of primer)	30secs	
72°C	1min	
72°C	7mins	

2.3.10.2 Transformation of Ecoli with plasmid DNA

10 μ l of the DNA extracted from the yeast cells or 1 μ l of plasmid DNA in all other cases was added into a vial of chemically competent Ecoli, mixed gently and incubated on ice for 30mins. Cells were heat-shocked for 30secs at 42°C and immediately transferred to ice. 250 μ l of room temperature SOC medium was added to the cells, which were then incubated at 37°C for 1hr with gentle shaking (200 rpm). Cells were pelleted by

centrifuging at 2000rpm for 5mins at room temperature and plated out onto either kanamycin or ampicillin (50µg/µl). Plates were incubated overnight at 37°C.

2.3.10.3 TOPO cloning

The TOPO cloning and transformation were carried out using the pcDNA3.1/V5-His TOPO TA Expression Kit (Invitrogen) according to the manufacturer's instructions. Briefly, 0.5µl of fresh PCR product, 1µl of salt solution, 1µl of TOPO vector and 2.5µl of sterile water were added to a sterile microfuge tube, mixed by pipetting and incubated for 30mins at room temperature. 2µl of this reaction was added to into vial of One Shot TOP10 chemically competent E.coli (Invitrogen), mixed gently and incubated on ice for 30mins. Cells were heat shocked for 30secs at 42°C and the tubes were immediately transferred to ice followed by the addition of 250µl of SOC medium. The cells were then incubated at 37°C for 1hr with agitation. 100µl and 200µl of the cells were spread on a prewarmed ampicillin plate (50µg/µl). Colonies were then screened using PCR to check for desired product (conditions shown below), DNA was isolated from the positive colonies using QIAprep kits and sequenced.

2.3.10.4 PCR screening of colonies

A small portion of a colony was scraped from the ampicillin plate using a sterile yellow tip and transferred to a sterile PCR tube containing 25µl of PCR buffer. As a large number of PCR screens were performed at any one time a 500µl stock of this buffer was prepared in a separate vial. This buffer contained; 50µl of 25mM MgCl₂, 50µl of 10X Thermophilic DNA Buffer, 10µl of 10mM dNTPs, 5µl of sense and antisense primers (100pmol/µl), 1µl of Taq DNA Polymcrasc, which was made up to a total volume of 500µl with distilled sterile water. Each portion of colony was resuspended in 25µl of this PCR buffer in a sterile PCR tube. The PCR conditions used to amplify the insert were as follows:

94°C	2mins	} 35 cycles
94°C	30secs	
47°C (variable depending on T _m of primer)	30secs	
72°C	1min	
72°C	7mins	

2.3.11 DNA sequencing

Inserts from the yeast two hybrid screen or PCR products were sequenced using the BigDye termination kit. The plasmid DNA (500ng) was mixed 3.2 pmol of primer and 8µl of Big Dye Sequencing mix and made up to a final volume of 20µl with sterile distilled water. The PCR conditions used were as follows:

96°C	30secs	} 25 cycles
50°C (variable depending on T _m of primer)	15secs	
60°C	4mins	

The resultant DNA was precipitated by adding 2µl of 3M NaOAc, pH 4.8 and 50µl of EtOH. After mixing, this solution was incubated on ice for 10mins. The precipitated DNA was pelleted by centrifuging at 13000rpm for 30mins at 4°C. The pellet was washed once with 70% ethanol and dried by heating in the PCR machine for 3mins at 80°C.

2.3.11.1 Sequence analysis

All DNA sequence analysis was performed using the Gene Jockey II program.

2.4 Yeast two hybrid analysis

2.4.1 Testing the bait plasmid for toxicity effects, transcriptional activation and effect on yeast mating efficiency

The details of this procedure are outlined in on pages 25 and 26 of the Clontech Pretransformed MATCHMAKER Libraries User Manual.

2.4.2 Preparation of SD/-Ade/-His/-Leu/-Trp plates

A combination of Minimal SD Agar base (for preparation of plates) or Minimal SD base (for liquid medium), both from Clontech were combined with the appropriate DO Supplement (Clontech) to produce a synthetic, defined minimal medium lacking one or more specific nutrients (details are listed in the Yeast Protocols Handbook from Clontech).. For example, to prepare sterile synthetic dropout (SD) agar plates lacking adenine (Ade), histidine (His), leucine (Leu) and tryptophan (Trp) (SD/-Leu/-Trp/-Ade/-His) then to each

litre of YPD Agar medium (70g YPD Agar medium per litre of distilled water) 0.6g of – Ade and 0.62g of –Leu, -Trp, -His DO supplement (Clontech) was added. Once medium was prepared it was heated until the agarose dissolved. Medium was allowed to cool slightly before pouring into the 150mm plates. The SD Agar plates were dried at room temperature for 3 days before use. To prepare YPD liquid medium the protocol is similar except YPD medium (50g per litre of distilled water) is used in place of the YPDA agar.

2.4.3 Preparation of competent yeast cells

AH109 cells were streaked from a glycerol stock on a YPD agar plate (70g of YPD Agar Medium powder (Clontech) dissolved in 1 litre of distilled water, autoclaved and cooled slightly before pouring into plates). Cells were grown agar side up at 30°C for ~3 days. One colony of these cells were picked using a sterile yellow tip and used to inoculate 50mls of sterile YPD medium (50g of YPD powder supplied by Clontech dissolved in 1 litre of distilled water and autoclaved to sterilise). Cells were grown overnight at 30°C with shaking. The next day this culture was transferred to a sterile falcon tube and the cells were pelleted by centrifugation at 3000g for 3mins at room temperature and the YPD medium was removed. Cells were rinsed with 50mls of sterile water and then pelleted by centrifugation at 3000 for a further 3mins. The water was removed and the cells were washed with ~12.5mls of filter sterilized LiSorb (100mM lithium acetate, 10mM Tris-HCl, pH 8.0, 1mM EDTA, 1M sorbitol) and centrifuged at 3000rpm for 5mins. The LiSorb was removed and cells were centrifuged for a further 5mins at 3000rpm at room temperature to remove any remaining LiSorb. Cells were then resuspended in 300µl of LiSorb. Carrier DNA (sonicated herring testes carrier DNA) was heat denatured for 5mins at 99°C and ~35µl was added to the yeast cells/LiSorb solution and mixed. Cells were aliquoted and stored at 80°C until required.

2.4.4 Transformation of DNA into AH109 yeast cells

The competent AH109 cells were thawed at room temperature and 1µl of plasmid DNA was added to 15µl of AH109s and mixed. 100µl of LiPEG (40% PEG (polyethylethe glycol), 0.1M TE buffer (0.1M Tris-HCl, 10mM EDTA, pH 7.5), 1M LiAc (lithium acetate, pH 7.5) were then added to the cells and mixed by vortexing. Cells were then incubated at room temperature for 20mins. 10µl of DMSO was added to the cells and mixed. Cells were then heat-shocked for 15mins in a 42°C water bath and then chilled on ice for 2mins. The cells were pelleted by centrifuging at 4000g for 3min and the resultant

supernatant was removed. The pelleted cells were resuspended in 200 μ l of PBS and plated onto SD/-Trp plates, which were incubated at 30°C agar side up for ~3 days.

2.4.5 Protein extraction from yeast

Yeast cells from which protein was to be extracted were scraped from plates using a sterile blue tip and resuspended in 1ml of ice-cold water. 150 μ l of 1.85M NaOH and 11 μ l of β -mercaptoethanol were added to the yeast cell suspension, mixed by vortexing and incubated on ice for 10mins. After this incubation, 150 μ l of 55% TCA was added to the yeast cell suspension, mixed by vortexing and incubated on ice for a further 10mins. Cells were then centrifuged at 14000rpm for 5mins at 4°C. The supernatant was removed and cells were centrifuged again briefly and any remaining TCA was removed. The cell pellet was resuspended in 150 μ l of 2X Laemmli buffer and boiled for 5mins to denature the protein.

2.4.6 Small scale yeast mating

One colony of each type (i.e., AH109[pGBKT7-PDE4A7] and Y187[pACT-RanBPM9] or AH109[pGBKT7-PDE4A7] and Y187[pACT-CBP]) was used to inoculate 0.5ml of 2X YPDA medium (100g of YPD powder per litre of distilled water, to which 30mls of adenine hemisulphate solution was added). Cells were resuspended by vortexing for 1min and then incubated at 30°C overnight with gentle shaking (200rpm). The appropriate controls included in the small scale yeast mating procedure were AH109[pGBKT7-53] mated with Y187[pTD1-1] as the positive control and AH109[empty-pGBKT7] mated with Y187[empty-pACT2], AH109[pGBKT7-PDE4A7] mated with Y187[empty-pACT2] as negative controls. The diploid yeast cells were plated out on SD/-Leu/-Trp/-Ade/-His plates and incubated at 37°C agar side up for 3-5 days. A small amount of each of the mated yeast cells were picked using a sterile yellow tip and resuspended in 5 μ l of sterile PBS. Each was gently pipetted onto an SD/-Leu/-Trp plate and grown for 1 day, so that each yeast mating grew as separate circles. This was in preparation for the β -galactosidase assay.

2.4.7 Large scale yeast mating

A large fresh colony of bait strain (AH109[pGBKT7-PDE4A7]) was used to inoculate a flask of 50mls of SD/-Trp medium. This flask was incubated overnight at 30°C

with shaking at 250-270 rpm. Once the OD₆₀₀ of this culture had reached >0.8 the cells were centrifuged at 1000g for 5mins and the supernatant was removed. The cell pellet was resuspended in the residual liquid by vortexing. The library culture was thawed in a room temperature water bath and mixed by gentle vortexing. The bait culture (AH109[pGBKT7-PDE4A7]) and the library were combined in a sterile 2-L flask, containing 45mls of 2X YPDA/Kan (YPDA containing 50µg/µl of kanamycin). Two 1ml aliquots of 2X YPDA/Kan were used to rinse the cells from the library tube. The flask was incubated at 30°C overnight with gentle swirling (30-50 rpm) to allow mating. The next day, this mating culture was transferred to a sterile centrifuge bottle and cells were pelleted by centrifuging at 1000g for 10mins. The mating flask was rinsed twice with 50mls of 2X YPDA/Kan. These rinses were combined and used to resuspend the first pellet. The cells were centrifuged for a further 10mins at 1000g and the resultant cell pellet was resuspended in 10mls of 0.5X YPDA/Kan. 750µl of this mating mixture was spread onto 150mm plates containing SD/-Ade/-His/-Leu/-Trp agar also referred to as quadruple dropout out (QDO) medium. These plates were incubated, colony side down, at 30°C until the appearance of colonies (typically between 8-21 days). Resultant colonies were streaked out a further twice onto SD/-Ade/-His/-Leu/-Trp agar to check they were 'authentic' two-hybrid positives.

2.4.8 Assay for β -galactosidase activity

β -galactosidase activity was determined by overlaying the diploid cells with a top agar containing the substrate of 5-bromo-4-chloro-3-indolyl- β -D-galactoside (X-Gal). Briefly, 289mM Na₂HPO₄, 211mM NaH₂PO₄ (pH 7.0), 20mM KCl, 2mM MgCl₂, and 1% (w/v) SDS were dissolved in 50mls of distilled water. Separately, 0.5g of low melting point agarose (Gibco) was made up to 45mls with distilled water and heated in a microwave until the agarose was dissolved. The agarose solution was allowed to cool to ~50°C before mixing with the previous solution. 1ml of 40mg/ml X-Gal was added to this agarose solution under mixing before slowly pouring over the plate of diploid yeast cells.

2.4.9 Plasmid isolation from yeast cells

To extract the library plasmid containing the insert of interest, a portion of the diploid yeast cells were scraped from the plate using a sterile blue tip and resuspended in 600µl of plasmid isolation buffer (1M sorbitol, 100mM EDTA and 14mM β -mercaptoethanol), followed by the addition of 8.5µl of lyticase. The yeast cell suspension

was heated at 30°C for 30-60mins and centrifuged at 7500rpm for 10mins. The resultant pellet was resuspended in 30µl of EB buffer (from the QIAprep Spin Miniprep Kit (Qiagen)).

2.5 Gene microarray analysis

Both the control and experimental samples were labelled with different fluors (Cyanine 3 or Cyanine 5) by mixing the following in a sterile PCR tube: 8µl of 5X First Strand reaction buffer (Superscript II, Life Technologies), 1.5µl of AncT mRNA primer (100pmol/µl), 3µl of 20mM ddNTP (-dCTP) (6.67mM each of dATP, dGTP, dTTP), 1µl of 2mM dCTP, 1µl of 1mM Cyanine 3 or Cyanine 5, 4µl of 0.1M DTT, 5µg of RNA (total RNA) and made up to a total volume of 40µl with RNase-free water. This labelling reaction was incubated at 65°C for 5mins, followed by a 5min incubation at 42°C. 2µl of reverse transcriptase (Superscript II, Life Technologies) was added to this mixture and was then incubated at 42°C for ~3hrs. This mix was briefly centrifuged and placed on ice. 4µl of 50mM EDTA (pH 8.0) and 2µl of 10M NaOH was added to the reaction. RNA was hydrolysed by incubating at 65°C for 20mins and then adding 4µl of 5M acetic acid. The control and test mixtures were then mixed together. DNA was precipitated by adding 100µl of isopropanol and incubated on ice for 30mins. Samples were centrifuged for 10mins at 4°C and the isopropanol was removed. The remaining pellet was rinsed with ice-cold 70% ethanol. Samples were pulse centrifuged and any remaining alcohol was removed by pipetting. Pellets were then resuspended in 5µl of RNase-free water. In a separate sterile PCR tube, 100µl of DIG Easy Hyb solution (Roche), 5µl of yeast tRNA were mixed and then incubated at 65°C for 2mins and cooled to room temperature. 30µl of this hyb solution was then added to each pooled pair of Cyanine 3 and Cyanine 5 labelled cDNA, mixed and then incubated at 65°C for a further 2mins and cooled back to room temperature. The hyb mixture was then pipetted onto the coverslip which was placed on a solid flat reliable surface. The slide was inverted and placed carefully onto the coverslip. Slides were then placed into a hybridization chamber (black microscope boxes) containing a small amount of DIG Easy Hyb solution and placed into a 37°C incubator for ~18 hrs. After this incubation coverslips were removed from the array slides by quickly dipping the array into 1X SSC (3M NaCl, 0.3M Na₃ Citrate, 1M HCl). Array slides were then placed into a staining rack and washed three times for 10mins in a clean slide staining box containing fresh 1X SSC buffer containing 0.1% SDS with gentle agitation. After the washes slides were rinsed in 1X SSC by plunging 4-6 times. Slides were dried at room temperature and stored in the dark until scanning.

Chapter 3

Intracellular Targeting of PDE4As

3.1 Introduction

The human PDE4A gene encodes four splice variants of which PDE4A4B (PDE46) [Sullivan et al., 1998], PDE4A10 [Rena et al., 2001] and PDE4A11 [TM3; unpublished] are long form isoenzymes that share an identical catalytic and C-terminal sequence but diverge at their N-terminal regions as a result of alternative 5' mRNA splicing. The fourth PDE4A splice variant, PDE4A7 (2EL) [Horton et al., 1995] is the only PDE4A found to undergo both 5' and 3' mRNA splicing, generating a PDE that contains both unique N- and C-terminal domains. PDE4A7 contains a 34bp insert, which results in premature termination of the open reading frame (ORF), producing an enzyme devoid of any catalytic PDE activity [Horton et al., 1995]. Transcripts of PDE4A7 have been detected in a number of tissues (Houslay Lab, unpublished), but the functional role of this protein remains to be elucidated.

PDEs are not randomly distributed throughout the cell, but are targeted to specific intracellular compartments. The idea that the unique N-terminal region of PDE4s may contain the information required for their subcellular targeting came originally from studies performed on the rat PDE4A isoform, PDE4A1 (RD1) [Scotland et al., 1995; Shakur et al., 1993]. PDE4A1 is found to be membrane-associated, both natively and when over-expressed. However, it becomes a fully soluble enzyme when its unique N-terminal region is removed, implying that the signal required for its membrane targeting is contained within its unique 25 amino acid residue N-terminal region [Shakur et al., 1993]. Following this discovery, the N-terminal regions of various other PDE4s were shown to mediate their intracellular targeting and interaction with other proteins. For example, the unique N-terminal domains of both PDE4A4B and PDE4D4 contain multiple PxxP motifs that allow these enzymes to interact with SH3 domain-containing proteins [M^oPhée et al., 1999], and the N-terminal region of PDE4D5 mediates its interaction with the RACK1 scaffold protein [Yarwood et al., 1999]. However, although removing the unique N-terminal region of PDE4A4B corresponds to a loss in its membrane localisation, the truncated species is still able to associate with the perinuclear region of the cell, implying that signals other than those located in the extreme N-terminal region are responsible for conferring targeting on PDE4A4B [Huston et al., 2000].

In this chapter attempts were made to identify targeting signals in PDE4A outwith the unique N-terminal region that characterises individual PDE4 isoforms. In this study, distribution analysis was performed on recombinant PDE4A4B. This is because it is impossible, as yet, to analyse endogenously expressed PDE4A4B. Despite the enormous efforts made by the MDII research group, no cell line we know of expresses PDE4A4B at the levels, which have allowed us to detect it unequivocally. This is because it is expressed at such low levels. Also, there is the potential to confuse PDE4A4B with PDE4A10 as both of these proteins co-migrate on SDS-PAGE. In addition the PDE4A4-specific antisera we have from Novartis is ten to one hundred fold less sensitive than that of the existing PDE4A C-terminal antisera. Thus, our group continue to examine PDE4A4B only in recombinant systems.

3.2 Results

3.2.1 Subcellular distribution of PDE4A4B (PDE46) and PDE4A4C (h6.1) in COS-1 cells

Before proceeding with this study it was essential to have an 'internal control'. I based this upon results obtained from previous PDE4A targeting analyses performed, in particular comparing the targeting of PDE4A4B (PDE46) to that of its truncate, PDE4A4C (h6.1). PDE4A4C (h6.1) was originally believed to be an authentic PDE4A long isoform. It was actually constructed from two over-lapping cDNA clones that we now know encompass amino acids 210 through to the extreme C-terminus of PDE4A4B [Bolger, Michaeli et al., 1993]. However, h6.1 also contains a unique N-terminal domain of 9 amino acids. The nucleotide sequences of PDE4A4B and h6.1 are aligned (*figure 3.1*), with the coloured residues representing the coloured domains shown in the subsequent schematic diagrams.

Lysates from COS-1 cells were transfected to express either PDE4A4B (*figure 3.2, panel A*) or h6.1 (*figure 3.3, panel A*). These transfected cell lysates were subjected to a basic subcellular fractionation in order to generate low speed (P1) and high speed (P2) pellet fractions as well as a high speed supernatant fraction (S2) (Materials and Methods 2.2.1). These fractions were then immunoprobed with the general PDE4A antiserum, which recognises the C-terminal domain located in all PDE4As. This is apart from the catalytically inactive PDE4A7 splice variant, as it is C-terminally truncated. PDE4A4B (121±3kDa) was found in the S2 soluble fraction and also with both the P1 and P2 particulate fractions (*figure 3.2, panel B* and see Table 3.1). In contrast h6.1 (98±2kDa)

whilst located both in the P1 and S2 fractions was absent from the P2 fraction (*figure 3.3, panel B* and see Table 3.1). These biochemical data correlate well with results of previous researchers [Huston et al., 1996] indicating that the basic subcellular fractionation protocol used here was suitable for the comparative membrane/particulate targeting analyses.

3.2.2 Analysis of transfected COS-1 cells using Laser Scanning Confocal Microscopy (LSCM)

Laser scanning confocal microscopy (LSCM) was utilised to investigate further the intracellular localisation of these various PDE4A proteins. COS-1 cells were transfected to express either PDE4A4B or h6.1. The cells were then fixed, permeabilised and incubated with the PDE4A general antiserum followed by the Alexa293-labelled anti-donkey antiserum for the specific fluorescent detection of the PDE4A proteins (Materials and Methods 2.2.5). Transfected cells were easy to identify as their fluorescence was more intense and defined than that of the surrounding cells, which were presumed to be untransfected. The fluorescence signal for PDE4A4B was found distributed throughout the cytosol with concentrated staining found in the area around the nucleus and the margins of the cell (*figure 3.2 panel C*). The fluorescent signal for h6.1 was found distributed throughout the cytosol with increased staining visualised around the nucleus (*figure 3.3 panel C*). However, this differed from PDE4A4B in that it was not found localised to the cell margins. Therefore, PDE4A4B does not become fully soluble upon removal of its unique N-terminal and instead can still associate with the perinuclear region of COS-1 cells. This suggested that motifs other than those found within the unique N-terminal region are responsible for conferring targeting on PDE4A4B. Again, these data are identical to those data previously published [Huston et al., 1996]. Such experiments support the idea that it is the N-terminal region of PDE4A4B leads to a loss in the fidelity of its intracellular targeting (compare *figure 3.2, panel C* with *figure 3.3, panel C*).

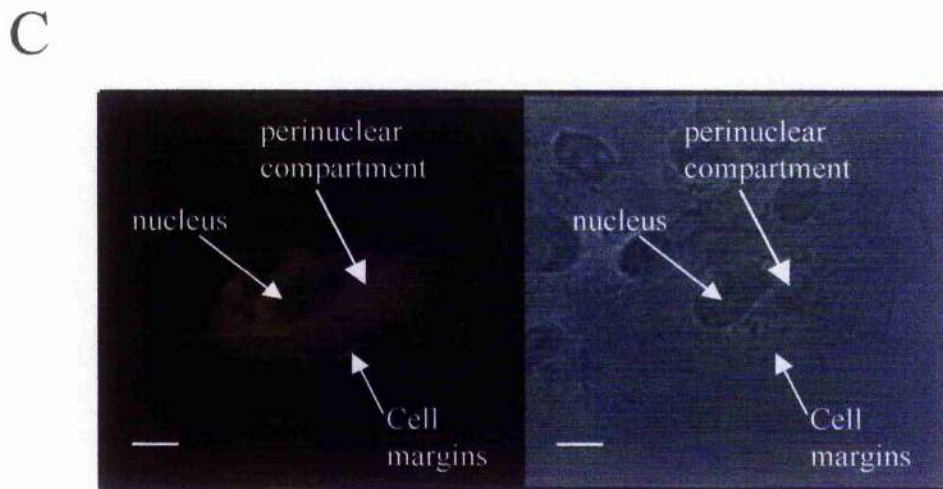
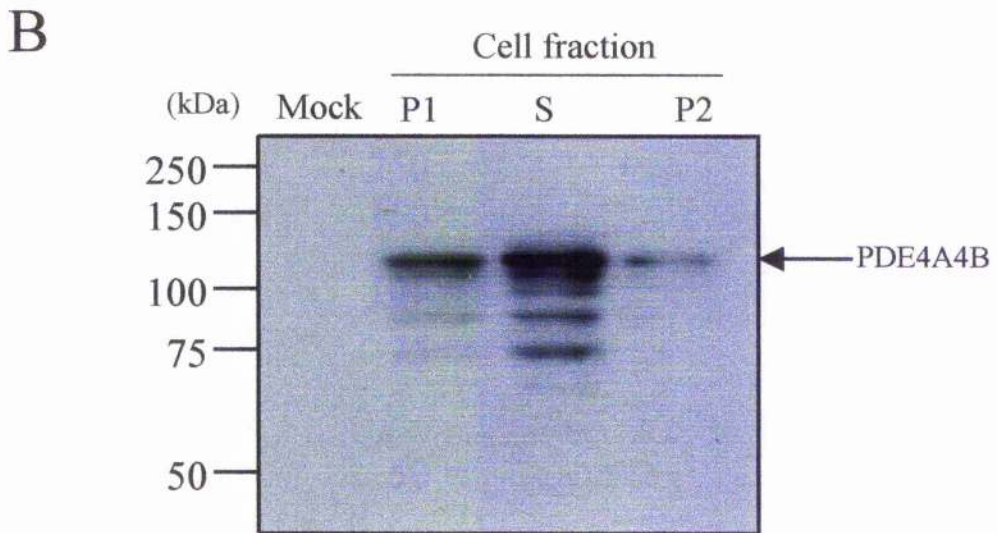
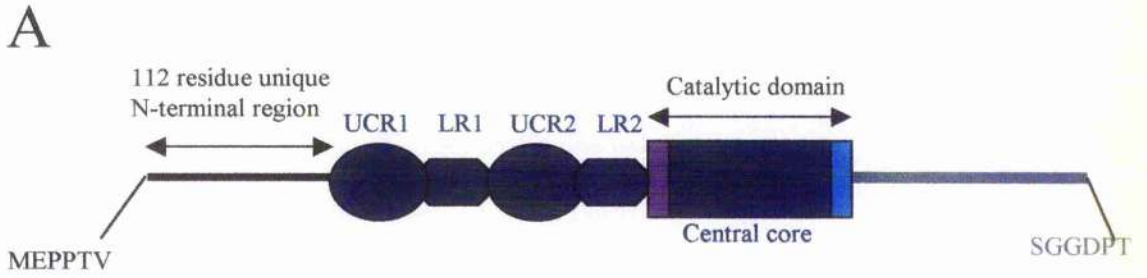
As I was able to reproduce the results from previous studies I concluded that both the subcellular fractionation and LSCM methods were suitable for use in the subsequent targeting analyses.

PDE46	MEPPTVPSERSLSLSLPGPREGQATLKPPPQHLWRQPRTPIRIQQRGYSDSAERAERERQ	60
h6.1	-----	
hyb1	-----	
hyb2	-----	
2EL	-----	
PDE46	PHRPIERADAMDTSDRPGLRTRRMSWPSSFHGTGTGSGGAGGGSSRRFEAENGPTPSPGR	120
h6.1	-----	
hyb1	-----	
hyb2	-----	
2EL	-----	
PDE46	SPLDSQASPGLVLHAGAATSQRRESFLYRSDSDYDMSPKTMSRNSSVTSEAHAEDLIVTP	180
h6.1	-----	
hyb1	-----	
hyb2	-----	
2EL	-----	
PDE46	FAQVLASLRSVRSNFSLLTNVPVPSNKRSPGGPTPVCKATLSEETCQQLARETLEELD	240
h6.1	----- HCFTFVTV PLGGPTPVCKATLSEETCQQLARETLEELD	40
hyb1	-----	
hyb2	----- HCFTFVTV PLGGPTPVCKATLSEETCQQLARETLEELD	40
2EL	-----	
PDE46	CLEQLETMQTYRSVSEMASHKFKRMLNRELTHLSEMSRSGNQVSEYISTTFLDKQNEVEI	300
h6.1	CLEQLETMQTYRSVSEMASHKFKRMLNRELTHLSEMSRSGNQVSEYISTTFLDKQNEVEI	100
hyb1	-----	
hyb2	CLEQLETMQTYRSVSEMASHKFKRMLNRELTHLSEMSRSGNQVSEYISTTFLDKQNEVEI	100
2EL	-----	
PDE46	PSPTMKEREKQQAPRPRPSQPPPPVPHLQPMQITGLKMLHNSLNNSNIPRFGVKTD	360
h6.1	PSPTMKEREKQQAPRPRPSQPPPPVPHLQPMQITGLKMLHNSLNNSNIPRFGVKTD	160
hyb1	-----MVLPSDQGFKLLGNVLQGPPEYRLLT	26
hyb2	PSPTMKEREKQQAPRPRPSQPPPPVPHLQPMQITGLKMLHNSLNNSNIPRFGVKTD	160
2EL	-----MVLPSDQGFKLLGNVLQGPPEYRLLT	26
PDE46	QEELLAQELENLNKWLNI FCVSDYAGGRSLTCIMYMFQERDLLKKFRIPVDTMVTYML	420
h6.1	QEELLAQELENLNKWLNI FCVSDYAGGRSLTCIMYMFQERDLLKKFRIPVDTMVTYML	220
hyb1	SGLRLHQELENLNKWLNI FCVSDYAGGRSLTCIMYMFQERDLLKKFRIPVDTMVTYML	86
hyb2	QEELLAQELENLNKWLNI FCVSDYAGGRSLTCIMYMFQERDLLKKFRIPVDTMVTYML	220
2EL	SGLRLHQELENLNKWLNI FCVSDYAGGRSLTCIMYMFQERDLLKKFRIPVDTMVTYML	86
PDE46	TLEDHYHADVAYHNSLHAADVLSQSTHVLLATPALDAVFTDLEILAALFAAAIHDVDHPGV	480
h6.1	TLEDHYHADVAYHNSLHAADVLSQSTHVLLATPALDAVFTDLEILAALFAAAIHDVDHPGV	280
hyb1	TLEDHYHADVAYHNSLHAADVLSQSTHVLLATPALDAVFTDLEILAALFAAAIHDVDHPGV	146
hyb2	TLEDHYHADVAYHNSLHAADVLSQSTHVLLATPALDAVFTDLEILAALFAAAIHDVDHPGV	280
2EL	TLEDHYHADVAYHNSLHAADVLSQSTHVLLATPALDAVFTDLEILAALFAAAIHDVDHPGV	146
PDE46	SNQFLINTNSELALMYNDESVLENHHLAVGFKLLQEDNCDFQNLKRQRQSLRKMVIDM	540
h6.1	SNQFLINTNSELALMYNDESVLENHHLAVGFKLLQEDNCDFQNLKRQRQSLRKMVIDM	340
hyb1	SNQFLINTNSELALMYNDESVLENHHLAVGFKLLQEDNCDFQNLKRQRQSLRKMVIDM	206
hyb2	SNQFLINTNSELALMYNDESVLENHHLAVGFKLLQEDNCDFQNLKRQRQSLRKMVIDM	340
2EL	SNQFLINTNSELALMYNDESVLENHHLAVGFKLLQEDNCDFQNLKRQRQSLRKMVIDM	206
PDE46	VLATDMSKHMTLLADLKTMTVETKKVTS SSVLLLDNYS DRIQVLRNMVHCADLSNPTKPLE	600
h6.1	VLATDMSKHMTLLADLKTMTVETKKVTS SSVLLLDNYS DRIQVLRNMVHCADLSNPTKPLE	400
hyb1	VLATDMSKHMTLLADLKTMTVETKKVTS SSVLLLDNYS DRIQVLRNMVHCADLSNPTKPLE	266
hyb2	VLATDMSKHMTLLADLKTMTVETKKVTS SSVLLLDNYS DRIQVLRNMVHCADLSNPTKPLE	400
2EL	VLATDMSKHMTLLADLKTMTVETKKVTS SSVLLLDNYS DRIQVLRNMVHCADLSNPTKPLE	266
PDE46	LYRQWTDRI MAEFFQQGDRE RERERGMEISPMCDKHTASVEKSQVGFIDYIVHPLWETWADL	660
h6.1	LYRQWTDRI MAEFFQQGDRE RERERGMEISPMCDKHTASVEKSQVGFIDYIVHPLWETWADL	460
hyb1	LYRQWTDRI MAEFFQQGDRE RERERGMEISPMCDKHTASVEKSQVGFIDYIVHPLWETWADL	326
hyb2	LYRQWTDRI MAEFFQQGDRE RERERGMEISPMCDKHTASVEKSQV QARGIDGRAQGGFY ---	457
2EL	LYRQWTDRI MAEFFQQGDRE RERERGMEISPMCDKHTASVEKSQV QARGIDGRAQGGFY ---	323

PDE46	VHPDAQEILDLTLEDNRDWYYSAIRQSPSPPPPEEESRGPFGHPPLPDKFQFELTLEEEEEEE	720
h6.1	VHPDAQEILDLTLEDNRDWYYSAIRQSPSPPPPEEESRGPFGHPPLPDKFQFELTLEEEEEEE	520
hyb1	VHPDAQEILDLTLEDNRDWYYSAIRQSPSPPPPEEESRGPFGHPPLPDKFQFELTLEEEEEEE	386
hyb2	-----	
2EL	-----	
PDE46	ISMAQIPCTAQEALTAQGLSGVEEALDATIAWEASPAQESLEVMAQEASLEAELEAVYLT	780
h6.1	ISMAQIPCTAQEALTAQGLSGVEEALDATIAWEASPAQESLEVMAQEASLEAELEAVYLT	580
hyb1	ISMAQIPCTAQEALTEQGLSGVEEALDATIAWEASPAQESLEVMAQEASLEAELEAVYLT	446
hyb2	-----	
2EL	-----	
PDE46	QQAQSTGSAPVAPDEFSSREEFVVAVSHSSPSALALQSPLLPAWRTL SVSEHAPGLPGLP	840
h6.1	QQAQSTGSAPVAPDEFSSREEFVVAVSHSSPSALALQSPLLPAWRTL SVSEHAPGLPGLP	640
hyb1	QQAQSTGSAPVAPDEFSSREEFVVAVSHSSPSALALQSPLLPAWRTL SVSEHAPGLPGLP	506
hyb2	-----	
2EL	-----	
PDE46	STAAEVEAQREHQAAKRACSACAGTFGEDTSALPAPGGGGSGGDPT	886
h6.1	STAAEVEAQREHQAAKRACSACAGTFGEDTSALPAPGGGGSGGDPT	686
hyb1	STAAEVEAQREHQAAKRACSACAGTFGEDTSALPAPGGGGSGGDPT	552
hyb2	-----	
2EL	-----	

Figure 3.1. Alignment of PDE4A4B (PDE46), PDE4A4C (h6.1), PDE4A7 (2EL), hyb1 and hyb2. Alignment of sequences was performed using the clustalw software (<http://www2.ebi.ac.uk/clustalw/>). The N-terminal of PDE4A4B is shown in black, the 9 residue unique N-terminal of h6.1 is shown in yellow, the regions of sequence common to all PDE4As is shown in dark blue, the N-terminal of the catalytic region found in all active PDE4As is shown in purple, the unique N-terminal of PDE4A7 is highlighted in green, the central core shared by all PDE4As is shown in blue, the C-terminal of PDE4A7 is shown in red and the C-terminal tail of all active PDE4As is shown in grey. The colour of these sequences corresponds to the coloured domains

Figure 3.2 Distribution of PDE4A4B (PDE46) in COS-1 cells. *A*, shows a schematic representation of the PDE4A4B protein with its unique 112 residue N-terminal shown in black, the UCR1, LR1, UCR2 and LR2 regions are shown in blue, the N-terminal of the catalytic unit (common to all active PDE4As) in purple, the central core in blue, the C-terminal of the catalytic unit (shared by all active PDE4As) is shown in aqua and the PDE4A C-terminal in grey. The first and last six amino acids of the protein are also indicated. *B*, COS-1 cells were either mock transfected or transfected with PDE4A4B construct and allowed to express for 48 hours. Cell lysates were lysed, disrupted and subjected to subcellular fractionation. 20µg of the S fraction and equal volumes of both the particulate fractions (P1 and P2) were separated by 10% SDS-PAGE before immunoprobining with the general PDE4A antisera. The migration of PDE4A4B is indicated, with the positions of standard protein molecular mass markers (in kDa) shown on the left. This immunoblot is representative of data from three separate experiments. *C*, COS-1 cells transfected with PDE4A4B were fixed, permeabilised and incubated with the general PDE4A antisera followed by Alexa-labelled anti-donkey antiserum used for the fluorescent detection of the enzyme. LSCM was used to image a section through the centre of the cell. The left hand panel shows the fluorescent image and the right hand panel shows the brightfield image of the transfected cell. The *horizontal white* bar shown in the panels is the 25µm scale marker.



3.2.3 Subcellular localisation of PDE4A7 (2EL)

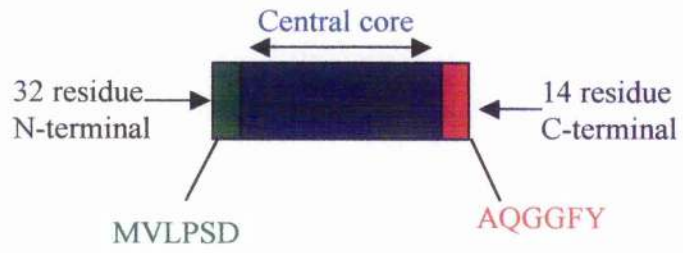
The *PDE4A* gene encodes the highly truncated, catalytically inactive PDE4A7 (2EL) enzyme. However, no studies have been done to analyse its intracellular distribution. Therefore the methods of general subcellular fractionation and LSCM were used to determine the intracellular location of this curious protein. That PDE4A7 is truncated at the C-terminal end means its expression cannot be detected using the general PDE4A antiscrum. Therefore, to overcome this problem PDE4A7 was engineered to contain the VSV-epitope tag (YTDIEMNRLGK) at its C-terminal. The nucleotide sequence of PDE4A7 has been aligned with both PDE4A4B and h6.1 (*figure 3.1*). The coloured residues represent the coloured domains shown in the subsequent schematic diagrams.

Subcellular analysis of COS-1 cells transfected with VSV-epitope tagged PDE4A7 (*figure 3.4, panel A*) were immunoprobed with the polyclonal anti-VSV antibody, which identified PDE4A7 as a 31 ± 5 kDa immunoreactive band associated exclusively with the P1 fraction (*figure 3.4, panel B*). As the P1 fraction contains both nuclear and cytoskeletal components, LSCM was used to determine the precise intracellular location of this protein. Once again, COS-1 cells were transfected to express PDE4A7, fixed, permeabilised and incubated with the polyclonal anti-VSV antibody followed by the Alexa293-labelled anti-goat antiserum for the fluorescent detection of this enzyme (Materials and Methods 2.2.5). Interestingly, the fluorescent signal for PDE4A7 was detected exclusively within the nuclear compartment (*figure 3.4, panel C*). One possibility then is that, as with previous studies done on PDE4 enzymes, the distribution of PDE4A7 is dependent on its unique N-terminal sequence. However, it is also possible that targeting of PDE4A7 could be achieved by its unique C-terminal region.

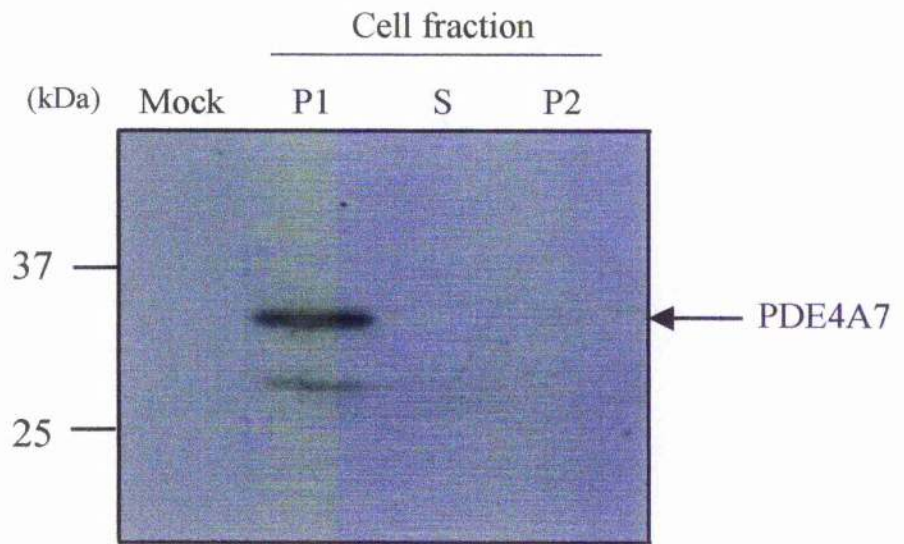
On the basis of previous studies performed whereby the unique N-terminal regions of PDE4s have been found to target them to specific intracellular locations, I expected that the extensively truncated PDE4A7 would be cytosolic. This was clearly not the case. So I set out to determine the basis for the nuclear localisation of PDE4A7 and why in contrast, PDE4A4B was found to be extranuclear. Initially, my strategy was to evaluate whether the N- or C- terminal regions of h6.1 allowed it to be targeted to the S2 fraction.

Figure 3.4 Distribution of PDE4A7 (2FL) in COS-1 cells. *A*, shows a schematic representation of PDE4A7 protein with its unique N-terminal highlighted in green, the central core in blue and the unique 14 residue C-terminal in red. The first and last six amino acids of the protein are also indicated. *B*, COS-1 cells were either mock transfected or transfected with the PDE4A7 construct and allowed to express for 48 hours. Cells were lysed, disrupted and subjected to subcellular fractionation. 20µg of the S fraction and equal volumes of both the particulate fractions (P1 and P2) were separated by 10% SDS-PAGE and immunoprobed with the polyclonal anti-VSV antibody. The migration of PDE4A7 is indicated, with the position of the standard protein molecular mass markers (in kDa) shown on the left. This immunoblot is representative of data from three separate experiments. *C*, COS-1 cells transfected with PDE4A7 were fixed, permeabilised and incubated with the VSV-polyclonal antibody followed by Alexa-labelled anti-goat antiserum used for the fluorescent detection of the enzyme. LSCM was used to image a section through the centre of the cell. The left hand panel shows the fluorescent image and the right hand panel shows the brightfield image of the transfected cell. The *horizontal white bar* shown in the panels is the 25µm scale marker.

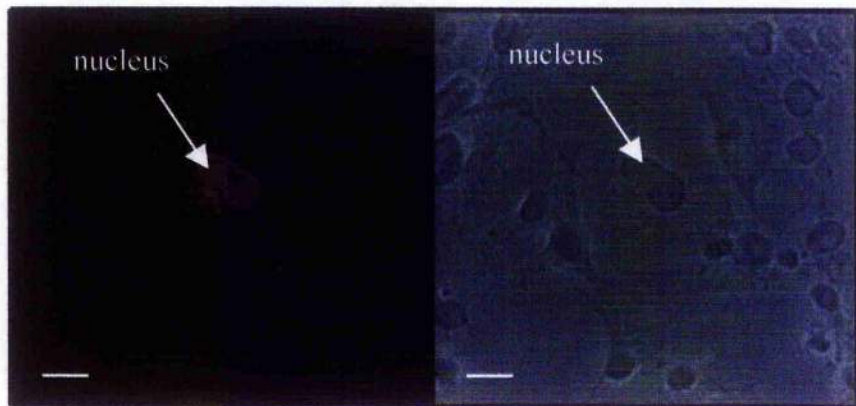
A



B



C



3.2.4 Subcellular distribution of the PDE4A7 chimeras, *hyb1* and *hyb2* in COS-1 cells

Targeting studies were performed on the PDE4A7 chimeras of *hyb1* and *hyb2* to evaluate whether fusing the N- or C-terminal regions of h6.1 to PDE4A7 could target it into the cytosol. *Hyb1* and *hyb2* were originally engineered to determine whether PDE4A7 was inactive by virtue of its C- or N-terminal truncation, respectively [Erdogan and Houslay, unpublished]. *Hyb1* is a fusion between the unique N-terminal 32 amino acids of PDE4A7 and the last 520 amino acids of h6.1 (also shared by all other active PDE4As) (*figure 3.5, panel A*), whereas *hyb2* is a fusion between the first 443 amino acids of h6.1 and the unique 14 amino acid C-terminal region of PDE4A7 (*figure 3.6, panel A*). *Hyb1* and *hyb2* sequences have been aligned with the other PDE4As (*figure 3.1*) with coloured residues corresponding to the coloured domains on the subsequent schematic diagrams.

Hyb1 was used here to determine whether replacing the C-terminal region of PDE4A7 with the C-terminal of h6.1 would cause PDE4A7 to target to the S2 fraction. Subcellular fractions of *hyb1*-transfected COS-1 cells were immunoprobed with the general PDE4A antisera, which identified *hyb1* as a 76 ± 2 kDa species located not only in the cytosol but also showing both P1 and P2 association (*figure 3.5, panel B*, Table 3.1 shows densitometry data). As the N-terminal region of PDE4A4B was found responsible for its association with the P2 fraction previously, it was surprising to find that *hyb1*, which contains the N-terminal of h6.1, was still capable of associating with this fraction. One possible explanation for the aberrant targeting of *hyb1* to the P2 fraction might be that extensive truncation has caused it to adopt a different conformation to that of h6.1, possibly resulting in the exposure of an otherwise masked targeting motif. If time had permitted, LSCM would have proved useful in identifying the precise intracellular location of *hyb1*. This is because association with P2 fraction does not necessarily suggest plasma membrane localisation, as the P2 fraction also contains endosomes, lysosomes, golgi stacks and cytoskeletal components.

Subcellular fractionation analyses of *hyb2* were performed to determine whether replacing the N-terminal region of PDE4A7 with the N-terminal of h6.1 would alter the targeting of the central core of PDE4A7. As it is C-terminally truncated, *hyb2* was also engineered to contain the VSV-epitope tag at its C-terminus. Subcellular fractionation of *hyb2*-transfected COS-1 cells was done and fractions were immunoprobed with the polyclonal anti-VSV antibody. This identified *hyb2* as a 49 ± 2 kDa species associated mainly with the P1 fraction (*figure 3.6, panel B*, Table 3.1 shows densitometry data) as

with PDE4A7. From these data I concluded that sequence within the C-terminal region of h6.1 was responsible for its S2 distribution. This might explain why PDE4A7, which is truncated at the C-terminus and therefore lacks this domain, cannot associate with the S2 fraction. These data also prove that the targeting information of PDEs is not strictly located within their unique N-terminal regions.

Table 3.1 Distribution of h6.1, hyb1 and hyb2 in COS-1 cells

These data are given as means \pm S.D. for three separate experiments.

Construct	Subcellular Fraction		
	P1 (%)	S (%)	P2 (%)
PDE4A4B	33 \pm 6	60 \pm 4	17 \pm 6
h6.1	20 \pm 4	80 \pm 4	-
hyb1	44 \pm 4	36 \pm 6	20 \pm 3
hyb2	92 \pm 5	8 \pm 4	-

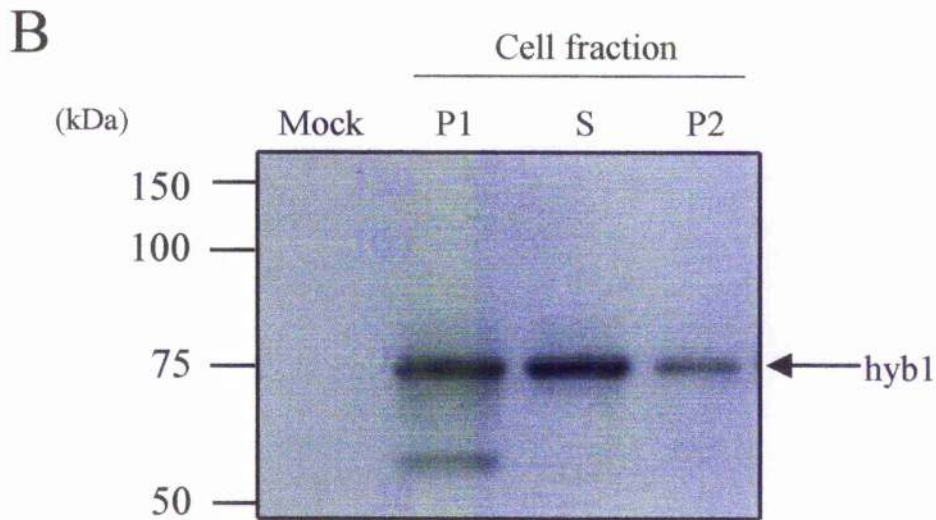
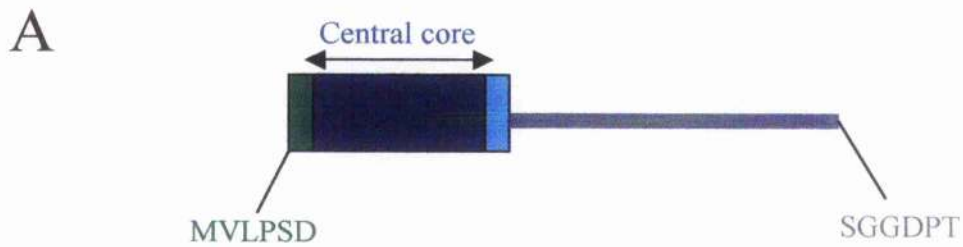


Figure 3.5 Subcellular localisation of *hyb1*. *A*, shows a schematic representation of the *hyb1* protein indicating the unique 32 residue N-terminal of PDE4A7 in green, the central core in blue, the C-terminal of the catalytic subunit shared by all active PDE4As shown in aqua and the PDE4A C-terminal tail in grey. The first and last six amino acids of the protein are also indicated. *B*, COS-1 cells were either mock transfected or transfected with the *hyb1* construct and allowed to express for 48 hours. Cell lysates were subjected to subcellular fractionation and 20 μ g of the S fraction and equal volumes of both the particulate fractions (P1 and P2) were separated by 10% SDS-PAGE. Fractions were immunoprobed with general PDE4A antiserum. This immunoblot is representative of data obtained from three separate experiments. The migration of *hyb1* is indicated, with the positions of the standard molecular weight markers on the left. The mock lysate lane was taken from the same gel as the sample lanes.

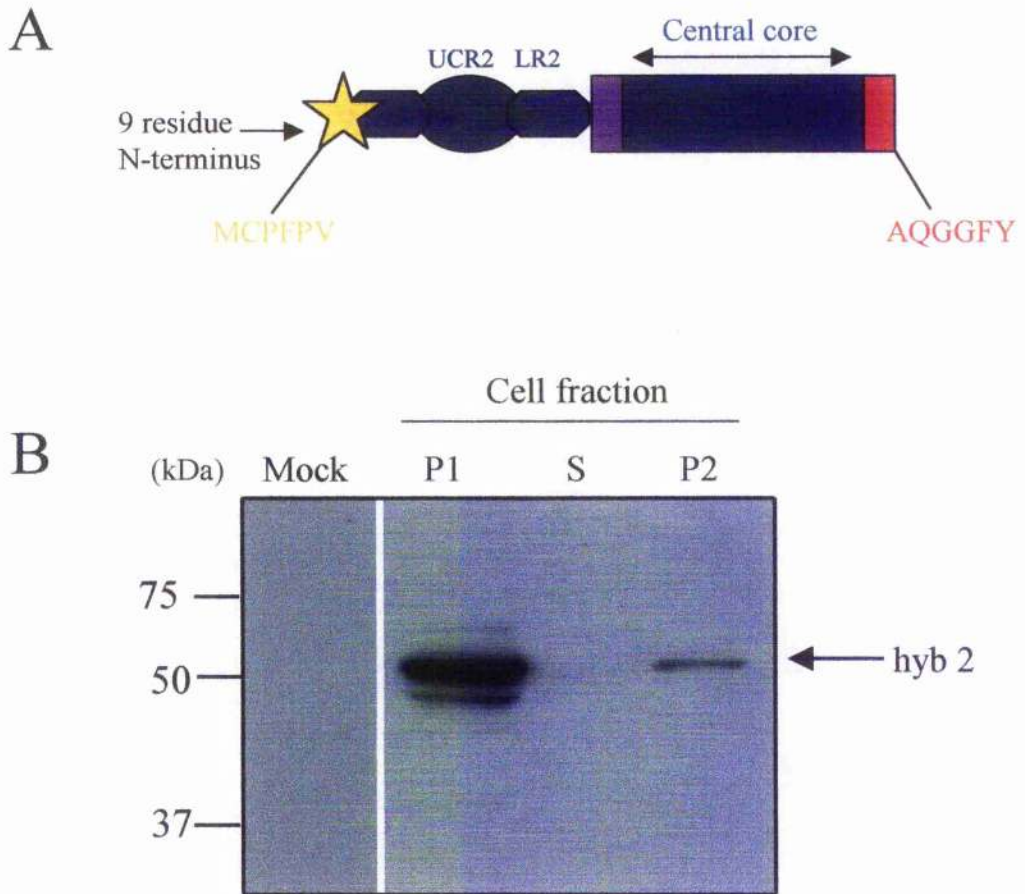


Figure 3.6 Subcellular localisation of hyb2. *A*, shows a schematic representation of the hyb2 protein indicating the unique 9 residue N-terminal in yellow, the sequence common to all PDE4As in blue, the N-terminal of catalytic subunit shared by all active PDE4As is shown in purple and the 14 residue C-terminal of PDE4A7 in red. The first and last six amino acids of the protein are also indicated. *B*, COS-1 cells were either mock transfected or transfected with the hyb2 construct and left to express for 48 hours. Cell lysates were subjected to subcellular fractionation. 20 μ g of the S fraction and equal volumes of both the particulate fractions (P1 and P2) were separated by 10% SDS-PAGE. Fractions were immunoprobed with the polyclonal anti-VSV antibody. This immunoblot is representative of data obtained from three separate experiments. The migration of hyb2 is indicated, with the positions of the standard protein molecular weight markers (in kDa) shown on the left. The mock lysate lane was taken from the same gel as the sample lanes.

3.2.5 Expression of *hyb1* truncates in COS-1 cells

My next aim was to gain insight into the basis for nuclear targeting of PDE4A7. Firstly I set out to determine whether the unique N- or C-terminal regions present in PDE4A7 were responsible for its P1 association. This was addressed by engineering two constructs. In the first construct (delta N-C), both the N- and C-terminal regions of PDE4A7 were deleted to leave the PDE4A core region. In the second construct only the C-terminal region of PDE4A7 was deleted (delta 309) to address whether the N-terminal of PDE4A7 harboured the targeting signal. As both of these constructs are C-terminally truncated, protein expression could not be detected using the general PDE4A antisera. To obviate this problem each truncate was engineered to contain a FLAG epitope tag (DYKDDDDK) at the C-terminal, which meant their expression could be detected by using the anti-FLAG antibody. COS-1 cells were transfected with each of the constructs, harvested and cell lysates were subjected to general subcellular fractionation before immunoblotting with the polyclonal FLAG antibody. The nucleotide sequences of the PDE4A7 truncates have been aligned with *hyb1* and PDE4A7. The coloured residues correspond to the coloured domains in the subsequent schematics (*figure 3.7*).

I expected that the extensively truncated delta N-C construct would be a fully soluble species and that association with the P1 would only occur when the PDE4A7 N-terminal was present. However, subcellular fractionation studies (Materials and Methods 2.2.1) identified the delta N-C construct (*figure 3.8, panel A*), as a 29 ± 3 kDa species associated exclusively with the low speed P1 fraction (*figure 3.8, panel B*). This result demonstrated that even in the absence of both the N- and C-terminals, the core of PDE4A7 (and of all PDE4As) was still targeted to the low speed P1 fraction. The next step was to determine whether the addition of the PDE4A7 unique N-terminal to the central core would alter this subcellular distribution. The delta 309 construct, which encodes amino acids 1-309 of the *hyb1* protein (*figure 3.10, panel A*) was associated with the P1 fraction only (31 ± 3 kDa) (*figure 3.10, panel B*). From these analyses I concluded that the sequence motif responsible for the P1 targeting of PDE4A7 was located within its central core and that the S2 targeting demonstrated by *hyb1* was due a motif located within its C-terminus. Determining the sequence motif in the *hyb1* C-terminus responsible for S2 distribution is of great interest as this C-terminal sequence is shared by all active long form PDE4s, and may therefore participate in their targeting.

In summary, residues within the C-terminal of *hyb1* appear to be involved in targeting it to the S2 fraction. In an attempt to identify the approximate location of this signal, C-terminal truncations of the *hyb1* construct were engineered (constructs were

made by Dr Ian McPhee). Again, each of these constructs were C-terminally truncated and were also engineered to contain the FLAG-epitope tag at their C-termini to allow detection of their expression by immunoblotting. The sequences of these *hyb1* truncates have been aligned with *hyb1* and PDE4A7, with coloured residues corresponding to the coloured domains in the subsequent schematics (*figure 3.7*).

The delta 328 construct, encoding amino acids 1-328 of *hyb1* (*figure 3.10, panel A*) was constructed to determine whether replacing the C-terminal of PDE4A7 with 19 amino acids from the C-terminal of *hyb1* would cause it to localise within the S2 fraction. Subcellular analyses identified delta 328 (32±4kDa) mainly within the P1 fraction, with some S2 distribution (*figure 3.10, panel B* and see Table 3.2). This demonstrated that the minimal common PDE4A C-terminal sequence required to confer S2 distribution on the PDE4A7 central core was located between amino acids 309 to 328 of the *hyb1* C-terminal region (corresponding to amino acids 643 to 662 of PDE4A4B). The most significant change in distribution was observed with the delta 410 construct, encoding amino acids 1-410 of *hyb1* (*figure 3.11, panel A* and see Table 3.2). This protein was identified as a 50±4kDa band in both the S2 and low speed P1 fractions, with some P2 association (*figure 3.10, panel B*). This data demonstrated that replacing the C-terminal of PDE4A7 with 101 amino acids from the PDE4A C-terminal caused the greatest shift of the PDE4A7 central core to the S2 fraction. To identify the motif responsible for allowing extranuclear targeting, then further truncations upstream of residue 328 in *hyb1* would have to be engineered and evaluated.

LSCM was performed on these constructs to determine their precise intracellular localisation, however, many problems were encountered with high background staining generated from the FLAG antibody, which made distinguishing between transfected and untransfected cells difficult. If time had permitted these constructs would have been engineered to contain the VSV-epitope tag instead because the anti-VSV antibody has been found in these studies to be more specific than the anti-FLAG antibody. Therefore, in the future it will be interesting to determine the precise intracellular distribution of *hyb1*, *hyb2* and the *hyb1* chimeras by using LSCM.

Table 3.2 Distribution of delta 328 and delta 410 in COS-1 cells

These data are given as means \pm S.D. for three separate experiments.

Construct	Subcellular Fraction		
	P1 (%)	S (%)	P2 (%)
delta 328	71 \pm 9	29 \pm 9	-
delta 410	55 \pm 4	37 \pm 5	8 \pm 4

hyb1	MVLPSDQGFKLLGNVLQGPEPYRLTSGRLRHQELENLNKWLNI FCVSDYAGGRSLTCI	60
NCTerm	-----QELLENLNKWLNI FCVSDYAGGRSLTCI	28
309	MVLPSDQGFKLLGNVLQGPEPYRLTSGRLRHQELENLNKWLNI FCVSDYAGGRSLTCI	60
328	MVLPSDQGFKLLGNVLQGPEPYRLTSGRLRHQELENLNKWLNI FCVSDYAGGRSLTCI	60
410	MVLPSDQGFKLLGNVLQGPEPYRLTSGRLRHQELENLNKWLNI FCVSDYAGGRSLTCI	60
2EL	MVLPSDQGFKLLGNVLQGPEPYRLTSGRLRHQELENLNKWLNI FCVSDYAGGRSLTCI	60
hyb1	MYMIFQERDLLKKFRI PVDTMVTYMLTLEDHYHADVAYHNSLHAADVLOSTHVLLATPAL	120
NCTerm	MYMIFQERDLLKKFRI PVDTMVTYMLTLEDHYHADVAYHNSLHAADVLOSTHVLLATPAL	88
309	MYMIFQERDLLKKFRI PVDTMVTYMLTLEDHYHADVAYHNSLHAADVLOSTHVLLATPAL	120
328	MYMIFQERDLLKKFRI PVDTMVTYMLTLEDHYHADVAYHNSLHAADVLOSTHVLLATPAL	120
410	MYMIFQERDLLKKFRI PVDTMVTYMLTLEDHYHADVAYHNSLHAADVLOSTHVLLATPAL	120
2EL	MYMIFQERDLLKKFRI PVDTMVTYMLTLEDHYHADVAYHNSLHAADVLOSTHVLLATPAL	120
hyb1	DAVFTDLEILAALFAAAIHDVDHPGVSNOFLINTNSELALMYNDESVLNHHLAVGFKLL	180
NCTerm	DAVFTDLEILAALFAAAIHDVDHPGVSNOFLINTNSELALMYNDESVLNHHLAVGFKLL	148
309	DAVFTDLEILAALFAAAIHDVDHPGVSNOFLINTNSELALMYNDESVLNHHLAVGFKLL	180
328	DAVFTDLEILAALFAAAIHDVDHPGVSNOFLINTNSELALMYNDESVLNHHLAVGFKLL	180
410	DAVFTDLEILAALFAAAIHDVDHPGVSNOFLINTNSELALMYNDESVLNHHLAVGFKLL	180
2EL	DAVFTDLEILAALFAAAIHDVDHPGVSNOFLINTNSELALMYNDESVLNHHLAVGFKLL	180
hyb1	QEDNCDI FQNL SKRQRQSLRKMVIDMVLATDMSKHMTLLADLKT MVETKKVTSSGVLLLD	240
NCTerm	QEDNCDI FQNL SKRQRQSLRKMVIDMVLATDMSKHMTLLADLKT MVETKKVTSSGVLLLD	208
309	QEDNCDI FQNL SKRQRQSLRKMVIDMVLATDMSKHMTLLADLKT MVETKKVTSSGVLLLD	240
328	QEDNCDI FQNL SKRQRQSLRKMVIDMVLATDMSKHMTLLADLKT MVETKKVTSSGVLLLD	240
410	QEDNCDI FQNL SKRQRQSLRKMVIDMVLATDMSKHMTLLADLKT MVETKKVTSSGVLLLD	240
2EL	QEDNCDI FQNL SKRQRQSLRKMVIDMVLATDMSKHMTLLADLKT MVETKKVTSSGVLLLD	240
hyb1	NYS DRIQVLRNMVHCADLSNPTKPLELYRQWTD RIMAEFFQQGDRERERGMEISPMCDKH	300
NCTerm	NYS DRIQVLRNMVHCADLSNPTKPLELYRQWTD RIMAEFFQQGDRERERGMEISPMCDKH	268
309	NYS DRIQVLRNMVHCADLSNPTKPLELYRQWTD RIMAEFFQQGDRERERGMEISPMCDKH	300
328	NYS DRIQVLRNMVHCADLSNPTKPLELYRQWTD RIMAEFFQQGDRERERGMEISPMCDKH	300
410	NYS DRIQVLRNMVHCADLSNPTKPLELYRQWTD RIMAEFFQQGDRERERGMEISPMCDKH	300
2EL	NYS DRIQVLRNMVHCADLSNPTKPLELYRQWTD RIMAEFFQQGDRERERGMEISPMCDKH	300
hyb1	TASVEKSQVGFIDYIVHPLWETWADLVHPDAQEILD TLEDNRDWYYSAIRQSPSPPEEE	360
NCTerm	TASVEKSQV-----	277
309	TASVEKSQV-----	309
328	TASVEKSQVGFIDYIVHPLWETWADLVH-----	328
410	TASVEKSQVGFIDYIVHPLWETWADLVHPDAQEILD TLEDNRDWYYSAIRQSPSPPEEE	360
2EL	TASVEKSQVQARGIDGRAQGGFY-----	323
hyb1	SRGPGHPPLPDKFQFELTLEEEEEEEISMAQIPCTAQEALTEQGLSGVEEALDATI AWEA	420
NCTerm	-----	
309	-----	
328	-----	
410	SRGPGHPPLPDKFQFELTLEEEEEEEISMAQIPCTAQEALTEQGLSGVEE-----	410
2EL	-----	
hyb1	SPAQESLEVMAQEASLEAELEAVYLTQQAQSTGSAPVAPDEFSSREEFVAVSHSSPSAL	480
NCTerm	-----	
309	-----	
328	-----	
410	-----	
2EL	-----	

```

hyb1  ALQSPLLPAWRRTLSVSEHAFGLPGLPSTAAEVEAQREHQAAKRACCSACAGTFGEDTSALP 540
NCterm -----
309   -----
328   -----
410   -----
2EL   -----

```

```

hyb1  APGGGGSGGDPT 552
NCterm -----
309   -----
328   -----
410   -----
2EL   -----

```

Figure 3.7. Alignment of hyb1 and PDE4A7 (2EL) with the engineered hyb1 chimeras. Alignment of these sequences were performed using the clustalw software (<http://www2.ebi.ac.uk/clustalw/>). The unique N-terminal of 2EL is highlighted in green, the central catalytic core shared by all PDE4As are shown in blue, the C-terminal of the catalytic domain found in all active PDE4As are shown in aqua, the C-terminal of 2EL is shown in red and the C-terminal tail shared by all active PDE4As is shown in grey. The colour of these sequences corresponds to the coloured domains of the schematics.

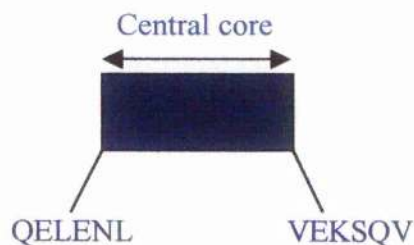
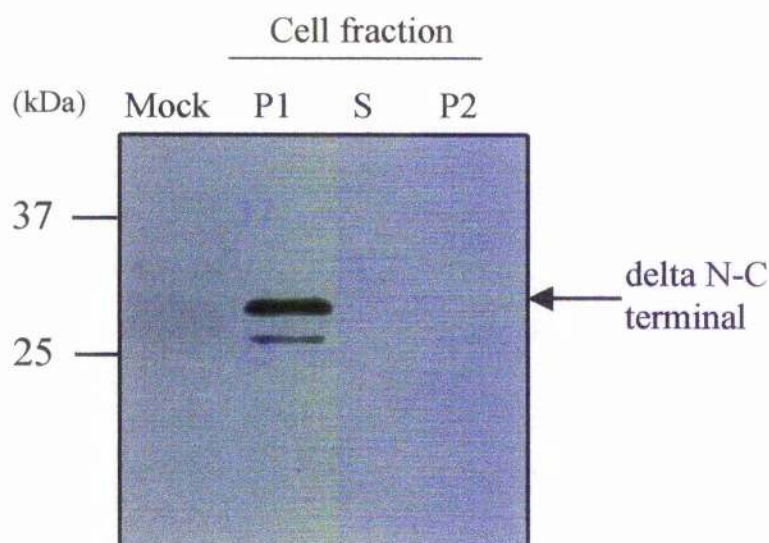
A**B**

Figure 3.8 Subcellular localisation of delta N-C terminal. *A*, shows a schematic representation of the delta N-C terminal that encodes the central core (blue). The first and last six amino acids of the protein are also indicated. *B*, COS-1 cells were either mock transfected or transfected with the delta N-C terminal construct and allowed to express for 48 hours. Cells were lysed, disrupted and subjected to subcellular fractionation. 20 μ g of the S fraction and equal volumes of both the particulate fractions (P1 and P2) were separated by 10% SDS-PAGE. Fractions were immunoblotted with the polyclonal anti-flag antibody.. This immunoblot is representative of data obtained from three separate experiments. The migration of delta N-C terminal is indicated, with the positions of the standard protein molecular mass standards (in kDa) shown on the left.

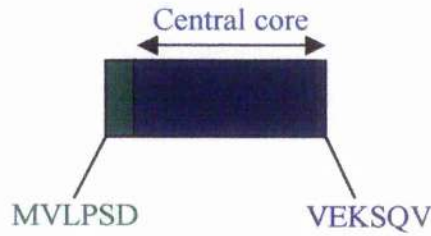
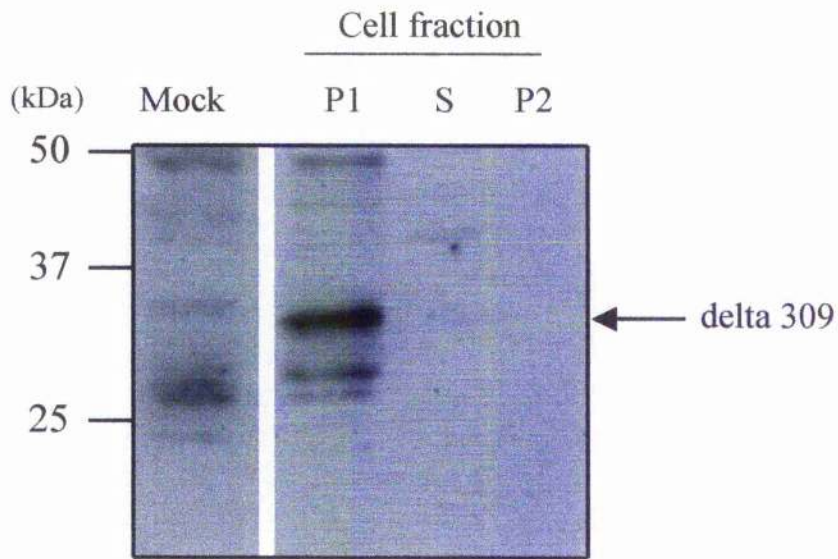
A**B**

Figure 3.9 Subcellular localisation of delta 309. *A*, shows a schematic representation of the delta 309 protein, with the unique 32 residue N-terminal of PDE4A7 shown in green and the central core domain in blue. The first and last six amino acids of the protein are also indicated. *B*, COS-1 cells were mock transfected or transfected with the delta 309 construct and allowed to express for 48 hours. Cells were lysed, disrupted and subjected to subcellular fractionation. 20 μ g of the S fraction and equal volumes of both the particulate fractions (P1 and P2) were separated by 10% SDS-PAGE. Fractions were immunoblotted with the polyclonal anti-flag antibody. This immunoblot is representative data from three separate experiments. The migration of delta 309 is indicated, with the position of the standard protein markers (in kDa) shown on the left. The mock lysate lane was taken from the same gel as the sample lanes.

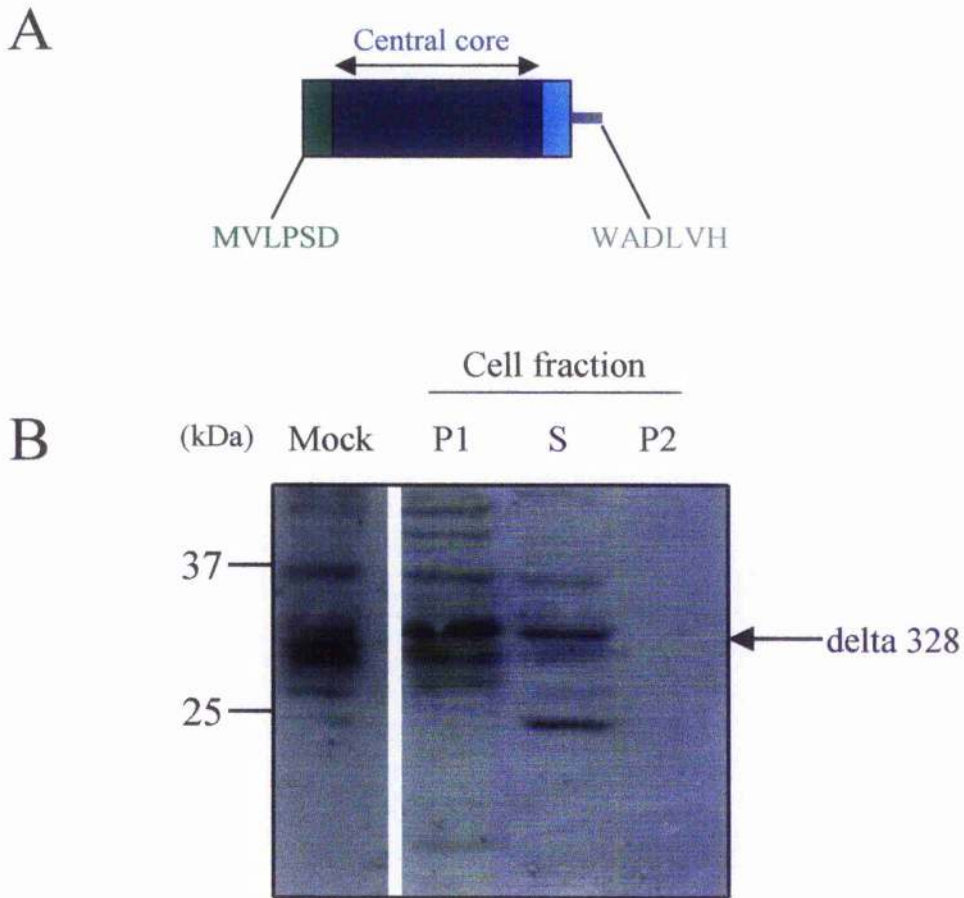
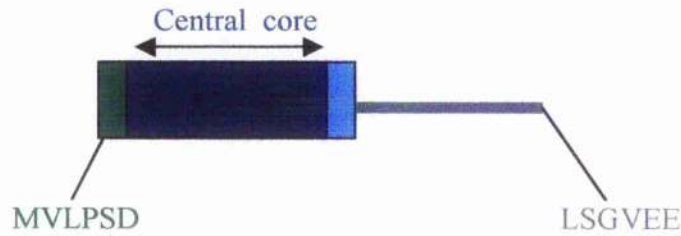


Figure 3.10 Subcellular localisation of delta 328. *A*, shows a schematic representation of the delta 328 protein indicating the unique 32 residue N-terminal of PDE4A7 in green, central core in blue, the C-terminal of the PDE4A catalytic unit (shared by all active PDE4As) in aqua and the truncated C-terminal tail of *hyb1* in grey. The first and last six amino acids of the protein are also indicated. *B*, COS-1 cells were either mock transfected or transfected with the delta 328 construct and allowed to express for 48 hours. Cells were lysed, disrupted and subjected to subcellular fractionation. 20 μ g of the S fraction and equal volumes of both the particulate fractions (P1 and P2) were separated by 10% SDS-PAGE. Fractions were immunoblotted with the polyclonal anti-flag antibody. This immunoblot is representative data from three separate experiments. The migration of delta 328 is indicated, with the positions of the standard protein molecular weight standards (in kDa) shown on the left. Both the mock lysate lane and sample lanes were taken from the same gel.

A



B

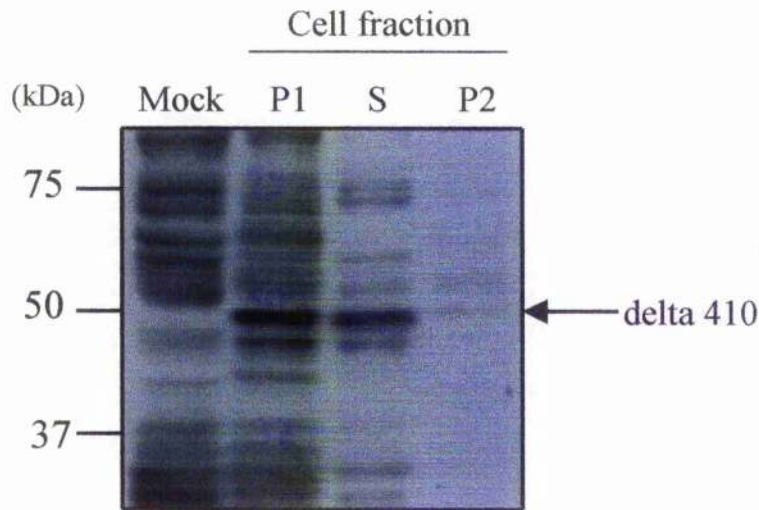


Figure 3.11 Subcellular localisation of delta 410. *A*, shows a schematic representation of the delta 410 protein indicating the unique 32 residue N-terminal of PDE4A7 in green, central core in blue, the C-terminal of the PDE4A catalytic unit (shared by all active PDE4As) in aqua and the truncated C-terminal tail of *hyb1* shown in grey. The first and last six amino acids of the protein are also indicated. *B*, COS-1 cells were either mock transfected or transfected with the delta N-C terminal construct and allowed to express for 48 hours. Cells were lysed, disrupted and subjected to subcellular fractionation. 20 μ g of the S fraction and equal volumes of both the particulate fractions (P1 and P2) were separated by 10% SDS-PAGE. Fractions were immunoblotted with the polyclonal anti-flag antibody. This immunoblot is representative of three separate experiments. The migration of delta 410 is indicated, with the positions of the standard molecular weight markers (in kDa) shown on the left.

3.2.6 Conclusions from targeting analysis of PDE4As

In summary, targeting studies performed on the *hyb1* and *hyb2* chimeras (section 3.2.4) demonstrated that replacing the C-terminal of PDE4A7 with the C-terminal region of *hyb1* was enough to cause some redistribution to the S2 fraction of COS-1 cells. Data from subcellular analyses performed on the *hyb1* truncates revealed that the minimum sequence required for S2 targeting was contained within amino acids 309 to 328 of the *hyb1* sequence. At this stage, the exact sequence motif responsible for this targeting was unknown.

3.2.7 Attempt to identify nuclear import and export signals on PDE4A7 and PDE4A4B, respectively.

The next aim was to gain more insight into the basis of nuclear entry for PDE4A7, as the nuclear import of proteins is a very tightly regulated process. Nuclear import is mediated by pores in the nuclear membrane called nuclear pore complexes (NPCs). The central channel of these pores allows the passive diffusion of smaller molecules (<40kDa) whereas the larger molecules (>40kDa) can only enter the nucleus by an energy-driven active transport process [Gorlich et al., 1999; Kaffman et al., 1999]. As PDE4A7 is only 32±3kDa in size it should, theoretically, be able to enter the nucleus by passive diffusion, however, this is unlikely as most of the proteins localised to the nuclear compartment are actively transported. Even proteins smaller (20-30kDa) than PDE4A7, such as histones [Kurz et al., 1997] depend on signal-mediated import. Proteins requiring active transport usually contain import signals that commonly fall into two categories, either consisting of 3-5 basic amino acid residues (monopartite) as first identified in the simian virus 40 (SV40) large T-antigen (PKKKRKV) [Kalderon et al., 1984], or of two basic stretches of amino acids separated by 10 amino acids (bipartite) as found in nucleoplasmin [Robbins et al., 1991].

Analysis of the PDE4A7 sequence for putative NLSs in PDE4As revealed two separate putative monopartite signals. KKFR is positioned between amino acids 72 and 75 and KKVT between amino acids 229 and 232 of PDE4A7. These NLS motifs are much shorter than the monopartite signal identified in the SV40 large T-antigen. However, a small basic motif of KRK has been shown to be sufficient to direct the nuclear import of the Src homology 2 domain-containing protein tyrosine phosphatase SHP-1 [Craggs et al., 2001]. If either KKFR or KKVT were NLSs in PDE4A7 then one might expect that all PDE4As would be capable of entering the nuclear compartment as these motifs are located

within the PDE4A central core domain that is shared by all PDE4As. However, PDE4A4B, which also harbours this sequence, is found outside the nucleus. Thus, it may be the large size of PDE4A4B that keeps it excluded from the nucleus, or, that only in the drastically truncated PDE4A7 do these putative NLSs become exposed. Alternatively, all PDE4A isoforms might have the ability to cycle through the nucleus, but that strong interactions with proteins outside the nucleus keep them excluded from this compartment.

Nucleolin was the first protein found to undergo nucleocytoplasmic shuttling [Borer et al., 1989], but ever since its discovery, a huge number of other proteins including steroid hormone receptors [Hache et al., 1999], transcription factors [Cartwright et al., 2000], cell cycle regulators [Pines et al., 1999] and transport receptors [Gorlich et al., 1999] have been found to cycle between the nucleus and cytoplasm. Shuttling proteins typically contain both an NLS and an NES [Mataj et al., 1998] although some proteins contain nucleocytoplasmic shuttling signals (NS) that are neither an NLS or an NES but can mediate both import and export [Michael., 2000]. The most common and researched type of NES contains a stretch of hydrophobic, leucine-rich residues and resemble the 'LX₍₁₋₃₎LX₍₂₋₃₎LXL' NES consensus [Kaffman et al., 1999; Wen et al., 1995]. Mutations of the crucial leucine residues in proteins containing well-characterised NESs were found to ablate their nuclear export [Henderson et al 2000].

Therefore, in order to cycle through the nucleus, PDE4As in addition to possessing an NLS, would also have to contain an NES. Analysis of the *hyb1* C-terminal sequence (also shared by all active PDE4As) for any putative NES was initially focussed to the sequence between amino acids 309 and 328 as this region was previously found to confer the cytosolic (S2) distribution on the central core of PDE4A7. However, no putative NESs were found in this region, but further downstream between amino acids 436 and 445 of *hyb1* (or amino acids 770 to 779 of PDE4A4B) the 'LEAELEAVYL' motif was identified, which resembled the common consensus NES motif. Therefore, the extranuclear targeting signal located within amino acids 309 and 328 may actually serve in mediating the interactions of the long forms with other proteins. I next hypothesised that both the active PDE4As and the inactive PDE4A7 were capable of entering the nucleus and that only the active PDE4A isoforms could exit from this compartment as they contained the C-terminal region that harbours the putative NES. To address these questions, the putative NLSs of PDE4A7 were removed by mutation and the putative NES was removed from *hyb1* by mutation.

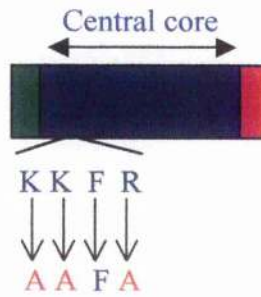
3.2.8 Mutational analysis of the putative nuclear import signal of PDE4A7

Firstly, to establish whether KKFR or KKVT were responsible for the nuclear import of PDE4A7, each domain was removed in the PDE4A7 protein by mutating the basic residues to aspartates (*figure 3.12, panel A* and *figure 3.13, panel A*) (engineered by Irene Gall). The subcellular fractions of COS-1 cells over-expressing either the KKFR or KKVT mutant were immunoblotted with the polyclonal VSV antibody which identified the 34±2kDa immunoreactive band of PDE4A7 only in the P1 fraction in both cases (*figure 3.12, panel B* and *figure 3.13, panel B*). If either of these motifs had been functional NLSs then an accumulation of these proteins within the S2 fraction would have been expected. This result suggested that neither the KKFR or KKVT motifs were responsible for import of PDE4A7 into the nucleus. In the future it would be interesting to analyse the targeting of these constructs using LSCM.

3.2.9 Mutational analysis of the putative export signal in PDE4A4B

Secondly to determine whether the putative NES found in the C-terminal of PDE4As was responsible for exporting them from the nuclear compartment, the leucine residues in this domain of *hyb1* were removed by mutation to aspartate (engineered by Irene Gall). As before, subcellular fractions of COS-1 cells over-expressing the *hyb1* NES mutant were immunoblotted with PDE4A antisera, but unfortunately this construct did not express. Therefore, the question of whether the 'LEAELEAVYL' motif of PDE4As functions as an NES remains to be resolved, as time constraints did not allow me to pursue this study any further.

A



B

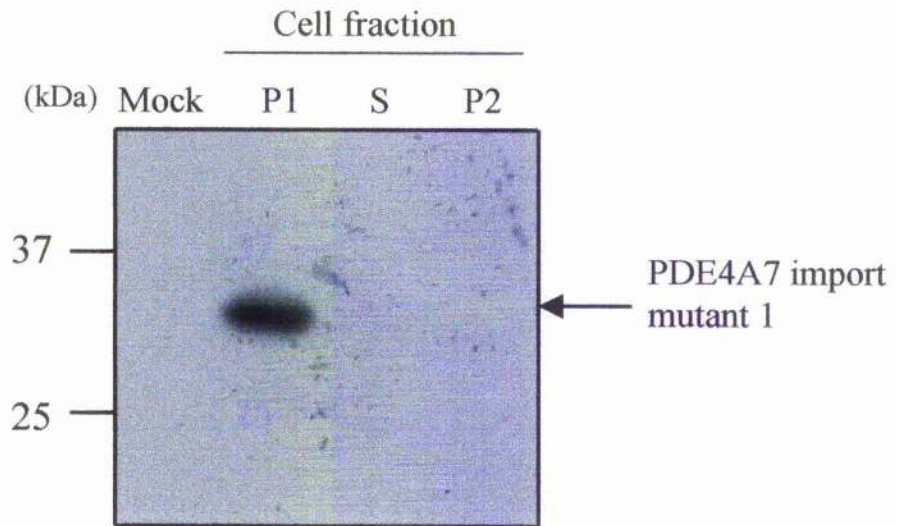
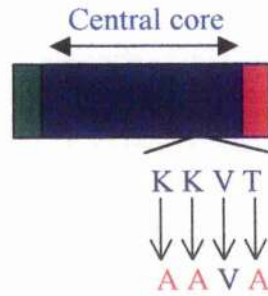


Figure 3.12 Subcellular localisation of PDE4A7 containing import mutation 1. *A*, shows a schematic representation of the PDE4A7 import mutant protein indicating the unique N-terminal of PDE4A7 in green, the central core in blue and the unique 14 residue C-terminal of PDE4A7 in red. The position of the amino acids that were mutated are also shown. *B*, COS-1 cells were either mock transfected or transfected with the KKFR PDE4A7 import mutant and allowed to express for 48 hours. Cells were lysed, disrupted and subjected to subcellular fractionation. 20 μ g of the S fraction and equal volumes of both the particulate fractions (P1 and P2) were separated by 10% SDS-PAGE. Fractions were immunoblotted with the polyclonal anti-VSV antibody. This immunoblot is representative of data from three separate experiments. The migration of the PDE4A7 import mutant is indicated, with the standard protein molecular weight standards (in kDa) shown on the left.

A



B

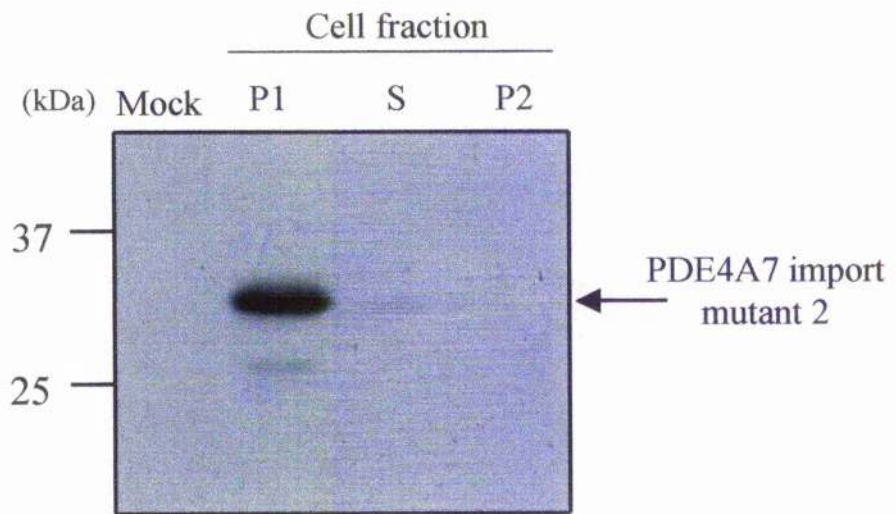


Figure 3.13 Subcellular localisation of PDE4A7 containing import mutation 2. *A*, shows a schematic representation of PDE4A7 import mutant 2 protein, with the unique N-terminal of PDE4A7 in green, the central core in blue and the unique 14 residue C-terminal of PDE4A7 in red. The position of the amino acids that were mutated are also indicated. *B*, COS-1 cells were either mock transfected or transfected with the KKVT PDE4A7 import mutant and allowed to express for 48 hours. Cells were lysed, disrupted and subjected to subcellular fractionation. 20µg of the S fraction and equal volumes of both the particulate fractions (P1 and P2) were separated by 10% SDS-PAGE. Fractions were immunoblotted with the polyclonal anti-VSV antibody. This immunoblot is representative of data from three separate experiments. The migration of the PDE4A7 import mutant is indicated with the positions of the standard molecular weight standards (in kDa) shown on the left.

3.2.10 Engineering an NES to the C-terminal of PDE4A7

My previous hypothesis was that PDE4A7 was restricted to the nuclear compartment because it lacked the PDE4A C-terminal containing the NES. However, it was yet to be proven whether an NES was capable of causing PDE4A7 to relocate to the cytosol. To address this question PCR was used to fuse the 'LQLPPLERLTLTYI' NES of PKI α onto the C-terminal of PDE4A7 cDNA. The sequence of the primers used are given below with the PCR conditions used for amplification described in Materials and Methods 2.3.10.1.

	Primer
	S= Sense A= Antisense
S	GATAATGGTGTCTTCCTTCAGACCAAGGC
A	GTTACTTTCCCAGCCTGTTTCATCTCTATATCGGTGTACAACGTTAGACGCTC CAACGGCGGCAGCTGCAGATAAAACCCAC

Table 3.3 Table showing the sense and antisense primers used to incorporate the NES of PKI α onto the C-terminal of PDE4A7

The sizes of the resultant PCR products were checked by 1% agarose gel electrophoresis, in which the clear band of PDE4A7 was detected as a 1000bp band in all cases (*figure 3.14, panel A*). The TOPO cloning kit from Invitrogen was used to insert the PDE4A7 NES-containing cDNA into the pcDNA3.1/V5-His-TOPO vector (Materials and Methods 2.3.10.3). These PCR products were used to transform Ecoli that were streaked out onto ampicillin plates and left to grow overnight at 30°C (colonies will only grow if they contain the TOPO vector carrying the ampicillin resistance gene) (Materials and Methods 2.3.10.2). Resultant colonies were PCR screened (Materials and Methods 2.3.10.3) to check that plasmids contained the PDE4A7 insert, only three of the six colonies screened were found to contain the PDE4A7 insert (*figure 3.14, panel B, lanes 1, 2 and 6*), therefore, a further six colonies were screened, of which another four were found to contain PDE4A7 (data not shown). These plasmids were then sequenced to confirm that PDE4A7 had been inserted into the TOPO vector in the correct orientation (Materials and Methods 2.3.11). Unfortunately all constructs contained numerous mutations in the attached NES. The only construct that was suitable for evaluation was one where a key leucine residue had been replaced with valine. As valine is also hydrophobic, it should not, theoretically, upset the 3:2:1 distribution of key hydrophobic residues. RanBP-1, which

undergoes nuclear export also contains a valine residue at this key position, therefore, there was the possibility that this mutated NES sequence of PKI α may still be recognised by its export receptor.

The NES of PKI α was chosen as export assays have shown that this is one of the most active export signals [Henderson et al., 2000]. Subcellular fractions of COS-1 cells over-expressing the PDE4A7 NES-containing protein were immunoblotted with the polyclonal VSV-antibody, which identified a 40 \pm 3kDa band of PDE4A7 only in the P1 fraction. This result indicated that PDE4A7 could not exit the nucleus by virtue of an exogenously added NES. A number of reasons may explain this finding. Firstly, the mutation of one of the important leucine residues to valine may have been enough to prevent this NES from being recognised by its cognate export receptor. It is possible that PDE4A7 is tightly associated with another protein in the nuclear compartment and that the export signal of PKI α was not strong enough to over-come this binding affinity. Also, PDE4A7 may adopt a conformation that masks the NES and prevents it from being recognised by the nuclear export machinery. Indeed, the NES of PKI α remains buried in this protein until PKI α interacts with its substrate of cAMP dependent kinase [Wen et al., 1995] indicating that presentation of this NES is crucial to its functioning.

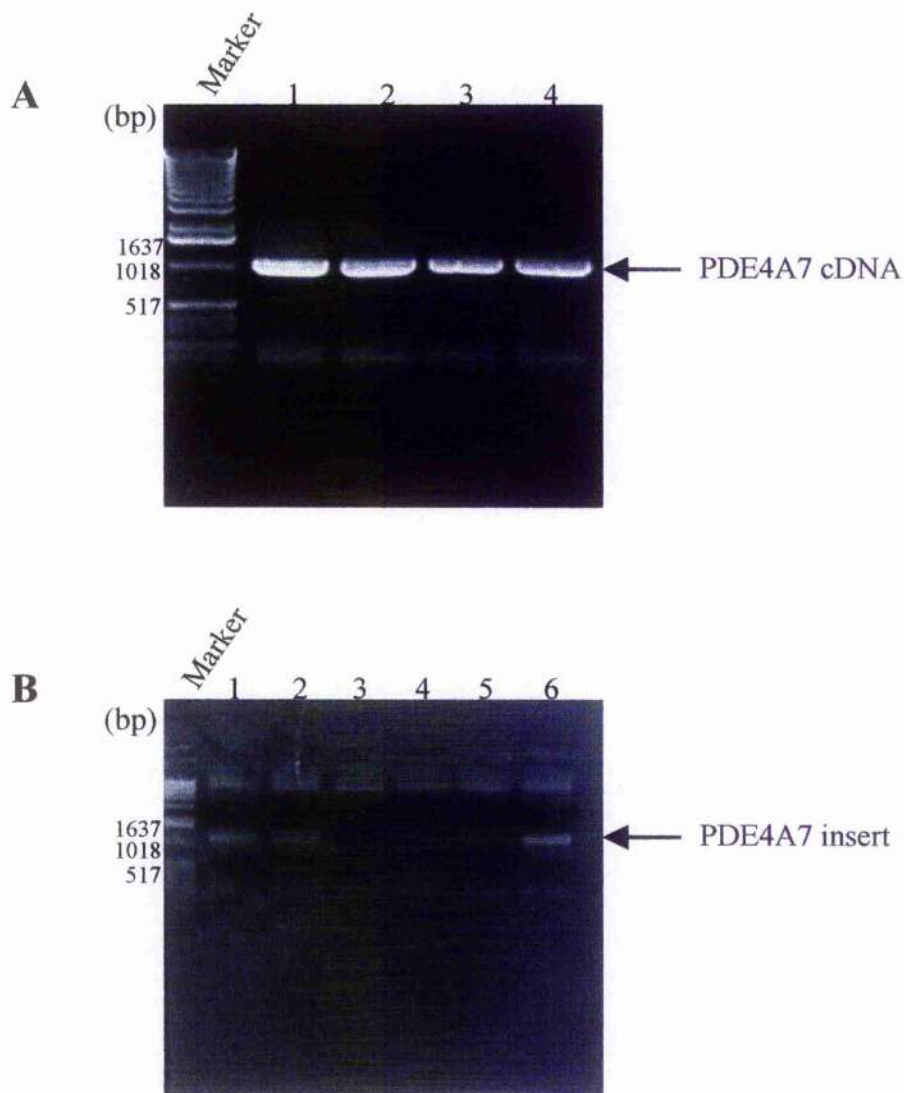


Figure 3.14 Engineering the NES of PKI α to the C-terminal of PDE4A7. *A*, PCR was used to fuse the NES of PKI α to the 3' end of PDE4A7 cDNA. PCR products were analysed by 1% agarose gel electrophoresis. *B*, PDE4A7 NES-containing cDNA was inserted into the TOPO cloning vector (see materials and methods). This TOPO vector was transformed into *E. coli* that were plated out onto ampicillin plates and grown overnight at 30°C. Resultant colonies were PCR screened using the T7 and PDE4A7 reverse NES primer to identify those vectors containing the PDE4A7 insert. Product sizes were analysed by 1% agarose gel electrophoresis. The migration of size markers (in bp) are indicated on the left.

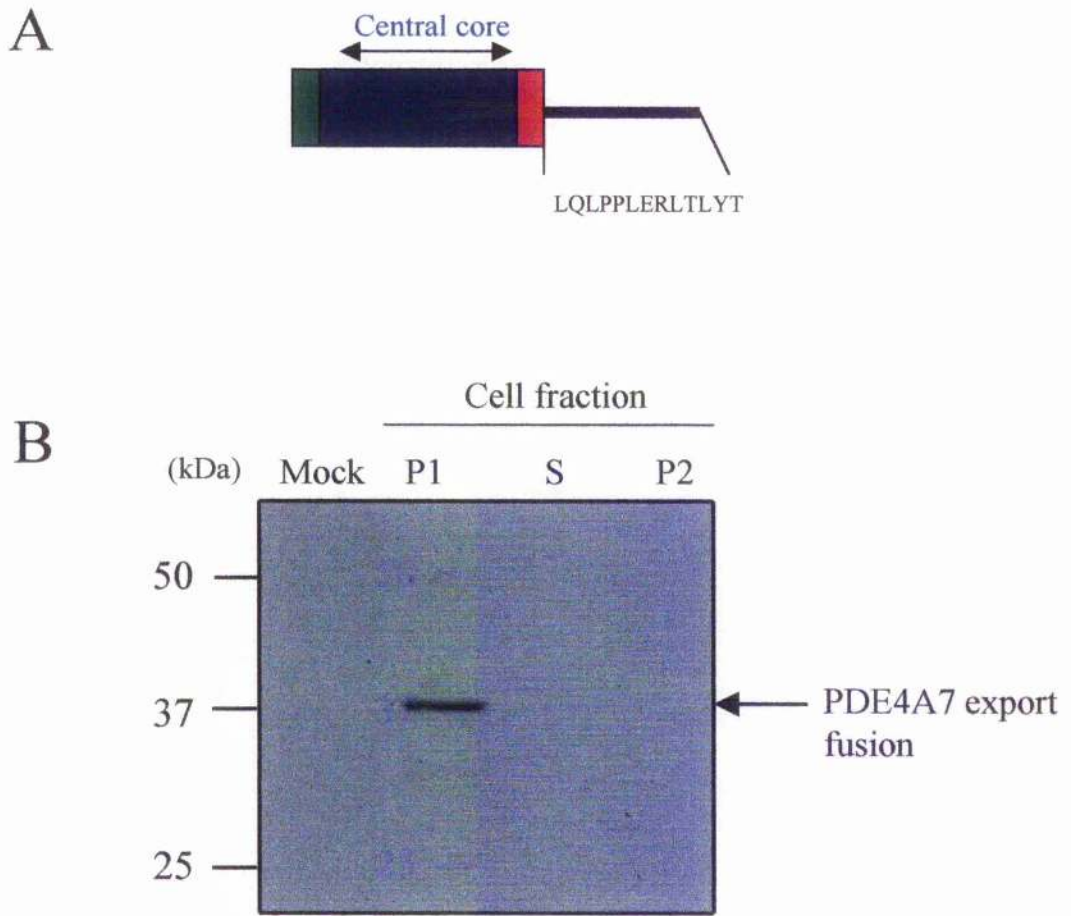


Figure 3.15 Subcellular localisation of PDE4A7 containing a NES. *A*, shows a schematic representation of the PDE4A7 NES-containing protein, with the unique 32 residue N-terminal of PDE4A7 shown in green, central core in blue, unique 14 residue C-terminal in red and the engineered NES in black. The position of the putative NES that was mutated is also shown. *B*, COS-1 cells were either mock transfected or transfected with the PDE4A7 export construct and allowed to express for 48 hours. Cells were lysed, disrupted and subjected to subcellular fractionation. 20 μ g of the S fraction and equal volumes of both the particulate fractions (P1 and P2) were separated by 10% SDS-PAGE. Fractions were immunoblotted with the polyclonal anti-VSV antibody. The migration of the PDE4A7 export protein is indicated, with position of the standard molecular mass protein standards (in kDa) shown on the left. This immunoblot is representative of data from three separate experiments.

3.3 Discussion

As the role of PDEs within cells is to regulate the levels of cyclic nucleotides, it was surprising to find that the PDE4A gene encoded a splice variant, PDE4A7, that is devoid of any catalytic activity. My study of this protein began by focussing on its intracellular targeting. I made the novel discovery that PDE4A7 was located exclusively to the nuclear compartment of COS-1 cells when over-expressed. This was interesting as previous work had demonstrated that a core complex formed from the catalytic unit and C-terminal were fully soluble, with targeting to membrane sites only achieved in the presence of isoform-specific N-terminals, thus I had expected that the highly truncated PDE4A7 would also be fully soluble [Scotland et al., 1995].

I next investigated whether replacing the unique N- or C-terminal regions of PDE4A7 with the N- and C-terminal regions common to all other PDE4As would alter its targeting. To address this the PDE4A7 chimeras of *hyb1* and *hyb2* were used. *Hyb1*, in which the unique C-terminal of PDE4A7 is fused to the C-terminal common to all active PDE4A isoforms was found in not only the particulate fractions (P1 and P2), but also in the S2 fraction. *Hyb2*, in which the unique C-terminal of PDE4A7 is fused to the N-terminal of h6.1, was found essentially in the P1 fraction. These studies demonstrated that the core of PDE4A7 could be targeted to the cytosol by replacing its unique C-terminal with 19 amino acids of the C-terminal region common to all PDE4As. I concluded that the signal that allowing for the extranuclear localisation of active PDE4As was contained within their C-terminals.

My next aim was to determine whether it was the unique N-terminal of PDE4A7 that was responsible for its targeting. To investigate this I used two constructs. In one construct, both the unique N- and C-terminal regions of PDE4A7 were deleted to leave only the central core that is common to all PDE4As (Δ N-C). The second construct only contained the core region and C-terminal of PDE4A7 (Δ 309). Both these constructs were found to associate exclusively with the P1 fraction of COS-1 cells. This was very surprising as I had expected that the central core alone would be fully soluble and that P1 distribution would only be restored when the N-terminal of PDE4A7 was present. I concluded from these analyses that the P1 association of PDE4A7 was mediated by sequence present in the central core and not the unique N- or C-terminal regions. This also proved that the S2 targeting of *hyb1* must be mediated by sequence in its C-terminal region.

In an attempt to identify the approximate location of this S2 signal in the PDE4A C-terminal, truncation analysis of the *hyb1* C-terminal region was performed. In one construct (delta 328), the C-terminal of PDE4A7 was replaced with 19 amino acids from the C-terminal sequence of *hyb1*. In the second construct (delta 410), the C-terminal of PDE4A7 was replaced with 101 amino acids from the *hyb1* C-terminal sequence. Subcellular analyses revealed that the minimal sequence required for to target the PDE4A7 core to the cytosol was contained within amino acids 309-328 of the *hyb1* C-terminal (amino acids 644 to 662 of PDE4A4B).

I next set out to identify the basis of PDE4A7 nuclear entry. On the basis that nuclear import is a highly regulated process and usually requires the presence of an NLS, I identified two putative NLSs namely KKFR and KKVT, located within the PDE4A7 central core. However, PDE4A4B, which also shares this core region is found located outside the nucleus. I hypothesised that the active PDE4A isoforms might cycle through the nucleus, but that stronger interactions outwith this compartment keep them excluded. The residues responsible for this interaction may reside within residues 309-328 of the *hyb1* C-terminus. Proteins that cycle between the nucleus and the cytosol typically contain both an NLS and NES. A putative NES was identified within the C-terminal of *hyb1* that is common to all PDE4As. This 'LEAELEAVYI.' motif was positioned between residues 436-445 in the *hyb1* sequence (between residues 770-779 of the PDE4A4B sequence). Therefore, I postulated that both active PDE4A long forms and PDE4A7 were capable of entering the nucleus, but that only the active forms could exit as they contained this NES. To address these questions both the NLSs and the NES were mutated. Subcellular analysis of the NLSs mutants demonstrated that neither KKVT nor KKFR were responsible for the nuclear import of PDE4A7. It would be interesting to mutate both sites together, in case just one of these signals alone can function to import the protein, even if the other one is no longer functional. Of course it is possible that PDE4A7 is transported to the nucleus by an unconventional NLS that bears no resemblance to the classical NLS motifs, such as the PPXXR motif found to mediate the import of Sam68 [Ishidate et al., 1997]. Alternatively, PDE4A7 may not contain any NLS itself but may gain entry into the nuclear compartment by piggybacking on a protein that does contain a classical NLS. Thus, as yet the transport mechanism for PDE4A7 remains to be elucidated.

The NES mutant of *hyb1* failed to express and whether the 'LEAELEAVYL' motif can act as an NES for the PDE4As remains to be investigated. Cycling of PDE4As could also be addressed in the future by treating cells over-expressing PDE4A4B (or other PDE4As) with the export inhibitor of Leptomycin B. Leptomycin B inhibits the nuclear

export receptor of CRM-1, which would be expected to cause PDE4A4B to accumulate in the nucleus. There is the possibility that PDE4As do not shuttle through the nucleus, and that after translation they simply reside in the cytosol. Even if an NLS was located in sequence common to both PDE4A7 and the other active PDE4As, this signal may be masked by the folding of PDE4A4B.

Finally, attempts were made to shift PDE4A7 from the nuclear compartment into the cytosol by fusing the NES of PKI α to the C-terminal region. In this study I expected to see PDE4A7 within the S2 fraction. However PDE4A7 was still associated exclusively with the P1 fraction. This suggested that such an NES may not suffice to 'pull' PDE4A7 out of the nucleus possibly because PDE4A7 may be tightly bound to another nuclear protein.

Here I have made a novel discovery that the highly truncated PDE4A7 is targeted to the nuclear compartment. This would suggest that PDE4A7 must have an important functional role within this compartment. The mechanism of nuclear localisation is unknown but I have demonstrated that a small portion from the C-terminal region found in all catalytically active PDE4A species is responsible for their S2 targeting.

Chapter 4

An attempt to identify PDE4A7 (2EL) interacting proteins

4.1 Introduction

As yet, the only PDE4A splice variant found to be exclusively localised within the nuclear compartment is the catalytically inactive PDE4A7 (2EL) splice variant. The mechanism used by PDE4A7 to gain entry to the nucleus remains to be elucidated. Originally, I postulated that PDE4A7 might be actively transported by virtue of sequences that resembled common nuclear localisation signals (NLSs). However, mutational analysis of the two putative NLSs found in PDE4A7 did not cause it to accumulate within the cytosol, as might be expected if they were functional NLSs. This suggests that PDE4A7 is transported into the nucleus by either an unconventional NLS or by a completely different process altogether. Although PDE4A7 is small enough to diffuse passively into the nucleus, literature has suggested that it is unlikely that even small proteins freely diffuse into this compartment and rather that their entry is strictly controlled [Gorlich et al., 1999]. It is possible that PDE4A7 contains no NLSs itself and that its nuclear entry is mediated by interacting with a protein that does contain an NLS. This process is called the 'piggy-back mechanism' and has been demonstrated by the (50kDa) glucokinase protein (GK), which enters into the nucleus by piggy-backing on the GK regulatory protein (GKRP) [Shiota et al., 1999].

In this chapter the yeast two-hybrid screening procedure was used to try and identify binding partners of PDE4A7. Identification of proteins interacting with PDE4A7 could give insight into the functional role of this curious protein within the cell and/or the mechanism used by PDE4A7 to gain entry into the nucleus (this project was performed with advice from Magda Magiera).

4.1.1 *The yeast two hybrid principal*

The yeast two-hybrid (Y2H) method uses the different functional domains of a transcription factor to study protein-protein interactions and was an idea first proposed over twenty years ago [Fields and Song., 1989]. The Matchmaker GAL4 Two-hybrid

System purchased from Clontech was used to identify putative binding partners for PDE4A7. This system is based on the principal that GAL4 cannot activate transcription unless its DNA binding domain (DNA-BD) and activation domain (AD) are physically associated. Usually, the DNA-BD and the AD are both part of the native GAL4 protein, but in the Matchmaker system these domains have been physically separated. The DNA-BD is derived from amino acids 1-147 of the yeast GAL4 protein and the activation domain from amino acids 768-881. Fusions of these domains to genes encoding proteins that may interact are generated using two different cloning vectors. Therefore the DNA-BD and AD domains will only interact if there is an association between the bait protein (in this case PDE4A7 which is fused to the DNA-BD) and the library protein (in this case human brain library fused to the AD) (*figure 4.1*). Interaction leads to the activation of reporter genes possessing promoters with GAL4-responsive elements. The expression of reporter genes allows yeast in which the protein-protein interaction has occurred to be detected by growing them on defined medium.

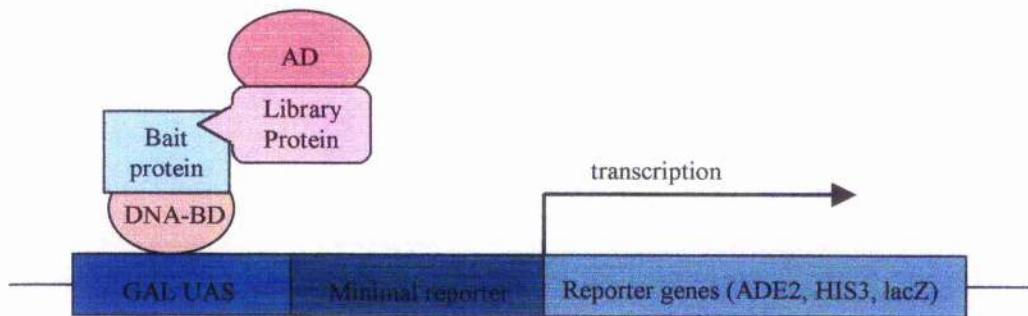


Figure 4.1 The yeast two-hybrid principle. GAL4 protein is a yeast transcription factor which activates genes involved in galactose metabolism. GAL4 binds to an Upstream Activating Sequence (UAS) which is located in GAL4-responsive genes. The GAL4 DNA binding (DNA-BD) and activation domains (AD) which are expressed as fusions are brought together as a result of protein-protein interaction causing expression of metabolic genes (in this case ADE2, HIS3, and lacZ) (diagram taken from the CLONTECH manual).

PDE4A7 cDNA. These PCR products were gel purified (Materials and Methods 2.3.6) and used in the subsequent digestions.

4.2.2 Digestion of pGBKT7 vector and PDE4A7 insert

Both the pGBKT7 vector and gel purified PDE4A7 cDNA (containing the appropriate restriction sites) were digested with the EcoRI and BamHI restriction enzymes (Material and Methods 2.3.7) and the product sizes were checked by 1% agarose gel electrophoresis. The digestion products were of the correct size as the PDE4A7 cDNA was detected as a band of 1000bp and the pGBKT7 vector as a ~7300bp band (*figure 4.3*). These products were gel purified (Materials and Methods 2.3.6) and used for ligation reactions (Materials and Methods 2.3.8).

Ecoli were transformed with the ligation products (Materials and Methods 2.3.10.2), plated onto kanamycin plates, to select for those bacteria containing the pGBKT7 vector (pGBKT7 contains the kanamycin resistance gene), and grown overnight at 30°C. Two checks were performed on plasmids from the resultant colonies to ensure they all contained the PDE4A7 insert. Firstly, colonies were PCR screened and product sizes were analysed by 1% agarose gel electrophoresis as before. The resultant PCR product from each colony was detected as a ~1000bp product, which is the correct size for the PDE4A7 (*figure 4.4*). Secondly, these plasmids were re-digested with EcoRI and BamHI enzymes to check that the PDE4A7 insert could be detected. The digested DNA was separated by agarose gel electrophoresis, which produced a band of ~7300bp representing the pGKBT7 vector and a 1000bp fragment corresponding to the PDE4A7 insert (data not shown).

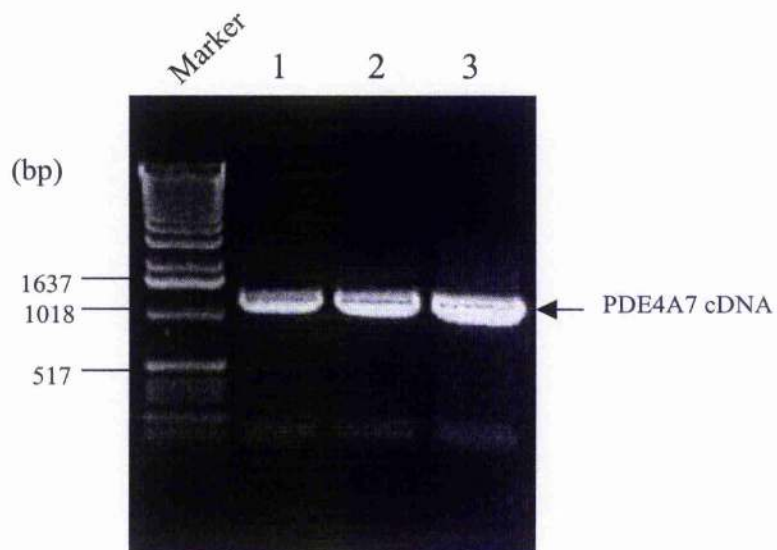


Figure 4.2 Incorporation of EcoRI and BamHI restriction sites into PDE4A7 cDNA. PCR was used to insert an EcoRI and a BamHI restriction sites at the 5' and 3' ends (respectively) of PDE4A7 cDNA. The PCR products were analysed by 1% agarose gel electrophoresis. The size markers (in bp) are shown on the left.

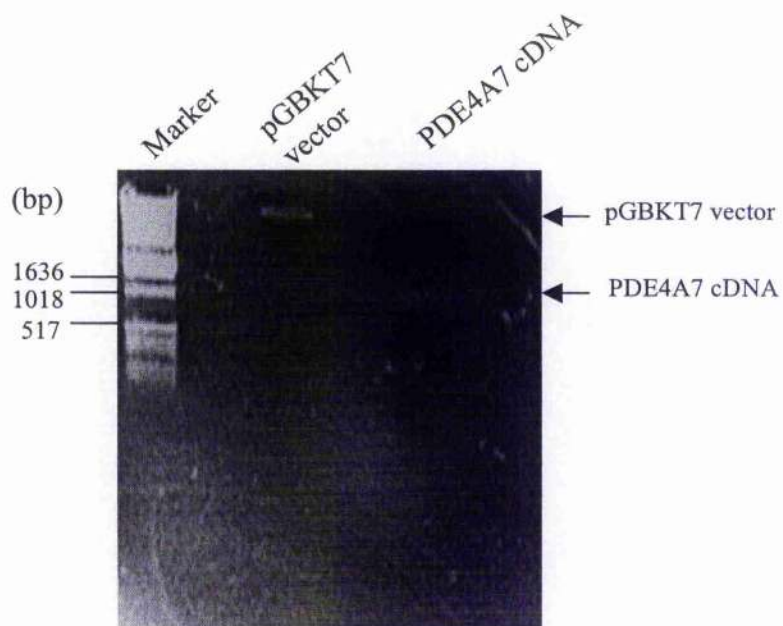


Figure 4.3 Digestion of the pGBKT7 vector and PDE4A7 cDNA. The pGBKT7 vector and PDE4A7 cDNA (containing the EcoRI and BamHI sites) were digested with the EcoRI and BamHI enzymes and product sizes were analysed by 1% agarose gel electrophoresis. The size markers (in bp) are shown on the left.

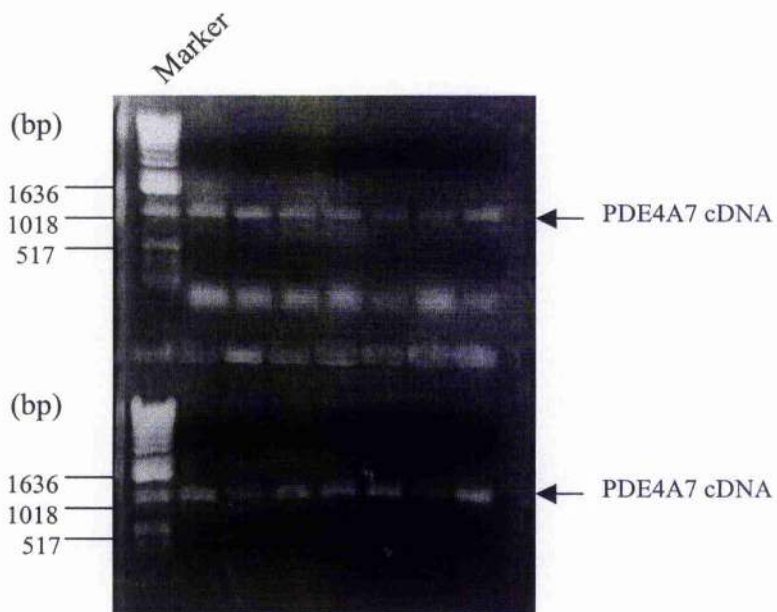


Figure 4.4 Identification of pGBKT7 vectors containing the PDE4A7 insert. The pGBKT7 vector and PDE4A7 cDNA were ligated, transformed into *E. coli*, plated onto ampicillin plates and grown overnight at 30°C. Resultant colonies were PCR-screened using the T7 and PDE4A7 BamHI primers to identify those PDE4A7 insert-containing pGBKT7 plasmids. Product sizes were analysed by 1% agarose gel electrophoresis. The migration size markers (in bp) are shown on the left.

4.2.3 Restriction analysis of pGBKT7-PDE4A7

To verify that the PDE4A7 cDNA had been inserted into pGBKT7 in the correct orientation, restriction analysis using the NcoI enzyme was performed (Materials and Methods 2.3.7). As well as a NcoI site present in multiple cloning region of the pGBKT7 vector, there is also a NcoI site at position 667 in the PDE4A7 sequence. Therefore, if PDE4A7 were inserted into the pGBKT7 vector correctly, a restriction digest should produce a DNA fragment of approximately 667bp. However, if PDE4A7 were inserted in the reverse orientation, restriction digestion with NcoI would produce a smaller fragment of 333bp.

The products of NcoI digestions performed on three of the putative pGBKT7-PDE4A7 plasmids were analysed by 1% agarose gel electrophoresis as before. All three plasmids were found to contain PDE4A7 in the correct orientation as only bands of ~667bp were detected from each digestion (*figure 4.4, lanes 1-3*). The DNA sequence of each of these plasmids were checked using automated sequencing (Materials and Methods 2.3.11), which also confirmed that the PDE4A7 insert was in the correct orientation.

4.2.4 Verification of PDE4A7 protein expression in the AH109 yeast reporter strain

To determine whether the PDE4A7 protein could be expressed successfully in the yeast reporter strain, the engineered pGBKT7-PDE4A7 construct was transformed into AH109 yeast cells (Materials and Methods 2.4.4). The pGBKT7 vector also encodes a c-Myc epitope tag (EQKLISEEDL) in frame with the GAL4 DNA-BD and bait protein. Thus, PDE4A7 expression could be detected using the anti c-Myc antibody. Protein was extracted from the AH109[empty-pGBKT7] or AH109[pGBKT7-PDE4A7] (Materials and Methods 2.4.5) and the resultant cell lysates were subjected to 10% SDS-PAGE electrophoresis and immunoblotted using the anti c-Myc antibody, which identified a 50kDa immunoreactive band representing PDE4A7, which was only detected in those AH109s that were transformed with pGBKT7-PDE4A7 (*figure 4.6*). PDE4A7 migrates at a higher molecular weight than normal because it is fused to the GAL4 activation domain. The previous result demonstrated that PDE4A7 could be expressed in AH109 cells and that any three of the engineered pGBKT7-PDE4A7 constructs would be suitable for use in the Y2H screen.

4.2.5 Testing for PDE4A7 bait protein toxicity effects

Preliminary tests were performed on the pGBKT7-PDE4A7 construct before proceeding with mating (these checks were carried out by Magda Magiera) see Materials and Methods 2.4.1). Firstly, the growth rates of AH109[empty-pGBKT7] and AH109[pGBKT7-PDE4A7] were compared to check the pGBKT7-PDE4A7 construct was non-toxic to the yeast. As growth rates were approximately the same it was concluded that this construct did not interfere with the growth of AH109s. Secondly, to check that PDE4A7 alone was incapable of inducing reporter gene activity, AH109s were co-transformed with pGBKT7-PDE4A7 and empty library vector pACT2 and compared with AH109s co-transformed with pGBKT7-p53 and pTD1-1, which are two proteins known to interact and therefore provided a positive control. These AH109s were then plated onto SD-Leu/-Trp and tested for β -galactosidase activity (Materials and Methods 2.4.8). Only colonies from those AH109s co-transformed with pGBKT7-p53 and pTD1-1 turned blue in colour as expected. Thus demonstrating that PDE4A7 alone was incapable of auto-activation. The final test was to check that the pGBKT7-PDE4A7 did not effect the mating efficiency of the yeast cells. In brief, the AH109[pGBKT7-PDE4A7] were mated with the Y187[pTD1-1] control strain and compared to the growth of Y187[pTD1-1] with AH109[pGBKT7-53] and subsequently plated on SD-Trp/-Leu. There were no major differences found in the mating efficiency (data not shown) indicating that the pGBKT7-PDE4A7 construct was suitable for use as bait in the Y2H screen.

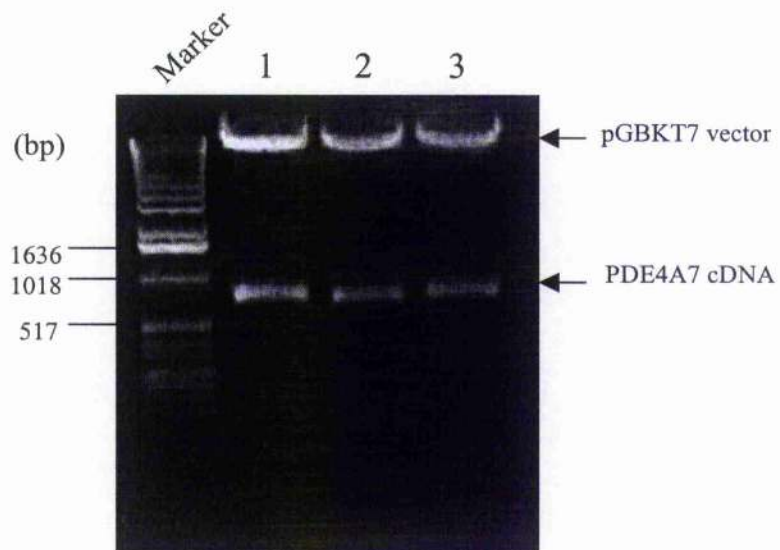


Figure 4.5 Restriction analysis of putative pGBKT7/PDE4A7 DNA. Putative pGBKT7/PDE4A7 DNA clones were digested using the NcoI enzyme and analysed by 1% agarose gel electrophoresis. The migration of the size markers are shown on the left.

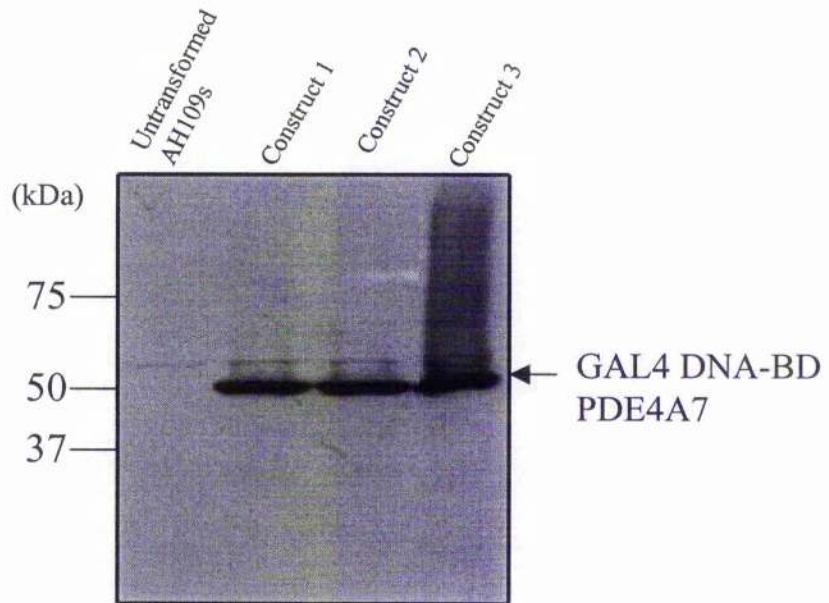


Figure 4.6 Verification of expression of PDE4A7 in AH109 yeast cells. AH109 yeast cells were transformed with the each of the three engineered pGBKT7/PDE4A7 constructs. Protein was extracted from pGBKT7/PDE4A7-transformed and untransformed AH109s (negative control) by TCA extraction and 20 μ g of each cell lysate was separated by 10% SDS-PAGE before immunoblotting with the anti-cMyc antibody. The migration of PDE4A7 containing the 16kDa GAL4D DNA-BD is indicated, with the positions of the standard protein molecular weight markers (in kDa) shown on the left.

4.2.6 Yeast mating

The previous tests showed that the pGBKT7-PDE4A7 bait was suitable for use in the Y2H screen. Therefore, AH109s containing the pGBKT7 bait were mated with Y187s containing the pACT2 library plasmid and plated onto selective quadruple dropout (QDO) medium (SD-Ade⁻/His⁻/Lcu⁻/Trp) (Materials and Methods 2.4.2, 2.4.7). This, QDO medium allows for the selection of yeast cells that have been transformed with plasmids carrying the appropriate nutritional marker. In this case the growth on -Lcu/-Trp selects for only those diploids containing the pACT2 and pGBKT7 plasmids, which introduce functional leucine and tryptophan genes (respectively). Secondly, the reason for omitting adenine and histidine from the medium, was that activation of the reporter genes encoding adenine and histidine would only occur in those diploids where the PDE4A7 bait interacts with a library insert. A total of seventy colonies were produced from this Y2H screen, however, to test if these colonies were true positives further analysis was required (see below).

4.2.7 Testing for β -galactosidase activity

Colonies produced from the yeast two-hybrid screen were plated out a further twice to increase the chance of selecting for true positives. Also, to confirm further that these resultant colonies were true positives, each were assayed for β -galactosidase activity (*figure 4.7*) (Materials and Methods 2.4.8). In colonies where an interaction between the bait and the library plasmid occurred the lacZ reporter gene was activated to produce the β -galactosidase enzyme, which catalysed X-gal to produce a blue coloured product. However, in those colonies where no interaction occurred the lacZ gene remained inactive and these cells were incapable of producing β -galactosidase for the degradation of X-gal, therefore these colonies remained white in colour. Out of the seventy colonies analysed only 20 turned blue. The library plasmid was rescued from each of these 20 colonies.

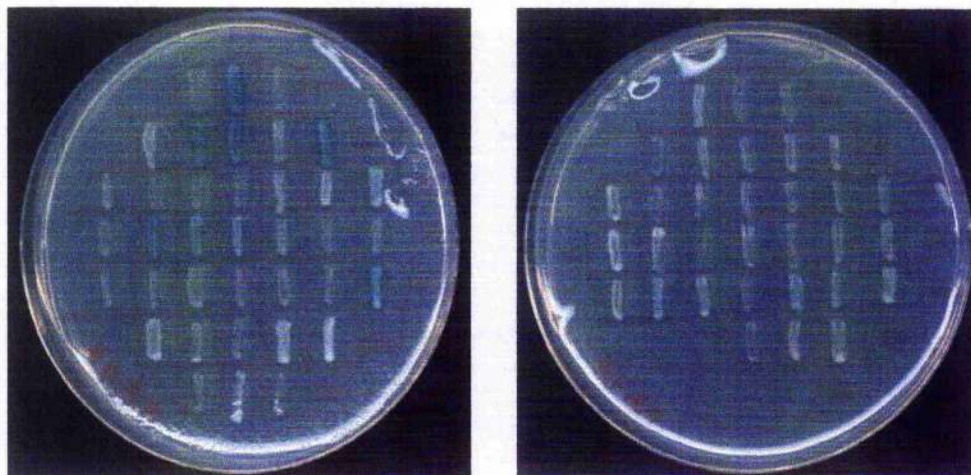


Figure 4.7 Testing positive colonies for β -galactosidase activity. AH109s containing the pGBKT7/PDE4A7 bait plasmid were mated with Y187s containing the pACT2 library-containing plasmid. Diploids were plated onto SD-Ade/-His/-Leu/-Trp and grown for 4-6 days at 30°C. Resultant positive colonies were re-streaked a further twice onto SD-Ade/-His/-Trp/-Leu. A sterile toothpick was used to streak surviving colonies out in a grid-like manner and grown for 2-4 days at 30°C, before assaying for β -galactosidase activity.

4.2.8 Rescue of the library plasmid

At this stage the yeast colonies contain a mixture of both the bait plasmid and the library plasmid, therefore, to identify the binding partner of PDE4A7 we had to enrich for the plasmid containing the library insert (Materials and Methods 2.4.9). In brief, both plasmids were isolated from the yeast colonies and the DNA was transformed into Ecoli unable to grow in the presence of ampicillin (Materials and Methods 2.3.10.2). The Ecoli were plated out on medium containing ampicillin so that only those Ecoli expressing the pACT2 plasmid (providing bacteria with the ampicillin resistance gene) would be rescued.

4.2.9 Proteins found to interact with PDE4A7 in the yeast two hybrid screen

All of the rescued activation plasmids were sequenced and the inserts were identified using the nucleotide blast search database located in the National Centre for Biotechnology Information (NCBI) website (<http://www.ncbi.nlm.nih.gov/BLAST/>). From a total of 20 colonies only 7 of the library plasmids generated quality sequence. Six binding partners were identified for PDE4A7, which included Ran binding protein 9 (RanBPM9), with five hits, CREB binding protein (CBP) with only one hit and mRNA from the human KIAA0160 gene with one hit. CBP is a nuclear protein that can bind to the phosphorylated form of the cAMP-responsive transcription factor CREB [Chirvia et al., 1993]. CBP participates in the activation of hundreds of different transcription. This suggested that PDE4A7 might also have an important role in the transcriptional regulation of various genes possibly of those involved in cAMP signalling. RanBPM9 is a 90kDa protein that is also found in the nucleus and in the cytoplasmic region surrounding the centrosome. It exists in a large complex of more than 670kDa. As yet the biological function of this complex remains to be elucidated [Nishitani et al., 2001], therefore it was hard to speculate the role for PDE4A7 within this protein complex. KIAA0160 is a relatively new gene for which the exact function remains to be elucidated [Nagase et al., 1995]. The nucleotide sequence of each of the inserts are shown in Table 4.1, with the areas of homology highlighted in grey. The nucleotide sequence of CBP, RanBPM and KIAA0160 have been aligned with those inserts that show sequence homology to them (*figure 4.8, figure 4.9 and figure 4.10, respectively*)

Table 4.1 Nucleotide sequences of inserts identified from the Y2H study

Insert identified	NCBI number	Nucleotide sequence of insert
CREB binding protein (Insert 1)	NM 004380	<p>TCCCCACCAA ACCCAAAAAA AGAGATCTCT ATGGCTTACC CATACGATGT TCCAGATTAC GCTAGCTTGG GTGGTCATAT GGCCATGGAG CCCCCGGGA TCCGAATTCG CGCCCGCTC GACGAGCAGG TGAATAATGGC TGAGAACTTG CTGGACGGAC CGCCCAACCC CAAAAGAGCC AACTCAGCT CGCCCGGTTT CTCGGCGAAT GACAGCACAG ATTTTGGATC ATTGTTTGAC TTGGAAAATG ATCTTCTGA TGAGCTGATA CCCAATGGAG GAGAATTAGG CCTTTTAAAC AGTGGGAACC TTGTTCAGA TGCTGCTTCC AAACATAAAC AACTGTCGGA GCTTCTACGA GGAGGCAGCG GCTCTAGTAT CAACCCAGGA ATAGGAAATG TGAGGCCAG CAGCCCGTG CAGCAGGGCC TGGGTGGCCA GGCTCAAGGG CAGCCGAACA GT</p>
RanBPM 9 (Insert 2)	NM 005493	<p>AAAGAGATCT CTATGGCTAC CCATACGATG TTCCAGATTA CGCTAGCTTG GGTGGTCATA TGGCCATGGA GGCCCGGGG ATCCGAATTC GCGGCCGCGT CGACCCGCT NCCCCTGCCT CAGCGGCTGC CCCCAGCAG GGGCCGCCC CTCCCCGGG CCTTGCAGCG GGCCCGGCC GGCTGGAGGA GCCCGAGCC CAGCTCTGGT GCGGGGAGC AGCGCCGCG CCCCCTTCC TCACGGGGAC TCGGCCCTGA ACGAGCAGGA GAAGGAGTTG CAGCGGCGGC TGAAGCGTCT CTACCCGCTG GTGGACGAAC AAGAGACGCC GCTGCTCGG TCCTGGAGCC CGAAGGACAA GTTCAG</p>
RanBPM 9 (Insert 3)	NM 005493	<p>CACCAAACCC AAAAAAAGAG ATCTCTATGG CTTACCCATA CGANGTTCCA GATTACGCTA GCTTGGGTGG TCATATGGCC ATGGAGGCC CGGGGATCCG AATTCGCGC CGCGTCGACC CGCCTCCCC TGCCTCAGG GCTGCCCCCG CCAGCGGGCC GCCGTCCCC GGGCCTTGA GCGGGCCCC GCCCGGCTGG AGGAGCCCGC ACCCCAGTCT TGGTGGCGGG CAGCAGCGCC CCGGCCCTC TCCCTCAGG GGAATCGGCC CTGAACGAGC AGGAGAAGGA GTTGCAGCGG CGGCTGAAGC GTCTTACCC GGGCTGGAC GAACAAGAGA CGCCGCTGCC TCGGTCTGG AGCCCGAAG ACAAGTTCAG CTAC</p>
RanBPM 9 (Insert 4)	NM 005493	<p>CCACCAACCC AAAAAGAATC TCTTGGCTAC CCATCGATGT TCCAGATTCCG CTAGCTTGGG TGGTCATATG GCATGGAGGC CCGGGGATCC GAATTCGCGG CCGCGTCGAC CCGTCCCC TGCTCAGCG GCTGCCCCCG CAGCGGGCCC GCCGTCCCC GGGCCTTGA AGCGGGCCCC GGCCCGGCTG GAGGAGCCCC GACCCAGCT CTGGTGGCGG GCAAGCAGCG CCGCGGCCCT CTTCCTCAC GGGGACTCGG CCCTGAACGA GCAGGAGAAG GAGTTGCAGC GCGGCTGAA GCGTCTTAC CCGGCCGTGG ACGAACAAGA GACGCCGCTG CCTCGTCTCT GGAGCCCGAA GGACAAGTTC A</p>
RanBPM 9 (Insert 5)	NM 005493	<p>AGAGATCTCT TGGCTNCCA TACGATGTTC CAGATTACGC TAGCTTGGGT GGTCATATGG CCATGGAGGC CCCGGGGATC CGAATTCGCG GNCGCTCGA CCCCTCCCC CTGCCTCAGC GGCTGCCCCC GCAGCGGGC CGCCCGCTCC CCCGGGCCTT GCAGCGGGCC CCGCGGGCT GGAGGAGCCC CGACCCAGC TCTGGTGGCG GGCAGCAGCG CCGGGGCCCT CTTCCTNAC GGGGACTCGG</p>
RanBPM 9 (Insert 6)	NM 005493	<p>AAGAGATCTC TATGGCTTAC CCATACNATG TTNCANATTC GCTNGCTNNG GTGGNCATAT GGCCATGGAG GCGCCGGTT CCGAATTCGC GGCCCGCTCG ACCCGCTCC CCCTGCCTCA GCGGCTGCC CCGCCAGCGG GCGCCCGCT CCCCCGGGCC TTGCAGCGGG CCGCGGCCG CTGGAGGAGC CCCGACCCCA GCTCTGGTGG CGGGCAGCAG GCGCGCGGCC CCCTTCCCTC ACGGGGACTC GGCCCTGAAC GAGCAGGAGA AGGAGTTGCA GCGGGCGCTG AAGCTCTCT ACCCGCGCT GGACGAACAA GAGACGCCG TGCTCGGTC CTGGAGCCCC AAGGACAAGT TCAGC</p>
KIAA0160 gene (Insert 7)	D63881	<p>AGATCTCTAT GGCTTACCCA TACGATGTTC CAGATTACGC TAGCTTGGGT GGTCATATGG CCATGGAGGC CCCGGGGATC CGAATTCGCG GCCGCTCGA CAAAAAAGA AAGGATGTAT GTTGTCCAAT AAGGCAAGTT CCCACAGGTA AAAAGCAGGT GCCTTTGAAT CCTGACCTCA ATCAAACAAA ACCTGGAAAT TTCCCGTCCC TTGCAGTTTC CAGTAATGAA TTTGAACCTA GTAACAGCCA CATGGTGAAG TCTTACTTGT TGCTATTTAG AGTGACTCGT CCAAGAAGAA GAGAGTTTAA TGGAATGATT AATGGAGAAA CCATGAAAAT ATTGATGTCA GTGAAGAGCT TCCAGCCAGA AGAAAAATGAA ATCGTGAGGA TGGGGAAAAG ACATTTGTTG CACAAATGAC ACTATTTGAT AAAAACAGTT AATGTTATG AACAGCGAG GCTCCACAA TGTCTGGAA ATGTTTTCAT TCTGAAGCAG AATATAATTA</p>

CBP	TGAGGAATCA	ACAGCCGCCA	TCTTGTGCGG	GACCCGACCG	GGGCTTCGAG	50
CBP	CGCGATCTAC	TCGGCCCCCG	CGGTCCCAGG	CCCCACAACC	GCCCGCGCTC	100
CBP	GCTCCTCTCC	CTCGCAGCCG	GCAGGGCCCC	CGACCCCGGT	CCGGGCCCTC	150
CBP	GCCGGCCCCG	CCGCCCGTGC	CCGGGGCTGT	TTTCGCGAGC	AGGTGAAAAT	200
Insert 1	-----	-----	-----	-----CGAGC	AGGTGAAAAT	
CBP	GGCTGAGAAC	TTGCTGGACG	GACCGCCCAA	CCCCAAAAGA	GCCAAACTCA	250
Insert 1	GGCTGAGAAC	TTGCTGGACG	GACCGCCCAA	CCCCAAAAGA	GCCAAACTCA	
CBP	GCTCGCCCCG	TTTCTCGGCG	AATGACAGCA	CAGATTTTGG	ATCATTGTTT	300
Insert 1	GCTCGCCCCG	TTTCTCGGCG	AATGACAGCA	CAGATTTTGG	ATCATTGTTT	
CBP	GACTTGAAAA	ATGATCTTCC	TGATGAGCTG	ATACCCAATG	GAGGAGAATT	350
Insert 1	GACTTGAAAA	ATGATCTTCC	TGATGAGCTG	ATACCCAATG	GAGGAGAATT	
CBP	AGGCCTTTTA	AACAGTGGGA	ACCTTGTTCC	AGATGCTGCT	TCCAAACATA	400
Insert 1	AGGCCTTTTA	AACAGTGGGA	ACCTTGTTCC	AGATGCTGCT	TCCAAACATA	
CBP	AACAACGTGC	GGAGCTTCTA	CGAGGAGGCA	GCGGCTCTAG	TATCAACCCA	450
Insert 1	AACAACGTGC	GGAGCTTCTA	CGAGGAGGCA	GCGGCTCTAG	TATCAACCCA	
CBP	GGAATAGGAA	ATGTGAGCGC	CAGCAGCCCC	GTGCAGCAGG	GCCTGGGTGG	500
Insert 1	GGAATAGGAA	ATGTGAGCGC	CAGCAGCCCC	GTGCAGCAGG	GCCTGGGTGG	
CBP	CCAGGCTCAA	GGGCAGCCGA	ACAGTGCTAA	CATGGCCAGC	CTCAGTGCCA	550
Insert 1	CCAGGCTCAA	GGGCAGCCGA	ACAGTG-----	-----	-----	
CBP	TGGGCAAGAG	CCCTCTGAGC	CAGGGAGATT	CTTCAGCCCC	CAGCCTGCCT	600
7601	TTTTTATTCC	TAGATGGAAC	TGCGACTTCC	GAGCCATGGA	AGGGTGGATT	7650
	GATGTTTAAA	GAAACAATAC	AAAGAATATA	TTTTTTTGTG	AAAAACCAGT	7700
	TGATTTAAAT	ATCTGGTCTC	TCTCTTTGGT	TTTTTTTGGG	CGGGGGGGTG	7750
	GGGGGGGTTT	TTTTTTTTTCC	GTTTTGTTTT	TGTTTGGGGG	GAGGGGGGTT	7800
	TTGTTTGGAT	TCTTTTTGTC	GTCATGCTG	GTGACTCATG	CCTTTTTTTA	7850
	ACGGGAAAAA	CAAGTTCATT	ATATTCATAT	TTTTTATTTG	TATTTTCAAG	7900
	ACTTTAAACA	TTTATGTTTA	AAAGTAAGAA	GAAAAATAAT	ATTTCAGAAT	7950
	GATTCCTGAA	ATAATGCAAG	CTTATAATGT	ATCCCGATAA	CTTTGTGATG	8000
	TTTCGGGAAG	ATTTTTTTCT	ATAGTGAACT	CTGTGGGCGT	CTCCCAGTAT	8050
	TACCCATGGAT	GATAGGAATT	GACTCCGGCG	TGCACACACG	TACACACCCA	8100
	CACACATCTA	TCTATACATA	ATGGCTGAAG	CCAAACTTGT	CTTGCAGATG	8150
	TAGAAATTGT	TGCTTTGTTT	CTCTGATAAA	ACTGGTTTTA	GACAAAAAAT	8200
	AGGGATGATC	ACTCTTAGAC	CATGCTAATG	TTACTAGAGA	AGAAGCCTTC	8250
	TTTTCTTTCT	TCTATGTGAA	ACTTGAAATG	AGGAAAAGCA	ATTCTAGTGT	8300
	AAATCATGCA	AGCGCTCTAA	TTCCTATAAA	TACGAAACTC	GAGAAGATTC	8350
	AATCACTGTA	TAGAATGGTA	AAATACCAAC	TCATTTCTTA	TATCATATTG	8400
	TTAAATAAAC	TGTGTGCAAC	AGACAAAAAG	GGTGGTCCTT	CTTGAATTCA	8450
	TGTACATGGT	ATTAACACTT	AGTGTTCGGG	GTTTTTTGTT	ATGAAAATGC	8500
	TGTTTTCAAC	ATTGTATTTG	GACTATGCAT	GTGTTTTTTC	CCCATTGTAT	8550
	ATAAAGTACC	GCTTAAAATT	GATATAAATT	ACTGAGGTTT	TTAACATGTA	8600
	TTCTGTCTTT	TAAGATCCCC	TGTAAGAATG	TTTAAGGTTT	TTATTTATTT	8650
	ATATATATTT	TTTGGTCTGT	TCTTTGTAAA	AAAAAAAAAA	AAAA	8650

Figure 4.8 Sequence alignment of the insert demonstrating homology to CREB binding protein (CBP). The nucleotide sequence of the insert demonstrating homology with the CBP protein has been aligned with the CBP protein nucleotide sequence. The CBP sequence is shown in black and the insert is shown in blue, with * marking the regions of insert sequence that do not align with CBP sequence.

```

RanBPM 9  CCGCCGTCGC  CCCC GCCTCC  CCCTGCCTCA  GCGGCTGCCC  CCGCCAGCGG  50
Insert 2  -----C CCGCCTCC  CCCTGCCTCA  GCGGCTGCCC  CCGCCAGCGG
Insert 3  -----C CCGCCTCC  CCCTGCCTCA  GCGGCTGCCC  CCGCCAGCGG
Insert 4  -----CTCC  CCCTGCCTCA  GCGGCTGCCC  CCGC*AGCGG
Insert 5  -----CTCC  CCCTGCCTCA  GCGGCTGCCC  CCGCCAGCGG
Insert 6  -----

RanBPM 9  GCGGCCGCT  CCCCCGGCC  TTGCAGCGGG  CCCCCGCCG  GCTGGAGGGG  100
Insert 2  GCGGCCGCT  CCCCCGGCC  TTGCAGCGGG  CCCCCGCCG  GCTGGAGGGG
Insert 3  GCGGCC***T  CCCCCGGCC  TTGCAGCGGG  CCCCCGCCG  GCTGGAGG*G
Insert 4  GCC*CCG*T  CCCCCGGCC  TTGCA*CGGG  CCCCCGCCG  GCTGGAGG*G
Insert 5  GCGGCCGCT  CCCCCGGCC  TTGCAGCGGG  CCCCCGCCG  GCTGGAGG*G
Insert 6  -----

RanBPM 9  CCCC GACCC  AGCTCTGGTG  GCGGGCAGCA  GCGCCGCGGC  CCCCTTCCCT  150
Insert 2  CCCC GACCC  AGCTCTGGTG  GCGGGCAGCA  GCGCCGCGGC  CCCCTTCCCT
Insert 3  CCCC GACCC  AGCTCTGGTG  GCGGGCAGCA  GCGCCGCGGC  CCCCTTCCCT
Insert 4  CCCC GACCC  AGCTCTGGTG  GCGGGCAGCA  GCGCCGCGGC  CCCCTTCCCT
Insert 5  CCCC GACCC  AGCTCTGGTG  GCGGGCAGCA  *CGCCGCGGC  CCCCTTCCCT
Insert 6  -----CGCCGCGGC  CCCCTTCCCT

RanBPM 9  CACGGGGACT  CGGCCCTGAA  CGAGCAGGAG  AAGGAGTTGC  AGCGGCGGCT  200
Insert 2  CACGGGGACT  CGGCCCTGAA  CGAGCAGGAG  AAGGAGTTGC  AGCGGCGGCT
Insert 3  CACGGGGACT  CGGCCCTGAA  CGAGCAGGAG  AAGGAGTTGC  AGCGGCGGCT
Insert 4  CACGGGGACT  CGGCCCTGAA  CGAGCAGGAG  AAGGAGTTGC  AGCGGCGGCT
Insert 5  *ACGGGGACT  CGG-----
Insert 6  CACGGGGACT  CGGCCCTGAA  CGAGCAGGAG  AAGGAGTTGC  AGCGGCGGCT

RanBPM 9  GAAGCGTCTC  TACCCGGCCG  TGGACGAACA  AGAGACGCCG  CTGCCTCGGT  250
Insert 2  GAAGCGTCTC  TACCCGGCCG  TGGACGAACA  AGAGACGCCG  CTGCCTCGGT
Insert 3  GAAGCGTCTC  TACCCGGCCG  TGGACGAACA  AGAGACGCCG  CTGCCTCGGT
Insert 4  GAAGCGTCTC  TACCCGGCCG  TGGACGAACA  AGAGACGCCG  CTGCCTCGGT
Insert 5  -----
Insert 6  GAAGCGTCTC  TACCCGGCCG  TGGACGAACA  AGAGACGCCG  CTGCCTCGGT

RanBPM 9  CCTGGAGCCC  GAAGGACAAG  TTCAGCTACA  TCGGCCTCTC  TCAGAACAAC  300
Insert 2  CCTGGAGCCC  GAAGGACAAG  TTCAG-----
Insert 3  CCTGGAGCCC  GAAGGACAAG  TTCAGCTAC-----
Insert 4  CCTGGAGCCC  GAAGGACAAG  TTC-----
Insert 5  -----
Insert 6  CCTGGAGCCC  GAAGGACAAG  TTCAGC-----

RanBPM 9  CTGCGGGTGC  ACTACAAAGG  TCATGGCAAA  ACCCAAAAG  ATGCCGCGTC  350
AGTTCGAGCC  ACGCATCCAA  TACCAGCAGC  CTGTGGGATT  TATTATTTTG  400
AAGTAAAAAT  TGTCAGTAAG  GGAAGAGATG  GTTACATGGG  AATTGGTCTT  450
TCTGCTCAAG  GTGTGAACAT  GAATAGACTA  CCAGGTTGGG  ATAAGCATTC  500
ATATGGTTAC  CATGGGGATG  ATGGACATTC  GTTTTGTTC  TCTGGAACTG  550
GACAACCTTA  TGGACCAACT  TTCACTACTG  GTGATGTCAT  TGGCTGTTGT  600
GTTAATCTTA  TCAACAATAC  CTGCTTTTAC  ACCAAGAATG  GACATAGTTT  650
AGGTATTGCT  TTCCTGACC  TACCGCCAAA  TTTGTATCCT  ACTGTGGGGC  700
TTCAAACACC  AGGAGAAGTG  GTCGATGCCA  ATTTTGGGCA  ACATCCTTTC  750
GTGTTTGATA  TAGAAGACTA  TATGCGGGAG  TGGAGAACCA  AAATCCAGGC  800
ACAGATAGAT  CGATTTCCCTA  TCGGAGATCG  AGAAGGAGAA  TGGCAGACCA  850
TGATACAAAA  AATGGTTTCA  TCTTATTTAG  TCCACCATGG  GACTGTGACC  900
ACAGCAGAGG  CCTTGGCCAG  ATCTACAGAC  CAGACCGTTC  TAGAAGAATT  950
AGCTTCCATT  AAGAATAGAC  AAAGAATTCA  GAAATGGTA  TTAGCAGGAA  1000
GAATGGGAGA  AGCCATTGAA  ACAACACAAC  AGTTATACCC  AAGTTTACTT  1050
GAAAGAAATC  CTAATCTCCT  TTTACATTA  AAAGTGCCTC  AGTTTATAGA  1100
AATGGTGAAT  GGTACAGATA  GTGAAGTACG  ATGTTTGGGA  GGCCGAAGTC  1150
CAAAGTCTCA  AGACAGTTAT  CCTGTTAGTC  CTCGACCTTT  TAGTAGTCCA  1200
AGTATGAGCC  CCAGCCATGG  AATGAATATC  CACAATTTAG  CATCAGGCAA  1250
AGGAAGCACC  GCACATTTT  CAGGTTTGA  AAGTTGTAGT  AATGGTGTA  1300

```

```

RanBPM 9  CCGCCGTCGC  CCCC GCCTCC  CCCTGCCTCA  GCGGCTGCCC  CCGCCAGCGG  50
Insert 2  -----C CCGCCTCC  CCCTGCCTCA  GCGGCTGCCC  CCGCCAGCGG
Insert 3  -----C CCGCCTCC  CCCTGCCTCA  GCGGCTGCCC  CCGCCAGCGG
Insert 4  -----CTCC  CCCTGCCTCA  GCGGCTGCCC  CCGC*AGCGG
Insert 5  -----CTCC  CCCTGCCTCA  GCGGCTGCCC  CCGCCAGCGG
Insert 6  -----

RanBPM 9  GCGGCCGCT  CCCCCGGCC  TTGCAGCGGG  CCCC GGCCG  GCTGGAGGGG  100
Insert 2  GCGGCCGCT  CCCCCGGCC  TTGCAGCGGG  CCCC GGCCG  GCTGGAGGGG
Insert 3  GCGGCC***T  CCCCCGGCC  TTGCAGCGGG  CCCC GGCCG  GCTGGAGG*G
Insert 4  GCC*CCG*T  CCCCCGGCC  TTGCA*CGGG  CCCC GGCCG  GCTGGAGG*G
Insert 5  GCGGCCGCT  CCCCCGGCC  TTGCAGCGGG  CCCC G*CCG  GCTGGAGG*G
Insert 6  -----

RanBPM 9  CCCC GACCC  AGCTCTGGTG  GCGGGCAGCA  GCGCCGCGGC  CCCCTTCCCT  150
Insert 2  CCCC GACCC  AGCTCTGGTG  GCGGGCAGCA  GCGCCGCGGC  CCCCTTCCCT
Insert 3  CCCC GACCC  AGCTCTGGTG  GCGGGCAGCA  GCGCCGCGGC  CCCCTTCCCT
Insert 4  CCCC GACCC  AGCTCTGGTG  GCGGGCAGCA  GCGCCGCGGC  CCCCTTCCCT
Insert 5  CCCC GACCC  AGCTCTGGTG  GCGGGCAGCA  *GCGCCGCGGC  CCCCTTCCCT
Insert 6  -----CGCCGCGGC  CCCCTTCCCT

RanBPM 9  CACGGGGACT  CGGCCCTGAA  CGAGCAGGAG  AAGGAGTTGC  AGCGGCGGCT  200
Insert 2  CACGGGGACT  CGGCCCTGAA  CGAGCAGGAG  AAGGAGTTGC  AGCGGCGGCT
Insert 3  CACGGGGACT  CGGCCCTGAA  CGAGCAGGAG  AAGGAGTTGC  AGCGGCGGCT
Insert 4  CACGGGGACT  CGGCCCTGAA  CGAGCAGGAG  AAGGAGTTGC  AGCGGCGGCT
Insert 5  *ACGGGGACT  CGG-----
Insert 6  CACGGGGACT  CGGCCCTGAA  CGAGCAGGAG  AAGGAGTTGC  AGCGGCGGCT

RanBPM 9  GAAGCGTCTC  TACCCGGCCG  TGGACGAACA  AGAGACGCCG  CTGCCTCGGT  250
Insert 2  GAAGCGTCTC  TACCCGGCCG  TGGACGAACA  AGAGACGCCG  CTGCCTCGGT
Insert 3  GAAGCGTCTC  TACCCGGCCG  TGGACGAACA  AGAGACGCCG  CTGCCTCGGT
Insert 4  GAAGCGTCTC  TACCCGGCCG  TGGACGAACA  AGAGACGCCG  CTGCCTCGGT
Insert 5  -----
Insert 6  GAAGCGTCTC  TACCCGGCCG  TGGACGAACA  AGAGACGCCG  CTGCCTCGGT

RanBPM 9  CCTGGAGCCC  GAAGGACAAG  TTCAGCTACA  TCGGCCTCTC  TCAGAACAAC  300
Insert 2  CCTGGAGCCC  GAAGGACAAG  TTCAG-----
Insert 3  CCTGGAGCCC  GAAGGACAAG  TTCAGCTAC-----
Insert 4  CCTGGAGCCC  GAAGGACAAG  TTC-----
Insert 5  -----
Insert 6  CCTGGAGCCC  GAAGGACAAG  TTCAGC-----

RanBPM 9  CTGCGGGTGC  ACTACAAAGG  TCATGGCAAA  ACCCAAAAG  ATGCCGCGTC  350
AGTTCGAGCC  ACGCATCCAA  TACCAGCAGC  CTGTGGGATT  TATTATTTTG  400
AAGTAAAAAT  TGTCAGTAAG  GGAAGAGATG  GTTACATGGG  AATTGGTCTT  450
TCTGCTCAAG  GTGTGAACAT  GAATAGACTA  CCAGGTTGGG  ATAAGCATTC  500
ATATGGTTAC  CATGGGGATG  ATGGACATTC  GTTTTGTTC  TCTGGAACTG  550
GACAACCTTA  TGGACCAACT  TTCACTACTG  GTGATGTCAT  TGGCTGTTGT  600
GTTAATCTTA  TCAACAATAC  CTGCTTTTAC  ACCAAGAATG  GACATAGTTT  650
AGGTATTGCT  TTCCTGACC  TACCGCCAAA  TTTGTATCCT  ACTGTGGGGC  700
TTCAAACACC  AGGAGAAGTG  GTCGATGCCA  ATTTTGGGCA  ACATCCTTTC  750
GTGTTTGATA  TAGAAGACTA  TATGCGGGAG  TGGAGAACCA  AAATCCAGGC  800
ACAGATAGAT  CGATTTCCCTA  TCGGAGATCG  AGAAGGAGAA  TGGCAGACCA  850
TGATACAAAA  AATGGTTTCA  TCTTATTTAG  TCCACCATGG  GACTGTGACC  900
ACAGCAGAGG  CCTTGGCCAG  ATCTACAGAC  CAGACCGTTC  TAGAAGAATT  950
AGCTTCCATT  AAGAATAGAC  AAAGAATTCA  GAAATGGTA  TTAGCAGGAA  1000
GAATGGGAGA  AGCCATTGAA  ACAACACAAC  AGTTATACCC  AAGTTTACTT  1050
GAAAGAAATC  CTAATCTCCT  TTTACATTA  AAAGTGCCTC  AGTTTATAGA  1100
AATGGTGAAT  GGTACAGATA  GTGAAGTACG  ATGTTTGGGA  GGCCGAAGTC  1150
CAAAGTCTCA  AGACAGTTAT  CCTGTTAGTC  CTCGACCTTT  TAGTAGTCCA  1200
AGTATGAGCC  CCAGCCATGG  AATGAATATC  CACAATTTAG  CATCAGGCAA  1250
AGGAAGCACC  GCACATTTT  CAGGTTTGA  AAGTTGTAGT  AATGGTGTA  1300

```

TATCAAATAA	AGCACATCAA	TCATATTGCC	ATAGTAATAA	ACACCAGTCA	1350
TCCAACCTGA	ATGTACCAGA	ACTAAACAGT	ATAAATATGT	CAAGATCACA	1400
GCAAGTTAAT	AACTTCACCA	GTAATGATGT	AGACATGGAA	ACAGATCACT	1450
ACTCCAATGG	AGTTGGAGAA	ACTTCATCCA	ATGGTTTCCT	AAATGGTAGC	1500
TCTAAACATG	ACCACGAAAT	GGAAGATTGT	GACACCGAAA	TGGAAGTTGA	1550
TTCAAGTCAG	TTGAGACGCC	AGTTGTGTGG	AGGAAGTCAG	GCCGCCATAG	1600
AAAGAATGAT	CCACTTTGGA	CGAGAGCTGC	AAGCAATGAG	TGAACAGCTA	1650
AGGAGAGACT	GTGGCAAGAA	CCTGCAAAAC	AAAAAATGT	TGAAGGATGC	1700
ATTCAAGTCTA	CTAGCATATT	CAGATCCCTG	GAACAGCCCA	GTTGGAAATC	1750
AGCTTGACCC	GATTCAGAGA	GAACCTGTGT	GCTCAGCTCT	TAACAGTGCA	1800
ATATTAGAAA	CCCACAATCT	GCCAAAGCAA	CCTCCACTTG	CCCTAGCAAT	1850
GGGACAGGCC	ACACAATGTC	TAGGACTGAT	GGCTCGATCA	GGAATTGGAT	1900
CCTGCGCATT	TGCCACAGTG	GAAGACTACC	TACATTAGCT	ATGCATTTCA	1950
AGAGCTCACA	CTTATATTGT	GGCATATAGT	CAACATGGAA	GTAGACCAGC	2000
TCTGCTGATT	TGAAATTTAG	ATTTTTTAAA	TTATGTACTG	GGGACAGGTT	2050
TTTGTGCTTT	TACATTGCTT	CCTAGTTTAC	AGCATGATGC	AAATGATTTT	2100
CTAACTTAGT	GTTAGGAGAA	ATTATTTTCC	ATCTTTAACC	TCTTAGTTGT	2150
CTAAGAGTTA	AATATTACTG	AATTTTCAGAC	GTTCAAATTG	ATCATCACAA	2200
ATCCTTTAAA	ACAATTACCT	AAAAGAAACC	AAAAATCCTG	CCTTCTTTGT	2250
GGGGGAGGGG	GGAGAGAGGG	GAAGGAAATG	GAACAAGTTG	TGTTTGTGTT	2300
AGCATGTGGG	TGATGTAAAC	TTCAAATTGG	GAGATGTTCC	GACCCC	2346

Figure 4.9 Sequence alignment of inserts demonstrating homology to the RanBPM9 protein. The nucleotide sequences of inserts demonstrating homology with RanBPM9 have been aligned with the RanBPM9 nucleotide sequence. The RanBPM9 sequence is shown in black and the insert is shown in blue, with * marking the regions of insert sequence that do not align with RanBPM9.

KIAA0160	CTCTGAGGAG	ACACTTTTTT	TTTCTCCCT	CCTTCCCTCC	TCTCTCTCTC	CCTTCCCTTC	60
	CCCTCTCTCT	CCCTCTCTCC	TCCTTCCCCC	CTCGGTCCGC	CGGAGCCTGC	TGGGGCGAGC	120
	GGTTGGTATT	GCAGGCGCTT	GCTCTCCGGG	GCCGCCCGCG	GGGTAGCTGG	CGGGGCGAGG	180
	AGGCAGGAAC	CGCGATGGCG	CCTCAGAAGC	ACGGCGGTGG	GGGAGGGGGC	GGCTCGGGGG	240
	CCAGCGCGGG	TCTCCGGGGA	GGCGGCTTCG	GGGGTTCGCG	GGCGGTGGCG	CGCGCGACGG	300
	CTTCGGGCGG	CAAATCCGGC	GGCGGGAGCT	GTGGAGGGGG	TGGCAGTTAC	TCGGCCTCCT	360
	CCTCCTCTCT	CGCGGCGGCA	GCGCGGGGGG	CTGCGGTGTT	ACCGGTGAAG	AAGCCGAAAA	420
	TGGAGCACGT	CCAGGCTGAC	CACGAGCTTT	TCCTCCAGGC	CTTTGAGAAG	CCAACACAGA	480
	TCTATAGATT	TCTTCGAACT	CGGAATCTCA	TAGCACCAAT	ATTTTTCACA	AGAACTCTTA	540
	CTTACATGTC	TCATCGAAAC	TCCAGAACAA	ACATCAAAAG	GAAAACATTT	AAAGTTGATG	600
	ATATGTTATC	AAAAGTAGAG	AAAATGAAAG	GAGAGCAAGA	ATCTCATAGC	TTGTCAGCTC	660
	ATTTGCAGCT	TACGTTTACT	GGTTTCTTCC	ACAAAAATGA	TAAGCCATCA	CCAAACTCAG	720
	AAAATGAACA	AAATTCGTGT	ACCCTGGAAG	TCCTGCTTGT	GAAAGTTTGC	CACAAAAAAA	780
KIAA0160	GAAAGGATGT	AAGTTGTCCA	ATAAGGCAAG	TTCCACAGG	TAAAAAGCAG	GTGCCTTTGA	840
Insert 7	GAAAGGATGT	A*GTTGTCCA	ATAAGGCAAG	TTCCACAGG	TAAAAAGCAG	GTGCCTTTGA	
KIAA0160	TTCCTGACCT	CAATCAAACA	AAACCCGGAA	ATTTCCCGTC	CCTTGCAGTT	TCCAGTAATG	900
Insert 7	TCCTGACCTT	CAATCAAACA	AAACC*GGAA	ATTTCCCGTC	CCTTGCAGTT	TCCAGTAATG	
KIAA0160	AATTTGAACC	TAGTAACAGC	CATATGGTGA	AGTCTTACTC	GTTGCTATTT	AGAGTGACTC	960
Insert 7	AATTTGAACC	TAGTAACAGC	CA*ATGGTGA	AGTCTTACT*	GTTGCTATTT	AGAGTGACTC	
KIAA0160	GTCCAGGAAG	AAGAGAGTTT	AATGGAATGA	TTAATGGAGA	AACCAATGAA	AATATTGATG	1020
Insert 7	GTCC*GGAAG	AAGAGAGTTT	AATGGAATGA	TTAATGGAGA	AACC*ATGAA	AATATTGATG	
KIAA0160	TCAATGAAGA	GCTTCCAGCC	AGAAGAAAAC	GAAATCGTGA	GGATGGGGAA	AAGACATTTG	1080
Insert 7	TCA*TGAAGA	GCTTCCAGCC	AGAAGAAAAC	GAAA*CGTGA	GGATGGGGAA	AAGACATTTG	
KIAA0160	TTGCACAAAT	GACAGTATTT	GATAAAAACA	GGCGCTTACA	GC'TTTTAGAT	GGGGAATATG	1140
Insert 7	TTGCACAAAT	GACAGTATTT	GATAAAAACA	GG-----			
KIAA0160	AAGTAGCCAT	GCAGGAAATG	GAAGAATGTC	CAATAAGCAA	GAAAAGAGCA	ACATGGGAGA	1200
	CTATTCTTGA	TGGGAAGAGG	CTGCCTCCAT	TCGAAACATT	TTCTCAGGGA	CCTACGTTGC	1260
	AGTTCACTCT	TCGTTGGACA	GGAGAGACCA	ATGATAAATC	TACGGCTCCT	ATTGCCAAAC	1320
	CTCTTGCCAC	TAGAAATTC	GAGAGTCTCC	ATCAGGAAAA	CAAGCTGGT	TCAGTTAAAC	1380
	CTACTCAAAC	TATTGCTGTT	AAAGAATCAT	TGACTACAGA	TCTACAAACA	AGAAAAGAAA	1440
	AGGATACTCC	AAATGAAAAC	CGACAAAAAT	TAAGAATATT	TTATCAGTTT	CTCTATAACA	1500
	ACAATACAAG	GCAACAAACT	GAAGCAAGAG	ATGACCTGCA	TTGCCCTTGG	TGTACTCTGA	1560
	ACTGCCGCCA	ACTTTATAGT	TTACTCAAGC	ATCTTAAACT	CTGCCATAGC	AGATTTATCT	1620
	TCAACTATGT	TTATCATCCA	AAAGGTGCTA	GGATAGATGT	TTCTATCAAT	GAGTGTATG	1680
	ATGGCTCCTA	TGCAGGAAAT	CCTCAGGATA	TTCATCGCCA	ACCTGGATTT	CCTTTTAGTC	1740
	GCAACGGACC	AGTTAAGAGA	ACACCTATCA	CACATATTCT	TGTGTGCAGG	CCAAAACGAA	1800
	CAAAAGCAAG	CATGTCTGAA	TTCTTGAAT	CTGAAGATGG	GGAAGTAGAA	CAGCAAAGAA	1840
	CATATAGTAG	TGGCCACAAT	CGTCTGTATT	TCCATAGTGA	TACCTGCCTA	CCTCTCCGTC	1920
	CACAAGAAAT	GGAAGTAGAT	AGTGAAGATG	AAAAGGATCC	TGAATGGCTA	AGAGAAAAAA	1980
	CCATTACACA	AATGGAAGAG	TTTTCTGATG	TTAATGAAGG	AGAGAAAAGAA	GTGATGAAAC	2040
	TCTGGAATCT	CCATGTCATG	AAGCATGGGT	TTATTGCTGA	CAATCAAATG	AATCATGCCT	2100
	GTATGCTGTT	TGTAGAAAAT	TATGGACAGA	AAATAATTAA	GAAGAATTTA	TGTCGAAACT	2160
	TCATGCTTCA	TCTAGTCAGC	ATGCATGACT	TTAATCTTAT	TAGCATAATG	TCAATAGATA	2220
	AAGCTGTTAC	CAAGCTCCGT	GAAATGCAGC	AAAAATTAGA	AAAGGGGAA	TCTGCTTCCC	2280
	CTGCAAACGA	AGAAATAACT	GAAGAACAAA	ATGGGACAGC	AAATGGATTT	AGTGAATTTA	2340
	ACTCAAAGA	GAAAGCTTTG	GAAACAGATA	GTGTCTCAGG	GGTTTCAAAA	CAGAGCAAAA	2400
	AACAAAAACT	CTGAAAAGCT	CTAACCCCAT	GTTATGGACA	AACACTGAAA	TTACATTTTA	2520
	GTTAGATGAA	GTAATGATT	TCAACAAGGA	TATTTGTATC	AGGGTCTAC	TTCACTTCTA	2580
	TATGCAGCAT	TACATGTATA	TCACTTTTAT	TGATGTCATT	AAAACATTC	GTACTTTAAG	2640
	CATGAAAAGC	AATATTTCAA	AGTATTTTTA	AACTCAACAA	ATGTCATCAA	ATATGTTGAA	2700
	TTGATCTAGA	AATTAATTTA	TATATAAATC	AGAATTTTTT	TGCATTTATG	AACGGCTGTT	2760
	TTTCTACTTT	GTAATTTGTA	GACATTTTCT	TGGGGAGGGA	AAATTTGAAAT	GGTTCCTTTT	2820
	TTTAGAAAT	GAAGTGTCT	TCATATGTCA	ACTACAGAAA	AGGAAAAAAA	TAGAAATTGA	2880
	AGGATTTTTA	TGAAATTATA	TTGCATTACT	ATTTGCAGTC	AAACTTTGAT	CCTTGTTTTT	2940
	GAAATCATTT	GTCAATTCGG	AATGAAAAAT	TATAATGTAA	TTTTACATTA	CATAAGTTCC	3000
	TTTTACAATT	AAAAAATAGC	ACTTCTTCAT	CTTATGCCTG	TTTGAGAAGA	TATTAATTTT	3060
	TCACATTTGTT	GACAGTGAAA	TGCTATGTTG	GTTTATAAGA	TTACAGACCA	TTTGTTTTCA	3180
	TGCTTGTPTT	GTTTTCTTTT	TTAATTTAGA	TAAATCACAC	GAAAAATTAAG	CTGTTTCATAT	3240
	CTTTAAATTA	GGATTGCAAA	CCAAGGAAAG	AACGCATTTG	AGATTTTAAG	ATGTCACCTA	3300
	TAAGGGGAGA	AGTGTCTTTA	AAAAGTCAAC	CAGAAAACCT	TTATGCCTTT	TATTTGTTTG	3360
	CAAGCATGTC	TTTGTAAATG	GTTTCATGAA	TAGAATATCC	AATAGAGATA	AGCTGACTTG	3420
	AATCATTTTG	AGCAATTTTG	CCCTGTGTTA	TATGTGTTTC	ACGCACATAT	TTGCAAGTTG	3480
	ATTTTCTCCA	ACAGAAAAGT	GATTCACACT	TGGCACATTA	ACAAGCACCA	ATAGGTTTTT	3540
	ATTCCAACCT	CGAGCACTGT	GGTTGAGTAA	CATCACCTCA	ATTTTTTATT	ATCCTTAAAG	3600
	ATATTGCATT	TTCATATTCT	TTATTTATAA	AGGATCAATG	CTGCTGTAAA	TACAGGTATT	3660
	TTAATTTTFA	AAATTTTATT	CCACCACCAT	CAGATGCAGT	TCCCTATTTT	GTTAATGAA	3720
	GGGATATATA	AGCTTTCTAA	TGGTGTCTTC	AGAAATTTAT	AAAAATGAAA	TACTGATTTG	3780

ACTGGTCTTT	AAGATGTGTT	TAAGTGTGAG	GCTATTTAAC	GAATAGTGTG	GATGTGATTT	3840
GTCATCCAGT	ATTAAGTTCT	TAGTCATTGA	TTTTTGTGTT	TAAAAAAAAA	TAGGAAAGAG	3900
GGAAACTGCA	GCTTTCATTA	CAGATTCCTT	GATTGGTAAG	CTCTCCAAAT	GATGAGTTCT	3960
AGTAAACTCT	GATTTTGGCC	TCTGGATAGT	AGATCTCGAG	CGTTTATCTC	GGGCTTTAAT	4020
TTGCTAAAAGC	TGTGCACATA	TGTAAAAAAAA	AAAAAAAAAA	GATTATTTTA	GGGGAGATGT	4080
AGGTGTAGAA	TTATTGCTTA	TGTCATTTCT	TAAGCAGTTA	TGCTCTTAAT	GCTTAAAAGA	4140
AGGCTAGCAT	TGTTTGACAA	AAAAGTTGGT	GATTCCCACC	CCAAATAGTA	ATAAAATTAC	4200
TTCTGTTGAG	TAAACTTTTT	ATGTCATCGT	AAAAGCTGGA	AAAATCCCTT	TGTTTCTATT	4260
TATAAAAAAA	GTGCTTTTCT	ATATGTACCC	TTGATAACAG	ATTTTGAAGA	AATCCTGTAA	4320
ATGATAAAG	CATTTGAATG	GTACAGTAGA	TGTAAAAAAAA	ATTCAGTTTA	AAAGAACATT	4380
TGTTTTTACA	TTAAATGTTT	ATTTGAAATC	AAATGATTTT	GTACATAAAG	TTCAATAATA	4440
T						4441

Figure 4.10 Sequence alignment of the insert that demonstrated homology to human mRNA for the KIAA0160 gene. The nucleotide sequence of the insert, demonstrating homology to the human KIAA0160 gene have been aligned with the nucleotide sequence for the mRNA from KIAA0160. The KIAA0160 mRNA sequence is shown in black and the insert is shown in blue, with * marking the regions of insert sequence that do not align with KIAA0160.

4.2.10 Attempt to confirm protein-protein interaction by co-immunoprecipitation

The next step was to try and provide independent confirmation of the putative interactions between PDE4A7 and CBP. This was attempted in mammalian cells (*in vivo*) by using the biochemical method of co-immunoprecipitation (Materials and Methods 2.2.2). It was impossible to check the PDE4A7-RanBPM9 or the PDE4A7-KIAA0160 interactions as no antibodies were available for the detection of these proteins. Therefore, only the PDE4A7-CBP interaction could be tested by co-immunoprecipitation.

COS-1 cells were either mock transfected or transfected to express VSV-tagged PDE4A7, lysates from these cells were homogenised and clarified by low speed centrifugation (Materials and Methods 2.2.2). The resultant supernatants were firstly incubated with protein A beads to check that PDE4A7 did not bind non-specifically to the beads alone. Next, the supernatants were incubated with either the polyclonal anti-CBP antibody or with control rabbit IgG (which acted as a negative control), followed by incubation with protein A beads. Resultant immunoprecipitates were analysed by 10% SDS-PAGE and immunoprobed with the polyclonal anti-VSV antibody for detection of the PDE4A7 protein. Although PDE4A7 (32±2kDa) was detected in the immunoprecipitate where the CBP antibody was used (*figure 4.11, lane 4*), it was also found to associate non-specifically with the protein A beads (*figure 4.11, lane 2*) and also the control rabbit IgG (*figure 4.11, lane 3*). No PDE4A7 was detected in the control, mock-transfected COS-1 cells (*figure 4.11, lane 5*). The data from this study did not provide conclusive evidence that PDE4A7 interacts specifically with the CBP protein as PDE4A7 was also detected in the immunoprecipitates from the controls. A possible reason why PDE4A7 was detected in the immunoprecipitate with CBP was because the initial clarification step was not performed at a high enough centrifugation speed. Therefore, to ensure complete clarification in the future the lysate should be centrifuged at 14000rpm for 10 minutes instead of 3000rpm for 10 minutes.

The lysis buffer used for harvesting the cells contained triton detergent, which breaks open the membranes in the cell and therefore PDE4A7 should be released into the supernatant fraction. However, the majority of PDE4A7 was detected within the pellet generated from the preliminary low speed spin (*figure 4.11, lane 1*). It is possible that not all nuclei have been broken open by this method of lysis and have therefore been pelleted in this low speed centrifugation step. Alternatively, it is likely that 2EL is associating with a protein that is triton insoluble. For example, early studies performed on 3T3 fibroblast-cells demonstrated that after cell lysis, the triton insoluble fraction contained nuclear and

cytoskeletal components [Trotter et al., 1978]. That 2BL is nuclear in COS-1 cells might explain why it is found majorly within the triton insoluble fraction. Once cellular membranes are broken open, many proteins are brought together. This can result in the formation of aggregates, which will also be pelleted by low speed centrifugation. The PDE4A7 that is found to associate with the control IgG immunoprecipitate and the protein A beads control may actually be residual PDE4A7 left over from the initial low speed spin or it may be that PDE4A7 is simply a 'sticky' protein. It was concluded that this method was not suitable for testing the PDE4A7 and CBP interaction. Alternative methods that could be used to test this interaction in the future would be to perform confocal analyses to check if these two proteins co-localise with each other, or, one could attempt a 'pull down assay'.

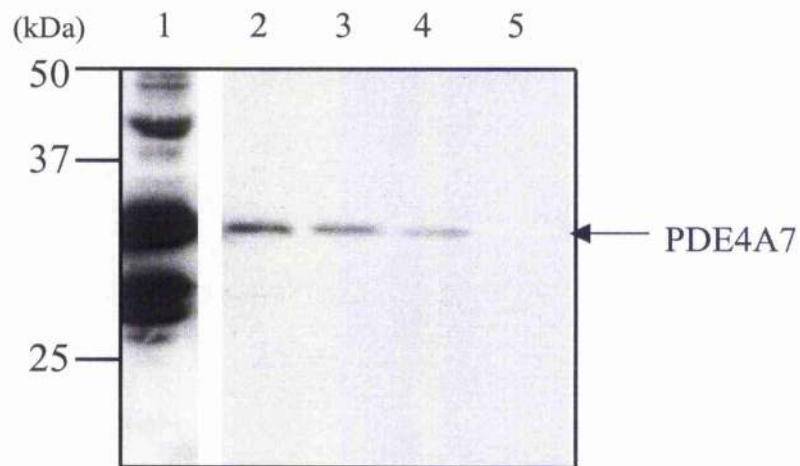


Figure 4.11 Testing for the *in vivo* interaction of CBP with PDE4A7. COS-1 cells were either mock transfected or transfected to over-express PDE4A7. After a 48 hour incubation period these cells were lysed, disrupted and centrifuged at a low speed to remove any cellular debris. Lysates were then immunoprecipitated with protein A beads alone followed by either control rabbit IgG or anti-CBP polyclonal antibody. Immunoprecipitates were subjected to 10% SDS-PAGE before immunoprobining with the polyclonal anti-VSV antibody. *Lanes 1-5* were taken from the same gel. The migration of the standard protein molecular weight standards are indicated on the left and the data are representative of two separate experiments. PDE4A7 was detected in the cellular debris pellet (*lane 1*). Lysates from COS-1 cells over-expressing PDE4A7 immunoprecipitated with protein A beads alone (*lane 2*), immunoprecipitated with control rabbit IgG (*lane 3*), immunoprecipitated with anti-CBP polyclonal antibody (*lane 4*). Lysates from mock transfected COS-1 cells immunoprecipitated with anti-CBP polyclonal antibody (*lane 5*).

4.2.11 Re-evaluating the possible interaction of PDE4A7 with RanBPM and CBP using the small scale Y2H

Putative interactions between PDE4A7 and either CBP or RanBPM were re-evaluated using small-scale yeast mating using the rescued library plasmids (Materials and Methods 2.4.6). Diploids produced from the mating were plated onto SD-Lcu/-Trp and incubated for 2-4 days at 30°C before testing for β -galactosidase activity (Materials and Methods 2.4.8). The details of the mating reactions performed are described below.

AH109[empty-pGBKT7] mated with Y187[empty-pACT2] acted as the negative control and colonies produced from this mating remained white in colour. This is because the AD and DNA-BD cannot interact unless they are brought into physical proximity by interacting proteins. Therefore resultant diploids are incapable of activating the reporter genes (*figure 4.12, a*). AH109[pGBKT7-53] mated with Y187[pTD1-1] acted as the positive control and these colonies were blue in colour. This is because BD-p53 interacts with AD-T-antigen to restore the GAL4 activity leading to transcriptional activation of the reporter genes (*figure 4.12, g and h*). AH109[pGBKT7-PDE4A7] mated with Y187[empty-pACT2] remained white as expected because PDE4A7 alone cannot autonomously activate the reporter genes (*figure 4.12, b*). When AH109[empty-pGBKT7] were mated with Y187[pACT2-CBP] the colony was white as expected (*figure 4.12, c*) but, AH109[pGBKT7-PDE4A7] mated with Y187[pACT2-CBP] also remained white in colour (*figure 4.12, d*) which was unexpected as CBP was identified as a positive binding partner for PDE4A7 previously in the large scale Y2H screen. When AH109[empty-pGBKT7] were mated with Y187[pACT2-RanBPM9] the colony turned blue when tested for β -galactosidase indicating that RanBPM9 alone was capable of autonomously activating the reporter genes (*figure 4.12, e*). However, when AH109[pGBKT7-PDE4A7] were mated with Y187[pACT2-RanBPM9] these colonies unexpectedly remained white, as if the presence of PDE4A7 abolished the ability of RanBPM9 to autonomously activate the reporter genes (*figure 4.12, f*). RanBPM9 is an example of an AD/library protein that can activate the reporter genes without the DNA-BD target protein present. This data suggested that both RanBPM9 and CBP were both artefacts. No conclusions were made regarding the KIAA0160 gene as its interaction with PDE4A7 was not re-tested.

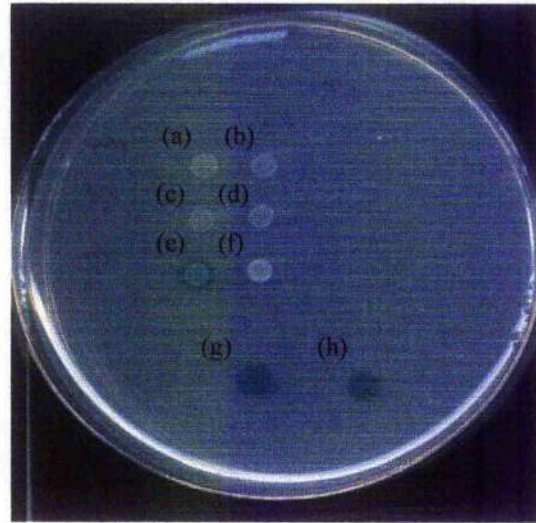


Figure 4.12 Re-testing the interaction of PDE4A7 with RanBPM and CBP. (a) AH109[pGBKT7/PDE4A7] mated with Y187[empty-pACT2], (b) AH109[empty-pGBKT7] mated with Y187[empty-pACT2] (negative control), (c) AH109[pGBKT7/PDE4A7] mated with Y187[pACT2/CBP], (d) AH109[empty-pGBKT7] mated with Y187[pACT2-CBP], (e) AH109[pGBKT7-PDE4A7] plasmid mated with Y187[pACT2/RanBPM], (f) AH109[empty-pGBKT7] mated with Y187[pACT2/RanBPM], (g) and (h) AH109[pGBKT7/p53] mated with Y187[pTD1-1] (positive control). Each of these combinations were mated using small scale yeast mating (Materials and methods) and were plated out onto SD-Trp/-Leu and and tested for β -galactosidase activity.

4.3 Discussion

The Y2H system was used to probe a human brain library with PDE4A7 in the hope of identifying possible binding partners for PDE4A7. The Y2H screen identified CBP, RanBPM9 and mRNA from the human KIAA0160 gene as binding partners for PDE4A7. However, when these interactions were re-tested by small-scale yeast mating CBP was no longer found to interact with PDE4A7 as the reporter genes remained inactive. Upon re-testing, RanBPM9 was found able to autonomously activate the reporter genes, but the presence of PDE4A7 seemed to ablate this interaction. There are many proteins that are classified as common false positives in the Y2H, including heat shock proteins (hsps), ribosomal proteins, mitochondrial proteins and zinc finger proteins [Golemis et al., 1997] to name a few. That RanBPM9 is a zinc finger containing protein may explain why this protein was able to activate the reporter genes in the absence of a DNA-BD-bait protein. As antibodies were available to the CBP protein I decided to test whether the PDE4A7-CBP interaction could be detected *in vivo* by using co-immunoprecipitation. The results of this study suggested that PDE4A7 was not specifically interacting with CBP, as PDE4A7 was found to bind non-specifically to the protein A beads and the control rabbit IgG. I concluded that this method was not suitable for the study of this interaction and that in the future the alternative approaches of confocal analysis and 'pull-down assays' should be attempted instead. The overall conclusion was that CBP and RanBPM were artefacts produced in the PDE4A7 Y2H screen. The potential interaction of PDE4A7 with KIAA0160 still needs to be evaluated as I did not have time to test this further. This is because my efforts were focussed on evaluating the other species because they were established examples of nuclear localised proteins.

Chapter 5

Assessing the potential effects of PDE4A7 (2EL) on gene regulation

5.1 Introduction

As the function of PDEs is to degrade the cyclic nucleotides into inactive 5' nucleoside monophosphates, it was surprising to find that the *PDE4A* gene also encoded a splice variant called PDE4A7 (2EL) that was incapable of hydrolysing either one of these second messengers. This raised the question of what possible function such a catalytically inactive product of the *PDE4A* gene may have within the cell. Many proteins that have been found to be devoid of catalytic activity, such as GRB2 [Tari et al., 2001] or AKAPs [Michel and Scott, 2002], act as scaffold proteins that bring important signalling proteins into complexes. Therefore, one possible function of PDE4A7 may be to mediate the interaction of other PDEs with important signalling proteins. However, that recombinant PDE4A7 was found localised to the nucleus of COS-1 cells might indicate that PDE4A7 could be involved in transcriptional regulation. This might provide a further route by which *PDE4A* gene products affect the transcription of various genes, for cAMP regulates the expression of various proteins through the action of CREB, with PDEs functioning to tailor cAMP levels.

Microarray has provided scientists with a method of analysing the expression patterns of thousands of genes in parallel. The microarray is a glass slide containing thousands of spots with each one representing a single gene. RNA is extracted from the test samples and reverse transcribed into fluorescently labelled cDNA by using fluor-derivatised nucleotides. Using different fluorescent dyes means that mRNA from the test sample and the control sample can be labelled in different colours, for example the control sample can be labelled with Cyanine 3 (CY3) (green) whereas the test sample can be labelled in Cyanine 5 (CY5) (red). These labelled cDNAs can be mixed and hybridised to the same microarray slide, which leads to competition between the test and the control cDNAs for the immobilised probes on the DNA chip. cDNA containing sequence that is complementary to the DNA on a given spot, will bind and be detected by its fluorescence when excited by a laser. The differences in mRNA levels between the control and test samples are calculated from the differences in the intensities of either CY3 or CY5

measured on each spot. Therefore, if RNA from the control sample (labelled with CY3) is most abundant, the spot will be green and indicates this gene has been down-regulated by experimental treatment; if the RNA from the experimental sample (labelled with CY5) is abundant the spot will be red and indicates that this gene has been up-regulated in response to experimental treatment. If both bind equally well to a spot it means there has been no effect on the regulation of that particular gene and the spot will be yellow. Finally, if neither bind then the spot will be black.

Studies performed on the PDE4A7 protein so far have been carried out using COS-1 cells as the model system, however, the slides available for the microarray study had been spotted with human cDNA. Therefore, the COS-1 cell system was not suitable for such analyses and had to be changed to a cell type of human origin. HEK-293 cells were used for this study, as they are well established as being readily transfectable, which was then confirmed here for PDE4A7 (see below). The major aim of the following study was to determine which genes are regulated in response to the over-expression of recombinant PDE4A7 using the techniques of gene microarray and RT-PCR.

5.2 Results

5.2.1 Expression of PDE4A7 in HEK-293 cells

HEK-293 cells were transiently transfected with a range of PDE4A7 plasmid DNA concentrations (0.5 μ g/ μ l, 1 μ g/ μ l, 2 μ g/ μ l and 5 μ g/ μ l) to determine whether it was possible to over-express PDE4A7 in this cell type and if so, the concentration of PDE4A7 plasmid DNA required to produce adequate expression of the PDE4A7 protein (Materials and Methods 2.1.3). The PDE4A7-transfected cell lysates were subjected to 10% SDS-PAGE before immunoprobing with the polyclonal anti-VSV antibody. The reason for using the anti-VSV antibody to detect PDE4A7 expression was because this protein contains a truncated C-terminal, which means that its expression cannot be detected using the general PDE4A antisera (discussed previously). Thus, PDE4A7 was engineered to contain a VSV epitope tag (YTDIEMNRLGK) at its C-terminal, which allows its expression to be detected using the anti-VSV antibody. VSV identified the 33 \pm 2kDa immunoreactive band of PDE4A7 only in those cells that were transfected with 5 μ g/ μ l of plasmid DNA (*figure 5.1*). This demonstrated that PDE4A7 could be over-expressed in this cell type and that 5 μ g/ μ l of DNA sufficed to produce detectable PDE4A7 expression by immunoblotting.

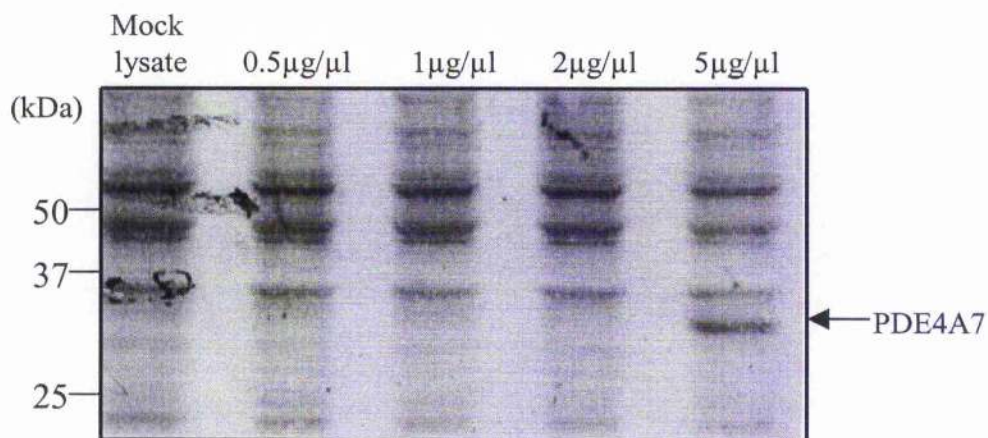


Figure 5.1 Expression of PDE4A7 in HEK-293 cells. Four plates of HEK-293 cells were transiently transfected with different amounts of DNA (indicated above). The cells were harvested, homogenised and centrifuged to remove cellular debris. 20 μg of protein from each cell lysate was subjected to 10% SDS-PAGE electrophoresis, followed by immunoblotting with the polyclonal anti-VSV antibody. The immunoreactive band of PDE4A7 is indicated above. Mock transfected HEK-293 lysate was run alongside the PDE4A7-transfected HEK-293 lysates as a negative control. Migration of standard molecular weight protein markers (in kDa) are shown on the left.

5.2.2 Using microarray to detect changes in gene expression in response to expression of recombinant PDE4A7

RNA was extracted from HEK-293 cells over-expressing either PDE4A7, which will be referred to as the test sample, or pcDNA3, referred to as the reference sample (Materials and Methods 2.3.9.1). pcDNA3-transfected HEK-293 cells were chosen as the negative control (reference sample) because PDE4A7 had previously been cloned into this vector. This meant that any changes observed in gene expression profiles could be attributed solely to the over-expression of PDE4A7 and also allowed us to correct for any expression changes that occur in response to the transfection procedure. The mRNA from the test sample was reverse transcribed to produce cDNA labelled with CY3, whereas the mRNA from the reference sample was used to generate cDNA labelled with CY5 (Materials and Methods 2.5). Equal amounts of these labelled cDNAs were mixed before hybridising to the microarray slides (Materials and Methods 2.5). It has been noted that CY5 does not incorporate as well as CY3, therefore, to correct for any incorporation bias, we prepared samples in which the test and control dyes were reversed. In this case the test sample was labelled with CY5 and the control sample with CY3. This process is referred to as 'fluor flip'. Two independent hybridisations to different microarray slides were performed for each treatment, with each including a 'fluor flip'. Results from the microarray study are shown as colour images whereby green represents the control sample data and red represents the test sample data and the two of these colour images are combined. Those genes demonstrating a similar response to the over-expression of PDE4A7 were grouped using the data analysis packages of CLUSTER and TREE VIEW [Schena, 1996 and Shalon et al., 1996]. These programmes enabled us to eliminate those genes that showed variability in their responses between the experiments, allowing us to focus on those genes that demonstrated consistent changes, in both the separate hybridisations and "fluor flip" process (normalisation and analysis of the gene microarray data was performed by Dr Steven Yarwood). The full data set generated from this microarray analysis is contained on the enclosed CD and can be accessed using Microsoft Excel.

Group A (*figure 5.2*) shows a cluster of those genes that were up-regulated in response to over-expression of PDE4A7, whereas group B (*figure 5.3*) shows those genes that were down-regulated in response to the over-expression of PDE4A7. Genes up-regulated in response to PDE4A7 over-expression included those involved in the cell cycle (e.g CDK5 and ETS) and those involved in G protein-mediated signalling (e.g GRK, Gz and A2A receptor). Genes down-regulated in response to PDE4A7 over-expression

included the A2B receptor and the ras-related C3 botulinum toxin substrate (C3), that are involved in generating cAMP and hydrolysing cGMP respectively. Before conclusions could be taken from this microarray analysis, I had to verify the gene expression changes using an alternative method.

Figure 5.2 Display of genes upregulated in response to over-expression of PDE4A7 in HEK-293 cells. HEK-293 cells were transfected with either pcDNA3 or PDE4A7 DNA and allowed to express for 48 hours. CY3- and CY5- labelled cDNAs were prepared from each of these samples and hybridised to a 1.7K human array (as described in Materials and Methods 2.5). Slides were subjected to confocal scanning and coloured images were generated. * mark those transcripts that were re-evaluated using RT-PCR analysis.

2EL 5 CY3
2EL 5 CY5
2EL 5 CY3
2EL 5 CY5

AA035031 GC-RICH SEQUENCE DNA-BINDING FACTOR GCF TRANSCRIPT
T78661 RAB GERANYLGERANYLTRANSFERASE ALPHA SUBUNIT EC 2.5.1
W86215 ETS-DOMAIN TRANSCRIPTION FACTOR ERF
W77759 TRANSCRIPTION FACTOR E2F1 E2F-1 RETINOBLASTOMA BINDI
R22307 Dup1PERIODIC TRYPTOPHAN PROTEIN 1 HOMOLOG KERATINOCY
W91932 PROLIFERATING CELL NUCLEAR ANTIGEN PCNA CYCLIN
H87204 CELL DIVISION PROTEIN KINASE 5 EC 2.7.1.- TAU PROTEI
W38310 ECOTROPIC VIRUS INTEGRATION 1 SITE PROTEIN
H17364 CAMP RESPONSE ELEMENT BINDING PROTEIN CRE-BP1 TRANSC*
H02641 VON HIPPEL-LINDAU DISEASE TUMOR SUPPRESSOR G7 PROTEI
W79411 ALPHA-2-HS-GLYCOPROTEIN PRECURSOR FETUIN ALPHA-2-Z-G
H17600 MICROTUBULE-ASSOCIATED PROTEIN 1B*
R81539 ER LUMEN PROTEIN RETAINING RECEPTOR 2 KDEL RECEPTOR
AA043477 TRISTETRAPROLINE TTP TIS11A TIS11 ZFP-36 GROWTH FA
AA044782 POLYPOSIS LOCUS PROTEIN 1 TB2 PROTEIN
AA069319 CREATINE KINASE, B CHAIN EC 2.7.3.2 B-CK.
AA001329 G2/MITOTIC-SPECIFIC CYCLIN A
T91426 CARBOXYPEPTIDASE M PRECURSOR EC 3.4.17.12 FRAGMENT
R13557 REPLICATION PROTEIN A 32 KD SUBUNIT RP-A RF-A REPLIC
R63760 PROBABLE G PROTEIN-COUPLED RECEPTOR GPR1
AA044453 X-LINKED PEST-CONTAINING TRANSPORTER
W67485 ZINC FINGER PROTEIN 136
AA022576 PAIRED MESODERM HOMEBOX PROTEIN 1 HOMEBOX PROTEI
R06476 FMET-LEU-PHE RECEPTOR FMLP RECEPTOR N-FORMYL PEPTIDE
N39399 UBIQUITIN-ACTIVATING ENZYME E1 HOMOLOG D8
N40660 Dup2PROTEASOME THETA CHAIN EC 3.4.99.46 MACROPAIN TH
W72937 CALDESMON CDM
H61280 Dup1GUANINE NUCLEOTIDE-BINDING PROTEIN, ALPHA-15 SUB
H69261 ALPHA-2-ANTIPLASMIN PRECURSOR ALPHA-2-PLASMIN INHIBI
R89708 LYSOSOME-ASSOCIATED MEMBRANE GLYCOPROTEIN 1 PRECURSO
W32673 Dup2TYROSINE-PROTEIN KINASE RYK PRECURSOR EC 2.7.1.1
W79895 METALLOTHIONEIN-IG MT-1G
R10588 PHOSPHATIDYLINOSITOL-GLYCAN-SPECIFIC PHOSPHOLIPASE D
R11719 PROLIFERATING-CELL NUCLEOLAR ANTIGEN P120 PROLIFERAT
R60825 STRESS-ACTIVATED PROTEIN KINASE JNK2 EC 2.7.1.- C-JU
AA011711 TRANSTHYRETIN PRECURSOR PREALBUMIN TBPA TTR ATTR
W15613 ADENOSINE A2A RECEPTOR*
N28517 Dup1SKI ONCOGENE C-SKI
R35713 VASCULAR ENDOTHELIAL GROWTH FACTOR RECEPTOR 2 PRECUR
R34925 PHOSPHOLIPASE D1 EC 3.1.4.4 PLD 1 CHOLINE PHOSPHATAS
AA121357 G PROTEIN-COUPLED RECEPTOR KINASE GRK5 EC 2.7.1.-
H87835 RECOVERIN CANCER ASSOCIATED RETINOPATHY PROTEIN CAR
H57207 PHOSPHOLEMMAN PRECURSOR
R74571 26S PROTEASOME REGULATORY SUBUNIT P31
R06476 FMET-LEU-PHE RECEPTOR FMLP RECEPTOR N-FORMYL PEPTIDE
N42428 40S RIBOSOMAL PROTEIN S24 S19
H57207 PHOSPHOLEMMAN PRECURSOR
H75353 DELTA-AMINOLEVULINIC ACID DEHYDRATASE EC 4.2.1.24 PO
R70292 IG KAPPA CHAIN C REGION
R19128 SPECTRIN ALPHA CHAIN, BRAIN SPECTRIN, NON-ERYTHROID
R20008 ALPHA-N-ACETYLGLUCOSAMINIDASE PRECURSOR EC 3.2.1.50
H17187 CALRETININ CR 29 KD CALBINDIN
R71967 C5A ANAPHYLATOXIN CHEMOTACTIC RECEPTOR C5A-R CD88 AN
H19564 GUANINE NUCLEOTIDE-BINDING PROTEIN GZ, ALPHA SUBUNIT
AA215295 Dup2PROBABLE UBIQUITIN CARBOXYL-TERMINAL HYDROLASE

Figure 5.3 Display of genes down-regulated in response to over-expression of PDE4A7 in HEK-293 cells. HEK-293 cells were transfected with either pcDNA3 or PDE4A7 DNA and allowed to express for 48 hours. CY3- and CY5- labelled cDNAs were prepared from each of these samples and hybridised to a 1.7K human array (as described in Materials and Methods 2.5). Slides were subjected to confocal scanning and coloured images were generated. * mark those transcripts that were re-evaluated using RT-PCR analysis.

U X S
U X S
S S S
L L L
L L L
L L L

R18606 Dup1DELTA-LIKE PROTEIN 1 PRECURSOR DELTA1
R81846 FERRITIN LIGHT CHAIN *
W68191 CLUSTERIN PRECURSOR COMPLEMENT-ASSOCIATED PROTEIN SP-40,40 COMPLEMENT CYTOLYSIS INHIBITOR CLI NA1 AND NA2 APOLIPOPROTEI
H74175 N-ACETYLLACTOSAMINE SYNTHASE EC 2.4.1.90 N-ACETYLGLUCOSAMINE BETA 1->4GALACTOSYLTRANSFERASE EC 2.4.1.38 LACTOSE SYNTHAS
R81846 FERRITIN LIGHT CHAIN
W05657 ETS-RELATED TRANSCRIPTION FACTOR ELF-1
AA047528 Dup12-19 PROTEIN PRECURSOR
T78665 Dup2EPHRIN-B2 PRECURSOR EPH-RELATED RECEPTOR TYROSINE KINASE LIGAND 5 LERK-5 HTK LIGAND HTK-L
R89564 SODIUM/POTASSIUM-TRANSPORTING ATPASE BETA-1 CHAIN EC 3.6.1.37 SODIUM/POTASSIUM-DEPENDENT ATPASE
AA055349 ADENOSINE A2B RECEPTOR
W31814 PROTEIN KINASE C, ZETA TYPE EC 2.7.1.- NPKC-ZETA.
AA001138 CARBOXYPEPTIDASE H PRECURSOR EC 3.4.17.10 CPH CARBOXYPEPTIDASE E CPE ENKEPHALIN CONVERTASE PROHORMONE PROCESSING CARB
H65733 ERYTHROID KRUPPEL-LIKE TRANSCRIPTION FACTOR EKLF ERYTHROID TRANSCRIPTION FACTOR
N34209 ALPHA-CENTRACTIN CENTRACTIN CENTROSOME-ASSOCIATED ACTIN HOMOLOG ACTIN-RPV ARP1
N23555 PUTATIVE GLUCOSAMINE-6-PHOSPHATE ISOMERASE EC 5.3.1.10 GLUCOSAMINE- 6-PHOSPHATE DEAMINASE OSCILLIN KIAA0060
W05657 ETS-RELATED TRANSCRIPTION FACTOR ELF-1
W31779 ALDEHYDE DEHYDROGENASE, E3 ISOZYME EC 1.2.1.3 GAMMA- AMINOBUTYRALDEHYDE DEHYDROGENASE EC 1.2.1.19 R-AMINOBUTYRALDEHYDE
AA010929 Dup1DNA-3-METHYLADENINE GLYCOSIDASE EC 3.2.2.21 3-METHYLADENINE DNA GLYCOSYLASE ADPG 3-ALKYLADENINE DNA GLYCOSYLASE N
W32991 INSULIN RECEPTOR PRECURSOR EC 2.7.1.112 IR
AA035789 ELONGATION FACTOR 1-DELTA EF-1-DELTA
R32131 INSULIN-LIKE GROWTH FACTOR II PRECURSOR IGF-II SOMATOMEDIN A
R60529 NT-3 GROWTH FACTOR RECEPTOR PRECURSOR EC 2.7.1.112 TRKC TYROSINE KINASE GP145-TRKC TRK-C
AA039289 PROTEIN KINASE CLK2 EC 2.7.1.- *
R25016 CD27L RECEPTOR PRECURSOR T-CELL ACTIVATION ANTIGEN CD27 T14
H29950 TOB PROTEIN TRANSDUCER OF ERBB-2
AA020759 NEURAL RETINA-SPECIFIC LEUCINE ZIPPER PROTEIN NRL D14S46E
AA011671 60S RIBOSOMAL PROTEIN L27A
R53336 Dup1RAS-RELATED C3 BOTULINUM TOXIN SUBSTRATE 3 P21-RAC3
AA039289 PROTEIN KINASE CLK2 EC 2.7.1.-
R53336 Dup1RAS-RELATED C3 BOTULINUM TOXIN SUBSTRATE 3 P21-RAC3 *
AA026838 HISTONE DEACETYLASE 1 HD1
R18606 Dup1DELTA-LIKE PROTEIN 1 PRECURSOR DELTA1
AA055349 ADENOSINE A2B RECEPTOR *
N40420 G1/S-SPECIFIC CYCLIN D1 PRAD1 ONCOGENE BCL-1 ONCOGENE
AA029730 LDLC PROTEIN
AA037541 CALCIUM-TRANSPORTING ATPASE ENDOPLASMIC RETICULUM TYPE EC 3.6.1.38, CLASS 2 HK1 SERCA2.
W04886 SPECTRIN BETA CHAIN, BRAIN SPECTRIN, NON-ERYTHROID BETA CHAIN FODRIN BETA CHAIN SPTBN1.
AA020759 NEURAL RETINA-SPECIFIC LEUCINE ZIPPER PROTEIN NRL D14S46E
AA134026 UBIQUITIN-CONJUGATING ENZYME E2-17 KD EC 6.3.2.19 UBIQUITIN-PROTEIN LIGASE UBIQUITIN CARRIER PROTEIN HR6A
R99156 CYCLIN-DEPENDENT KINASES REGULATORY SUBUNIT 1 CKS-1

5.2.3 Using RT-PCR to detect changes in gene expression in response to PDE4A7 over-expression

Although gene microarray has provided researchers with a valuable tool for analysing the expression of thousands of genes simultaneously, this method is still in its infancy and problems exist with irregularities in spot shape and size, noise and data analysis, which are all pitfalls that can lead to misinterpretation of the expression profiles of many genes [Schuchhardt et al., 2000]. Normally microarray data is verified by using RT-PCR or Northern blotting to retest the expression changes of the candidate genes. Here, RT-PCR was used to verify the changes in gene expression detected in HEK-293 cells in response to the over-expression of PDE4A7. Seven candidate genes were chosen for further analysis, as it would not have been feasible to analyse large numbers of genes given the time available.

RNA was extracted from HEK-293 cells over-expressing either PDE4A7 or pcDNA3 (negative control) and each was reverse transcribed into cDNA, which served as a template in the subsequent PCR reactions, where gene specific primers were used to detect the target gene of interest (Materials and Methods 2.3.9.1, 2.3.9.2, 2.3.9.3). In addition each PCR reaction contained primers to detect the housekeeping gene of cyclophilin, an RNA that provides an internal control to which the target genes can be normalised. Other common housekeeping genes used as internal controls are glyceraldehyde-3-phosphate-dehydrogenase (GADPH) and β -actin because their expression is normally constitutive and their levels remain unchanged despite any experimental treatments, providing ideal internal controls [Bustin, 2000]. To ensure the target gene was detected within the linear range of amplification, each PCR reaction was performed at increasing cycle numbers (15, 20, 25, 30 and 35 cycles).

5.2.4 Primer design

The primers for each target gene and the cyclophilin control were designed according to the nucleotide sequences provided by the National Centre for biotechnology Information (NCBI) database(<http://www.ncbi.nlm.nih.gov/>). Primer pairs amplified each of the target genes as 350bp products and the internal control of cyclophilin as a 250bp product. The nucleotide sequence of target used to generate the primer pairs are shown in *figures 5.4-5.11*, with the sequence used to generate the sense (5') and antisense (3') primers highlighted in yellow and red, respectively. The actual primer pairs and the PCR

reaction conditions used for amplification of each of the target genes are shown in Table 5.1.

```

1   AATTTTCAGC TGTTCTTTGC TCAATAATAA CTTTTTTTATC ACCAAGATAT CTCTCTAAGT
61  TTTTGACATA TTCCTCATTT GTTTTGATAA AAGTTTTTCTT ATTTTCTTAG AAAAAATAAGT
121 TACTAAAAGT CATATATCAT TGTATATCTT CAAAATATTG CTTAAACTA GGACTTGTAT
181 TTAAATGTTT TTTCTTCTTA AAGACAATTT GCAGGTGCC TCAGGAACCC TGAAGCTGGG
241 CTGAGCCATG ATGCTGCTGC CAGAACCCTT GCAGAGGGCC TGGTTTCAGG AGACTCAGAG
301 TCCTCTGTGA AAAAGCCCTT GGAGAGCGCC CCAGCAGGGC TGCACTTGGC TCCTGTGAGG
361 AAGGGGCTCA GGGGTCTGGG CCCCTCCGCC TGGGCCGGGC TGGGAGCCAG GCGGGCGGCT
421 GGGCTGCAGC AATGGACCGT GAGCTGGCCC AGCCCGCGTC CGTGCTGAGC CTGCTGTGCG
481 TCTGTGGCCA TGCCCATCAT GGGCTCCTCG GTGTACATCA CGGTGGAGCT GCCCATTGCT
541 GTGCTGGCCA TCCTGGGCAA TGTGCTGGTG TGCTGGGCCG TGTGGCTCAA CAGCAACCTG
601 CAGAACGTCA CCAACTACTT TGTGGTGTCA CTGGCGGCGG CCGACATCGC AGTGGGTGTG
661 CTCGCCATCC CCTTTGCCAT CACCATCAGC ACCGGGTTC TGCCTGCCTG CCACGGCTGC
721 CTCTTCATTG CCTGCTTCGT CCTGGTCCTC ACGCAGAGCT CCATCTTCAG TCTCTGGCC
781 ATGCCATTG ACCGCTACAT TGCATCCGC ATCCCGCTCC GGTACAATGG CTTGGTGACC
841 GGCACGAGGG CTAAGGGCAT CATTGCCATC TGCTGGGTGC TGTCGTTTGC CATCGGCCTG
901 ACTCCCATGC TAGGTTGGAA CAACTGCGGT CAGCCAAAGG AGGGCAAGAA CCACTCCCAG
961 GGCTGCGGGG AGGGCCAAGT GGCCTGTCTC TTTGAGGATG TGGTCCCCT GAACTACATG
1021 GTGTACTTCA ACTTCTTTGC CTGTGTGCTG GTGCCCTGC TGCTCATGCT GGGTGTCTAT
1081 TTGCGGATCT TCCTGGCGGC GCGACGACAG CTGAAGCAGA TGGAGAGCCA GCCTCTGCCG
1141 GGGGAGCGGG CACGGTCCAC ACTGCAGAAG GAGGTCCATG CTGCCAAGTC ACTGGCCATC
1201 ATTGTGGGGC TCTTTGCCCT CTGCTGGCTG CCCCTACACA TCATCAACTG CTTCACTTTC
1261 TTCTGCCCCG ACTGCAGCCA CGCCCCTCTC TGGCTCATGT ACCTGGCCAT CGTCTCTCC
1321 CACACCAATT CGGTTGTGAA TCCCTTCATC TACGCCTACC GTATCCGCGA GTTCCGCCAG
1381 ACCTTCCGCA AGATCATTCT CAGCCACGTC CTGAGGCAGC AAGAACCTTT CAAGGCAGCT
1441 GGCACCAAGT CCCGGGTCTT GGCAGCTCAT GGCAGTGACG GAGAGCAGGT CAGCCTCCGT
1501 CTCAACGGCC ACCCGCCAGG AGTGTGGGCC AACGGCAGTG CTCCCCACCC TGAGCGGAGG
1561 CCCAATGGCT ACGCCCTGGG GCTGGTGAGT GGAGGGAGTG CCCAAGAGTC CCAGGGGAAC
1621 ACGGGCCTCC CAGACGTGGA GCTCCTTAGC CATGAGCTCA AGAGAGTGTG CCCAGAGCCC
1681 CCTGGCCTAG ATGACCCCCT GGCCAGGAT GGAGCAGGAG TGTCTGATG ATTCATGGAG
1741 TTTGCCCTT CCTAAGGGAA GGAGATCTT ATCTTCTGG TTGGCTGAC CAGTCACGTT
1801 GGGAGAAGAG AGAGAGTGCC AGGAGACCCT GAGGGCAGCC GGTTCCTACT TTGGACTGAG
1861 AGAAGGGAGC CCCAGGCTGG AGCAGCATGA GGCCAGCAA GAAGGGCTTG GGTTCAGG
1921 AAGCAGATGT TTCATGCTGT GAGGCCTTG ACCAGGTGGG GGCCACAGCA CCAGCAGCAT
1981 CTTTGCTGGG CAGGGCCCAG CCCTCCACTG CAGAAGCATC TGGAAGCACC ACCTTGCTCTC
2041 CACAGAGCAG CTTGGGCACA GCAGACTGGC CTGGCCCTGA GACTGGGGAG TGGCTCCAAC
2101 AGCCTCTG CACCCACACA CCACTCTCCC TAGACTCTCC TAGGGTTCAG GAGCTGCTGG
2161 GCCCAGAGGT GACATTTGAC TTTTTTCCA GGAAAATGT AAGTGTGAGG AAACCCTTTT
2221 TATTTTATTA CCTTTCCTC TCTGGCTGCT GGGTCTGCCG TCGTCTGCTG TGCTAACCTG
2281 GCACCAGAGC CTCTGCCCGG GGAGCCTCAG GCAGTCTCT CCGTGTGCTA CAGCTGCCAT
2341 CCACTTCTCA GTCCAGGGC CATCTCTTGG AGTGACAAAG CTGGGATCAA GGACAGGGAG
2401 TTGTAACAGA GCAGTGCCAG AGCATGGCC CAGGTCCCAG GGGAGAGGTT GGGGCTGGCA
2461 GGCCACTGGC ATGTGCTGAG TAGCGCAGAG CTACCCAGTG AGAGGCCTTG TCTAACTGCC
2521 TTCTCTCTA AAGGGAATGT TTTTTTCTGA GATAAAATAA AAACGAGCCA CA

```

Figure 5.4 Nucleotide sequence of the A2AR (NCBI: S46950). The nucleotide sequence used to generate the sense (5') and antisense (3') primers for the amplification of the A2AR transcript are highlighted in yellow and red respectively. The actual nucleotide sequence of the primers used are shown in Table 5.1.

```

1   GTACCAGGCC CATTTCCTCT TCTGTTACAT CTTCCCTAATG GACAAAACCAT GCCTGTTGCT
61  ATTCTGCAT CAATTACAAG TTCTAATGTG CATGTTCCAG CTGCAGTCCC ACTCGTTCGA
121 CCAGTCACCA TGGTGCCTAG TGTTCCAGGA ATCCCAGGTC CTTCCTCTCC CCAACCAGTA
181 CAGTCAGAAG CAAAAATGAG ATTAAAAGCT GCTTTGACCC AGCAACATCC TCCAGTTACC
241 AATGGTGATA CTGTCAAAGG TCATGGTAGC GGATTGGTTA GGACTCAGTC AGAGGAATCT
301 CGACCGCAGT CATTACAACA GCCAGCCACA TCCACTACAG AAACCTCCGGC TTCTCCAGCT
361 CACACAACCT CACAGACCCA AAGTACAAGT GGTTCGTCGGA GAAGAGCAGC TAACGAAGAT
421 CCTGATGAAA AAAGGAGAAA GTTTTTAGAG CGAAATAGAG CAGCAGCTTC AAGATGCCGA
481 CAAAAAAGGA AAGTCTGGGT TCAGTCTTTA GAGAA GAAAG CTGAAGACTT GAGTTCATTA
541 AATGGTCAGC TGCAGAGTGA AGTCACCCTG CTGAGAAATG AAGTGGCACA GCTGAAACAG
601 CTTCTTCTGG CTCATAAAGA TTGCCCTGTA ACCGCCATGC AGAAGAAATC TGGCTATCAT
661 ACTGCTGATA AAGATGATAG TTCAGAAGAC ATTTCAAGTC CGAGTAGTCC ACATACAGAA
721 CTATACAGC ATAGTTCGGT CAGCACATCC AATGGAGTCA GTTCAACCTC CAAGGCAGAA
781 GCTGTAGCCA CTTCAAGTCT CACCCAGATG GCGGAC CAGA GTACAGAGCC TGCTCTTTCA
841 CAGATCGTTA TGGCTCCTTC CTCCCAGTCA CAGCCCTCAG GAAGTTGATT AAAAACCTGC
901 AGTACAACAG TTTTAGATAC TCATTAGTGA CTTCAAAGGG AAATCAAGGA AAGACCAGTT
961 TCCATTTATG CGAAATCTGT GGTTGTAAT TTTTTTTTTT ACTTGAAAT AAATTTGGCT
1021 CTAAAGTTGG TGTAGCAGCA GTTGATCAGA CTGAAAAACG GTTTTTAGTC TCTGGAAAAA
1081 GACTGATTTT GCTTTTTTTA TAAATATTAT TAGATTTATT AATTTTTCTG TGCTCAATGT
1141 GTAAATTGTA TTATAATTCA TTGTGATTTA TTTCACTTTT AATTTGCTGG TGTTTTAATA
1201 AATGGGGGTG TTAGCTG

```

Figure 5.5 Nucleotide sequence of CREB protein (NCBI: M31630). The nucleotide sequence used to generate the sense (5') and antisense (3') primers for the amplification of the CREB protein transcript are highlighted in yellow and red respectively. The actual nucleotide sequence of the primers used are shown in Table 5.1.

```

1   CAGGACAAAA GATCCTTCAT CACCGAAGTG ACGTTTTAGA AACAGTGGTC CTGATCAACC
61  CTTCTGATGA AGCAGTCAGC ACCGAGGTGC GCTTAATGAT CACTGATGCT GCCCGACACA
121 AGCTGCTCGT GCTGACCGGG CAGTGCTTTG AAAATACCGG AGAGCTCATT CTCCAGTCCG
181 GCTCTTTTCTC CTTCCAGAAC TTCATAGAGA TTTTCACCGA TCAAGAGATC GGGGAGTTAC
241 TAAGCACCAC CCATCCTGCC AACAAAGCCA GCTTAACCCT GTTCTGTCCT GAAGAAGGGG
301 ACTGGAAGAA CTCCAATCTT GACAGACACA ATCTCCAAGA CTTTCATCAAT ATTAAACTCA
361 ATTCAGCTTC TATCTTGCCA GAAATGGAAG GACTTTCTGA GTTTACCGAG TATCTCTCAG
421 AATCAGTGGG AGTCCCATCT CCCTTTGACA TCTTGGAACC TCCCACATCG GGTGGATTTT
481 TGAAGCTCTC CAAGCCCTGC TGTTATATTT TTCCAGGAGG GAGGGGCGAT TCTGCCTTGT
541 TTGCAGTGAA TGGTTTCAAT ATGCTCATCA ATGGCGGATC AGAGAGAAAA TCCTGCTTCT
601 GGAAGCTCAT CCGACACTTA GACCGAGTGG ACTCCATCCT GTCACCCAC ATTGGGGATG
661 ACAATTTGCC TGGGAATAAAC AGCATGTTAC AGCGGAAAAT TGCAGAGCTC GAGGAAGAAC
721 AGTCCAGGG CTCCACCACA AATAGTGACT GGATGAAAAA CCTCATCTCC CCTGACTTAG
781 GAGTTGTATT TCTCAATGTA CCTGAAAATC TCAAAAATCC AGAGCCAAAC ATCAAGATGA
841 AGAGAAGCAT AGAAGAAGCC TGCTTCACTC TCCAGTACCT AAACAAATG TCCATGAAAC
901 CAGAACCTCT GTTTAGAAGT GTAGGCAATA CTATTGATCC TGTCATTCTT TTCCAAAAAA
961 TGGGAGTAGG TAAACTTGAG ATGTATGTGC TTAATCCAGT CAAGAGCAGC AAGGAAATGC
1021 AGTATTTTAT GCAGCAGTGG ACTGGTACCA ACAAAGACAA GGCTGAATTC ATTCT ----

-----
7441 AGAGAGAGAG AGCGCGGGGAG AGAGTGAGAG AGAGTGAGAG CACAAAGATA ACGCAGGAGA
7501 GAGAGAGAGA AAGAATGAGA AAGAAAAGGA ATGCAAGAGA AGGAGATGTA ATGACAGAGA
7561 GTTCTGGTGA GATACCCAGA GAGAAAAAGA GAGAGCAGGG TGGGGTAAGG AGGAGAAAAT
7621 AAACCAACAA TTAGGTCTGC ATTTTCTCAG GCAGTAGGCA TTCTTTAGTC TACATAGGCA
7681 AAGTTTTCCA TTTTGTGTCAG TCTGAGTCAT CAAAAAGAGT CTTAATTTTC TAAAACAAGT
7741 TGGCTAGAAG AAAGTAAAAA GAACAACACT TGTTATGAGG GCATGTGATA TTTTCACATC
7801 TTAATTAAGC TCCTTCAGTT TGAAGGCTGC ACACTGACAT AATGTAGTGA GTGTAGACTG
7861 GCCATGCAAG TGGTTTGGGC CCCATTGAGA ACTCTCAGAC TCTAAACACA CAAGTAGATT
7921 GATCTAAGGC ATGCTCCAGC CATTGTCCAC CCACTTAGTC CACTCTGAGT CGATTAACCT
7981 GCATGCAGCA ACACCCAAGT CCACCCAAT TAACTGAAGC AAATACCAA GCAGTTGGGA
8041 GTACATATGG TAGACAATTT GCCTTAGGAA GTGACTTGAA TGTACAAAGA TACTTGATGC
8101 ACTTATTTTT TAATGTGAGA CAGCAAGTTT ATAAAACATC CATATAGGAT TATAGATACT
8161 TAAAGGAACA CGTGGGTGAG CGTGTGTGGG GGTACTAGAA GCTGATCTGA TTGGTCCAAC
8221 AGTTTGATGC TGAGTCATGC GTGTTGAATC CCACTTCAGT GCACCTGTGG CCTCTCAGTC
8281 AAACAAGTTG TGCCTTTCAC AGCTTCTTTA CTA CTGCAAG TTCAAGACTG AAATGGCTTC
8341 TATGATCAGA ACTGGGAAAA CAGTGAATCT TATGGTGGAA GAGGTTCTCA GCAAGTGTAC
8401 AGTATTTACC TTCCTTTGTC TTACATTGGC TTTTAAATTT TTCCATTAAT TTCAACATAA
8461 TTATGGGAAC AAGTGACAG AAGAATTTT TTTTAAAGAT ATGTGAGAAC TTTTCATAGA
8521 TGAACTTTTT AACAAATGTT TTCATTTACA GGAAATGCA AAGAAAATTC TCAAGTGATA
8581 GTCTTTTTTT TTAAGTGTTC CGTAAGACAA AAATGAATA ATGTTTTTTG AAGTTCTGGC
8641 AAGATTGAAG TCTGATATTG CAGTAATGAT ATTTATTAAA AACCCATAAC TACCAGGAAT
8701 AATGATACCT CCCACCCCTT GATTCCATA ACATAAAAGT GCTACTTGAG AGTGGGGGAG
8761 AATGGCATGG TAGGCTACTT TTCAGGGCCT TGACAAGTAC ATCACCCAGT GGTATCCTAC
8821 AACTTCTTT CAAGATCTC AACCATGAGG TAAAAGAGCC AAGTTCAAAG AACCCTAGCA
8881 CAAATTTGCT TTGGGATTTT CTTTCTGGA

```

Figure 5.6 Nucleotide sequence of the MAP1B protein (NCBI: XM 003704). The nucleotide sequence used to generate the sense (5') and antisense (3') primers for the amplification of the MAP1B transcript are highlighted in yellow and red respectively. The actual nucleotide sequence of the primers used are shown in Table 5.1.

```

1   ATGCAGGCCA TCAAGTGTGT GGTGGTGGGA GATGGGGCCG TGGGCAAGAC CTGCCTTCTC
61  ATCAGCTACA CCACCAACGC CTTTCCCGGA GAGTACATCC CCACCGTGT T GACAACATAT
121 TCAGCCAATG TGATGGTGGG CAGCAAGCCA GTGAACCTGG GGCTGTGGGA CACTGCTGGG
181 CAGGAGGACT ACGACCGTCT CCGGCCGCTC TCCTATCCAC AGACGGACGT CTTCTCATC
241 TGCTTCTCCC TCGTCAGCCC AGCCTCTTAT GAGAACGTCC GCGCCAAGTG GTTCCAGAA
301 GTGCGGCACC ACTGCCCCAG CACACCCATC ATCCTGGTGG GCACCAAGCT GGACCTGCGG
361 GACGACAAGG ACACCATCGA GAAACTGAAG GAGAAGAAGC TGGCTCCCAT CACCTACCCG
421 CAGGGCCTGG CACTGGCCAA GGAGATTGAC TCGGTGAAAT ACCTGGAGTG CTCAGCCCTC
481 ACCCAGAGAG GCCTGAAAAC CGTGTTCGAC GAGGCCATCC GGGCCGTGCT GTGCCCTCAG
541 CCCACGCGGC AGCAGAAGCG CGCCTGCAGC CTCTCTAG

```

Figure 5.7 Nucleotide sequence of the C3 protein (NCBI: M29871). The nucleotide sequence used to generate the sense (5') and antisense (3') primers for the amplification of the C3 protein transcript are highlighted in yellow and red respectively. The actual nucleotide sequence of the primers used are shown in Table 5.1.

```

1   AGTTGTTGCT TATGATGTGT GAGTGAACAT ATGCCATGCC TGGCCTTTTT TGTGGTTAGC
61  TCCTTCTTGC CAACCAACCA TGAGCTCCCA GATTCGTCAG AATTATTCCA CCGACGTGGA
121 GGCAGCCGTC AACAGCCTGG TCAATTTGTA CCTGCAGGCC TCCTACACCT ACCTCTCTCT
181 GGGCTTCTAT TTCGACCGCG ATGATGTGGC TCTGGAAGGC GTGAGCCACT TCTCCGCGA
241 ACTGGCCGAG GAGAAGCGCG AGGGCTACGA GCGTCTCCTG AAGATGCAA ACCAGCGTGG
301 CGGCCGCGCT CTCTTCCAGG ACATCAAGAA GCCAGCTGAA GATGAGTGGG GTAAAACCC
361 AGACGCCATG AAAGCTGCCA TGACCCTGGA GAAAAAGCTG AACLAGGCC TTTTGGATCT
421 PCATGCCCTG GGTTCTGCCC GCACGGACCC CCATCTCTGT GACTTCCTGG AGACTCACTT
481 CCTAGATGAG GAAGTGAAGC TTATCAAGAA GATGGGTGAC CACCTGACCA ACCTCCACAG
541 GCTGGGTGGC CCGGAGGCTG GGCTGGGCGA GTATCTCTTC GAAAGGCTCA CTCTCAAGCA
601 CGACTAAGAG CCTTCTGAGC CCAGCGACTT CTGAAGGGCC CTTGCAAAG TAATAGGGCT
661 TCTGCCTAAG CCTCTCCCTC CAGCCAATAG GCAGCTTTCT TAACTATCCT AACAAACCTT
721 GGA

```

Figure 5.8 Nucleotide sequence of the FLCK protein (NCBI: M10119). The nucleotide sequence used to generate the sense (5') and antisense (3') primers for the amplification of the FLCK protein transcript are highlighted in yellow and red respectively. The actual nucleotide sequence of the primers used are shown in Table 5.1.

```

1   ATGAAATCGT TAGCACCTTA GGAGAGGGGA CCTTCGGCCG AGTTGTACAA TGTGTTGACC
61  ATCGCAGGGG TGGGGCTCGA GTTGCCCTGA AGATCATTAA GAATGTGGAG AAGTACAAGG
121 AAGCAGCTCG ACTTGAGATC AACGTGCTAG AGAAAATCAA TGAGAAAGAC CCTGACAACA
181 AGAACCTCTG TGTCCAGATG TTGACTGGT TTGACTACCA TGGCCACATG TGTATCTCCT
241 TTGAGCTTCT GGGCCTTAGC ACCTTCGATT TCCTCAAAGA CAACAACACTAC CTGCCCTACC
301 CCATCCACCA AGTGCGCCAC ATGGCCTTCC AGCTGTGCCA GGCTGTCAAG TTCCTCCATG
361 ATAACAAGCT GACACATACA GACCTCAAGC CTGAAAATAT TCTGTTTGTG AATTGAGACT
421 ATGAGCTCAC CTACAACCTA GAGAAGAAGC GAGATGAGCG CAGTGTGAAG AGCACAGCTG
481 TGCGGGTGGT AGACTTTGGC AGTGCCACCT TTGACCATGA GCACCATAGC ACCATTGTCT
541 CCACTCGCCA TTACCGAGCA CCAGAAGTCA TCCTTGAGTT GGGCTGGTCA CAGCCTTGTG
601 ATGTGTGGAG TATAGGCTGC ATCATCTTTG AATACTATGT GGGATTCACC CTCTTCCAGA
661 CCCATGACAA CAGAGAGCAT CTAGCCATGA TGGAAAGGAT CTTGGGTCTT ATCCCTTCCC
721 GGATGATCCG AAAGACAAGA AAGCAGAAAT ATTTTTACCG GGGTCGCCTG GATTGGGATG
781 AGAACACATC AGCTGGGCGC TATGTTTCGTG AGAACTGCAA ACCGCTGCGG CGGTATCTGA
841 CCTCAGAGGC AGAGGAACAC CACCAGCTCT TCGATCTGAT TGAAAGCATG CTAGAGTATG
901 AACCAGCTAA GCGGCTGACC TTGGGTGAAG CCCTTCAGCA TCCTTTCTTC GCCCGCCTTC
961 GGGCTGAGCC GCCCAACAAG TTGTGGGACT CCAGTCGGGA TATCAGTCGG TGACGATCAG
1021 GCCCTGGGCC CCCCTGCATC TTTTATAGCA GTGGGTGTCC AGTCCAGGAC ACTGGTGCTT
1081 TTTTATACAA GAGAACGAGC CAGAGTTCAC TCCTTCCTCC TGGCTCTCTA TATACCTGTG
1141 AATATGTGAA ATAGTGTAAT TATGAAAGAA CTTGTACCTA TCACTTCAAC CCCTGCCTTG
1201 TACATAATAC TATTCCATCC ACACAGTTTC CACCCTCACC TGCCCCCTCA TACGGAGTTG
1261 GATGGGGGCC GAGTGAGGTA ACCAGGTGGC ATCTACCCCA TGTTTTATAA GGAATTTTGT
1321 ACAGTCTTTG TGAAATAAAA TAACGTGCTT CATTTGACCC CC

```

Figure 5.9 Nucleotide sequence of the CLK2 protein (NCBI: XM002188). The nucleotide sequence used to generate the sense (5') and antisense (3') primers for the amplification of the CLK2 protein transcript are highlighted in yellow and red respectively. The actual nucleotide sequence of the primers used are shown in Table 5.1.

```

1   GGGCAATTTG TTAGTTATCC GCCGCCACCA AGACGCGGCA CGGCGCCTGG ACCGGAGGGG
61  CCCC GCGCGG GCGCGAACTT TGGGCTCGGG CGAGTGGGTG GTGCTCCGCC CAGCCCGAGA
121 CGGGCGGGCG CGCGGGCCAA TGGGTGCCGC CTCTTGGCCG CGGGGGGCCC CGACCCGTGG
181 GTCCCGGCCA CCAGCGCCCC AGCCCCGAGG CTCAGAAGCG GCAGGCGGAG GCGCGGTCCG
241 GGCCTATGG CCATGCCCGG CGGGTCTCAC GCGGCTGCC CTGCCCCGGC GCGCCTTCGG
301 TAGGGGGCGC CCGGGGCCCA GCTGGCCCGG CCATGCTGCT GGAGACACAG GACGCGCTGT
361 ACGTGGCGCT GGAGCTGGTC ATCGCCGCGC TTTCGGTGGC GGGCAACGTG CTGGTGTGCG
421 CCGCGGTGGG CACGGCGAAC ACTCTGCAGA CGCCACCAA CTACTTCCTG GTGTCCCTGG
481 CTGCGGCCGA CGTGGCCGTG GGGCTCTTCG CCATCCCCTT TGCCATCACC ATCAGCCTGG
541 GCTTCTGCAC TGA TTTCTAC GGCTGCCTCT TCCTCGCCTG CTTCTGTGCTG GTGCTCACGC
601 AGAGCTCCAT CTT CAGCCTT CTGGCCGTGG CAGTCGACAG ATACCTGGCC ATCTGTGTC
661 CGCTCAGGTA TAAAAGTTG GTCACGGGGA CCCGAGCAAG AGGGGTCATT GCTGTCTCT
721 GGGTCCTTGC CTTTGGCATC GGATTGACTC CATTCCTGGG GTGGAACAGT AAAGACAGTG
781 CCACCAACAA CTGCACAGAA CCCTGGGATG GAACCACGAA TGAAAGCTGC TGCCTTGTGA
841 AGTGTCTCTT TGAGAATGTG GTCCCCATGA GCTACATGGT ATATTTCAAT TTCTTTGGGT
901 GTGTTCTGCC CCCACTGCTT ATAATGCTGG TGATCTACAT TAAGATCTTC CTGGTGGCCT
961 GCAGGCAGCT TCAGCGCACT GAGCTGATGG ACCACTCGAG GACCACCCTC CAGCGGGAGA
1021 TCCATGCAGC CAAGTCACTG GCCATGATTG TGGGGATTTT TGCCCTGTGC TGTTACCTG
1081 TGCATGCTGT TAACTGTGTC ACTCTTTTCC AGCCAGCTCA GGGTAAAAAT AAGCCCAAGT
1141 GGGCAATGAA TATGGCCATT CTTCTGTAC ATGCCAATC AGTTGTCAAT CCCATTGTCT
1201 ATGCTTACCG GAACCGAGAC TTCCGCTACA CTTTTACAA AATTATCTCC AGGTATCTTC
1261 TCTGCCAAGC AGATGTCAAG AGTGGGAATG GTCAGGCTGG GGTACAGCCT GCTCTCGGTG
1321 TGGGCCTATG ATCTAGGCTC TCGCCTCTTC CAGGAGAAGA TACAAATCCA CAAGAAACAA
1381 AGAGGACACG GCTGGTTTTT ATTGTGAAAG ATAGCTACAC CTCACAAGGA AATGGACTGC
1441 CTCTCTTGAG CACTTCCCTG GAGCTACCAC GTATCTAGCT AATATGTATG TGTCAGTAGT
1501 AGGCTCCAAG GATTGACAAA TATATTTATG ATCTATTCAG CTGCTTTTAC TGTGTGGATT
1561 ATGCCAACAG CTTGAATGGA TTCTAACAGA CTCTTTTGTT TTTAAAAGTC TGCCTTGTTT
1621 ATGGTGGAAA ATTACTGAAA CTATTTTACT GTGAAACAGT GTGAACTATT ATAATGCAAA
1681 TACTTTTTTAA CTTAGAGGCA ATGAAAAAT AAAAGTTGAC TGTACTAAAA ATG

```

Figure 5.10 Nucleotide sequence of the A2BR (NCBI: X68487). The nucleotide sequence used to generate the sense (5') and antisense (3') primers for the amplification of the A2BR transcript are highlighted in yellow and red respectively. The actual nucleotide sequence of the primers used are shown in Table 5.1.

1 GAATTCCCTT GTAAGGTTTT CTTAACAAAA CACCAGTCAC ATAAGTGCAT TTTATTTTAT
61 ATTTTTGTTT ATTTATTTGA GACGGAGTCT CTTGTCTCTC AGGCTGGAGT GCAGTGGCGC
121 CATCTCTGCT CGCTGCAACC TCCACCTCCT GGGTTCCAGC GATTCTCCTG CCTCAGCCTC
181 CCGAGGGGGT AGCTGGGACT ACAGGTGCGC ACCACCATGC CCAGCTAATT TTGTATTTTT
241 CGTAGAGATG GGGTTTCACC ATGTTGTCCA GGCTGGTCTT GAACTCCTGA CCTCAGGTGA
301 TCCTCCCGCC TCGGCCTCCC AAAGTGCTGG AATTACAGGC GTGATCCACC GCACCCGGCC
361 TATTTTTTGA GAGAGGGTCA CACTCTGTCTG TCCCGGCTGG AATGCAGTGA TGGATCACC
421 GCCCACTACA GCCTCGACCT CCGGGCTCAA GCAATCCTCC CCGCCAGCC TCCTGAGTAG
481 CGAGCGCCTC GACGCCCAGC TAATTTTTAT TTTTATTTAT TTTTTGTAG AGACGGCGTC
541 TCTCTAAGAT GCCCAGGCTG GTGGCCGGTG TCGAACTCCT AAGATGAAGC GATCCTCCCC
601 GGCCTTGGCC TCCGCGCCTC CTAAAGCGCC AGGTATGAGC CACCGCGCCT GGCCTACAAG
661 TGCATTTTAA TTAAAGTATT ATTAATGTCT TTGCCTGAAG AAATTCGCTT TAAATTGTG
721 ACTTATCTTT CACCCAAAAA TCAAAGCACA ATTCAGCCCC GAGGCGGGGG CGGTAGGAGC
781 TGGGCGGGGC GGGGGCAGGG AAAGACCAGG AGCAGAGATT CAAAAAGAGT AAGAGGGCAA
841 AATGTGCATA ATGCATCTTC ACAGGTAAGA GCCTGGCCAG GCTCCTGTTT TAATGGCTTC
901 CTCCTGAAGA AGATTCAAGC AGAGTGTAAG ATATTTTCGG AAAGTAGAGC ATTTTGAAAAG
961 CATTTTATAA TCTCTCAAAA CCGGAGACTG CTCCTGTCCC ACCTCGTTAG AGAAAAACAGC
1021 GATGCTCAAA GGCAACCTCC TTCCTGACAT TGCCTGGTAG GACGCGACGT GGTGTTTGCC
1081 CGCGCGGAAT GCGGACGCAA GGCTGCTCCT AGGTCTCGGG GACGCGCCAT CCCATTTC
1141 GCTCGCGGAG GCGTAGGGTC CGGGCGCGGG ACCCCAGTCG ACCTTGACTG GCGGCGCGAC
1201 CTTGAGGCCT GCGTTCGCCT CAGTTGCCCC CTCTGTGCAA TGGGGAGACG CGCCTCATCG
1261 CTTGACAACG GCCGAAGAGC CGCCGCGCTT CCGTCTCCCG CGTGCGCGCG CCATGCTGCC
1321 CACCCCGTTC CCGCACTGAC CCTCCCCCGT GCCCCGCGTC CCGTACTGCC GCCCCGCCCC
1381 GAGTCCCATG CCGCAGCCAC CGCGACGGAG CCCGCAGGCG GGAACCTGCC TCCGCGCGTT
1441 AGCGCGCACG CGCGCCTCAT GTGTGCTCCC CATCAGCGCC GGCTTCCGTC TATAGGCCAG
1501 ATGCACTGTC ACTCTGGCGA AGTCGCAGAC CCGATTGGCC GGGACGGAGG CGCGAGACCG
1561 GGTTGCGGGC GGGGCCGAAC GTGGTATAAA ACGGGCGGGA GGCCAGGCTC GTGCCGTTTT
1621 GCAGACGCCA CCGCCGAGGA AAACCGTGTA CTATTAGCCA TGGTCAACCC CACCGTGTTT
1681 TTCGACATTG CCGTCGACGG CGAGCCCTTG GGCCGCGTCT CCTTTGAGGT CGGGCGGGCG
1741 GCGGCGTGCG GGAATGGGGC CCAGAAAGTG GGCCGGGGTC GGGGTGGGTG GTAGCGCCCC
1801 AAAGGCCCGG GCGCGGGGCG ACCCTGCTTG AGGGGCGAGC GCGGGCGGGC TGCGGCGCCA
1861 TTTCTGACG AGGGGCCATT TTGGGAGGTC CGCGAGTCG GGGAGGAGGC CGGGACGCGG
1921 CGGACAAAGG CAGGCGGGGC GGCTGCGAGG CCGTTGGGGG AGGGGGCCCC CGTCCGCCCC
1981 CCGCCTCAT GTGGCCGCGC CCTGTCTCTG CCGACGCACG TGCTCGGCGG CCGCGCTCAG
2041 GTCCGCGCCT TGAGAGTCGT TGTCCGCCCT AGCTTGGCCT GGGCGCCGCA GACCGGAGCC
2101 AGAAGCACGC TCGCGGGGGC TTGCGACCGC CTTCTGGGA AGCTGTCCCC TGGCAGGCAT
2161 GGGTGCTTTA CATCCTGAGC TGGGAAGCTG TTTGCTTGAG GGTTTTTCTC AAGGATCGAG
2221 GCGCGGTGTG AGCCCGTCCA TGCTCGGTCC TGTAGATCCC GGGAGGCCAT GTTATAAAAG
2281 GAGACTTGCT GGGATGTGAC GGGTTGCCAC TTGAAATATC TTCCATTTGG ATAAAGTAGG
2341 AATATTTATA CATGTGCCCC AAACGTCCCT CCGTGTCCCC CACCCCAAG CGGAAATGTG
2401 AAAATGGGCC TTGCCTTTGC TGGTGCCCAA GGACCGCCTT CCACTGCAGT GACGGCGCTG
2461 CTGGCCACAA GGCAGGCCTC TTCCGACCAA GGTGGATTAC CAGTGATTAC CTAATTAGTT
2581 TTGAGAGCGT TAAATGAGTT CTTAAAGATC AGTTGTAATT ATAGCATAGT ATCTAAACTT
2641 GCGCGGTGTC TTCAAAGTTA AATATTGAGT ACGATTCCGT TCCAGTTAAC ATGGATAGAC
2701 CTTAGGGAGT AGCGAAATAG GATGTTAGTG GTTTTATTCC TTTAAATCAC ATCTCAAAAG
2761 GCCACCAATG GCTAGTTTGG ATCTTATTCC GAAAATAGAT TGATCCTCAT GCAGTCTTCG
2821 GAAACTGTC ATGTTAATCC ACACCCACC CCACCTATGA GTGTAGTCAA AGCTGGTAAG
2941 TGACAAGGGC TTTGCTGGAA ACTTGGCCTG ACCTAATGTT GGGCATCAGG TTACCCAAAAG
3001 AGCTTCAGGG AAATGAGAAA GGACTTGAGC GTCTTGATGA GAATGGAGGG GTAACGCCA
3061 ATGAGGGCTT TGGCTTTAGC GAAAGTCTGA AAGGGAAGCC ATAGGAACTT AAACGTACCG
3121 ACTATAAAGC TCTGAGAAAA GCTGATGTTT TAGAAAGACC ATACATTCTA GGTACAAATA
3181 CCTAAAAACT AAAAAATAAG TACGTTGGCC AGGCGGGCGG ATCACGAAGT CAGGAGATTG
3241 AGACCATCCT GGGCCCCTGG TGAAACCCCA CCTCTATTAA AAATACAAAA ATTAGCTGGG
3301 CGTGGTGGCG CTTGCCTGTA ATCTCAGCTA CTCTAGAGGC TGAGGCAGGA GATCGCTTGA

3361 ACCCCGGAGG CGGAGGCTGC AGTGAGCCGA GATCGTGCCA CTGCACTCCA GCCTGGTGAC
 3421 AGCGAGACTC TTGTCTCAAA AAAAAAAAAAG TACATTGCTA TAAGAGAAGT GCACACGGAT
 3481 ACTAGTAGTT AATTCAGTCA CATCTGTGAA ATAGCTTATA AAATGCTACT TTTAAACAAG
 3541 CTGTTTTTAT GAAAGGGCTT GTAAATGTTT ATGGTATTTA AGCTACCTCT CTAGCCATAA
 3601 CGTATTATAC ATTCAAGAAA GGTTCAAAAC CAGATATACT AGAAACCAAT CTTTATTTTT
 3661 TACCCCACTA CTAGGTAAGG GCCTGGATAC CAAGAAGTGA CTGCTCATCT AATCCATAAA
 3721 GCTATGTTAA CAGATTGGAG GTAGTAGCAT TTTCATTACA AGTGACTAAA AGAACAGCTG
 3781 TTTACCCCTG ATCGTGCAGC AGTGCTTGCT GTTCCTTAGA ATTTTGCCTT GTAAGTTCTA
 3841 GTGATGTACT AAAAGTTTGA GACACTTTCT AGAAGTCTCA CTATTTAAGT TATGACTAGT
 3961 ATTGGATTTT TGGCATGTCT TTGGGTTTCA TGTTTCTTAA CCCAAGTCC TGCAGGGCCT
 4021 TATGGCTGTC AGGAGCAGTT CTTGGGAATT AAAGTAATTA CTGAAGAAGT ATTCTAGTGA
 4081 GAAAATGAAT TTATGACTCA GAAGCCCCTA AAGACATGGG TACTAAGCAA CAAAATAAGC
 4141 AGATGTTAAT TAACTGTAAT TTTCTCTTAC AGCTGTTTGC AGACAAGTCC CCAAAGACAG
 4201 CAGTTTGGTC CATTTTCTAA GTTTAACAAA GATGTTCCAA TTGTGACAGT TTGTGTGTGT
 4261 GTGTGTATAT ATATATTTTT ATGTATGTAT ATATGTGTTT AATTTTTTTTT TAAACAGAAA
 4321 ATTTTCGTGC TCTGAGCACT GGAGAGAAAG GATTTGGTTA TAAGGGTTC TGCTTTCACA
 4381 GAATTATTCC AGGGTTTATG TGTCAGGTAC GAAATTTACT GAATTTTATT TTATTTGGGT
 4441 TTCTACCATT CGGTTCTATT TAACCCTTCT ATTCAGTTTG AACTTGGGTT TAAAGTTTGA
 4561 ACCTTGCAGA TTTGGCACAC TTCATGGTTA TGTTGTCAGA AGTGACATTT TTCCTATATG
 4621 TTGACAGGGT GGTGACTTCA CACGCCATAA TGGCACTGGT GGCAAGTCCA TCTATGGGGA
 4681 GAAATTTGAA GATGAGAACT TCATCCTAAA GCATACGGGT CCTGGCATCT TGCCATGGC
 4741 AAATGCTGGA CCCAACACAA ATGGTTCCCA GTTTTTCATC TGCCTGCCA AGAGTGAGTG
 4801 GTAAGGGTAC AACATGGCAC ACTAACCACC TGAATAATG AAAAGTTGCC CTGGGGGGAA
 4861 CGGAACAAAC ACTACTTTTC TTCAACCTTT GCTTCCACAG ACTTTTTTCAT CCCTAAGATA
 4921 TATGATAGAA ACTTGGCCCT TAGCTGGGTG GTTGAATTAG GTGCTACTTT TTTGAGATGG
 5041 AGTTTTGCTC TGTTGCCAGG TTGGAGTGCA GTGGCACAAT CTGGGCTCAC TGCAACCTCT
 5101 GCCTCCTGGG TTCAAGCGAT TCTCCTGCCT TGGCCTCCTG AGTAGCTGAG AATACAGATG
 5161 TGTGCCAGCA TGCCTGGCTA ATTTTTTGTA TTTTGTGGA GACGGGGTTT CATCATGTTG
 5221 GCCAAGCTGG TCTTGAAGTC GTGACTTAAG GTGAACCACC TGCCTTGGCC CCCCAAAGTG
 5281 CTGGGATTTT AGGCATGAGC CACTGCGCCC AACCAATTAA GTGCTTTTTT TTTTTTTTTT
 5341 CTTTTCTCAG ACTGGATCTC GCTCTTATCT CCCAGGTTGG AGTGCAGTGG TGCCATCTCA
 5401 GGAACACAG GCATGCACCA CCACTCCAG CTAAATTGTG TATTATTAGT AGAGCGGAT
 5521 TTACCATGTT GTCCAGGCTG GTCTCGAAGT CCTGGGCTCA AGTGATCTGC CTGCCTTGAC
 5581 CCCCCGAAG TGCTGGGATT ACAGGCATGA GCCACTGTGC CCACCAATT AAGTGCTGCT
 5641 TTTGTTTTGT TTGTTTTTGG GGGAGGGGGG CGCAATTCAT TCTATATGTG TAACTCTTTT
 5761 TTGAGATGGA GTTTCGCTCT GTCGCCCAGG CTGGAGTGCA GTGGCGCGAT CTCGGCTCAC
 5821 TGCAAGCTCC GCCTCCCAGG TTCACGCCAT TCTCCTGCCT CAGCCTCCCG AGTAGCTGGG
 5881 ACTATAGGCA CATGCCACCA TGCCCAGGCTA ATTTTTTGTA TTTTATAGT AGACAGGTT
 5941 TCACCGTGTT AGCCAGGATG GTCTCGATCT CCTGACCTCG TGATCCGCC GCCTTGGCCT
 6001 CCCAAAGTGC TGGGATTACA GCGGTGAGCC ACCGCACCCG GCCTATATGT GTAACCTTTT
 6061 AATGGTAATT GGAGAATCAT GTTTAATGAC ATTTAGTACA AAAGGCTTCA GTTAAAAAAA
 6121 AAAAAAAAAA GCTACCTTTC TCGTCTTGGT TCATGACACA TGGAGGCTGC TTGTTTGTGG
 6181 TTGCCAGTCA TAATGATTGT TCTTCTTTTT CAAGTTTGA TGGCAAGCAT GTGGTGTGTTG
 6241 GCAAAGTGAA AGAAGGCATG AATATTGTGG AGGCCATGGA GCGCTTTGGG TCCAGGAATG
 6301 GCAAGACCAG CAAGAAGATC ACCATTGCTG ACTGTGGACA ACTCGAATAA GTTTGACTTG
 6361 TGTTTTATCT TAACCACCAG ATCATTCTT CTGTAGCTCA GGAGAGCACC CCTCCACCCC
 6421 ATTTGCTCGC AGTATCCTAG AATCTTTGTG CTCTCGCTGC AGTTCCCTTT GGGTTCATG
 6481 TTTTCTTGT TCCCTCCCAT GCCTAGCTGG ATTGCAGAGT TAAGTTTATG ATTATGAAAT
 6541 AAAAATAAAA TAACAATTGT CCTCGTTTGA GTTAAGTGTG GATGTAGGCT TTATTTTAAAG
 6601 CAGTAATGGG TTAATTCTGA AACATCACTT GTTTGCTTAA TTCTACACAG TACTTAGATT
 6661 TTTTTTACTTTCCAGTCCCAGGAAGTGTCAATGTTTGTGAGTGGAAATAT

Figure 5.11 Nucleotide sequence of cyclophylin (NCBI: X52851). The nucleotide sequence used to generate the sense (5') and antisense (3') primers for the amplification of the cyclophylin transcript are highlighted in yellow and red respectively. Actual nucleotide sequence of the primers used are shown in Table 5.1.

Target Gene	Primer		Fragment Size (bp)	Cycle conditions		
	S=Sense	A=Antisense		D	A	E
A2A receptor	S A	GGGCTCCCTCGGTGTACATCACGGTGG CCATTGTACCGGAGCGGGATGCGGATG	350	94°C 15 secs	65°C 15 secs	68°C 1 min
A2B receptor	S A	GCTGCTGGAGACACAGGACGCGCTGTA CGTGACCAAACCTTTATACCTGAGCGG	350	94°C 15 secs	80°C 15 secs	68°C 1 min
cAMP response element binding protein	S A	GAAAGTCTGGGTTCCAGTCTTTAGAGAA CTGTGAAAGAGCAGGCTCTGTACTCTG	350	94°C 15 secs	55°C 15 secs	68°C 1 min
Protein kinase CLK2	S A	GATGTTTGACTGGTTTGACTACCATGG CGAGTGGAGACAATGGTCTATGGTGC	350	94°C 15 secs	60°C 15 secs	68°C 1 min
Dup 1 ras-related C3 botulinum toxin	S A	GCCATCAAGTGTGTGGTGGTGGGAGAT CAGGTCCAGCTTGGTGCCACCAGGAT	350	94°C 15 secs	60°C 15 secs	68°C 1 min
Ferritin light chain kinase	S A	GAGCTCCCAGATTCGTCAGAATTATTC CAGGGCATGAAGATCCAAAAGGGGCTG	350	94°C 15 secs	60°C 15 secs	68°C 1 min
Microtubule-associated protein IB	S A	GATGCTGCCCGACACAAGCTGCTCGTG CAAAGGGAGATGGGACTTCCACTGATT	350	94°C 15 secs	60°C 15 secs	68°C 1 min
Cyclophilin	S A	GTGCTCTGAGCACTGGAGAGAAAAGGAT GTCTTGCCAGTGCAGATGAAAACTGG	250	Conditions used for cyclophilin matched conditions for the transcript to be amplified		

Table 5.1 Table showing primers and conditions for RT-PCR reactions. Sequences of the sense (S) and antisense (A) RT-PCR primers are shown alongside the gene they detect. An initial 2 min denaturation step at 94°C was performed for each transcript tested. The temperatures and hold times for the denaturation (D), annealing (A) and elongation (E) stages of the PCR cycles are shown. A range of cycles were performed in each case ranging from 15 - 35 cycles. The expected size of the fragments amplified are given in base pairs (bp)

5.2.5 Checking for PDE4A7 expression in HEK-293 cells

cDNA template was prepared from HEK-293 cells over-expressing either PDE4A7 or pcDNA3 (Materials and Methods 2.3.9.2). However, before proceeding with RT-PCR analysis, it was important to determine that these transfections were successful by checking for PDE4A7 protein expression. Transfected HEK cell lysates were subjected to 10% SDS-PAGE electrophoresis before immunoprobing with the polyclonal anti-VSV antibody, which identified the 34kDa immunoreactive band of PDE4A7 only in those cells transfected with PDE4A7 (*figure 5.12*). Experiment 1 and experiment 2 show the results of two separate sets of transfections. The cDNA produced from each of these experiments were used in the subsequent RT-PCR reactions.

For all the mRNA transcripts investigated two ethidium bromide gels are shown, demonstrating the results of two separate RT-PCR reactions in which the template cDNAs used were generated from the two separate transfected HEK cell populations (mentioned previously). These will be referred to as experiment 1 and experiment 2. Products from each of the RT-PCR reactions were separated by 1.5% agarose gel electrophoresis (*figures 5.13-5.18*). The predicted and observed weights for each of the transcripts are shown in Table 5.2. Each of these bands were found to increase in intensity with increasing cycle number, indicating that all the products were detected within the linear range of amplification. Each RT-PCR reaction contains a negative control where cDNA template was replaced with sterile water. No bands were detected in any of the negative controls.

The adenosine A2A receptor (A2AR), cAMP response element binding protein (CREB) and microtubule-associated protein 1B (MAP1B) were genes seemingly up-regulated in response to over-expression of PDE4A7, as detected by microarray analysis. When re-evaluated with RT-PCR no changes were detected for either the A2AR or MAP1B transcripts (*figures 5.13 and 5.15*, respectively). However, CREB appeared to be down-regulated (visually) in response to the over-expression of PDE4A7 (*figure 5.14*), which disagreed with the microarray data. The intensity of the CREB and cyclophilin bands at cycle 30 were measured (using the Kodak 1 ID programme) for both the control and experimental samples. When the ratio value (CREB:cyclophilin) from the experimental sample (HEK-293 cells over-expressing PDE4A7) was compared to that of the control sample (HEK-293 cells over-expressing pcDNA3), no significant difference was found (data not shown). This was the case for both experiment 1 and experiment 2. It was concluded that CREB expression was unaffected by the over-expression of PDE4A7. Dup 1 ras-related C3 botulinum toxin (C3), ferritin light chain kinase (FLCK) and protein kinase CLK2 (CLK2) were genes seemingly down-regulated in response to PDE4A7 over-

expression using microarray analysis. However, when these gene expression changes were re-evaluated with RT-PCR analysis (*figures 5.16, 5.17 and 5.18*, respectively), only CLK2 appeared to be down-regulated (visually) in response to PDE4A7 over-expression (at cycle 30) in both experiment 1 and experiment 2 (*figure 5.18*). The intensity of the CLK2 and cyclophilin bands at cycle 30 were measured (using the Kodak 1 ID programme) for both the control and experimental samples. When the ratio value (CLK2:cyclophilin) from the experimental sample (HEK-293 cells over-expressing PDE4A7) was compared with the ratio value (CLK2:cyclophilin) from the control sample (HEK-293 cells over-expressing pcDNA3), no significant difference was found. This was the case for both experiments. Therefore, it was concluded that CLK2 expression remained unchanged in response to the over-expression of PDE4A7. The A2B receptor transcript could not be amplified, indicating a problem with the primer design (data not shown). A comparison of the gene expression changes observed in these candidate genes from both microarray analysis and RT-PCR analysis are listed in Table 5.2.

Table 5.2 Comparison of the predicted and observed molecular sizes (in bp) for the target genes.

Target Gene	Predicted Size (bp)	Observed Size (bp)
Adenosine A2A receptor	350	347±11
cAMP response element binding protein	350	337±25
Microtubule-associated protein 1B	350	339±16
Dup 1 ras-related C3 botulinum toxin substrate	350	352±12
Ferritin light chain	350	363±10
Protein kinase CLK2	350	356±9
Cyclophilin	250	250±6

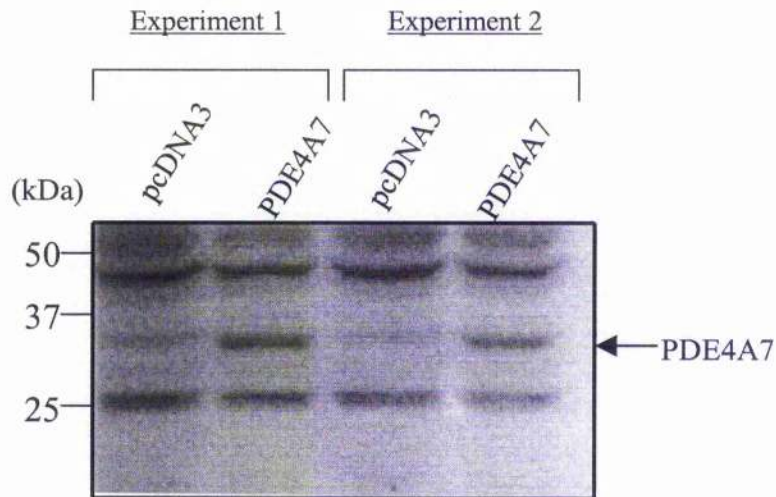


Figure 5.12 Detecting expression of PDE4A7 in cell lysates used for RT-PCR analysis. HEK-293 cells were transiently transfected with either PDE4A7 plasmid DNA or pcDNA3 plasmid DNA. These sets of transfections were performed on two separate occasions and the cell lysates separated on the same gel, labelled as experiment 1 or experiment 2 above. Cells were harvested in lysis buffer, homogenised and centrifuged to remove cellular debris. Lysates were subjected to 10% SDS-PAGE gel electrophoresis before immunoprobing with the anti-VSV polyclonal antibody. The immunoreactive band of PDE4A7 is indicated. Migration of the standard protein molecular weight markers (in kDa) are shown on the left.

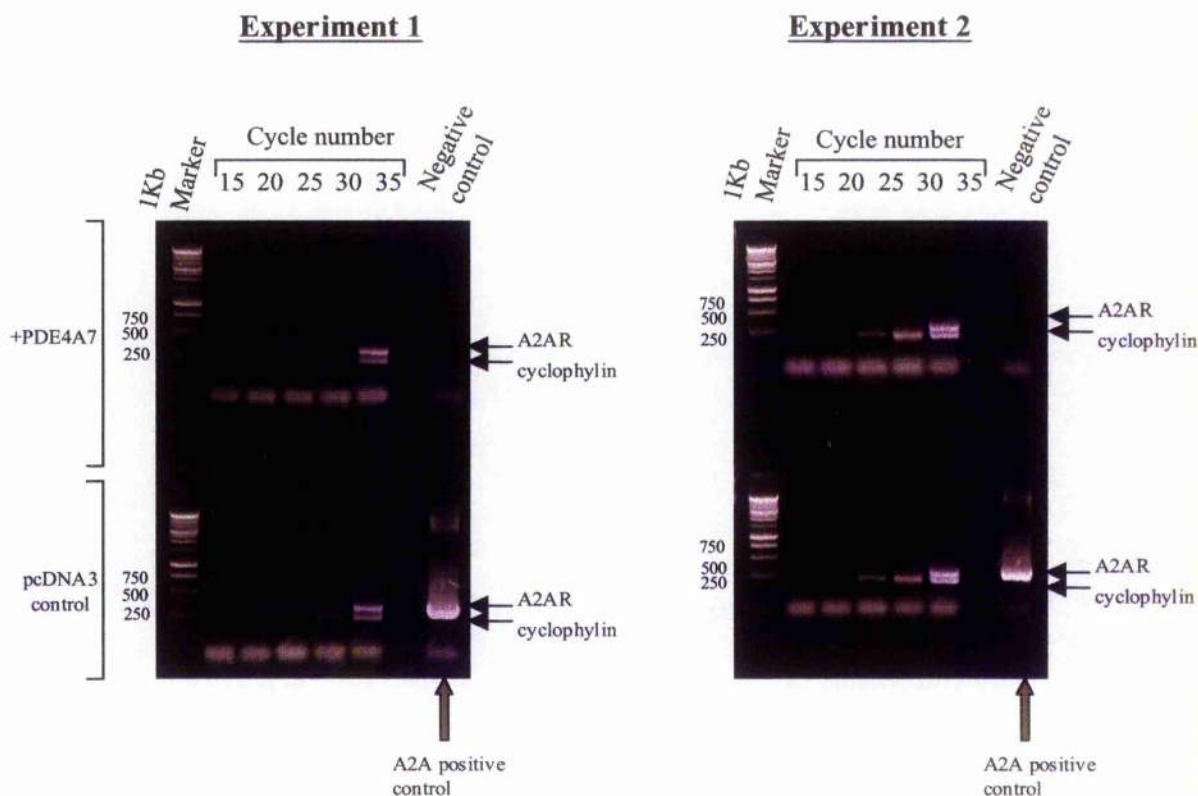


Figure 5.13 Changes in the adenosine A2A receptor (A2AR) transcript level in response to over-expression of PDE4A7. cDNA was generated from HEK-293 cells over-expressing either pcDNA3 or PDE4A7 plasmid DNA. PCR products were fractionated electrophoretically on 1.5% agarose gels, stained with ethidium bromide and visualised using a UV transilluminator. Two sets of primer pairs were included in each PCR reaction, one pair were designed to amplify a 350bp fragment representing the A2A transcript and the other primer pair were designed to amplify a 250bp fragment representing the control transcript of cyclophilin. Both bands are clearly labelled on the above gels. The two gels labelled experiment 1 and experiment 2 show the data obtained from two separate studies. The upper panel of each gel shows the change in A2A transcript level in HEK-293 cells in response to over-expression of PDE4A7 plasmid DNA, whereas the lower panels illustrate changes in A2A transcript level in HEK-293 cells in response to the over-expression of pcDNA3 plasmid DNA (negative control). The molecular size standards (in bp) are shown on the left.

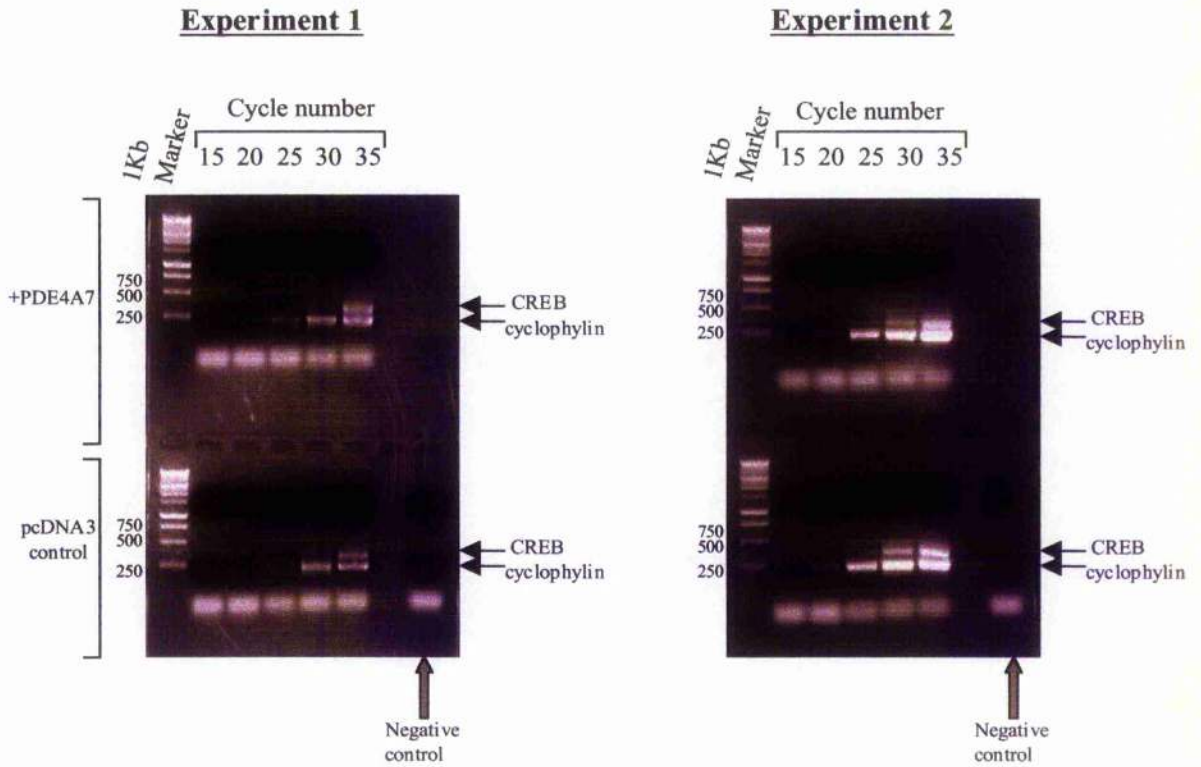


Figure 5.14 Changes in cAMP response element binding protein (CREB) transcript level in response to over-expression of PDE4A7. cDNA was generated from HEK-293 cells over-expressing either pcDNA3 or PDE4A7 plasmid DNA. PCR products were fractionated electrophoretically on 1.5% agarose gels, stained with ethidium bromide and visualised using a UV transilluminator. Two sets of primer pairs were included in each PCR reaction, one pair were designed to amplify a 350bp fragment representing the CREB transcript and the other primer pair were designed to amplify cyclophilin as a 250bp fragment. Both bands are clearly labelled on the above gels. The two gels labelled experiment 1 and experiment 2 show the data obtained from two separate studies. The upper panel of each gel shows the change in CREB transcript level in HEK-293 cells in response to over-expression of PDE4A7 plasmid DNA, whereas the lower panels show the changes in CREB transcript level detected in HEK-293 cells in response to the over-expression of pcDNA3 plasmid DNA (negative control). The molecular size standards (in bp) are shown on the left.

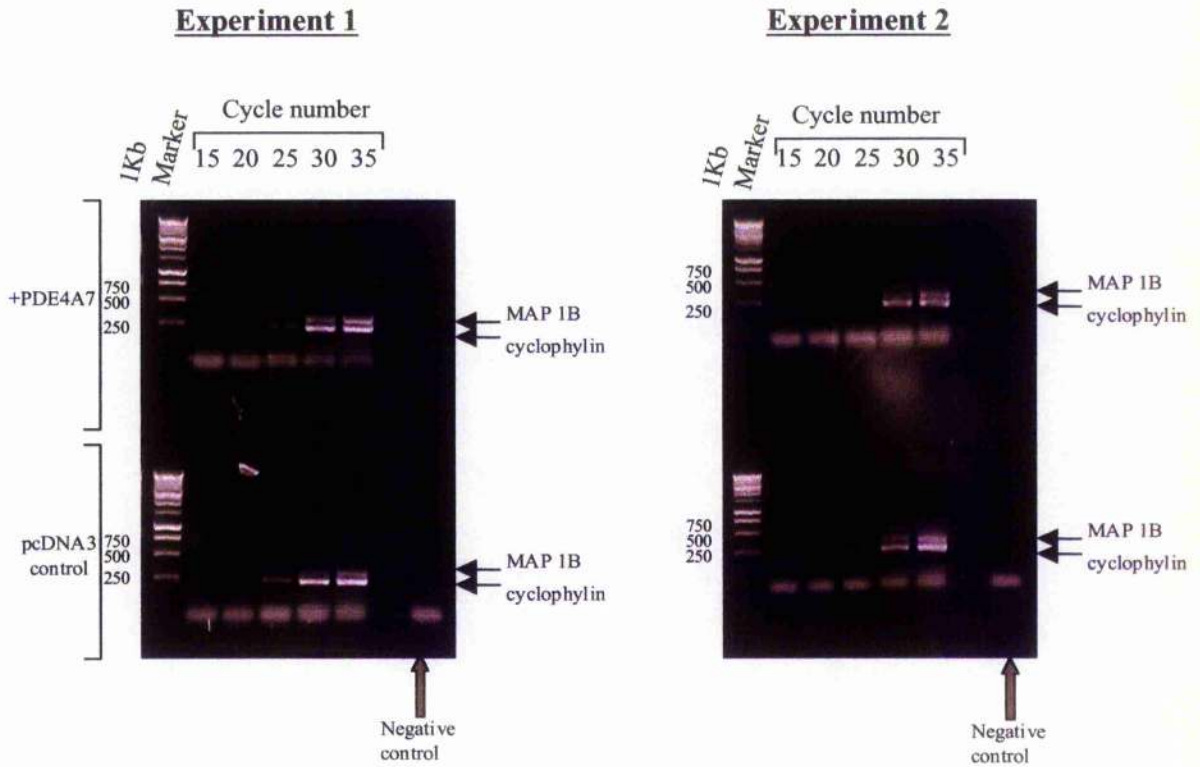


Figure 5.15 Changes in microtubule-associated protein 1B (MAP1B) transcript level in response to over-expression of PDE4A7. cDNA was generated from HEK-293 cells over-expressing either pcDNA3 or PDE4A7 plasmid DNA. PCR products were analysed by 1.5% agarose gel electrophoresis. Two sets of primer pairs were included in each PCR reaction, one pair were designed to amplify MAP1B as a 350bp fragment and the other primer pair were designed to amplify cyclophilin as a 250bp fragment. Both bands are clearly labelled on the above gels. The two gels labelled experiment 1 and experiment 2 show the data obtained from two separate studies. The upper panel of each gel shows the change in MAP1B transcript level in HEK-293 cells caused by the over-expression of PDE4A7 plasmid DNA, whereas the lower panels show the changes in MAP1B transcript level caused by over-expression of pcDNA3 plasmid DNA in HEK-293 cells (negative control). The molecular size markers are indicated on the left.

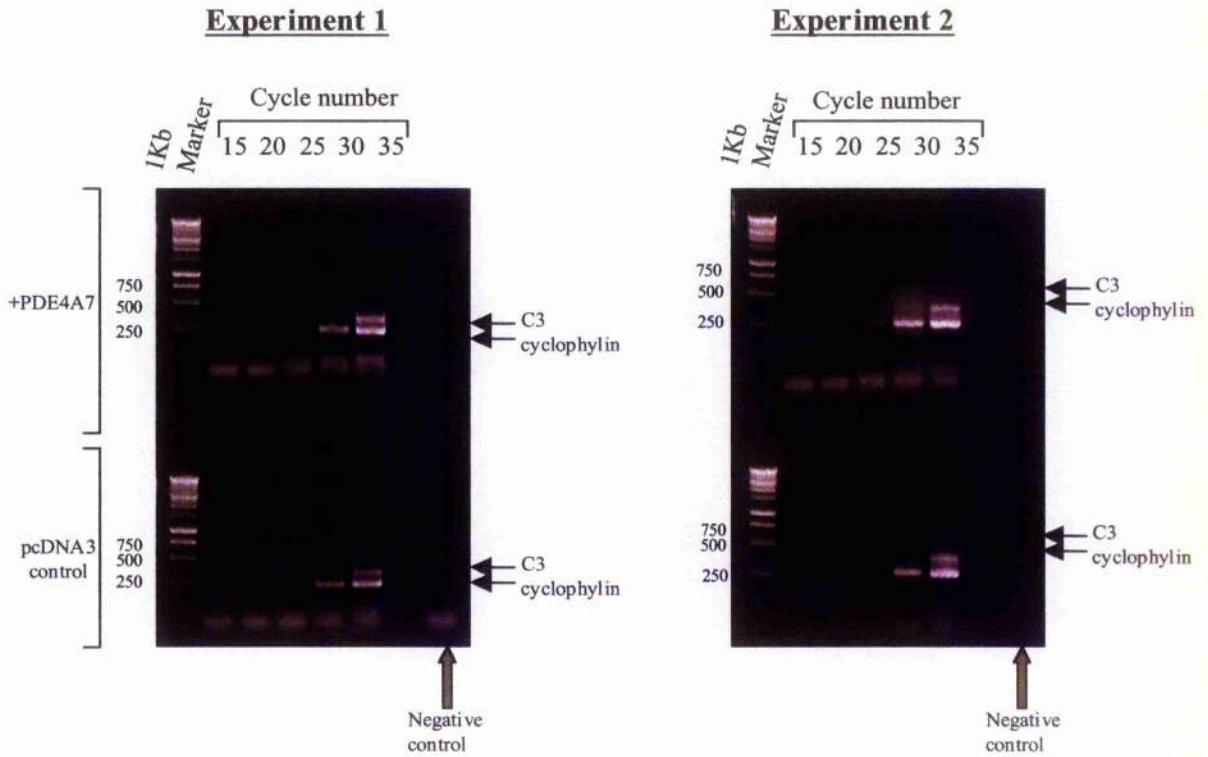


Figure 5.16 Changes in C3 botulinum toxin substrate (C3) transcript level in response to over-expression of PDE4A7. cDNA was generated from HEK-293 cells over-expressing either pcDNA3 or PDE4A7 plasmid DNA. PCR products were fractionated electrophoretically on 1.5% agarose gels, stained with ethidium bromide and visualised using a UV transilluminator. Two sets of primer pairs were included in each PCR reaction, one pair were designed to amplify a 350bp fragment representing the C3 transcript and the other primer pair were designed to amplify a 250bp fragment of the cyclophilin control transcript. Both bands are clearly labelled on the above gels. The two gels labelled experiment 1 and experiment 2 show the data obtained from two separate studies. The upper panel of each gel shows the change in C3 transcript level in HEK-293 cells in response to over-expression of PDE4A7 plasmid DNA, whereas the lower panels show the changes in C3 transcript level detected in HEK-293 cells in response to the over-expression of pcDNA3 plasmid DNA (negative control). The molecular size standards (in bp) are shown on the left.

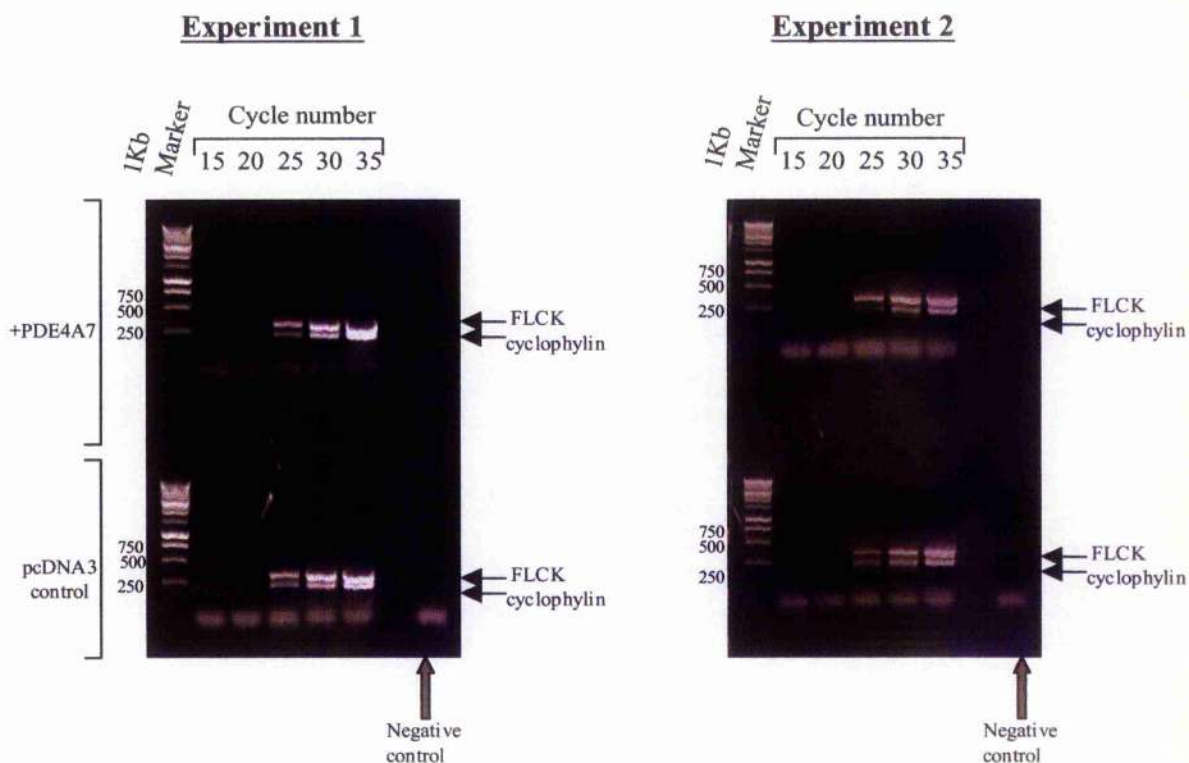


Figure 5.17 Changes in ferritin light chain kinase (FLCK) transcript level in response to over-expression of PDE4A7. cDNA was generated from HEK-293 cells over-expressing either pcDNA3 or PDE4A7 plasmid DNA. PCR products were analysed by 1.5% agarose gel electrophoresis. Two sets of primer pairs were included in each PCR reaction, one pair were designed to amplify FLCK as a 350bp fragment and the other primer pair were designed to amplify cyclophylin as a 250bp fragment. Both bands are clearly labelled on the above gels. The two gels labelled experiment 1 and experiment 2 show the data obtained from two separate studies. The upper panel of each gel shows the change in FLCK transcript level in HEK-293 cells caused by the over-expression of PDE4A7 plasmid DNA, whereas the lower panels show the changes in FLCK transcript level caused by over-expression of pcDNA3 plasmid DNA in HEK-293 cells (negative control). The molecular size standards (in bp) are shown on the left.

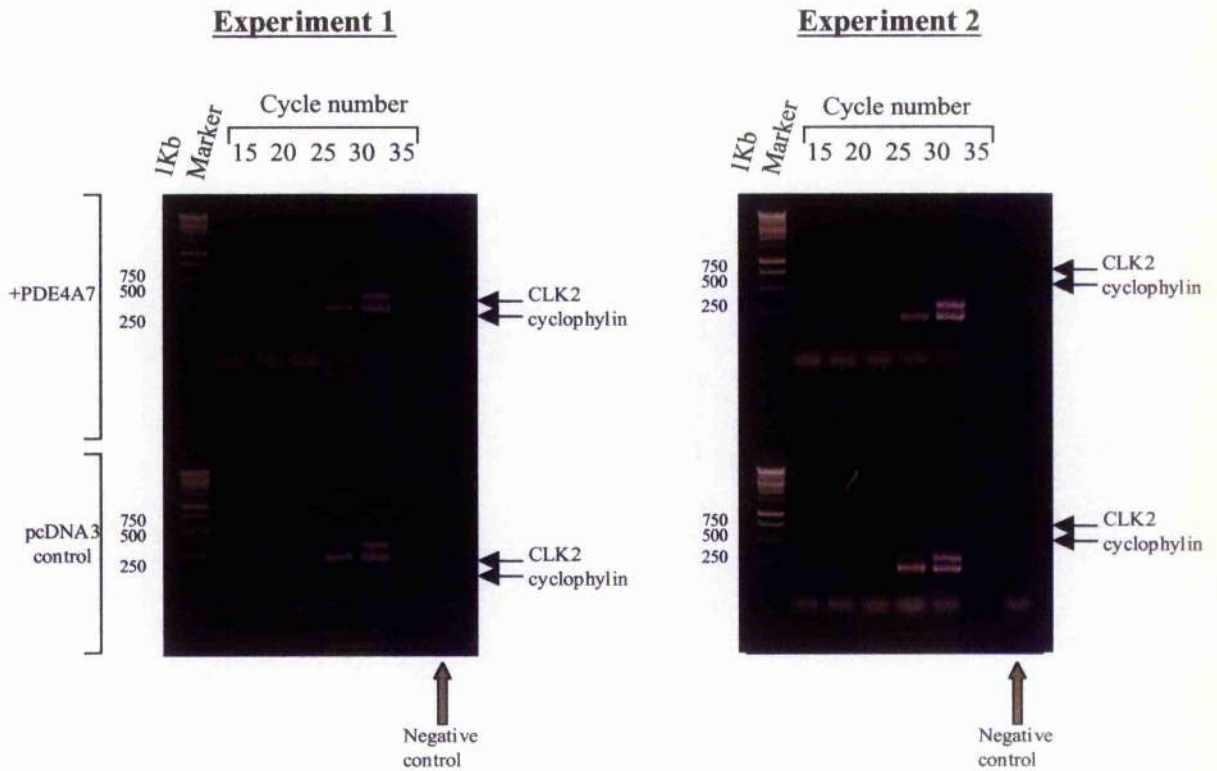


Figure 5.18 Changes in protein kinase CLK2 (CLK2) transcript level in response to over-expression of PDE4A7. cDNA was generated from HEK-293 cells over-expressing either pcDNA3 or PDE4A7 plasmid DNA. PCR products were analysed by 1.5 % gel electrophoresis. Two sets of primer pairs were included in each PCR reaction, one pair were designed to amplify a 350bp fragment representing the CLK2 transcript and the other primer pair were designed to amplify cyclophilin as a 250bp fragment. Both bands are clearly labelled on the above gels. The two gels labelled experiment 1 and experiment 2 show the data obtained from two separate studies. The upper panel of each gel shows the change in CLK2 transcript level in response to over-expression of PDE4A7 plasmid DNA in HEK-293 cells, whereas the lower panels shows the changes in CLK2 transcript level detected in HEK-293 cells in response to the over-expression of pcDNA3 plasmid DNA (negative control). The molecular size standards (in bp) are shown on the left.

Target Gene	Method of Analysis	
	Gene Microarray	RT-PCR
Adenosine A2A receptor	upregulated	unchanged
cAMP response element binding protein	upregulated	unchanged
Microtubule-associated protein 1B	upregulated	unchanged
Dup 1 ras-related C3 botulinum toxin substrate	downregulated	unchanged
Ferritin light chain	downregulated	unchanged
Protein kinase CLK2	downregulated	unchanged
Adenosine A2B receptor	downregulated	not detected

Table 5.3 Comparison of the gene expression changes detected using gene microarray and RT-PCR analysis.

5.4 Discussion

In this study microarray analysis was used to determine the changes in the gene expression profile of HEK-293 cells caused by the over-expression of PDE4A7. A number of interesting genes were regulated in response to PDE4A7, which included the genes encoding for proteins involved in cAMP signalling such as the A2A receptor, A2B receptor, and CREB. Before making conclusions about gene regulation based on the data obtained from microarray analysis it was important to evaluate potential changes by using an alternative technique. This is because microarray technology has been criticised for generating false positive data. Problems associated with microarray that can lead to the production of misleading data include non-specific background, slide inhomogeneities caused by hybridisation occurring differently in different parts of the slide and variations in pin geometry, which can cause the deposition of differing amounts of target DNA onto the slide.

RT-PCR was used to re-evaluate the expression changes detected for seven genes from the microarray study. Unfortunately I was unable to identify any major differences in transcript level between the control cells and those over-expressing PDE4A7 for any of the targets. This suggested that microarray had generated false positive data. An alternative explanation for the lack of data correlation from these two methods is that the RNA used for microarray analysis was extracted from a different population of PDE4A7-transfected HEK-293 cells to that RNA used for RT-PCR analysis. This made direct comparison of the data obtained from the two methods difficult as small differences in the transfection efficiency of PDE4A7, differences in the time when the cells were harvested and differences in RNA quality are all factors that could have influenced the differences in the gene expression profiles of the HEK-293 cells detected by microarray and RT-PCR analysis. A better approach would have been to generate HEK cells stably transfected with PDE4A7 on an inducible promoter and from these cells prepare enough RNA for use in both microarray and RT-PCR analysis. This would obviate the problems of differences in transfection efficiency and would have allowed the direct comparison of gene microarray data with RT-PCR data.

In conclusion, I was unable to confirm the gene expression changes detected with microarray for the A2AR, CREB, MAP1A, C3, and FLCK genes by using RT-PCR analysis. That time only allowed me to re-evaluate the changes in a small number of the microarray candidates, leaves the possibility that other genes did demonstrate authentic changes.

Another problem with this study was the presumption that by over-expressing PDE4A7 we would only detect gene expression changes in those genes specifically regulated by this protein. It is probable that the high expression levels of PDE4A7 might have upset many other biochemical processes in the cell, resulting in gene changes that may not have occurred as a direct influence of PDE4A7. A way of addressing the actions of endogenous PDE4A7 would be to identify a cell line that natively expresses this protein and then to specifically downregulate its expression. Such approaches have traditionally used antisense technologies, which have been found to be problematic and inefficient. However, recently researchers have described a method that could prevent this problem [Brummelkamp et al., 2002]. It was demonstrated that RNA interference could be achieved by using a mammalian expression vector (pSUPER vector) to suppress the expression of a desired gene. Therefore, an alternative approach to identify those genes specifically regulated by PDE4A7 would be to identify cell lines that express PDE4A7 natively and then to treat those cells with a pSUPER vector designed to suppress the expression of the PDE4A7 gene. By comparing the gene expression profiles of cells expressing endogenous PDE4A7 (as positive control) to those cells treated with the pSUPER vector specific for PDE4A7 suppression using the methods of microarray and RT-PCR analysis, it would be possible to identify those genes specifically regulated by the PDE4A7 protein.

It is possible that PDE4A7 might interact with other transcription factors or affect regulatory transcriptional complexes that are involved in controlling the expression of other PDE4As. As PDE genes were not present on the gene microarray chip used for this study, this question remains unanswered. Therefore, useful future experiments would be to investigate the changes in the regulation of other PDE genes in response to either over-expression of recombinant PDE4A7 or to the down-regulation of native PDE4A7 using either microarray or RT-PCR analysis. PDE4A mRNA levels have been found to increase in response to elevated cAMP levels in U937 human monocytic cells [Engels et al., 1994], Mono-Mac-6 cells [Verghese et al., 1995] and Jurkat cells [Engels et al., 1994] and in some cell types can decrease PDE4A mRNA [Erdogan et al., 1997]. PDE4A7 may therefore have an active role to play in these processes.

Chapter 6

Partial characterisation of the novel cyclic AMP-specific phosphodiesterase PDE4A11 (TM3)

6.1 Introduction

As already discussed in the Introduction (section 1.4), the PDE4 enzyme family contains ~18 isoforms encoded by four different genes (4A, 4B, 4C, 4D). PDE4 enzymes all possess a highly conserved catalytic core for the hydrolysis of cAMP and in addition possess two other highly conserved regions of sequence, located N-terminal to the catalytic core. These regions are called UCR1 and UCR2 for Upstream Conserved Region 1 and 2, respectively. Those PDE4 enzymes possessing both a UCR1 and UCR2 region are referred to as long isoforms, those lacking a UCR1 region but contain an intact UCR2 region are referred to as short isoforms and finally those containing a truncated UCR2 are termed super-short isoforms. In addition, each isoform contains a unique N-terminal sequence, which has been shown to target these enzymes to specific intracellular locations.

The human *PDE4A* gene encodes the two long isoforms of PDE4A4B (PDE46) [Huston et al., 1996] and PDE4A10 [Rena et al., 2001], the supershort isoform called PDE4A1 (RD1) and the N- and C-terminally truncated isoform called PDE4A7 (2EL) [Horton et al., 1995]. As both PDE4A4B and PDE4A10 each have a unique N-terminal, exon 1 will differ between each of these long isoforms and for any other long forms identified in the future. Exon 14, which encodes for the C-terminal tail should be the same for each of these PDE4A isoforms with the exception of PDE4A7, which undergoes 3' splicing within exon 14 (*figure 6.1*). That PDEs within a particular gene group contain identical sequence in their C-terminal tails is an attribute that has been utilised to generate antisera, which recognises a peptide sequence found only within the C-terminal sequence specific to a particular gene family.

Here, I have attempted partial characterisation studies on the novel PDE4A11 (TM3) isoform. It was suggested originally that 'TM3' may be C-terminally truncated and be catalytically inactive as was seen for PDE4A7. However, the TM3 construct contains sequence for a novel PDE4A together with extraneous sequence originating from a cloning artefact as this does not appear in the genomic sequence. Inspection of the PDE4A gene has allowed for the identification of a unique exon for a novel PDE4A, called PDE4A11

(sequence given in *figure 6.2*). This contains some of the sequence seen in TM3 [Sullivan et al., 1998].

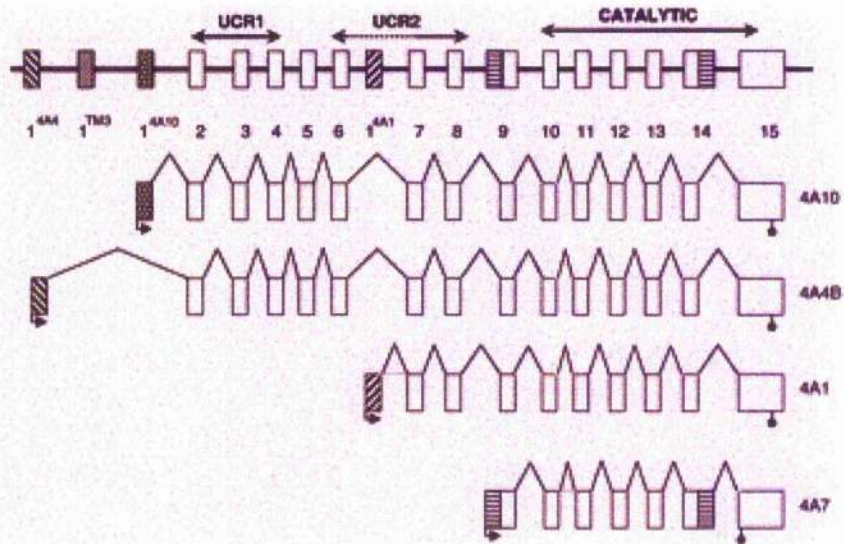


Figure 6.1 Structure of the PDE4A gene. The structure of the PDE4A gene is shown in at the top. The exons are shown as boxes, which are joined together by horizontal lines, which represent the introns. Initiation and stop codons are represented in this diagram by arrows and filled circles, respectively. This diagram was taken from [Rena et al., 2001].

1	MARPRGLGRI	PELQLVAFPV	AVAAEDEAFL	PEPLAPRAPR	RPRSPPSSPV
51	FFASPSPTFR	RRLRLLRSCQ	DLGRQAWAGA	GFEAENGPTP	SPGRSPLDSQ
101	ASPGVLHAG	AATSQRRESF	LYRSDSDYDM	SPKTMSRNSS	VTSEAHAEDL
151	IVTPFAQVLA	SLRSVRSNFS	LLTNVPVPSN	KRSPLGGPTP	VCKATLSEET
201	CQQLARETLE	ELDWCLEQLE	TMQTYRSVSE	MASHKFKRML	NRELTHLSEM
251	SRSGNQVSEY	ISTTFLDKQN	EVEIPSPTMK	EREKQQAPRP	RPSQPPPPPV
301	PHLQPMSQIT	GLKCLMHSNS	LNNSNIPRFG	VKTDQEELLA	QELENLNKWG
351	LNIFCVSDYA	GGRSLTCIMY	MIFQERDLLK	KFRIPVDTMV	TYMLTLEDHY
401	HADVAYHNSL	HAADVLRQSTH	VLLATPALDA	VFTDLEILAA	LFAAAIHDVD
451	HPGVSNQFLI	NTNSEALMY	NDESVLENHH	LAVGFKLLQE	DNCDIFQNLS
501	KRQRQSLRKM	VIDMVLATDM	SKHMTLLADL	KTMVETKKVT	SSGVLLLDNY
551	SDRIQVLRNM	VHCADLSNPT	KPLELYRQWT	DRIMAEFFQQ	GDRERERGME
601	ISPMCDKHTA	SVEKSQVGF I	DYIVHPLWET	WADLVHPDAQ	EILD TLEDNR
651	DWYYSAIRQS	PSPPEEEESR	GPGHPPLPDK	FQFELTLEE	EEEEISMAQI
701	PCTAQEALTA	QGLSGVEEAL	DATI AWEASP	AQESLEVMAQ	EASLEAELEA
751	VYLTQQAQST	GSAPVAPDEF	SSREEFVVAV	SHSSPSALAL	QSPLLPAWRT
801	LSVSEHAPGL	PGLPSTAAEV	EAQREHQAAK	RACSACAGTF	GEDTSALPAP
851	GGGGSGGDPT				

Figure 6.2 Amino acid sequence of HSPDE4A11 (TM3). The unique 81 amino acid N-terminal region of HSPDE4A11 is shown in blue and the sequence that is shared by all other long form human PDE4As is shown in black.

6.2 Results

6.2.1 Distinguishing between the different PDE4A long isoforms

Preliminary expression studies using SDS-PAGE analysis revealed that HSPDE4A11 migrates as a similar size to the other PDE4A long-forms of HSPDE4A4B and HSPDE4A10. Indeed, this offered the potential for confusing the identity of these enzymes in SDS-PAGE analyses. However, this problem was encountered previously with HSPDE4A10 and HSPDE4A4B, but was overcome by producing antisera that specifically recognised peptide sequence contained only within the unique N-terminal of one particular isoform or another. This led to the production of a PDE4A4B N-terminal specific, affinity purified antibody (by Novartis), which recognises the peptide sequence of 'PPEEESRGP GHPPLPK' found only within the unique N-terminal of HSPDE4A4B. We developed the PDE4A10 N-terminal specific antibody, which recognises the peptide sequence of 'MAMPPTGPESLTHFPFSDDED' located only within the unique N-terminal sequence of HSPDE4A10 [Rena et al., 2001]. This has allowed us to distinguish between these two long form PDE4A isoenzymes. As yet, there is no antibody available for the specific detection of the novel HSPDE4A11.

To check the HSPDE4A10- and HSPDE4A4B-specific antisera would not cross-react with HSPDE4A11, COS-7 cell lysates transfected with either pSV-SPORT4A4B or pcDNA3.1-4A11 were subjected to subcellular fractionation followed by 10% SDS-PAGE analysis (Materials and Methods 2.2.1). The nitrocellulose membrane was firstly immunoprobed with the HSPDE4A4B N-terminal specific antisera, which identified a 125kDa immunoreactive band in all three fractions of those COS-7 cells transfected to express HSPDE4A4B (*figure 6.3*). No bands were detected for the HSPDE4A10 standard, or in those cell lysates over-expressing HSPDE4A11. This demonstrated that the HSPDE4A4B-specific antisera only detected HSPDE4A4B and did not cross-react with HSPDE4A11.

The same nitrocellulose membrane was next immunoprobed with the HSPDE4A10 N-terminal specific antisera, which detected a 121kDa immunoreactive species only in the lane containing the HSPDE4A10 standard (*figure 6.4*). This demonstrated that the HSPDE4A10-specific antisera did not cross-react with HSPDE4A11.

Finally, the nitrocellulose was immunoprobed with the general PDE4A C-terminal antisera, which recognises peptide sequence located within the C-terminal of all known human PDE4As (with the exception of the C-terminally truncated PDE4A7 enzyme). Only when the general PDE4A antisera was used, did bands appear in the lanes containing

those COS-7 lysates over-expressing HSPDE4A11 (*figure 6.5*). These analyses demonstrated that the PDE4A4B- and PDE4A10-specific antisera were suitable for distinguishing between these three long form isoenzymes, until antisera is generated for the specific detection of HSPDE4A11.

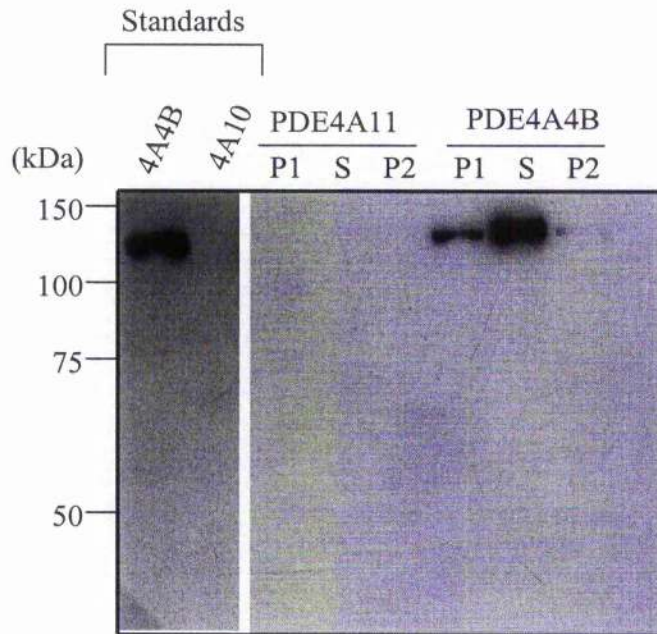


Figure 6.3 Immunoprobings HSPDE4A11 and HSPDE4A4B COS-7 cell lysates with the HSPDE4A4B-specific antisera. COS-7 cells were transfected with either pSV.SPORT4A4B or pcDNA3.1-TM3 and allowed to express for 48 hours. Cells were lysed, disrupted and subjected to subcellular fractionation. 15 μ g of the S fraction and equal volumes of both the particulate fractions (P1 and P2) were separated by 10% SDS-PAGE and immunoprobed using HSPDE4A4B N-terminal specific antisera. The migration of standard protein molecular mass markers are indicated on the left. All lanes came from the same gel.

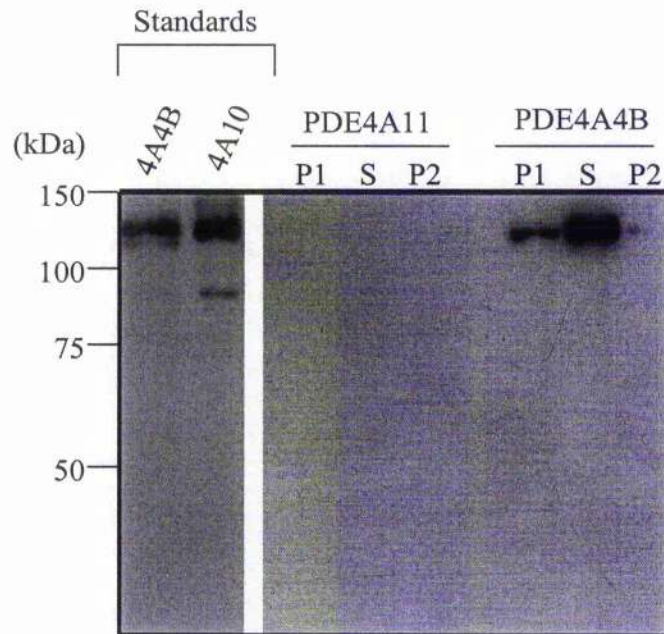


Figure 6.4 Immunoprobings HSPDE4A11 and HSPDE4A4B COS-7 cell lysates with the HSPDE4A10-specific antisera. The nitrocellulose membrane previously immunoprobed with the HSPDE4A4B N-terminal specific antibody was re-probed with HSPDE4A10 N-terminal specific antisera. Migration of the standard protein molecular weight markers are indicated on the left. All lanes came from the same gel.

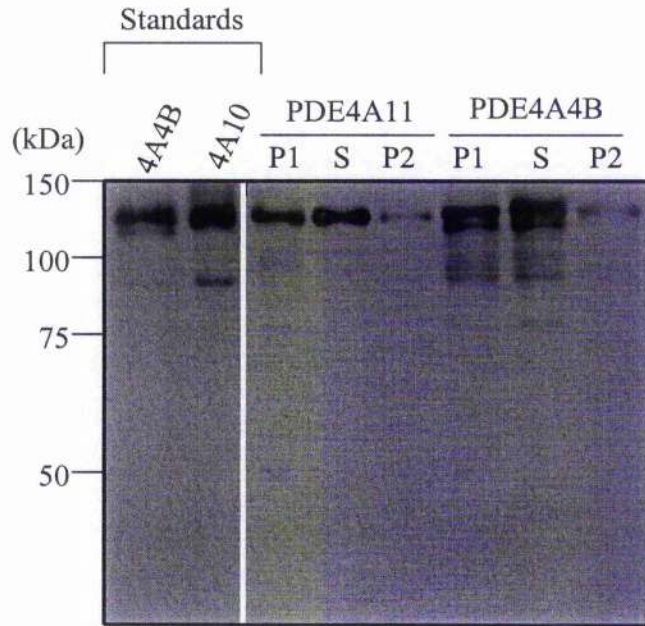


Figure 6.5 Immunoprobings HSPDE4A11 and HSPDE4A4B COS-7 cell lysates with general PDE4A antisera. The nitrocellulose membrane previously immunoprobed with both the HSPDE4A4B N-terminal specific antisera and HSPDE4A10 N-terminal specific antisera was re-probed with antisera specific for the common C-terminal region of human PDE4A isoforms.. Migration of the standard protein molecular weight markers are indicated on the left. All lanes came from the same gel.

6.2.2 Localisation of HSPDE4A11 in transiently transfected COS-7 cells

Lysates from COS-7 cells transfected with either pSV-SPORT4A4B or pcDNA3.1-4A11 were subjected to subcellular fractionation into a low speed particulate fraction (P1), high speed soluble fraction (S2) and a high speed particulate fraction (P2), before being subjected to 10% SDS-PAGE analysis (Materials and Methods 2.2.1). HSPDE4A4B was included as an 'internal control' because the distribution of this enzyme has already been established. Immunoblotting was performed using the general PDE4A C-terminal specific antibody [Huston et al., 1996], which identified immunoreactive bands in all three cellular fractions of those cells transfected with either pSV-SPORT4A4B or pcDNA3.1-4A11 (figure 6.6). From these immunoblots the molecular size for the novel HSPDE4A11 was calculated from its RF values. The calculated molecular size for PDE4A11 was 118 ± 2 (n=3; mean \pm S.D.).

Quantitative immunoblotting analyses demonstrated that PDE4A11 was distributed equally between the soluble (S2) and particulate fractions (P1, P2) (Table 6.1). Similar results were obtained when the distribution of HSPDE4A11 activity (1 μ M cAMP substrate) was calculated (Table 6.1). When the distributions of both HSPDE4A11 and HSPDE4A4B were compared they were found to be very similar (Table 6.1).

If time had permitted LSCM would have been used to visualise the precise intracellular localisation in intact COS-7 cells as cellular disruption may cause the release of PDE4A11 from any protein that it may interact with. This has been shown in previous studies whereby cellular disruption analyses of COS-7 cells over-expressing either HSPDE4A4B and HSPDE4A10, suggested that both these enzymes were predominantly located within the soluble fraction [Huston et al., 1996; Rena et al., 2001]. In contrast, LSCM studies actually demonstrated that HSPDE4A4B was found predominantly at the cell margins and with structures throughout the cell body, and that HSPDE4A10 was localised mainly to the perinuclear region of COS-7 cells [Huston et al., 1996; Rena et al., 2001]. Therefore, according to LSCM analyses these enzymes should have been associated with the particulate fractions of the COS-7 cells, which was clearly not the case after cellular disruption. This highlights the importance of performing LSCM analysis for HSPDE4A11.

Table 6.1 Distribution of HSPDE4A11 and HSPDE4A4B in COS-7 cells

These data are given as means \pm S.D. for three separate experiments.

Fraction	Distribution of 4A11 (quantitative immunoblotting) (%)	Distribution of 4A11 (activity) (%)	Distribution of 4A4B (quantitative immunoblotting) (%)	Distribution of 4A4B (activity) (%)
Particulate (P1, P2)	48.5 \pm 2.1	53 \pm 1.5	55 \pm 6.6	60 \pm 4.2
Soluble (S2)	51.5 \pm 2.1	47 \pm 1.5	45 \pm 6.6	40 \pm 4.2

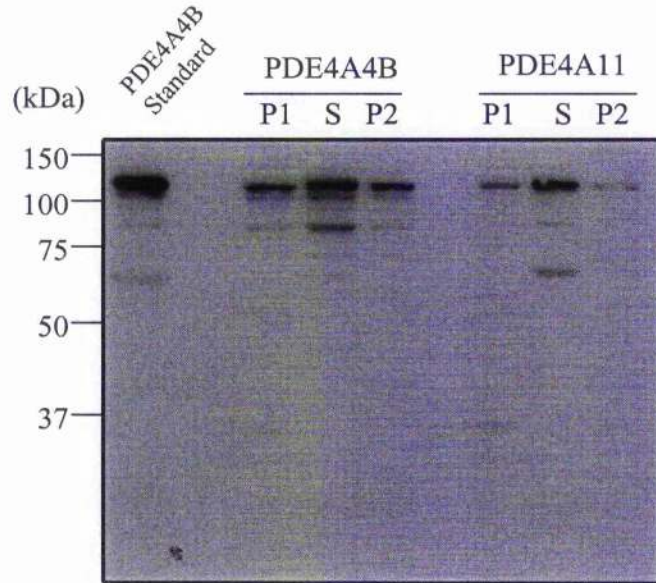


Figure 6.6 Subcellular distribution of HSPDE4A11. COS-7 cells were transfected with either pSV.SPORT4A4B or pcDNA3.1-4A11 and allowed to express for 48 hours. Cell lysates were then subjected to subcellular fractionation and 20 μ g of the S fraction and equal volumes of both particulate fractions(P1 and P2) were separated by 10% SDS-PAGE and immunoprobed with the general PDE4A C-terminal specific antisera. The migration of protein molecular mass markers are indicated on the left. This blot is representative of results obtained from three separate experiments.

6.3 Kinetic evaluation of HSPDE4A11

6.3.1 K_m and relative V_{max} values of HSPDE4A11 expressed in transfected COS-7 cells

Kinetic evaluation was performed on the HSPDE4A11 activity found in both the soluble (S2) and particulate (P1,P2) fractions of transfected COS-7 cells. To determine the K_m value for the PDE4A11 enzyme, PDE assays were performed (Materials and Methods 2.4.6.2), except instead of using 1 μ M cAMP a range of cAMP substrate concentrations were used (0.1-100 μ M). The data was analysed by computer fitting to the hyperbolic form of the Michaelis-Menton equation using the Ultrafit programme (Biosoft, Cambridge, U.K). These data showed that the HSPDE4A11 activity in both the soluble (S2) and particulate fractions (P1, P2) had very similar K_m values (graphs of kinetic data for the soluble and particulate fractions shown in figures 6.6 and 6.7 respectively and data values are listed in Table 6.2). Also the K_m values for HSPDE4A11 were very similar to those K_m values that were obtained previously for the HSPDE4A4B and HSPDE4A4B enzymes [Huston et al., 1996; Rena et al., 2001]. Next, attempts were made to determine whether the relative V_{max} values for HSPDE4A11 in these various fractions are different. To do this I determined the relative amount of HSPDE4A11 protein found in each of the fractions by using quantitative immunoblotting. The relative V_{max} for the HSPDE4A11 protein found in each of these fractions were calculated using the following equation (adaptation of Michaelis- Menton equation):

$$V = \frac{V_{max} [S]}{[S] + K_m}$$

The V_{max} data demonstrated that particulate HSPDE4A11 protein was less active than the soluble form (Table 6.2). A possible explanation for this finding might be that the association of HSPDE4A11 with the particulate fraction has altered the conformation of the catalytic unit. However, this would have to be addressed further by determining the IC_{50} values for inhibition of HSPDE4A11 in the different fractions by rolipram. If the forms of HSPDE4A11 found in the different fractions showed significant differences in their sensitivity to rolipram, then it could be concluded that they exist in different conformational states. Indeed, HSPDE4A4B has been found to exist in two conformationally distinct states, whereby the particulate species is more sensitive to rolipram than the soluble form [Huston, Pooley et al., 1996]. When the V_{max} for soluble

(S2) HSPDE4A11 was compared with the V_{max} for soluble (S2) HSPDE4A4B, HSPDE4A11 was found to be a less active enzyme (Table 6.3).

Table 6.2 Properties of HSPDE4A11 expressed in COS-7 cells

Values given are means with errors as S.D. for separate determinations done on three separate experiments. The V_{max} values are given relative to that for soluble HSPDE4A11, which is set as unity.

Assay	Soluble (S2) HSPDE4A11	Particulate (P1,P2) HSPDE4A11
K_m (μ M)	2.5 \pm 0.4	2.44 \pm 0.7
Relative V_{max}	(1)	0.74 \pm 0.6

Table 6.3 Comparison of the relative V_{max} obtained for soluble (S2) HSPDE4A4B and HSPDE4A11

The relative V_{max} of soluble HSPDE4A11 is compared with the V_{max} of soluble HSPDE4A4B (given here as unity). Values given are means with errors as S.D. for separate determinations done on two separate experiments.

Assay	Soluble (S2) HSPDE4A4B	Soluble (S2) HSPDE4A11
Relative V_{max}	(1)	0.41 \pm 0.005

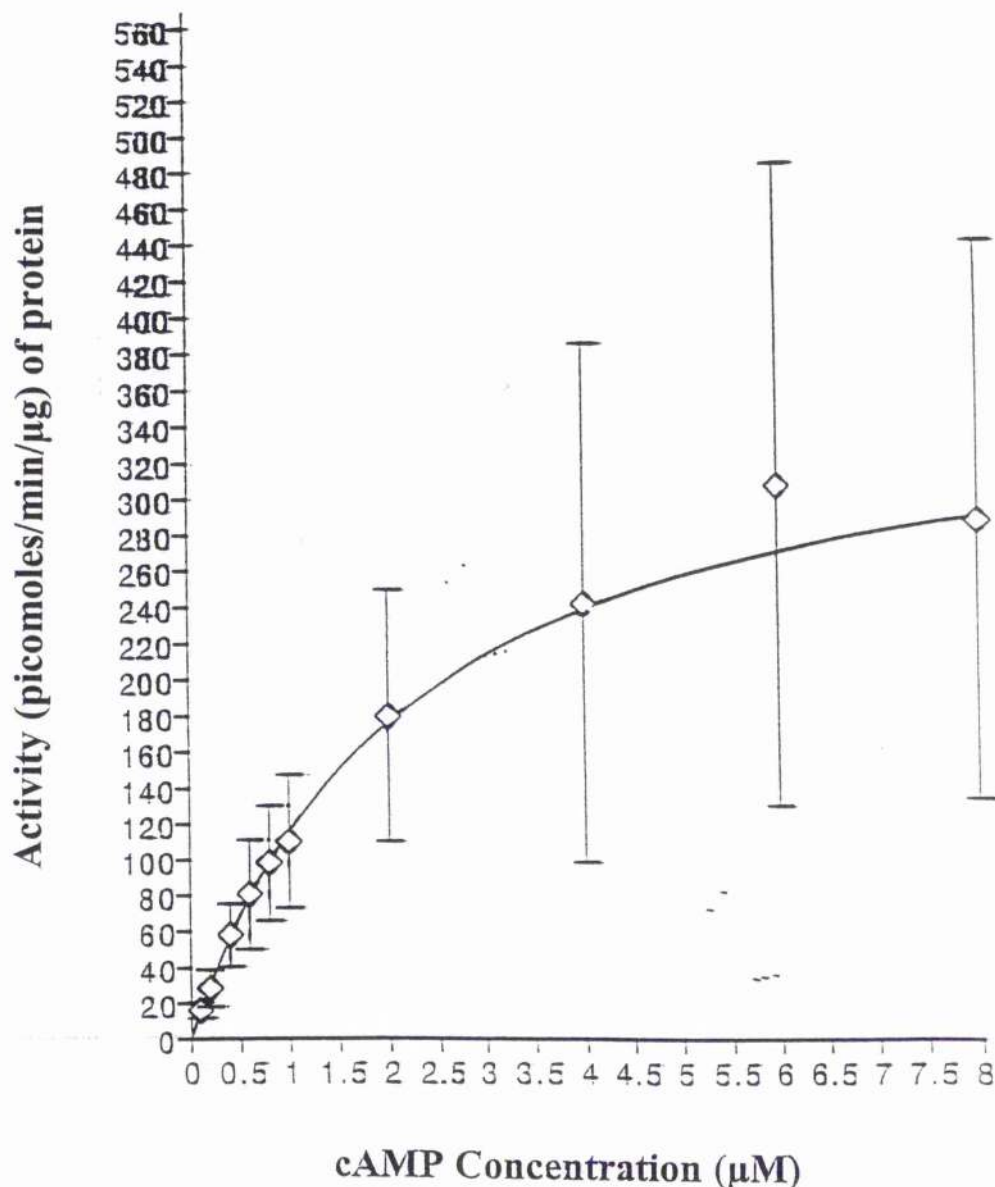


Figure 6.7 Analysis of the K_m for particulate PDE4A11 expressed in COS-7 cells. COS-7 cells were transfected with pcDNA3.1-4A11 and allowed to express for 48 hours. Cells were harvested, lysed and particulate fractions (P1 and P2) were prepared as described in *Materials and Methods*. PDE activity was measured over a range of cAMP substrate concentrations. Data was analysed by computer fitting to the hyperbolic form of the Michaleis-Menton equation using the Ultrafit programme (Biosoft). Data shown are the means of three separate experiments done on different cell transfections with errors as SD.

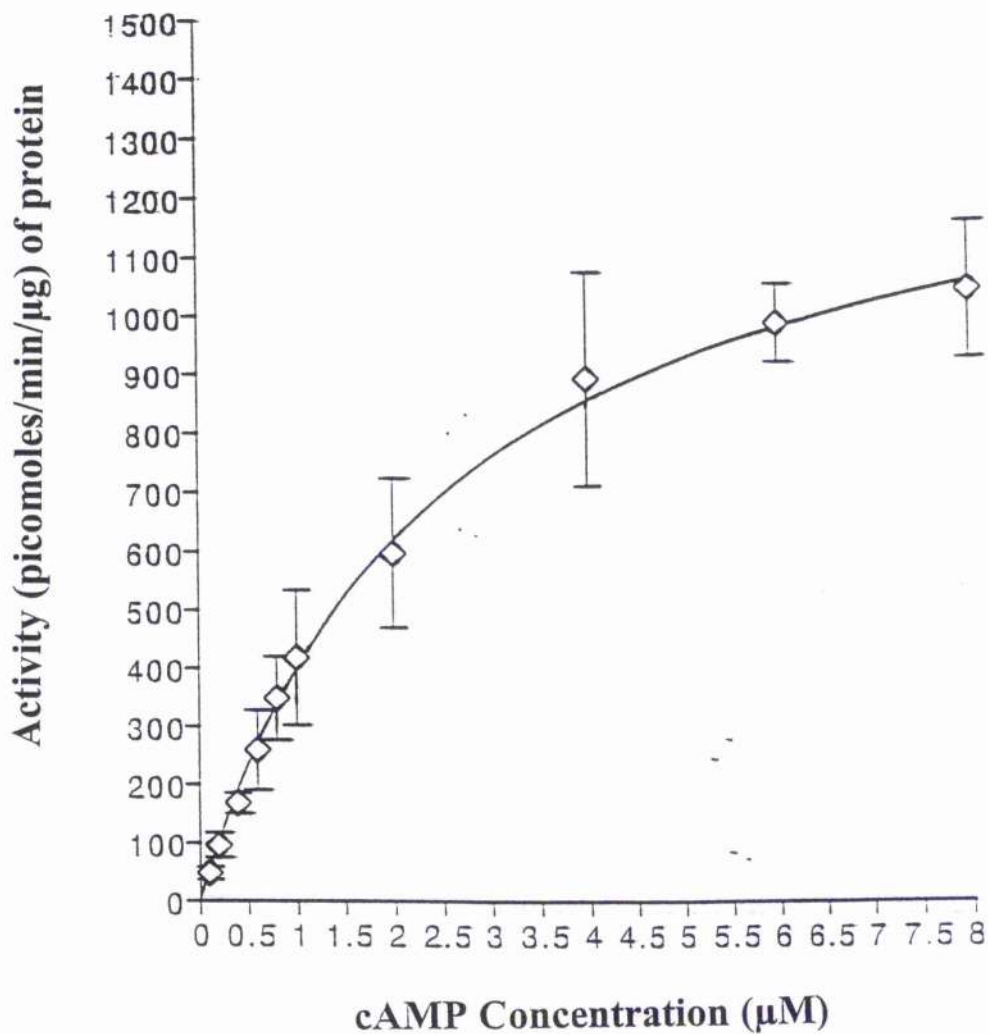


Figure 6.8 Analysis of the K_m for soluble PDE4A11 expressed in COS-7 cells. COS-7 cells were transfected with pcDNA3.1-4A11 and allowed to express for 48 hours. Cells were harvested, lysed and supernatant fractions (S2) were prepared as described in *Materials and Methods*. PDE activity was measured over a range of cAMP substrate concentrations. Data was analysed by computer fitting to the hyperbolic form of the Michaleis-Menton equation using the Ultrafit programme (Biosoft). Data shown are the means of two separate experiments done on different cell transfections with errors as SD.

6.3 Discussion

In this study, I performed partial characterisation studies on a novel PDE4A long isoform called HSPDE4A11. I have demonstrated from subcellular analyses of transfected COS-7 cells that HSPDE4A11 has a similar distribution to that of the established HSPDE4A4B isoform. Obviously, to gain better insight into the intracellular localisation of this protein LSCM analysis would be required. This is because cellular disruption has already been shown to cause the release of particulate-associated proteins into the soluble fraction [Huston et al., 1996; Rena et al., 2001]. I have also demonstrated that the V_{max} of soluble HSPDE4A11 protein is similar to that of the particulate species. That the error values for K_m and V_{max} data are high and to reduce these errors experiments will have to be repeated.

Chapter 7

General Discussion

cAMP is involved in regulating a diverse range of signalling processes. The enzymes that generate cAMP (adenylyl cyclases), detect cAMP (PKA) and degrade cAMP (PDEs) are all involved in controlling the levels of this key second messenger. The multiple isoforms of each of these enzymes and their distinct regulatory properties and intracellular locations all serve to produce a compartmentalised cell-specific cAMP response [Houslay and Milligan, 1997].

The PDE enzymes provide the sole means of degrading cyclic nucleotides in cells and, therefore, play a central role in the controlling the levels of both cAMP and cGMP by hydrolysing them into 5'-nucleoside monophosphates. Without these PDE enzymes we would fail to see gradients of cAMP in cells and levels of cAMP would rise such that the sustained activation of PKA would ensue [Houslay and Milligan, 1997].

PDEs are currently grouped into 11 gene families of which seven families (1, 2, 3, 4, 7, 8, 11) are able to functionally hydrolyse cAMP. The cAMP-specific PDE4 family are of particular interest within our laboratory as inhibitors of these enzymes have been found to serve as anti-inflammatory agents and anti-depressant agents, signifying not only that PDE4 enzymes provide targets for novel therapeutics, but also are functionally important species [Houslay, 2001]. Indeed, the high interspecies conservation of PDE4 enzymes, coupled with lack of polymorphisms in coding regions suggest a strong evolutionary pressure to keep intact this complex gene family.

PDE4 enzymes are encoded by four genes, which each generate multiple isoforms by alternative 5' mRNA splicing. The distinct N-terminal regions of these enzymes can serve to target them to either distinct intracellular compartments or to interact with cytosolic signalling scaffold proteins as well as conferring regulatory properties on them [Houslay, 1996].

As the central role of PDEs within cells is to regulate the levels of cyclic nucleotides, it was surprising to find that the *PDE4A* gene encoded a splice variant, called PDE4A7 (2EL) that is devoid of any cAMP-specific PDE catalytic activity [Horton et al., 1995].

This observation attracted my attention and caused me to investigate this protein further. I began my study by focussing on its intracellular localisation, which then led me on to attempt to gain insight into its possible functional role. Thus, in Chapter 3 I

investigated the targeting of PDE4A7 using the methods of general subcellular fractionation and Laser Scanning Confocal Microscopy (LSCM). I made the novel finding that this protein was located exclusively to the nuclear compartment when over-expressed in COS-1 cells. This came as a great surprise as previous work had shown that a core complex formed from the catalytic unit and the C-terminal region was cytosolic, with targeting to distinct membrane sites being achieved by the isoform-specific N-terminal region [Shakur, Pryde et al., 1993]. I thus fully expected that the extensively truncated PDE4A7, consisting of a truncated catalytic core together with small, unique N- and C-terminal regions would also be a soluble, cytosolic protein.

I thus demonstrated that although PDE4A7 and PDE4A4B share an identical central core region they are localised to very different intracellular locations. The initial aim of my study was thus to determine whether the unique N- and C-terminal regions of PDE4A7 underpinned its targeting to the nucleus. As a first attempt to address this I studied chimeras that replaced these regions with those of a PDE4A construct that had a defined intracellular targeting. This was PDE4A4C, also known as h6.1, which is found in both the cytosolic S2 fraction as well as the particulate P1 fraction, due, presumably to the action of its N-terminal region. The PDE4A7 chimeras generated were called hyb1 and hyb2. In hyb1, the unique C-terminal of PDE4A7 was replaced with the C-terminal region that is found in all PDE4A isoforms, including h6.1. I was able to show that the hyb1 construct was located not only in the particulate (P1 and P2) fractions but, crucially, the S2 fraction of COS-1 cells. In hyb2, the unique N-terminal of PDE4A7 was replaced with the N-terminal region common to all PDE4A isoforms, including h6.1. Hyb2 was essentially located within the P1 particulate fraction. This indicated that the addition of the PDE4A common C-terminal region conferred S2 targeting upon PDE4A7. I thus concluded that the signal responsible for allowing PDE4 isoforms to have extranuclear localisation and to appear in the cytosolic fraction was located within the C-terminal region found in all known catalytically active PDE4A long and short isoforms.

My next aim was to gain insight into the basis for nuclear targeting of PDE4A7. I set out first to determine whether the unique N-terminal of PDE4A7 was responsible for directing it to the nucleus. To address this point two constructs were engineered. In one construct the unique N- and C-terminal domains of PDE4A7 were deleted, to yield a core region and in the other construct only the unique C-terminal region of PDE4A7 was removed. I expected that the central core alone would be a fully soluble species and would become targeted only when the PDE4A7 N-terminal was present. However, this was not the case. Instead both constructs were found to associate with the P1 particulate fraction. From these analyses I concluded that the targeting signal responsible for the P1 association

of PDE4A7 was located within the central core and not the unique N- or C-terminal regions. These data also enforced the idea that the signal responsible for the cytosolic (S2) targeting of *hyb1* arose from sequence located C-terminal to the central core. I thus attempted to identify the approximate region of where this signal was located in the PDE4A C-terminal region by using truncation analyses of the *hyb1* chimera. Two constructs were engineered to address this question. The first of these, called, delta 328 contained 19 amino acids of the C-terminal sequence of *hyb1* (also shared by all active PDE4As) fused to the PDE4A7 core and N-terminal. The second of these, called, delta 410 contained 101 amino acids of the PDE4A C-terminal sequence fused to the PDE4A7 core and N-terminal region.

Subcellular analyses of transfected COS-1 cells showed that delta 328 was distributed between both the P1 and S2 fractions whilst delta 410 was found to associate with the P1, S2 with a small amount found in the P2 fraction. From these studies I concluded that the minimal common PDE4A C-terminal sequence required to target the PDE4A7 central core to the S2 fraction was located between amino acids 309-328 of *hyb1*. To try and identify the motif responsible for allowing extranuclear targeting, further truncations upstream of residue 328 in *hyb1* would have to be engineered and evaluated. This would further localise the targeting motif, whose sequence could then be determined by point mutations.

Next, I attempted to elucidate the basis of nuclear entry of PDE4A7. The majority of proteins that are imported into the nuclear compartment possess an NLS. These take the form of either a stretch of 3-5 basic amino acid residues (monopartite) or of two basic stretches of amino acids separated by 10 amino acids (bipartite) [Kalderon et al., 1984; Robbins et al., 1991]. On this basis, PDE4A7 was found to contain two putative NLSs, namely KKFR and KKVT, positioned between amino acids 72-75 and amino acids 229-232 of the *hyb1* sequence, respectively. That these signals are located within the central core of PDE4A7 made sense, as in previous studies, I demonstrated that the central core of PDE4A7 was able to target exclusively to the P1 fraction, as with PDE4A7. However PDE4A4B, which also harbours this sequence, is found outside the nucleus. This suggested the possibility either that only in the extensively truncated PDE4A7 protein were these NLSs exposed or, alternatively, that all PDE4As might have the ability to cycle through the nucleus. In order to cycle, most proteins contain both an NLS and an NES [Mattaj et al., 1998]. I next hypothesised that if PDE4As were to contain an NES then it would presumably be located in the common PDE4A C-terminal region. This is because *hyb1* is found within the S2 fraction whilst appropriate C-terminal truncation of this species led to ablation of cytosolic targeting. Thus, I analysed this common PDE4A C-

terminal sequence for the presence of any putative NESs. However, the only putative NES that I was able to identify in PDE4A4B was indeed found in the C-terminal region of PDE4A4B. However, this motif (LEAELEAVYL) was found between amino acids 436 and 445 of *hyb1* (corresponding to amino acids 770-779 of PDE4A4B), rather than being located between residues 309-328 of *hyb1* (corresponding to residues 643-662 of PDE4A4B) that were previously found to be responsible for S2 targeting. To determine whether these putative NLSs and NES were functional, I investigated the targeting of constructs whereby these signals were removed by mutation of key residues. However, mutation of the putative NLSs on PDE4A7 did not cause this protein to re-localise to the S2 fraction, which demonstrated that these motifs did not provide the basis for targeting to the nucleus. I had also hoped to examine whether mutation of the 'LEAELEAVYL' motif would cause *hyb1* to accrue in the nucleus. However, unfortunately the NES mutant did not express. It is also possible that amino acids 309-328 of the *hyb1* C-terminal (corresponding to amino acids 643-662 of PDE4A4B) contain a novel type of NES. To evaluate this further, truncation/mutation analyses need to be performed in order to pin down the exact requirements (as already suggested). It would then be useful to see if such an NES could serve to re-target other nuclear localised proteins. From these various analyses I concluded that KKFR and KKVT were not acting as NLSs for PDE4A7 and that it gained entry into the nucleus by either passive diffusion or by piggy-backing on another protein that does contain an NLS. I have yet to prove whether PDE4A4B can cycle through the nucleus. Cycling could be addressed in the future by treating cells over-expressing PDE4A4B with the CRM-1 export inhibitor Leptomycin B and seeing if PDE4A4B accumulates in the nucleus as a result. However, it is possible that the active PDE4As are too large to enter into the nuclear compartment, or that once synthesised in the cytosol they associate with other proteins in the S2 fraction.

In chapter 4, I attempted to identify binding partners for PDE4A7, in the hope that this would give insight into both the functional role and nuclear import mechanism of PDE4A7. Using the yeast two hybrid screening procedure, I identified three possible binding partners for the PDE4A7 protein; CREB-binding protein (CBP) is a nuclear protein, which is involved in transcriptional activation of a number of genes [Chirvia, Kwok et al., 1993]; KIAA0160, which is a new functional gene with no known function to date [Nagase, Seki et al., 1995]; RanBPM9 was the most abundant insert identified. RanBPM9 is a nuclear localised protein and has been found to exist in a large complex of more than 670kDa, although its precise function remains to be elucidated [Nishitani, Hirose et al., 2001]. That CBP is involved in transcriptional regulation of many different genes suggested the potential of a similar role for PDE4A7. The interaction with

RanBPM9 was of interest as it is possible PDE4A7 could be imported into the nucleus by piggy-backing on either RanBPM9 or one of the other proteins contained in the large RanBPM9 complex. Also uncovering the biological function of the RanBPM9 complex would give insight into another possible functional role of PDE4A7. However, upon further analysis I demonstrated that both CBP and RanBPM9 were false positives generated from the yeast two-hybrid screen whereby upon re-testing RanBPM9 was found to autonomously activate the reporter genes and CBP was no longer found to interact with PDE4A7. However, the possibility remains that KIAA0160 is an authentic binding partner for PDE4A7 and thus its potential interaction needs to be evaluated. Unfortunately I did not have time to study this further as I had focussed on evaluating the other species. This is because nothing is known of KIAA0160, whilst the other species provided established examples of nuclear localised proteins.

Yeast two-hybrid is one of the most popular methods for the detection of protein-protein interactions as it is simple, rapid and inexpensive. However, there are a number of disadvantages to this system. For example, the yeast system may not provide the post-translational modifications required for native folding, or for certain interactions to occur. Conversely, protein-protein interactions that occur in the yeast system may not occur in the proteins' native environment. Also, the GAL4 domain may interfere with the ability of the fusion proteins to interact. The major disadvantage noted for this system is the tendency to produce false positives, which has occurred in this case. There are a number of common false positives, which include heat shock proteins (hsps), ribosomal proteins, mitochondrial proteins and zinc finger proteins [Golemis et al., 1997]. That RanBPM9 is a zinc finger containing protein may explain why it was able to activate reporter genes in the absence of a DNA-BD-bait protein. False positives can be generated if the bait or prey proteins affect the colony viability, which in turn would allow colonies to grow even under selective conditions. However, few false positives can be explained mechanistically.

An alternative method that could be used in the future to identify binding partners for PDE4A7 is that of mass spectrometry, which allows the identification of protein complexes. There are four steps to this procedure. Step 1 is to construct a vector encoding tagged PDE4A7, which we already have. The tagged PDE4A7 would be transfected into the cell type of interest. Next, PDE4A7 would be immunopurified alongside its interacting partners and mass spectrometry would be used to unambiguously identify the binding partners (details of mass spectrometry method are given in Figeys et al., 2001).

That PDE4A7 was localised to the genomic centre of the cell, I proposed that the function of PDE4A7 might be to regulate the transcription of genes involved in cAMP signalling. To address this I used the methods of gene microarray and RT-PCR. From the

gene microarray analysis I demonstrated that over-expression of recombinant PDE4A7 affected the regulation of many genes including the cAMP response element binding protein (CREB), adenosine A2A and adenosine A2B receptors (A2AR and A2BR, respectively). As microarray is a new technique and has been criticised for generating false-positive data, I decided to try and verify the changes of seven of the candidate genes using the method of RT-PCR. I was unable to confirm the gene expression changes identified in the gene microarray study using RT-PCR analysis. However, expression changes for a large number of genes were detected from gene microarray analysis and given the time available it would not have been possible to re-evaluate them all. Therefore it is possible that many of the expression changes in other candidate genes were authentic.

Researchers should be aware that the microarray method is new and there are still pitfalls associated with the methodology, therefore all data must be re-evaluated by an alternative means. To increase the reliability of microarray data it has been suggested that microarray experiments should be repeated between five and nine times. This is because data can vary greatly between experiments due to fluctuations in probe, target and array preparation, in the hybridization process, background and effects resulting from image processing. In this case, microarray experiments were only repeated twice. This was because the technique was being used only as an initial screening tool to assess which genes may be possible candidates to investigate by RT-PCR. In hindsight, it would have been better to increase the number of repeats as the resulting data was quite variable. Another point to note is that no statistical analysis was performed on the microarray data therefore, any change above baseline level was considered to be a genuine change. In contrast, many researchers choose to omit those genes that do not have their expression modified by 1.5 or 2.0 fold as they are classified insignificant. As already discussed RT-PCR did not confirm the microarray data, this is probably because RT-PCR is only sensitive enough to detect 1.5 to 2.0 fold changes in expression, however, those genes from microarray that were re-evaluated demonstrated changes in expression levels less than this threshold. In conclusion, RT-PCR was not sensitive enough to detect the small changes in gene expression found in microarray. In future, numerous replicates, stricter normalisation and statistical analysis of microarray results should produce more reliable data that can be verified independently by alternative methodology if the changes are authentic.

In this study I have demonstrated that PDE4A7 is targeted exclusively to the nuclear compartment. This has not been shown for any of the other PDE4s, suggesting that PDE4A7 must have an important functional role within this compartment. The most logical reason for this is that PDE4A7 affects gene transcription, perhaps by interacting with a transcription factor per se or affecting a regulatory transcriptional complex. My

studies have established a novel feature of PDE4A enzymes, namely that the cytosolic targeting is associated with a small portion of the C-terminal region found in the catalytically active PDE4A species. However, as yet, the exact basis for both the nuclear targeting and cytosolic targeting remain to be established.

In the future, it would be interesting to determine the binding partners for PDE4A7 by using mass spectrometry (as already discussed) as opposed to the yeast two-hybrid, which could help unravel the mystery behind the function of this protein and the basis of its targeting. It would also be interesting to determine whether PDE4A7 can affect the expression levels of other PDEs. This could be addressed by using the gene chips (now available) that have been spotted with PDE cDNAs. It has already been demonstrated that PDE4A7 is incapable of hydrolysing cAMP because of its truncated catalytic site, however, it remains to be ascertained whether PDE4A7 is still able to bind cAMP. If proven to bind cAMP, then a potential role for PDE4A7 could be protect certain PDE isoforms from becoming activated. This could be evaluated by conducting a cAMP binding assay as described in Rannels et al., 1983.

Finally, in Chapter 6, I performed preliminary characterisation studies on the novel PDE4A isoform, called HSPDE4A11. In this study, I demonstrated that HSPDE4A11 migrates as a 118kDa protein in both the soluble and particulate fractions. The results from the biochemical analyses done on disrupted COS-7 cells suggest that the majority of HSPDE4A11 exists as a soluble species. However, as cellular disruption can cause the release of these proteins from their binding partners, it will be interesting to determine the distribution of this protein in intact cells by using LSCM analyses.

The soluble and particulate forms of HSPDE4A11 demonstrated similar K_m values to each other and also to the other long human isoforms of HSPDE4A4B and HSPDE4A10. The soluble form of HSPDE4A11 was found to have a similar V_{max} to that of the particulate form. In order to draw valid conclusions from this data these experiments will have to be repeated to reduce the error values.

References

- Alvarez, E., I. C. Northwood, F. A. Gonzalez, D. A. Latour, A. Seth, C. Abate, T. Curran, and R. J. Davis. 1991. Pro-Leu-Ser/Thr-Pro is a consensus primary sequence for substrate protein phosphorylation. Characterization of the phosphorylation of c-myc and c-jun proteins by an epidermal growth factor receptor threonine 669 protein kinase. *J.Biol.Chem.* 266:15277-15285.
- Artemyev, N. O., V. Y. Arshavsky, and R. H. Cote. 1998. Photoreceptor phosphodiesterase: interaction of inhibitory gamma subunit and cyclic GMP with specific binding sites on catalytic subunits. *Methods* 14:93-104.
- Ashman, D. F., Lipton, R., Melicow, M. M. and Price, T. D. 1963. Isolation of adenosine 3', 5'-monophosphate and guanosine 3', 5'-monophosphate from rat urine. *Biochem. Biophys. Res. Comm.* 11:330-334.
- Baillie, G., S. J. MacKenzie, and M. D. Houslay. 2001. Phorbol 12-myristate 13-acetate triggers the protein kinase A-mediated phosphorylation and activation of the PDE4D5 cAMP phosphodiesterase in human aortic smooth muscle cells through a route involving extracellular signal regulated kinase (ERK). *Mol.Pharmacol.* 60:1100-1111.
- Baillie, G. S., S. J. MacKenzie, I. McPhee, and M. D. Houslay. 2000. Sub-family selective actions in the ability of Erk2 MAP kinase to phosphorylate and regulate the activity of PDE4 cyclic AMP-specific phosphodiesterases. *Br.J.Pharmacol.* 131:811-819.
- Banky, P., M. G. Newlon, M. Roy, S. Garrod, S. S. Taylor, and P. A. Jennings. 2000. Isoform-specific differences between the type Ialpha and IIalpha cyclic AMP-dependent protein kinase anchoring domains revealed by solution NMR. *J.Biol.Chem.* 275:35146-35152.
- Beard, M. B., J. C. O'Connell, G. B. Bolger, and M. D. Houslay. 1999. The unique N-terminal domain of the cAMP phosphodiesterase PDE4D4 allows for interaction with specific SH3 domains. *FEBS Lett.* 460:173-177.

- Beard, M. B., A. E. Olsen, R. E. Jones, S. Erdogan, M. D. Houslay, and G. B. Bolger. 2000. UCR1 and UCR2 domains unique to the cAMP-specific phosphodiesterase family form a discrete module via electrostatic interactions. *J.Biol.Chem.* 275:10349-10358.
- Beard, M. B., E. Huston, L. Campbell, I. Gall, I. McPhee, S. Yarwood, G. Scotland, and M. D. Houslay. 2002. In addition to the SH3 binding region, multiple regions within the N- terminal noncatalytic portion of the cAMP-specific phosphodiesterase, PDE4A5, contribute to its intracellular targeting. *Cell Signal.* 14:453-465.
- Beavo, J. A., M. Conti, and R. J. Heaslip. 1994. Multiple cyclic nucleotide phosphodiesterases. *Mol.Pharmacol.* 46:399-405.
- Beavo, J. A. 1995. Cyclic nucleotide phosphodiesterases: functional implications of multiple isoforms. *Physiol Rev.* 75:725-748.
- Bloom, T. J. and J. A. Beavo. 1996. Identification and tissue-specific expression of PDE7 phosphodiesterase splice variants. *Proc.Natl.Acad.Sci.U.S.A* 93:14188-14192.
- Bolger, G., Michaeli, T., Martins, T., St John, T., Steiner, B., Rodgers, L., Riggs, M., Wigler, M., Ferguson, K. 1993. A family of human phosphodiesterases homologous to the dunce learning and memory gene product of *Drosophila melanogaster* are potential targets for antidepressant drugs. *Molecular & Cellular Biology.* 13:6558-6571.
- Bolger, G. B., I. McPhee, and M. D. Houslay. 1996. Alternative splicing of cAMP-specific phosphodiesterase mRNA transcripts. Characterization of a novel tissue-specific isoform, RNPDE4A8. *J.Biol.Chem.* 271:1065-1071.
- Bolger, G. B., S. Erdogan, R. E. Jones, K. Loughney, G. Scotland, R. Hoffmann, I. Wilkinson, C. Farrell, and M. D. Houslay. 1997. Characterization of five different proteins produced by alternatively spliced mRNAs from the human cAMP-specific phosphodiesterase PDE4D gene. *Biochem.J.* 328 (Pt 2):539-548.
- Borer, R. A., C. F. Lehner, II. M. Eppenberger, and E. A. Nigg. 1989. Major nucleolar proteins shuttle between nucleus and cytoplasm. *Cell* 56:379-390.

- Brummelkamp, T. R., R. Bernards, and R. Agami. 2002. A system for stable expression of short interfering RNAs in mammalian cells. *Science* 296:550-553.
- Bunemann, M. and M. M. Hosey. 1999. G-protein coupled receptor kinases as modulators of G-protein signalling. *J.Physiol* 517 (Pt 1):5-23.
- Bustin, S. A. 2000. Absolute quantification of mRNA using real-time reverse transcription polymerase chain reaction assays. *J.Mol.Endocrinol.* 25:169-193.
- Cartwright, P. and K. Helin. 2000. Nucleocytoplasmic shuttling of transcription factors. *Cell Mol.Life Sci.* 57:1193-1206.
- Charbonneau, H., N. Beier, K. A. Walsh, and J. A. Beavo. 1986. Identification of a conserved domain among cyclic nucleotide phosphodiesterases from diverse species. *Proc.Natl.Acad.Sci.U.S.A* 83:9308-9312.
- Chini, C. C., J. P. Grande, E. N. Chini, and T. P. Dousa. 1997. Compartmentalization of cAMP signaling in mesangial cells by phosphodiesterase isozymes PDE3 and PDE4. Regulation of superoxidation and mitogenesis. *J.Biol.Chem.* 272:9854-9859.
- Chrivia, J. C., M. D. Uhler, and G. S. McKnight. 1988. Characterization of genomic clones coding for the C alpha and C beta subunits of mouse cAMP-dependent protein kinase. *J.Biol.Chem.* 263:5739-5744.
- Chrivia, J. C., R. P. Kwok, N. Lamb, M. Hagiwara, M. R. Montminy, and R. H. Goodman. 1993. Phosphorylated CREB binds specifically to the nuclear protein CBP. *Nature* 365:855-859.
- Colledge, M. and J. D. Scott. 1999. AKAPs: from structure to function. *Trends Cell Biol.* 9:216-221.
- Conti, M. and S. L. Jin. 1999. The molecular biology of cyclic nucleotide phosphodiesterases. *Prog.Nucleic Acid Res.Mol.Biol.* 63:1-38.
- Corbin, J. D. and S. H. Francis. 1999. Cyclic GMP phosphodiesterase-5: target of sildenafil. *J.Biol.Chem.* 274:13729-13732.

- Craggs, G. and S. Kellie. 2001. A functional nuclear localization sequence in the C-terminal domain of SHP-1. *J.Biol.Chem.* 276:23719-23725.
- Davis, R. L., H. Takayasu, M. Eberwine, and J. Myres. 1989. Cloning and characterization of mammalian homologs of the *Drosophila dunce+* gene. *Proc.Natl.Acad.Sci.U.S.A* 86:3604-3608.
- Davis, R. L. and B. Dauwalder. 1991. The *Drosophila dunce* locus: learning and memory genes in the fly. *Trends Genet.* 7:224-229.
- de Rooij, J., F. J. Zwartkruis, M. H. Verheijen, R. H. Cool, S. M. Nijman, A. Wittinghofer, and J. L. Bos. 1998. Epac is a Rap1 guanine-nucleotide-exchange factor directly activated by cyclic AMP. *Nature* 396:474-477.
- de Rooij, J., H. Rehmann, M. van Triest, R. H. Cool, A. Wittinghofer, and J. L. Bos. 2000. Mechanism of regulation of the Epac family of cAMP-dependent RapGEFs. *J.Biol.Chem.* 275:20829-20836.
- Degerman, E., P. Belfrage, and V. C. Manganiello. 1997. Structure, localization, and regulation of cGMP-inhibited phosphodiesterase (PDE3). *J.Biol.Chem.* 272:6823-6826.
- Dodge, K. L., S. Khouangsathiene, M. S. Kapiloff, R. Mouton, E. V. Hill, M. D. Houslay, L. K. Langeberg, and J. D. Scott. 2001. mAKAP assembles a protein kinase A/PDE4 phosphodiesterase cAMP signaling module. *EMBO J.* 20:1921-1930.
- Dousa, T. P. 1999. Cyclic-3',5'-nucleotide phosphodiesterase isozymes in cell biology and pathophysiology of the kidney. *Kidney Int.* 55:29-62.
- Erdogan, S. and M. D. Houslay. 1997. Challenge of human Jurkat T-cells with the adenylate cyclase activator forskolin elicits major changes in cAMP phosphodiesterase (PDE) expression by up-regulating PDE3 and inducing PDE4D1 and PDE4D2 splice variants as well as down-regulating a novel PDE4A splice variant. *Biochem.J.* 321 (Pt 1):165-175.
- Fawcett, L., R. Baxendale, P. Stacey, C. McGrouther, I. Harrow, S. Soderling, J. Hetman, J. A. Beavo, and S. C. Phillips. 2000. Molecular cloning and characterization of a distinct human phosphodiesterase gene family: PDE11A. *Proc.Natl.Acad.Sci.U.S.A* 97:3702-3707.

- Feliciello, A., M. E. Gottesman, and E. V. Avvedimento. 2001. The biological functions of A-kinase anchor proteins. *J.Mol.Biol.* 308:99-114.
- Fields, S. and O. Song. 1989. A novel genetic system to detect protein-protein interactions. *Nature* 340:245-246.
- Figeys, D., L. McBroom, and M. Moran. 2001. Mass Spectrometry for the study of protein-protein interactions. *Methods* 24;230-239
- Fischer, U., J. Huber, W. C. Boelens, I. W. Mattaj, and R. Luhrmann. 1995. The HIV-1 Rev activation domain is a nuclear export signal that accesses an export pathway used by specific cellular RNAs. *Cell* 82:475-483.
- Fisher, D. A., J. F. Smith, J. S. Pillar, S. H. St Denis, and J. B. Cheng. 1998. Isolation and characterization of PDE8A, a novel human cAMP-specific phosphodiesterase. *Biochem.Biophys.Res.Commun.* 246:570-577.
- Fisher, D. A., J. F. Smith, J. S. Pillar, S. H. St Denis, and J. B. Cheng. 1998. Isolation and characterization of PDE9A, a novel human cGMP-specific phosphodiesterase. *J.Biol.Chem.* 273:15559-15564.
- Florio, S. K., R. K. Prusti, and J. A. Beavo. 1996. Solubilization of membrane-bound rod phosphodiesterase by the rod phosphodiesterase recombinant delta subunit. *J.Biol.Chem.* 271:24036-24047.
- Fujishige, K., J. Kotera, and K. Omori. 1999. Striatum- and testis-specific phosphodiesterase PDE10A isolation and characterization of a rat PDE10A. *Eur.J.Biochem.* 266:1118-1127.
- Fujishige, K., J. Kotera, H. Michibata, K. Yuasa, S. Takebayashi, K. Okumura, and K. Omori. 1999. Cloning and characterization of a novel human phosphodiesterase that hydrolyzes both cAMP and cGMP (PDE10A). *J.Biol.Chem.* 274:18438-18445.
- Gardner, C., N. Robas, D. Cawkill, and M. Fidock. 2000. Cloning and characterization of the human and mouse PDE7B, a novel cAMP- specific cyclic nucleotide phosphodiesterase. *Biochem.Biophys.Res.Commun.* 272:186-192.

- Gether, U. and B. K. Kobilka. 1998. G protein-coupled receptors. II. Mechanism of agonist activation. *J.Biol.Chem.* 273:17979-17982.
- Gether, U. 2000. Uncovering molecular mechanisms involved in activation of G protein-coupled receptors. *Endocr.Rev.* 21:90-113.
- Glavas, N. A., C. Ostenson, J. B. Schaefer, V. Vasta, and J. A. Beavo. 2001. T cell activation up-regulates cyclic nucleotide phosphodiesterases 8A1 and 7A3. *Proc.Natl.Acad.Sci.U.S.A* 98:6319-6324.
- Gluzman, Y. 1981. SV40-transformed simian cells support the replication of early SV40 mutants. *Cell* 23:175-182.
- Golemis, E. A. and V. Khazak. 1997. Alternative yeast two-hybrid systems. The interaction trap and interaction mating. *Methods Mol.Biol.* 63:197-218.
- Gopal, V. K., S. H. Francis, and J. D. Corbin. 2001. Allosteric sites of phosphodiesterase-5 (PDE5). A potential role in negative feedback regulation of cGMP signaling in corpus cavernosum. *Eur.J.Biochem.* 268:3304-3312.
- Gorlich, D. and U. Kutay. 1999. Transport between the cell nucleus and the cytoplasm. *Annu.Rev.Cell Dev.Biol.* 15:607-660.
- Grange, M., C. Sette, M. Cuomo, M. Conti, M. Lagarde, A. F. Prigent, and G. Nemoz. 2000. The cAMP-specific phosphodiesterase PDE4D3 is regulated by phosphatidic acid binding. Consequences for cAMP signaling pathway and characterization of a phosphatidic acid binding site. *J.Biol.Chem.* 275:33379-33387.
- Guipponi, M., H. S. Scott, J. Kudoh, K. Kawasaki, K. Shibuya, A. Shintani, S. Asakawa, H. Chen, M. D. Lalioti, C. Rossier, S. Minoshima, N. Shimizu, and S. E. Antonarakis. 1998. Identification and characterization of a novel cyclic nucleotide phosphodiesterase gene (PDE9A) that maps to 21q22.3: alternative splicing of mRNA transcripts, genomic structure and sequence. *Hum.Genet.* 103:386-392.
- Hache, R. J., R. Tse, T. Reich, J. G. Savory, and Y. A. Lefebvre. 1999. Nucleocytoplasmic trafficking of steroid-free glucocorticoid receptor. *J.Biol.Chem.* 274:1432-1439.

- Hamm, H. E. 1998. The many faces of G protein signaling. *J.Biol.Chem.* 273:669-672.
- Han, P., X. Zhu, and T. Michaeli. 1997. Alternative splicing of the high affinity cAMP-specific phosphodiesterase (PDE7A) mRNA in human skeletal muscle and heart. *J.Biol.Chem.* 272:16152-16157.
- Han, P., C. F. Fletcher, N. G. Copeland, N. A. Jenkins, L. M. Yaremko, and T. Michaeli. 1998. Assignment of the mouse Pde7A gene to the proximal region of chromosome 3 and of the human PDE7A gene to chromosome 8q13. *Genomics* 48:275-276.
- Hanifin, J. M., S. C. Chan, J. B. Cheng, S. J. Tofte, W. R. Henderson, Jr., D. S. Kirby, and E. S. Weiner. 1996. Type 4 phosphodiesterase inhibitors have clinical and in vitro anti-inflammatory effects in atopic dermatitis. *J.Invest Dermatol.* 107:51-56.
- Hanoune, J. and N. Defer. 2001. Regulation and role of adenylyl cyclase isoforms. *Annu.Rev.Pharmacol.Toxicol.* 41:145-174.
- Harrison, S. A., D. H. Reifsnyder, B. Gallis, G. G. Cadd, and J. A. Beavo. 1986. Isolation and characterization of bovine cardiac muscle cGMP-inhibited phosphodiesterase: a receptor for new cardiotonic drugs. *Mol.Pharmacol.* 29:506-514.
- Harrison, T., F. Graham, and J. Williams. 1977. Host-range mutants of adenovirus type 5 defective for growth in HeLa cells. *Virology* 77:319-329.
- Hartzell, H. C. and R. Fischmeister. 1986. Opposite effects of cyclic GMP and cyclic AMP on Ca²⁺ current in single heart cells. *Nature* 323:273-275.
- Hashimoto, Y., R. K. Sharma, and T. R. Soderling. 1989. Regulation of Ca²⁺/calmodulin-dependent cyclic nucleotide phosphodiesterase by the autophosphorylated form of Ca²⁺/calmodulin-dependent protein kinase II. *J.Biol.Chem.* 264:10884-10887.
- Hayashi, M., K. Matsushima, H. Ohashi, H. Tsunoda, S. Murase, Y. Kawarada, and T. Tanaka. 1998. Molecular cloning and characterization of human PDE8B, a novel thyroid-specific isozyme of 3',5'-cyclic nucleotide phosphodiesterase. *Biochem.Biophys.Res.Commun.* 250:751-756.

- Hayes, J. S., L. L. Brunton, and S. E. Mayer. 1980. Selective activation of particulate cAMP-dependent protein kinase by isoproterenol and prostaglandin E1. *J.Biol.Chem.* 255:5113-5119.
- Henderson, BR., Eleftheriou, A. 2000. A comparison of the activity, sequence specificity, and CRM1-dependence of different nuclear export signals. *Experimental Cell Research.* 256:213-224.
- Hoffmann, R., I. R. Wilkinson, J. F. McCallum, P. Engels, and M. D. Houslay. 1998. cAMP-specific phosphodiesterase HSPDE4D3 mutants which mimic activation and changes in rolipram inhibition triggered by protein kinase A phosphorylation of Ser-54: generation of a molecular model. *Biochem.J.* 333 (Pt 1):139-149.
- Hoffmann, R., G. S. Baillie, S. J. MacKenzie, S. J. Yarwood, and M. D. Houslay. 1999. The MAP kinase ERK2 inhibits the cyclic AMP-specific phosphodiesterase HSPDE4D3 by phosphorylating it at Ser579. *EMBO J.* 18:893-903.
- Horton, Y. M., M. Sullivan, and M. D. Houslay. 1995. Molecular cloning of a novel splice variant of human type IVA (PDE-IVA) cyclic AMP phosphodiesterase and localization of the gene to the p13.2- q12 region of human chromosome 19 [corrected]. *Biochem.J.* 308 (Pt 2):683-691.
- Houslay, M. D., G. Scotland, L. Pooley, S. Spence, I. Wilkinson, F. McCallum, P. Julien, N. G. Rana, A. M. Michie, S. Erdogan, and . 1995. Alternative splicing of the type-IVA cyclic AMP phosphodiesterase gene provides isoform variants with distinct N-terminal domains fused to a common, soluble catalytic unit: 'designer' changes in Vmax, stability and membrane association. *Biochem.Soc.Trans.* 23:393-398.
- Houslay, M. D. 1996. The N-terminal alternately spliced regions of PDE4A cAMP-specific phosphodiesterases determine intracellular targeting and regulation of catalytic activity. *Biochem.Soc.Trans.* 24:980-986.
- Houslay, M. D. and G. Milligan. 1997. Tailoring cAMP-signalling responses through isoform multiplicity. *Trends Biochem.Sci.* 22:217-224.

- Houslay, M. D. 1998. Adaptation in cyclic AMP signalling processes: a central role for cyclic AMP phosphodiesterases. *Semin.Cell Dev.Biol.* 9:161-167.
- Houslay, M. D., M. Sullivan, and G. B. Bolger. 1998. The multienzyme PDE4 cyclic adenosine monophosphate-specific phosphodiesterase family: intracellular targeting, regulation, and selective inhibition by compounds exerting anti-inflammatory and antidepressant actions. *Adv.Pharmacol.* 44:225-342.
- Houslay, M. D. 2001. PDE4 cAMP-specific phosphodiesterases. *Prog.Nucleic Acid Res.Mol.Biol.* 69:249-315.
- Huang, Z., Y. Ducharme, D. Macdonald, and A. Robichaud. 2001. The next generation of PDE4 inhibitors. *Curr.Opin.Chem.Biol.* 5:432-438.
- Hurley, J. H. 1999. Structure, mechanism, and regulation of mammalian adenylyl cyclase. *J.Biol.Chem.* 274:7599-7602.
- Huston, E., L. Pooley, P. Julien, G. Scotland, I. McPhee, M. Sullivan, G. Bolger, and M. D. Houslay. 1996. The human cyclic AMP-specific phosphodiesterase PDE-46 (HSPDE4A4B) expressed in transfected COS7 cells occurs as both particulate and cytosolic species that exhibit distinct kinetics of inhibition by the antidepressant rolipram. *J.Biol.Chem.* 271:31334-31344.
- Huston, E., S. Lumb, A. Russell, C. Catterall, A. H. Ross, M. R. Steele, G. B. Bolger, M. J. Perry, R. J. Owens, and M. D. Houslay. 1997. Molecular cloning and transient expression in COS7 cells of a novel human PDE4B cAMP-specific phosphodiesterase, HSPDE4B3. *Biochem.J.* 328 (Pt 2):549-558.
- Huston, E., M. Beard, F. McCallum, N. J. Pyne, P. Vandenabeele, G. Scotland, and M. D. Houslay. 2000. The cAMP-specific phosphodiesterase PDE4A5 is cleaved downstream of its SH3 interaction domain by caspase-3. Consequences for altered intracellular distribution. *J.Biol.Chem.* 275:28063-28074.
- Ishidate, T., S. Yoshihara, Y. Kawasaki, B. C. Roy, K. Toyoshima, and T. Akiyama. 1997. Identification of a novel nuclear localization signal in Sam68. *FEBS Lett.* 409:237-241.

- Jin, S. L., T. Bushnik, L. Lan, and M. Conti. 1998. Subcellular localization of rolipram-sensitive, cAMP-specific phosphodiesterases. Differential targeting and activation of the splicing variants derived from the PDE4D gene. *J.Biol.Chem.* 273:19672-19678.
- Jin, S. L., F. J. Richard, W. P. Kuo, A. J. D'Ercole, and M. Conti. 1999. Impaired growth and fertility of cAMP-specific phosphodiesterase PDE4D-deficient mice. *Proc.Natl.Acad.Sci.U.S.A* 96:11998-12003.
- Jin, S. L. and M. Conti. 2002. Induction of the cyclic nucleotide phosphodiesterase PDE4B is essential for LPS-activated TNF-alpha responses. *Proc.Natl.Acad.Sci.U.S.A* 99:7628-7633.
- Juilfs, D. M., H. J. Fulle, A. Z. Zhao, M. D. Houslay, D. L. Garbers, and J. A. Beavo. 1997. A subset of olfactory neurons that selectively express cGMP-stimulated phosphodiesterase (PDE2) and guanylyl cyclase-D define a unique olfactory signal transduction pathway. *Proc.Natl.Acad.Sci.U.S.A* 94:3388-3395.
- Jurevicius, J. and R. Fischmeister. 1996. cAMP compartmentation is responsible for a local activation of cardiac Ca²⁺ channels by beta-adrenergic agonists. *Proc.Natl.Acad.Sci.U.S.A* 93:295-299.
- Kaffman, A. and E. K. O'Shea. 1999. Regulation of nuclear localization: a key to a door. *Annu.Rev.Cell Dev.Biol.* 15:291-339.
- Kakiuchi, S. and R. Yamazaki. 1970. Calcium dependent phosphodiesterase activity and its activating factor (PAF) from brain studies on cyclic 3',5'-nucleotide phosphodiesterase (3). *Biochem.Biophys.Res.Comm.* 41:1104-1110.
- Kakkar, R., R. V. Raju, and R. K. Sharma. 1999. Calmodulin-dependent cyclic nucleotide phosphodiesterase (PDE1). *Cell Mol.Life Sci.* 55:1164-1186.
- Kalderon, D., B. L. Roberts, W. D. Richardson, and A. E. Smith. 1984. A short amino acid sequence able to specify nuclear location. *Cell* 39:499-509.
- Kawasaki, H., G. M. Springett, N. Mochizuki, S. Toki, M. Nakaya, M. Matsuda, D. E. Housman, and A. M. Graybiel. 1998. A family of cAMP-binding proteins that directly activate Rap1. *Science* 282:2275-2279.

- Keely, S. L. 1977. Activation of cAMP-dependent protein kinase without a corresponding increase in phosphorylase activity. *Res. Commun. Chem. Pathol. Pharmacol.* 18:283-290.
- Kotera, J., K. Fujishige, Y. Imai, E. Kawai, H. Michibata, H. Akatsuka, N. Yanaka, and K. Omori. 1999. Genomic origin and transcriptional regulation of two variants of cGMP-binding cGMP-specific phosphodiesterases. *Eur. J. Biochem.* 262:866-873.
- Kurz, M., Doenecke, D., Albig, W. 1997. Nuclear transport of H1 histones meets the criteria of a nuclear localization signal-mediated process. *Journal of Cellular Biochemistry.* 64:573-578.
- Laemmli, U. K. 1970. Cleavage of structural proteins during the assembly of the head of bacteriophage T4. *Nature* 227:680-685.
- Lee, D. C., D. F. Carmichael, E. G. Krebs, and G. S. McKnight. 1983. Isolation of a cDNA clone for the type I regulatory subunit of bovine cAMP-dependent protein kinase. *Proc. Natl. Acad. Sci. U.S.A* 80:3608-3612.
- Li, L., C. Yee, and J. A. Beavo. 1999. CD3- and CD28-dependent induction of PDE7 required for T cell activation. *Science* 283:848-851.
- Li, Y. and C. S. Rubin. 1995. Mutagenesis of the regulatory subunit (RII beta) of cAMP-dependent protein kinase II beta reveals hydrophobic amino acids that are essential for RII beta dimerization and/or anchoring RII beta to the cytoskeleton. *J. Biol. Chem.* 270:1935-1944.
- Liu, A. Y. 1982. Differentiation-specific increase of cAMP-dependent protein kinase in the 3T3-L1 cells. *J. Biol. Chem.* 257:298-306.
- Liu, H. and D. H. Maurice. 1999. Phosphorylation-mediated activation and translocation of the cyclic AMP-specific phosphodiesterase PDE4D3 by cyclic AMP-dependent protein kinase and mitogen-activated protein kinases. A potential mechanism allowing for the coordinated regulation of PDE4D activity and targeting. *J. Biol. Chem.* 274:10557-10565.
- Loughney, K., T. R. Hill, V. A. Florio, L. Uher, G. J. Rosman, S. L. Wolda, B. A. Jones, M. L. Howard, L. M. McAllister-Lucas, W. K. Sonnenburg, S. H. Francis, J. D. Corbin, J. A. Beavo,

- and K. Ferguson. 1998. Isolation and characterization of cDNAs encoding PDE5A, a human cGMP-binding, cGMP-specific 3',5'-cyclic nucleotide phosphodiesterase. *Gene* 216:139-147.
- Loughney, K., P. B. Snyder, L. Uher, G. J. Rosman, K. Ferguson, and V. A. Florio. 1999. Isolation and characterization of PDE10A, a novel human 3', 5'-cyclic nucleotide phosphodiesterase. *Gene* 234:109-117.
- MacFarland, R. T., B. D. Zelus, and J. A. Beavo. 1991. High concentrations of a cGMP-stimulated phosphodiesterase mediate ANP-induced decreases in cAMP and steroidogenesis in adrenal glomerulosa cells. *J.Biol.Chem.* 266:136-142.
- MacKenzie, S. J., S. J. Yarwood, A. H. Peden, G. B. Bolger, R. G. Vernon, and M. D. Houslay. 1998. Stimulation of p70S6 kinase via a growth hormone-controlled phosphatidylinositol 3-kinase pathway leads to the activation of a PDE4A cyclic AMP-specific phosphodiesterase in 3T3-F442A preadipocytes. *Proc.Natl.Acad.Sci.U.S.A* 95:3549-3554.
- MacKenzie, S. J. and M. D. Houslay. 2000. Action of rolipram on specific PDE4 cAMP phosphodiesterase isoforms and on the phosphorylation of cAMP-response-element-binding protein (CREB) and p38 mitogen-activated protein (MAP) kinase in U937 monocytic cells. *Biochem.J.* 347:571-578.
- MacKenzie, S. J., G. S. Baillie, I. McPhee, G. B. Bolger, and M. D. Houslay. 2000. ERK2 mitogen-activated protein kinase binding, phosphorylation, and regulation of the PDE4D cAMP-specific phosphodiesterases. The involvement of COOH-terminal docking sites and NH2-terminal UCR regions. *J.Biol.Chem.* 275:16609-16617.
- Macphee, C. H., S. A. Harrison, and J. A. Beavo. 1986. Immunological identification of the major platelet low-K_m cAMP phosphodiesterase: probable target for anti-thrombotic agents. *Proc.Natl.Acad.Sci.U.S.A* 83:6660-6663.
- Manganiello, V. C., E. Degerman, C. J. Smith, V. Vasta, H. Tornqvist, and P. Belfrage. 1992. Mechanisms for activation of the rat adipocyte particulate cyclic-GMP-inhibited cyclic AMP phosphodiesterase and its importance in the antilipolytic action of insulin. *Adv.Second Messenger Phosphoprotein Res.* 25:147-164.

- Manganiello, V.C., Tanaka, T., and Murashima, S. 1990. Cyclic GMP-stimulated cyclic nucleotide phosphodiesterases. In *Isoenzymes of Cyclic Nucleotide Phosphodiesterases*, J.A.Beavo and M.D.Houslay, eds. (New York: Wiley) 61-68.
- Marchmont, R.J., and Houslay, M.D. 1980. A peripheral and intrinsic enzyme constitute the cAMP phosphodiesterase activity of rat liver plasma membranes. *Biochemical Journal* 187:381-392
- Martin, E. L., S. Rens-Domiano, P. J. Schatz, and H. E. Hamm. 1996. Potent peptide analogues of a G protein receptor-binding region obtained with a combinatorial library. *J.Biol.Chem.* 271:361-366.
- Matousovic, K., J. P. Grande, C. C. Chini, E. N. Chini, and T. P. Dousa. 1995. Inhibitors of cyclic nucleotide phosphodiesterase isozymes type-III and type-IV suppress mitogenesis of rat mesangial cells. *J.Clin.Invest* 96:401-410.
- Mattaj, I.W., Englmeier, L. 1998. Nucleocytoplasmic transport: the soluble phase. *Annual Review of Biochemistry.* 67:265-306.
- McAllister-Lucas, L. M., W. K. Sonnenburg, A. Kadlecck, D. Seger, H. L. Trong, J. L. Colbran, M. K. Thomas, K. A. Walsh, S. H. Francis, J. D. Corbin, and . 1993. The structure of a bovine lung cGMP-binding, cGMP-specific phosphodiesterase deduced from a cDNA clone. *J.Biol.Chem.* 268:22863-22873.
- McPhee, I., L. Pooley, M. Lobban, G. Bolger, and M. D. Houslay. 1995. Identification, characterization and regional distribution in brain of RPDE-6 (RNPDE4A5), a novel splice variant of the PDE4A cyclic AMP phosphodiesterase family. *Biochem.J.* 310 (Pt 3):965-974.
- McPhee, I., S. J. Yarwood, G. Scotland, E. Huston, M. B. Beard, A. H. Ross, E. S. Houslay, and M. D. Houslay. 1999. Association with the SRC family tyrosyl kinase LYN triggers a conformational change in the catalytic region of human cAMP-specific phosphodiesterase HSPDE4A4B. Consequences for rolipram inhibition. *J.Biol.Chem.* 274:11796-11810.
- Meacci, E., M. Taira, M. Moos, Jr., C. J. Smith, M. A. Movsesian, E. Degerman, P. Belfrage, and V. Manganiello. 1992. Molecular cloning and expression of human myocardial cGMP-inhibited cAMP phosphodiesterase. *Proc.Natl.Acad.Sci.U.S.A* 89:3721-3725.

- Michael, W. M. 2000. Nucleocytoplasmic shuttling signals: two for the price of one. *Trends Cell Biol.* 10:46-50.
- Michel, J. J. and J. D. Scott. 2002. AKAP mediated signal transduction. *Annu.Rev.Pharmacol.Toxicol.* 42:235-257.
- Montminy, M. 1997. Transcriptional regulation by cyclic AMP. *Annu.Rev.Biochem.* 66:807-822.
- Mou, H. and R. H. Cote. 2001. The catalytic and GAF domains of the rod cGMP phosphodiesterase (PDE6) heterodimer are regulated by distinct regions of its inhibitory gamma subunit. *J.Biol.Chem.* 276:27527-27534.
- Muller, T., P. Engels, and J. R. Fozard. 1996. Subtypes of the type 4 cAMP phosphodiesterases: structure, regulation and selective inhibition. *Trends Pharmacol.Sci.* 17:294-298.
- Murashima, S., T. Tanaka, S. Hockman, and V. Manganiello. 1990. Characterization of particulate cyclic nucleotide phosphodiesterases from bovine brain: purification of a distinct cGMP-stimulated isoenzyme. *Biochemistry* 29:5285-5292.
- Nagase, T., N. Seki, A. Tanaka, K. Ishikawa, and N. Nomura. 1995. Prediction of the coding sequences of unidentified human genes. IV. The coding sequences of 40 new genes (KIAA0121-KIAA0160) deduced by analysis of cDNA clones from human cell line KG-1. *DNA Res.* 2:167-210.
- Naro, F., C. Sette, E. Vicini, A. De, V, M. Grange, M. Conti, M. Lagarde, M. Molinaro, S. Adamo, and G. Nemoz. 1999. Involvement of type 4 cAMP-phosphodiesterase in the myogenic differentiation of L6 cells. *Mol.Biol.Cell* 10:4355-4367.
- Nemoz, G., C. Sette, and M. Conti. 1997. Selective activation of rolipram-sensitive, cAMP-specific phosphodiesterase isoforms by phosphatidic acid. *Mol.Pharmacol.* 51:242-249.
- Newlon, M. G., M. Roy, Z. E. Hausken, J. D. Scott, and P. A. Jennings. 1997. The A-kinase anchoring domain of type IIalpha cAMP-dependent protein kinase is highly helical. *J.Biol.Chem.* 272:23637-23644.

- Nishitani, H., E. Hirose, Y. Uchimura, M. Nakamura, M. Umeda, K. Nishii, N. Mori, and T. Nishimoto. 2001. Full-sized RanBPM cDNA encodes a protein possessing a long stretch of proline and glutamine within the N-terminal region, comprising a large protein complex. *Gene* 272:25-33.
- O'Connell, J. C., J. F. McCallum, I. McPhee, J. Wakefield, E. S. Houslay, W. Wishart, G. Bolger, M. Frame, and M. D. Houslay. 1996. The SH3 domain of Src tyrosyl protein kinase interacts with the N-terminal splice region of the PDE4A cAMP-specific phosphodiesterase RPDE-6 (RNPDE4A5). *Biochem.J.* 318 (Pt 1):255-261.
- Owens, R. J., S. Lumb, K. Rees-Milton, A. Russell, D. Baldock, V. Lang, T. Crabbe, M. Ballesteros, and M. J. Perry. 1997. Molecular cloning and expression of a human phosphodiesterase 4C. *Cell Signal.* 9:575-585.
- Patel, T. B., Z. Du, S. Pierre, L. Cartin, and K. Scholich. 2001. Molecular biological approaches to unravel adenylyl cyclase signaling and function. *Gene* 269:13-25.
- Pedarzani, P. and J. F. Storm. 1995. Protein kinase A-independent modulation of ion channels in the brain by cyclic AMP. *Proc.Natl.Acad.Sci.U.S.A* 92:11716-11720.
- Pines, J. 1999. Four-dimensional control of the cell cycle. *Nature Cell Biology.* 1:E73-79
- Ponting, C. P. and P. Bork. 1996. Pleckstrin's repeat performance: a novel domain in G-protein signaling? *Trends Biochem.Sci.* 21:245-246.
- Pooley, L., Y. Shakur, G. Rena, and M. D. Houslay. 1997. Intracellular localization of the PDE4A cAMP-specific phosphodiesterase splice variant RD1 (RNPDE4A1A) in stably transfected human thyroid carcinoma FTC cell lines. *Biochem.J.* 321 (Pt 1):177-185.
- Rahn, T., L. Ronnstrand, M. J. Leroy, C. Wernstedt, H. Tornqvist, V. C. Manganiello, P. Belfrage, and E. Degerman. 1996. Identification of the site in the cGMP-inhibited phosphodiesterase phosphorylated in adipocytes in response to insulin and isoproterenol. *J.Biol.Chem.* 271:11575-11580.
- Rena, G., F. Begg, A. Ross, C. MacKenzie, I. McPhee, L. Campbell, E. Huston, M. Sullivan, and M. D. Houslay. 2001. Molecular cloning, genomic positioning, promoter identification,

- and characterization of the novel cyclic amp-specific phosphodiesterase PDE4A10. *Mol.Pharmacol.* 59:996-1011.
- Robbins, J., S. M. Dilworth, R. A. Laskey, and C. Dingwall. 1991. Two interdependent basic domains in nucleoplasmin nuclear targeting sequence: identification of a class of bipartite nuclear targeting sequence. *Cell* 64:615-623.
- Schena, M. 1996. Genome analysis with gene expression microarrays. *Bioessays* 18:427-431.
- Schuchhardt, J., D. Beule, A. Malik, E. Wolski, H. Eickhoff, H. Lehrach, and H. Herzog. 2000. Normalization strategies for cDNA microarrays. *Nucleic Acids Res.* 28:F47.
- Scotland, G. and M. D. Houslay. 1995. Chimeric constructs show that the unique N-terminal domain of the cyclic AMP phosphodiesterase RD1 (RNPDE4A1A; rPDE-IVA1) can confer membrane association upon the normally cytosolic protein chloramphenicol acetyltransferase. *Biochem.J.* 308 (Pt 2):673-681.
- Scott, J. D., M. B. Glaccum, M. J. Zoller, M. D. Uhler, D. M. Helfman, G. S. McKnight, and E. G. Krebs. 1987. The molecular cloning of a type II regulatory subunit of the cAMP-dependent protein kinase from rat skeletal muscle and mouse brain. *Proc.Natl.Acad.Sci.U.S.A* 84:5192-5196.
- Sette, C. and M. Conti. 1996. Phosphorylation and activation of a cAMP-specific phosphodiesterase by the cAMP-dependent protein kinase. Involvement of serine 54 in the enzyme activation. *J.Biol.Chem.* 271:16526-16534.
- Shabb, J. B. 2001. Physiological substrates of cAMP-dependent protein kinase. *Chem.Rev.* 101:2381-2411.
- Shakur, Y., J. G. Pryde, and M. D. Houslay. 1993. Engineered deletion of the unique N-terminal domain of the cyclic AMP- specific phosphodiesterase RD1 prevents plasma membrane association and the attainment of enhanced thermostability without altering its sensitivity to inhibition by rolipram. *Biochem.J.* 292 (Pt 3):677-686.
- Shakur, Y., K. Takeda, Y. Kenan, Z. X. Yu, G. Rena, D. Brandt, M. D. Houslay, E. Degerman, V. J. Ferrans, and V. C. Manganiello. 2000. Membrane localization of cyclic nucleotide phosphodiesterase 3 (PDE3). Two N-terminal domains are required for the efficient

- targeting to, and association of, PDE3 with endoplasmic reticulum. *J.Biol.Chem.* 275:38749-38761.
- Shalon, D., Smith, S. J., Brown, P. O. 1996. A DNA microarray system for analyzing complex DNA samples using two-color fluorescent probe hybridization. *Genome Research.* 6:639-645.
- Sharma, R. K. and J. H. Wang. 1985. Differential regulation of bovine brain calmodulin-dependent cyclic nucleotide phosphodiesterase isoenzymes by cyclic AMP-dependent protein kinase and calmodulin-dependent phosphatase. *Proc.Natl.Acad.Sci.U.S.A* 82:2603-2607.
- Shiota, C., J. Coffey, J. Grimsby, J. F. Grippo, and M. A. Magnuson. 1999. Nuclear import of hepatic glucokinase depends upon glucokinase regulatory protein, whereas export is due to a nuclear export signal sequence in glucokinase. *J.Biol.Chem.* 274:37125-37130.
- Skalhegg, B. S. and K. Tasken. 2000. Specificity in the cAMP/PKA signaling pathway. Differential expression, regulation, and subcellular localization of subunits of PKA. *Front Biosci.* 5:D678-D693.
- Soderling, S. H., S. J. Bayuga, and J. A. Beavo. 1998. Cloning and characterization of a cAMP-specific cyclic nucleotide phosphodiesterase. *Proc.Natl.Acad.Sci.U.S.A* 95:8991-8996.
- Soderling, S. H., S. J. Bayuga, and J. A. Beavo. 1998. Identification and characterization of a novel family of cyclic nucleotide phosphodiesterases. *J.Biol.Chem.* 273:15553-15558.
- Soderling, S. H., S. J. Bayuga, and J. A. Beavo. 1999. Isolation and characterization of a dual-substrate phosphodiesterase gene family: PDE10A. *Proc.Natl.Acad.Sci.U.S.A* 96:7071-7076.
- Soderling, S. H. and J. A. Beavo. 2000. Regulation of cAMP and cGMP signaling: new phosphodiesterases and new functions. *Curr.Opin.Cell Biol.* 12:174-179.
- Solberg, R., M. Sandberg, V. Natarajan, P. A. Torjesen, V. Hansson, T. Jahnsen, and K. Tasken. 1997. The human gene for the regulatory subunit RI alpha of cyclic adenosine 3', 5'-monophosphate-dependent protein kinase: two distinct promoters provide differential regulation of alternately spliced messenger ribonucleic acids. *Endocrinology* 138:169-181.

- Sonnenburg, W. K., S. D. Rybalkin, K. E. Bornfeldt, K. S. Kwak, I. G. Rybalkina, and J. A. Beavo. 1998. Identification, quantitation, and cellular localization of PDE1 calmodulin-stimulated cyclic nucleotide phosphodiesterases. *Methods* 14:3-19.
- Stacey, P., S. Rulten, A. Dapling, and S. C. Phillips. 1998. Molecular cloning and expression of human cGMP-binding cGMP-specific phosphodiesterase (PDE5). *Biochem.Biophys.Res.Commun.* 247:249-254.
- Sullivan, M., G. Rena, F. Begg, L. Gordon, A. S. Olsen, and M. D. Houslay. 1998. Identification and characterization of the human homologue of the short PDE4A cAMP-specific phosphodiesterase RD1 (PDE4A1) by analysis of the human HSPDE4A gene locus located at chromosome 19p13.2. *Biochem.J.* 333 (Pt 3):693-703.
- Sullivan, M., A. S. Olsen, and M. D. Houslay. 1999. Genomic organisation of the human cyclic AMP-specific phosphodiesterase PDE4C gene and its chromosomal localisation to 19p13.1, between RAB3A and JUND. *Cell Signal.* 11:735-742.
- Sunahara, R. K., C. W. Dessauer, R. E. Whisnant, C. Kleuss, and A. G. Gilman. 1997. Interaction of G α with the cytosolic domains of mammalian adenylyl cyclase. *J.Biol.Chem.* 272:22265-22271.
- Sutherland, E. W. and Rall, T. W. 1958. Fractionation and characterization of a cyclic adenine ribonucleotide formed by tissue particles. *J.Biol.Chem.* 232:1077-1091.
- Swinnen, J. V., K. E. Tsikalas, and M. Conti. 1991. Properties and hormonal regulation of two structurally related cAMP phosphodiesterases from the rat Sertoli cell. *J.Biol.Chem.* 266:18370-18377.
- Szpirer, C., J. Szpirer, M. Riviere, J. Swinnen, E. Vicini, and M. Conti. 1995. Chromosomal localization of the human and rat genes (PDE4D and PDE4B) encoding the cAMP-specific phosphodiesterases 3 and 4. *Cytogenet.Cell Genet.* 69:11-14.
- Tang, W. J. and A. G. Gilman. 1995. Construction of a soluble adenylyl cyclase activated by G α and forskolin. *Science* 268:1769-1772.
- Tari, A. M. and G. Lopez-Berestein. 2001. GRB2: a pivotal protein in signal transduction. *Semin.Oncol.* 28:142-147.

- Tasken, K. A., P. Collas, W. A. Kemmner, O. Witezak, M. Conti, and K. Tasken. 2001. Phosphodiesterase 4D and protein kinase a type II constitute a signaling unit in the centrosomal area. *J.Biol.Chem.* 276:21999-22002.
- Taylor, S. S., D. R. Knighton, J. Zheng, L. F. Ten Eyck, and J. M. Sowadski. 1992. Structural framework for the protein kinase family. *Annu.Rev.Cell Biol.* 8:429-462.
- Taylor, S. S., D. R. Knighton, J. Zheng, L. F. Ten Eyck, and J. M. Sowadski. 1992. Structural framework for the protein kinase family. *Annu.Rev.Cell Biol.* 8:429-462.
- Tesmer, J. J. and S. R. Sprang. 1998. The structure, catalytic mechanism and regulation of adenylyl cyclase. *Curr.Opin.Struct.Biol.* 8:713-719.
- Thomas, M. K., S. H. Francis, S. J. Beebe, T. W. Gettys, and J. D. Corbin. 1992. Partial mapping of cyclic nucleotide sites and studies of regulatory mechanisms of phosphodiesterases using cyclic nucleotide analogues. *Adv.Second Messenger Phosphoprotein Res.* 25:45-53.
- Thompson, W. J. and M. M. Appleman. 1971. Multiple cyclic nucleotide phosphodiesterase activities from rat brain. *Biochemistry* 10:311-316.
- Torphy, T. J., H. L. Zhou, and L. B. Cieslinski. 1992. Stimulation of beta adrenoceptors in a human monocyte cell line (U937) up-regulates cyclic AMP-specific phosphodiesterase activity. *J.Pharmacol.Exp.Ther.* 263:1195-1205.
- Torphy, T. J. 1998. Phosphodiesterase isozymes: molecular targets for novel antiasthma agents. *Am.J.Respir.Crit Care Med.* 157:351-370.
- Torphy, T. J., M. S. Barnette, D. C. Underwood, D. E. Griswold, S. B. Christensen, R. D. Murdoch, R. B. Nieman, and C. H. Compton. 1999. Ariflo (SB 207499), a second generation phosphodiesterase 4 inhibitor for the treatment of asthma and COPD: from concept to clinic. *Pulm.Pharmacol.Ther.* 12:131-135.
- Turko, I. V., T. L. Haik, L. M. McAllister-Lucas, F. Burns, S. H. Francis, and J. D. Corbin. 1996. Identification of key amino acids in a conserved cGMP-binding site of cGMP-binding phosphodiesterases. A putative NKXnD motif for cGMP binding. *J.Biol.Chem.* 271:22240-22244.

- Verde, I., G. Pahlke, M. Salanova, G. Zhang, S. Wang, D. Coletti, J. Onuffer, S. L. Jin, and M. Conti. 2001. Myomegalin is a novel protein of the golgi/centrosome that interacts with a cyclic nucleotide phosphodiesterase. *J.Biol.Chem.* 276:11189-11198.
- Verghese, M. W., R. T. McConnell, J. M. Lenhard, L. Hamacher, and S. L. Jin. 1995. Regulation of distinct cyclic AMP-specific phosphodiesterase (phosphodiesterase type 4) isozymes in human monocytic cells. *Mol.Pharmacol.* 47:1164-1171.
- Verne, J., E. Fournier, P. Gervais, S. Hebert, and N. Richshoffer. 1973. Direct stimulant effect of cyclic AMP and dibutyryl cAMP on glycogenolysis by hepatocytes in histiotypic culture. *Biomedicine.* 19:130-132.
- Vicini, F. and M. Conti. 1997. Characterization of an intronic promoter of a cyclic adenosine 3',5'- monophosphate (cAMP)-specific phosphodiesterase gene that confers hormone and cAMP inducibility. *Mol.Endocrinol.* 11:839-850.
- Wang, P., P. Wu, K. M. Ohleth, R. W. Egan, and M. M. Billah. 1999. Phosphodiesterase 4B2 is the predominant phosphodiesterase species and undergoes differential regulation of gene expression in human monocytes and neutrophils. *Mol.Pharmacol.* 56:170-174.
- Wen, W., J. L. Meinkoth, R. Y. Tsien, and S. S. Taylor. 1995. Identification of a signal for rapid export of proteins from the nucleus. *Cell* 82:463-473.
- Yan, C., A. Z. Zhao, J. K. Bentley, and J. A. Beavo. 1996. The calmodulin-dependent phosphodiesterase gene PDE1C encodes several functionally different splice variants in a tissue-specific manner. *J.Biol.Chem.* 271:25699-25706.
- Yan, S. Z., Z. H. Huang, V. D. Rao, J. H. Hurlcy, and W. J. Tang. 1997. Three discrete regions of mammalian adenylyl cyclase form a site for G α activation. *J.Biol.Chem.* 272:18849-18854.
- Yang, J. and S. Kornbluth. 1999. All aboard the cyclin train: subcellular trafficking of cyclins and their CDK partners. *Trends Cell Biol.* 9:207-210.
- Yarwood, S. J., M. R. Steele, G. Scotland, M. D. Houslay, and G. B. Bolger. 1999. The RACK1 signaling scaffold protein selectively interacts with the cAMP-specific phosphodiesterase PDE4D5 isoform. *J.Biol.Chem.* 274:14909-14917.

Yuasa, K., J. Kotera, K. Fujishige, H. Michibata, T. Sasaki, and K. Omori. 2000. Isolation and characterization of two novel phosphodiesterase PDE11A variants showing unique structure and tissue-specific expression. *J.Biol.Chem.* 275:31469-31479.

